Functional Characterisation of Arabidopsis under Acidic and Aluminium Stresses

Jayakumar Bose, B.Sc (Agriculture),
M.Sc (Soil Science and Agricultural Chemistry)

This thesis is presented for the degree of
Doctor of Philosophy
at
The University of Western Australia
Faculty of Natural and agricultural Sciences
School of Earth and Environment

August 2010

THE UNIVERSITY OF

WESTERN AUSTRALIA

STATEMENT OF ORIGINAL CONTRIBUTION

The research presented in this thesis is an original contribution to the field of plant physiology. The thesis has been completed during the course of enrolment in a PhD degree at the University of Western Australia, and has not been used previously for a degree or diploma at any other institution.

This thesis contains work accepted to be published and/or work prepared for publication, all of which has been co-authored. I contributed all of the hands-on work for all papers. Withrop Professor Zed Rengel and Dr Olga Babourina provided overall supervision, advice with experimental designs, critical comments and corrections on the manuscripts.

Jayakumar Bose	Professor Zed Rengel
Signature:	Signature:
Candidate	Coordinating Supervisor

August. 2010

DEDICATED TO MY BELOVED PARENTS

Acknowledgment

This research project would not have been possible without the support of many people. In this regard, I proclaim my thanks to Winthrop Professor Zed Rengel for the meticulous supervision, patient guidance, incessant help, encouragement, advice and constructive criticism he has provided throughout my research. I have been extremely lucky to have a supervisor who is very quick in responding and cared so much about everything. I also would like to acknowledge the extra financial support from him at the end of my PhD candidature. Although the past four years have passed quickly and the topic proved to be very challenging, I am sure that the knowledge I have gained will prepare me well for future research.

With deep respect and esteem, I am indebted to my co-supervisor Dr Olga Babourina, whose door is always open for me. Olga was always there to give me the advice, support and encouragement needed to continue in my research and be able to face many problems. I really thank Olga for the opportunity to work alongside her and get so much hands-on experience with the confocal microscope and MIFE systems.

I am privileged to place on record my heartfelt gratitude to Associate Professor Sergey Shabala for his extensive help and input during membrane potential measurements, and particularly for his critical comments on the manuscripts and magnesium flux recalculation.

I wish to express my deep regards and appreciation to all the staff members of School of Earth and Environment who helped me in one way or another during the course of the study. I express my whole hearted thanks to Professor Krishnapillai Sivasithamparam and the late Dr. Tissa Senneratna for their caring and advice when necessary. I gratefully acknowledge Michael Smirk and Paul Damon (for unforgettable fishing trips!!) for analytical and technical assistance. Thanks also goes to IT support office members for their timely and patient help with computer technique and problems, and to office members for their routine help with my study.

I wish to thank my countless pals in the Soil Science and Plant Nutrition Group and from outside for all the timely help when required by me: laughs and coffee!! Wouldn't have made it without you.

I wish to acknowledge the University of Western Australia for awarding me the Endeavour International Postgraduate Research Scholarship and University Postgraduate Award (International Student) to go through this wonderful research journey. I am grateful for the opportunities this award provided me.

I would also like to take this opportunity to thank the Australian Research Council for the financial support for my experiments, and to The Centre for Microscopy, Characterisation and Analysis, The University of Western Australia for their facilities and technical support.

Last but not least for the constant, unfailing inspiration and encouragement, unbound love, affection and care, unswerving support and motivation given throughout my academic life (22 years!!), my parents Bose and Tamilselvi, brother Kaviarasu, sister Ponmalar and beautiful wife Maheswari are gratefully acknowledged.

I thank God, humbly and wholeheartedly for making me abide through the phases of life till now.

Any omission in this acknowledgement is not meaning a lack of gratitude.

Abstract

Low pH and Al^{3+} toxicity coexist in acid soils, affecting root growth. Thus, Al^{3+} toxicity is always studied at low pH. Decades of research showed that Al^{3+} toxicity mechanisms are complex and still unclear. The reason for such ambiguity about Al^{3+} toxicity may be due to poor knowledge about the accompanying low pH stress (H^+ toxicity) because (i) low-pH stress alone can cause poor root growth in diverse plant species, and (ii) plants are usually grown (for a long period) or just conditioned (for a few hours) in a low-pH (≈4.5) medium before applying Al^{3+} treatments. Hence, low-pH and combined low-pH/Al^{3+} stresses need to be separated in order to understand stress-specific toxicity and tolerance mechanisms in plants and ultimately to breed genotypes that are more tolerant of these two stresses in acidic soils.

Arabidopsis thaliana mutants differing in Al sensitivity were used in this dissertation together with the wild type (Col-0) to characterise low-pH and combined low-pH/Al^{3+} toxicity and multiple tolerance mechanisms. One Al-tolerant mutant, *alr104*, which has high rhizosphere alkalinising capacity and two Al-sensitive mutants, *als3* (defective in redistribution of accumulated Al away from Al-sensitive tissues) and *als5* (defective in the Al exclusion mechanism), were tested. I would write as… One Al-tolerant mutant, *(alr104*) and two Al-sensitive mutants, (*als3* and *als5)* were tested. Tolerant genotype *alr104* has high rhizosphere alkalinising capacity, whilst *als3* is defective in redistribution of accumulated Al away from Al-sensitive tissues and *als5* is defective in the Al exclusion mechanism.

The distal elongation zone of the root is the primary zone of Al toxicity: the zone acts as 'plant command centre' to integrate sensory inputs caused by diverse environmental stimuli into adaptive mechanisms. In addition, the importance of the mature root zone for plant nutrient acquisition is also beyond doubt. Accordingly, all the measurements (e.g. H^+, K^+, Ca^{2+} and Mg^{2+} fluxes, rhizosphere pH, plasma membrane potential, intracellular pH, intracellular Mg^{2+} concentration) were made at least at the distal elongation zone and the mature zone to establish root-zone-specific responses under low-pH and combined low-pH/Al^{3+} stresses.

Arabidopsis thaliana wild type roots showed H^+ influx at the root apex (meristem, distal and proximal elongation zone) and H^+ efflux at the mature zone at pH

5.5. The low-pH treatment induced H^+ influx and caused cytoplasmic acidification in the distal elongation and the mature zone. Earlier reports showed that the genes regulating cytoplasmic pH were down-regulated in the low-pH-hypersensitive *Arabidopsis stop1* mutant. Thus, cytoplasmic acidification is likely to be responsible for poor root growth in the low-pH treatment. The combined low-pH/Al^{3+} treatment either decreased H^+ influx into the distal elongation zone or induced H^+ efflux from the mature zone. In both cases, there would be increased concentrations of H^+ ions in the rhizosphere. Given that such H^+ concentrations in the rhizosphere would be lower in the distal elongation zone (where net H^+ influx was measured) than in the mature zone (net H^+ efflux measured), this finding would explain the higher Al^{3+} sensitivity of the distal elongation zone in comparison to the mature zone. Modulation of cytosolic pH by low-pH/Al^{3+} stress can act as a cellular messenger to activate/inactivate transporters and enzymes and, in turn, regulate the synthesis and subsequent release of organic acid anions.

Low-pH stress induced an increase in rhizosphere pH in the distal elongation and mature zones, whereas combined low-pH/Al^{3+} stress resulted in lower rhizosphere pH in both root zones, suggesting that Al^{3+} stress affects the normal rhizosphere alkalisation process required to cope with the low-pH environments.

After long-term exposure (7 d), Al^{3+} stress resulted in higher shoot K^+ concentrations in the wild type compared to low-pH stress alone. Consistent with this observation, in short-term studies, low-pH stress elicited K^+ efflux, whereas 100-µM Al^{3+} stress inhibited K^+ efflux in the distal elongation and induced influx in the mature zone. A close link between K^+ fluxes and the plasma membrane potential (E_m) was observed. In the distal elongation and mature zones, the low-pH treatment induced plasma membrane depolarisation (1-30 min), which was significantly ($P \leq 0.05$) diminished (1-25 min of exposure) and eventually turned into hyperpolarisation (25-60 min) when combined low-pH/100 µM Al^{3+} stress was imposed. After 60 min of exposure, low-pH caused E_m depolarisation, while low-pH/100 µM Al^{3+} caused E_m hyperpolarisation. The E_m depolarisation induced by low-pH stress may either activate K^+ outward-rectifying channels (KORC are activated at E_m potentials greater than -80 mV) or inactivate K^+ inward-rectifying channels (KIRC require E_m in the range of -80 to -150 mV for activation), thereby resulting in net K^+ efflux. By contrast, Al^{3+} effects on E_m (less initial depolarisation and subsequent hyperpolarisation) could either

inactivate KORC or activate KIRC, thereby resulting in inhibition of K^+ efflux in the distal elongation and induced influx in the mature zone.

Al^{3+} toxicity impairs uptake of Ca^{2+} and Mg^{2+}, but the underlying physiology is poorly understood. Short-term (1 h) and long-term (7 d) Al^{3+} exposure studies using *Arabidopsis thaliana* wild type seedlings were compared to characterise the primary and secondary effects of Al^{3+} toxicity on Ca^{2+} and Mg^{2+} uptake. Intracellular Mg^{2+} activity was monitored under low-pH and combined low-pH/Al^{3+} stress using Mg^{2+}-specific fluorescent dye and fluorescent lifetime imaging (FLIM) analysis for the first time in intact root cells.

In short-term experiments, high Al^{3+} concentration (500 μM) induced Mg^{2+} efflux, but moderate Al^{3+} concentrations (50 and 100 μM) induced Mg^{2+} influx in both the distal elongation and mature root zones, resulting in a concomitant rise in intracellular Mg^{2+} concentration. Enhanced Mg^{2+} uptake under moderate concentrations of Al might play a crucial role in organic acid synthesis and release. Only high concentrations of Al (500 μM) and/or prolonged Al exposure reduced Mg^{2+} uptake, suggesting inhibition of the activity of plasma membrane cation channels permeable to Mg^{2+}. In contrast, all three Al^{3+} concentrations (50, 100 and 500 μM) induced Ca^{2+} efflux in both root zones. Thus, short-term Ca^{2+} fluxes (but not those of Mg^{2+}) are impaired by Al^{3+}, whereas long-term exposure to Al^{3+} has a similar inhibitory effect on the accumulation of both Ca^{2+} and Mg^{2+}. Immediate Al^{3+}-induced disturbance in Ca^{2+} uptake may be associated with the primary cause of Al^{3+} toxicity in *Arabidopsis thaliana*.

Arabidopsis mutants differed in their responses to low-pH and Al^{3+} stresses: *als5* grew well under low-pH stress and poorly under Al^{3+} stress, whereas *als3* was sensitive and *alr104* tolerant to both stresses. The capacity of *Arabidopsis* mutants to maintain Ca^{2+} and Mg^{2+} uptake from acidic environments may contribute to low-pH and Al^{3+} tolerance. Indeed, low-pH-tolerant mutants (*als5* and *alr104*) maintained higher Ca^{2+} and Mg^{2+} concentrations in roots, had greater Mg^{2+} influx and showed better? faster? recovery from low-pH-induced inhibition of Ca^{2+} influx compared with the low-pH-sensitive wild type and *als3* mutant. Under combined low-pH/Al^{3+} treatment, Al-tolerant genotypes (wild type and *alr104*) maintained higher Ca^{2+} and Mg^{2+} accumulation than Al-sensitive genotypes (*als3* and *als5*). Further, Al-tolerant genotypes (wild type and *alr104*) showed recovery from Al-induced Ca^{2+} efflux, had

higher Mg^{2+} influx and higher intracellular Mg^{2+} concentration than Al-sensitive genotypes (*als3* and *als5*).

Plant capacity to take up K^+ or retain more K^+ in tissues has been previously suggested as the low-pH tolerance mechanism.However, this hypothesis was not supported because low-pH-sensitive *als3* mutant retained more K^+ and showed lower K^+ efflux than low-pH tolerant *alr104* mutant. The *alr104* and *als5* mutants exhibited higher H^+ influxes and higher rhizosphere pH than the wild type and *als3* at the distal elongation and mature zones.Thus, enhanced capacity of *als5* and *alr104* mutants to alkalinise the rhizosphere and take up H^+ from a low-pH environment contributes to the low-pH tolerance in these mutants. Higher tolerance to combined low-pH/Al stress in the wild type and *alr104* mutant compared with *als3* and *als5* coincided with a higher resting E_m followed by E_m depolarisation throughout the combined stress treatment, higher K^+ efflux and higher H^+ influx, all of which are linked to the plant capacity to make the rhizosphere less acidic.

In conclusion, this project demonstrated that low-pH and combined low-pH/Al^{3+} stresses differentially affect root tissues and, consequently, the rhizosphere. The capacity of some *Arabidopsis* genotypes to alkalinise the rhizosphere and take up H^+ from low-pH environment is responsible for the low-pH and combined low-pH/Al^{3+} tolerance. Less disturbed Ca^{2+} and Mg^{2+} uptake also helps *Arabidopsis* genotypes to cope with low-pH and combined low-pH/Al^{3+} stresses. Maintenance of K^+ efflux together with E_m depolarisation coincided with Al tolerance. However, retention of high K^+ and/or low K^+ efflux under low-pH stress did not contribute to low-pH tolerance.

This project developed a new method to measure intracellular Mg^{2+} concentration dynamics using Mg^{2+}-specific fluorescent dye and fluorescent lifetime imaging (FLIM) analysis. Furthermore, this thesis contains an interesting observation that Al^{3+} stress enhanced Mg^{2+} influx and elevated cytosolic Mg^{2+} concentration in Al-tolerant genotypes within the first hour of exposure. Considering a pivotal role of intracellular Mg^{2+} in regulation of H^+-ATPase activity and organic acid synthesising enzymes, this elevated Mg^{2+} may fuel organic acid synthesis inside the cytoplasm for subsequent release in Al-tolerant genotypes. Further work, particularly characterizing activities of H^+-ATPase and organic acid synthesising enzymes in Al-tolerant genotypes together with monitoring cytosolic Mg^{2+} concentration, is eagerly awaited to address this hypothesis.

Publications Arising from this Thesis

Bose J, Babourina O, Shabala S, and Rengel Z. 2010. Aluminum-dependent dynamics of ion transport in *Arabidopsis*: Specificity of low pH and aluminium responses. **Physiologia Plantarum,** 139:401-412 (Chapter 4)

Bose J, Babourina O, Shabala S, and Rengel Z. 2010 Aluminium-induced ion transport in *Arabidopsis*: the relationship between Al tolerance and root ion flux. **Journal of Experimental Botany,** 61 (11):3163-3175 (Chapter 6)

Bose J, Babourina O, and Rengel Z. Aluminium affects Ca^{2+} and Mg^{2+} uptake in the roots of intact *Arabidopsis thaliana* plants (**Submitted to Journal of Plant Physiology;** Chapter 5)

Bose J, Babourina O, and Rengel Z. Low-pH and aluminium tolerance in Arabidopsis is linked to increased calcium and magnesium uptake **(Submitted to Journal of Experimental Botany;** Chapter 7**)**

List of Abbreviations

BSM	basal salt medium (0.1 mM $CaCl_2$ + 1 mM KCl + 0.2 mM $MgCl_2$, pH 5.5)
CEC	Cation exchange capacity
DEZ	distal elongation zone
E_m	plasma membrane potential
FLIM	fluorescence lifetime imaging
HACC	hyperpolarisation-activated cation channels
KORC	potassium outward-rectifying channels
KIRC	potassium inward-rectifying channels
MIFE	microelectrode ion flux estimation
MZ	mature zone
NORC	non-selective outward-rectifying channels
NSCC	non-selective cation channel
OAA	organic acid anions
PM	plasma membrane
PEZ	proximal elongation zone
ROS	reactive oxygen species
RBC	root border cells

Table of Contents

List of Figures

List of Tables

Chapter 1

Introduction

Soil acidity is one of the most significant problems limiting food production world-wide. It is estimated that at least 40%, and potentially up to 70%, of the world's arable land is acidic (von Uexkull and Mutert, 1995). Soil acidification is a natural process that occurs as the result of weathering of acidic parent material and leaching of basic cations. Other factors such as intensive agriculture, cultivation of legumes, use of acid-forming fertilizers and acid rain can also increase soil acidity. Thus, the problem of acid soils is exacerbated over time in both the severity and the extent (Rengel, 2004). In Australia, there is more than 33 million hectares of acid soils and an additional 55 million hectares of moderately acidic soils; costing farmers close to $1 billion each year in lost yields (see http://www.csiro.au/files/files/pjyt.pdf).

Acid soils can be made productive by applying lime, but such an option is often too expensive and machinery intensive, so it is of limited use in addressing soil acidity in extensive agriculture. Often, soil acidity is most severe in the subsoil where incorporation of liming material into the subsoil acidity is technically difficult (Rengel, 2004; Tang *et al.*, 2000). However, many plant species are well adapted to growing in acid soils, suggesting there is some scope to breed and engineer plants with high tolerance to acid soils. Nevertheless, breeding for acid soil tolerance has achieved only limited progress world-wide so far because of the complex interplay between mineral toxicities (Al^{3+} and Mn^{2+}) and deficiencies (NH_4^+-N, P, Ca^{2+}, Mg^{2+} and MoO_4^{2-}) in addition to H^+ toxicity in various acidic soils (Kochian *et al.*, 2004).

In the complex acid-soil syndrome, aluminium toxicity poses a major threat to plant growth by inhibiting root growth (Kochian *et al.*, 2004). Aluminium as the Al^{3+} ion is the most rhizotoxic form (Kochian, 1995); its activity peaks at around pH 4.2-4.3 (Kinraide, 1993; Taylor *et al.*, 2000). Therefore, Al^{3+} toxicity is always studied in combination with low-pH stress (H^+ toxicity). Despite decades of research, Al^{3+} toxicity

mechanisms remain unclear, which might be due to poor knowledge about the accompanying low-pH stress that can hamper root growth in diverse plant species. Hence, low-pH and combined low-pH/Al^{3+} stresses need to be separated in order to understand the stress-specific toxicity and tolerance mechanisms in plants and ultimately to breed genotypes that are more tolerant of these two stresses in acidic soils.

Given that low-pH and combined low-pH/Al^{3+} stresses affect root growth, roots have been the focus of research to decipher the mechanisms of toxicity and tolerance in plants. It was shown that low pH causes irreversible damage to primary and lateral roots in *Arabidopsis*, with the pattern of damage being different from the one caused by Al^{3+} rhizotoxicity (Koyama *et al.*, 2001; Koyama *et al.*, 1995). Further, an *Arabidopsis* QTL analysis suggested that Al^{3+} tolerance and low-pH tolerance are controlled by different genes (Ikka *et al.*, 2007). In contrast, low-pH hypersensitive *Arabidopsis stop1* (sensitive to proton rhizotoxicity1) mutant is also hypersensitive to Al^{3+} (Iuchi *et al.*, 2007; Sawaki *et al.*, 2009). Therefore, it appears that H^+ and Al^{3+} toxicities and tolerances are controlled by some separate and some common mechanisms, which need to be elucidated.

This thesis was aimed at clarifying the mechanisms of low-pH and combined low-pH/Al^{3+} toxicity tolerance in plants using *Arabidopsis thaliana* as the model system. The nutrient dynamics in an Al-tolerant mutant (*alr104*) and two Al-sensitive mutants (*als3* and *als5*) were examined along with the wild type (Col-0) under low-pH and combined low-pH/Al^{3+} stress.

The second chapter summarises the current literature pertinent to low-pH and combined low-pH/Al^{3+} toxicity and tolerance mechanisms in plants. That chapter also (i) describes Mg^{2+} homeostasis inside plant cells, and (ii) characterises the mechanisms hypothesised to operate in Al-tolerant and Al-sensitive *Arabidopsis* mutants (*alr104*, *als3* and *als5*) under combined low-pH/Al^{3+} stress. The third chapter outlines the experimental techniques employed in this thesis. The fourth chapter characterises the effects of low-pH and combined low-pH/Al^{3+} stresses on H^+ and K^+ fluxes, rhizosphere pH, intracellular pH and plasma membrane potential of the wild type. The fifth chapter elucidates the effects of low-pH and combined low-pH/Al^{3+} stresses on Ca^{2+} and Mg^{2+} fluxes and intracellular Mg^{2+} dynamics in the wild type. The sixth and seventh chapters

examine the physiology of multiple tolerance mechanisms (such as rhizophere alkalisation, maintenance of Ca^{2+}, Mg^{2+} and K^{+} uptake processes as well as intracellular Mg^{2+} homeostasis) operating in the *Arabidopsis* mutants under low-pH and combined low-pH/Al^{3+} stresses. The eighth chapter discuss the outcome of this thesis and ninth chapter describes conclusions and future work.

Chapter 2

Literature Review

2.1 Soil acidity

Acidic soils are formed mainly due to the weathering of acidic parent material and the leaching of basic cations by soil water. As a result, soils in high rainfall areas and older soils exhibit greater acidity. A number of other factors also contribute to soil acidification, including imbalances in the nitrogen, carbon and sulphur cycles (Goulding *et al.*, 1998; Mannion, 1998); use of NH_4^+-forming fertilisers (Rowell and Wild, 1985; Tang *et al.*, 2000); atmospheric acidification (Galloway, 1989; Vries and Breeuwsma, 1987); nitrogen fixation by legumes (Bolan *et al.*, 1991; Shen *et al.*, 2004a) and excessive uptake of cations by plants (Shen *et al.*, 2004a). Thus, soil acidification is a continuous process, which means the problem of acid soils is exacerbated over time in severity and extent (Rengel, 2004).

In acidic soils, plant growth may be limited by various toxicities (H^+, Al^{3+}, Mn^{2+}) and deficiencies (NH_4^+-N, P, Ca^{2+}, Mg^{2+} and MoO_4^{2-}) (for references, see Kidd and Proctor, 2001). Among these complex factors, Al^{3+} and low-pH (H^+ toxicity) stresses are highly correlated with poor plant growth (Rangel *et al.*, 2005).

Aluminium (Al) is the third most abundant element in the earth's crust behind oxygen and silicon, mostly present as insoluble aluminosilicates and oxides. Aluminium becomes increasingly soluble when the pH decreases below 5. Its chemistry is complex, and the toxicity of different Al species remains unclear even in simple nutrient solutions (Kinraide, 1991). Root elongation studies indicated that trivalent cationic $Al(H_2O)_6^{3+}$ (hereafter Al^{3+} for convenience), polynuclear hydroxyl-Al complexes such as ($AlO_4Al_{12}(OH)_{24}(H_2O)_{12}^{7+}$) (hereafter Al_{13} for convenience) and Al-fluoride complexes are clearly rhizotoxic, whilst Al-phosphate, Al-hydroxide and Al-organic acid complexes are non rhizotoxic to plants (Kinraide, 1990, 1991; Matsumoto, 2000; Poschenrieder *et al.*, 2008). The Al^{3+} ion is the most relevant toxic form in acid soils (Kochian, 1995). The Al^{3+} activity often peaks at around pH 4.2-4.3 (Kinraide, 1993;

Taylor *et al.*, 2000). Hence, Al^{3+} toxicity experiments need to be conducted around this pH to avoid interference by the formation of other Al species.

Al^{3+} and H^{+} toxicities often coexist in acid soils, affecting root growth. Literature reports suggest that low pH alone can affect growth in diverse plant species (e.g. Arnon and Johnson, 1942). Further, there are low-pH soils (e.g. organic soils) where Al^{3+} ions are either not present or present in low concentrations, thereby H^{+} ions dominate the composition of the soil solution (Kidd and Proctor, 2001). These H^{+}-ion-dominated soils account for a high proportion of acid soils around the globe. For instance, histosols occupy 200 million ha worldwide (Brady and Weil, 1990). Hence, low-pH and combined low-pH/Al^{3+} stresses need to be separated in order to understand stress-specific toxicity and tolerance mechanisms in plants and to breed genotypes that are more tolerant of these two stresses in acidic soils. However, these types of experiments have seldom been reported in the literature (Lazof and Holland, 1999; Samac and Tesfaye, 2003; Vitorello *et al.,* 2005).

2.2 Al^{3+} toxicity in plants

2.2.1 Inhibition of root growth and root region affected by Al^{3+} toxicity

An early symptom of Al^{3+} toxicity to plants is inhibition of root growth, becoming measurable within minutes of exposure to micromolar concentrations of Al^{3+} (see Delhaize and Ryan, 1995; Rengel, 2004 for references). Thus, roots have been the focus of research to decipher the mechanisms of Al^{3+} toxicity and tolerance in plants.

Root growth is a complex and dynamic phenomenon that involves a series of biochemical and physiological processes differing in various root tissues (Street, 1966; Wang *et al.*, 2006). *Arabidopsis thaliana* roots have five distinct zones along the longitudinal axis: root cap, meristem (zone of active cell division), transition zone or distal elongation zone (in this dissertation abbreviated as DEZ; zone of slow cell growth in length and width), proximal elongation zone (PEZ, zone of rapid cell growth in length without growth in width) and mature zone (MZ, zone of root hairs). These zones differ distinctly in anatomy, growth pattern and presumably in plant signalling in response to environmental stimuli (Verbelen *et al.*, 2006).

Detailed investigations of the spatial sensitivity to Al^{3+} in different root zones revealed that the root apex (Ryan *et al.*, 1993), particularly the distal elongation zone within the root apex (Illes *et al.*, 2006; Kollmeier *et al.*, 2000; Sivaguru and Horst, 1998), is the primary site of Al^{3+} toxicity. The distal elongation zone (due to its specific architecture) has extraordinary capability to sense various environmental stimuli and act as a "plant command centre" to integrate sensory inputs into adaptive responses (Baluška *et al.*, 2004). Accordingly, the distal elongation zone needs to be studied in detail for a greater understanding of the primary mechanisms of Al^{3+} toxicity and tolerance. However, Al^{3+} toxicity and tolerance studies on distal elongation zone are relatively rare. Some studies have shown that Al^{3+} also affects physiological and biochemical processes in other root zones, such as the root cap, meristem, elongation zone and mature zone (Brady *et al.*, 1993; Olivetti *et al.*, 1995; Rengel, 1996).

Being the longest, the mature zone accounts for more than 90% of root biomass and is the principal area for nutrient absorption (Bibikova and Gilroy, 2002; Gahoonia and Nielsen, 1998; Parker *et al.*, 2000). For example, Ahn *et al.* (2004b) found that 10 out of 15 K^+ transporters (*KT/KUPs*) get expressed in the mature zone. Further, Ca^{2+} and Mg^{2+} uptake at the mature zone is different to that at the root apex (Demidchik *et al.*, 2002; Ferguson and Clarkson, 1975, 1976; Guo *et al.*, 2010; Kiegle *et al.*, 2000; Newman, 2001). Recently, Babourina and Rengel (2009) found that Al^{3+} concentration in the internal tissues of the mature zone is higher than in the cortex; therefore, the response of the mature zone to Al^{3+} might be different from that of the distal elongation zone. Hence, it is important to examine the mature root zone to understand root-tissue-specific adaptation mechanisms to combat Al^{3+} stress.

2.2.2 Inhibition of cell division and cell elongation

Early work by Clarkson (1965) revealed that Al^{3+} toxicity strongly altered root development and pointed at the hampering of cell division by Al^{3+} ions as a primary cause of root growth inhibition. Indeed, (i) binding of Al to nucleic acid in root tips along with inhibition of cell division (Matsumoto *et al.*, 1976b; Morimura *et al.*, 1978) and (ii) reduction in the mitotic index along with different abnormalities such as chromosome bridges, breaks, sticky metaphases, nuclear dissolution, cell death and in some cells chromosome duplication under Al^{3+} stress have been observed in maize or

onion roots (De Campos and Viccini, 2003). In contrast, Al^{3+}-induced stimulation of cell division was also reported under low concentrations of Al^{3+}, mainly in cell culture experiments. For example, cell cycle activity was enhanced in the Al-tolerant cell culture line of *Coffea arabica*, while inhibition was observed in the Al-sensitive cell line (Valadez-Gonzalez *et al.*, 2007).

Al^{3+}-induced alterations of the cell cycle received considerable attention in recent years because (i) it has been well established that Al can enter the symplasm quite rapidly (Babourina and Rengel, 2009; Silva *et al.*, 2000); (ii) Al^{3+} could alter the cell cycle through a signalling cascade without the need for Al to reach nuclei of meristematic cells (Poschenrieder *et al.*, 2009). Further, Al^{3+} toxicity is not restricted to inhibition of root length. More detailed temporal and spatial study on the maize root cell patterning under Al^{3+} stress revealed that 5-min Al^{3+} exposure was sufficient to inhibit cell division in the proximal meristem zone and stimulate cell division in the distal elongation zone. Protrusion of an incipient lateral root was observed in the distal elongation zone after 180 min. These observations suggest a rapid change in cell patterning events along the root axis upon short-time Al^{3+} exposure(Doncheva *et al.*, 2005).

Stiffening of cell walls and consequent inhibition of root growth has been observed in response to Al^{3+} stress under different experimental conditions (Jones *et al.*, 2006; Ma *et al.*, 2004; Tabuchi and Matsumoto, 2001). Indeed, large amounts of Al accumulate in the cell walls and intercellular spaces of root tips. For example, 85 to 99.9% of Al was found in the apoplasm of root cells (Ma, 2007). Apart from precipitation of Al on the root surface and in intercellular spaces, binding of an exchangeable form of Al to the negative charges of the pectin substances in the cell wall was also observed (Blamey, 2001). In an *in vitro* study, Al treatment did not cause cell wall stiffening in dead root tips of maize (Ma *et al.*, 2004) indicating it is a biochemical process and not purely physical cross-linking between pectin material and Al^{3+}. This leads to the conclusion that Al binds to the newly formed cell wall material, which is required for cell elongation growth, thereby altering mechanical properties of cell wall and hampering cell elongation (Ma, 2007; Ma *et al.*, 2004). The cross-linking of other polar cell wall constituents, such as hydroxyproline-rich glycoproteins (HRGPs) by

reactive oxygen species in combination with callose deposition, has been shown to inhibit cell elongation in *Arabidopsis thaliana* (De Cnodder *et al.*, 2005).

2.2.3 Production of reactive oxygen species (ROS)

Reactive oxygen species are natural by-products of aerobic respiration formed when oxygen is partially reduced. ROS production can be toxic to plant cells or can act as signalling molecules depending on the circumstances (Scholz-Starke *et al.*, 2005). ROS are essential for (i) root elongation because quenching of root ROS resulted in inhibition of root elongation in *Arabidopsis thaliana* (Demidchik *et al.*, 2003), (ii) regulation of hyperpolarisation-activated cation channels (HACC) present in the epidermis of the root elongation zone (Demidchik *et al.*, 2003; Foreman *et al.*, 2003), and (iii) activation of potassium outward-rectifying channel (KORC) and a non-selective cation channel (NSCC), which mediate, respectively, K^+ efflux and Ca^{2+} influx in root hair tips of C3 and C4 plants (Demidchik *et al.*, 2003).

The formation of ROS in response to Al^{3+} has been observed in many studies (Babourina *et al.*, 2006; Darko *et al.*, 2004; Jones *et al.*, 2006; Tahara *et al.*, 2008; Tamás *et al.*, 2004), even though Al^{3+} is not a transition metal and therefore cannot catalyse redox reactions. However, Al^{3+} in combination with iron caused peroxidation of lipids in the plasma membrane of soybean (Cakmak and Horst, 1991) and rice roots (Meriga *et al.*, 2004) and cultured tobacco cells (Ono *et al.*, 1995; Yamamoto *et al.*, 1997). Further, Al^{3+} induced the expression of several genes encoding antioxidant enzymes such as glutathione S-transferase, peroxidase and superoxide dismutase (SOD) in *Arabidopsis thaliana* (Ezaki *et al.*, 2000; Richards *et al.*, 1998), which established the significance of ROS production under Al^{3+} toxicity.

A number of hypotheses have been proposed for Al^{3+}-induced rapid production of ROS, including dysfunction of mitochondria (Yamamoto *et al.*, 2002), formation of aluminium superoxide semi-reduced radicals (Exley, 2004) and activation of oxidising enzymes (Šimonovicová *et al.*, 2004a; Šimonovicová *et al.*, 2004b). However, time-dependent studies demonstrated that cell death and protein oxidation occurred several hours after the cessation of root growth (Boscolo *et al.*, 2003; Šimonovicová *et al.*, 2004b). For example, ROS production and loss of growth was observed after 12 h in tobacco (Yamamoto *et al.*, 2002). Considering the time taken to

produce ROS, it appears ROS production may not be the primary mechanism of Al^{3+} toxicity. Yamamoto *et al* (2002) suggested that ROS production is not important for root growth inhibition, but rather important for callose biosynthesis. Indeed, cross-linking of ROS with hydroxyproline-rich glycoproteins (HRGPs) was accompanied by callose deposition and was shown to be an important mechanism for inhibition of cell elongation induced by the ethylene precursor 1-aminocyclopropane-1-carboxylic acid (ACC) in *Arabidopsis thaliana* (De Cnodder *et al.*, 2005).

2.2.4 Disturbance of cytoskeleton

Cytoskeletal structures (microtubules and microfilaments) are pivotal for cell divisions and the elongation of the growing root (cf. Kochian *et al.*, 2005; Sivaguru *et al.*, 1999; Sivaguru *et al.*, 2000). Al-induced disturbance to organisation of microtubules and microfilaments in the root cells was well documented (e.g Amenos *et al.*, 2009; Sivaguru *et al.*, 1999; Sivaguru *et al.*, 2003). Such Al-induced structural changes in the root cells might underlie morphological changes and structural malformations observed in Al-stressed roots (Kochian *et al.*, 2005).

2.2.5 Changes in the plasma membrane properties

As Al can enter the symplasm quite rapidly (Babourina and Rengel, 2009; Silva *et al.*, 2000), Al^{3+} stress is likely to occur at the plasma membrane (Ahn and Matsumoto, 2006). Al^{3+} has a strong affinity for the plasma membrane surface (560-fold stronger than Ca^{2+}) (Akeson *et al.*, 1989). Yermiyahu et al. (1997) demonstrated that the surface charge of the plasma membrane vesicles isolated from the Al-sensitive wheat cv. Scout was 26% lower than that of vesicles from the Al-tolerant cv. Atlas, allowing more Al to bind to the Scout vesicles, thereby causing greater Al toxicity compared with Atlas. Moreover, Ahn *et al.* (2001) reported that 50 μM Al neutralized the surface charge of the plasma membrane and caused a surface potential shift from −20 to +1 mV in squash roots. These results indicated that membrane surface charge regulated the accessibility of Al ions to cells. Indeed, strong correlation was observed between Al^{3+} toxicity and the concentration of adsorbed Al on the membrane surface, as calculated by Gouy-Chapman-Stern model (Kinraide, 1994; Kinraide *et al.*, 1992). Such binding of Al to the plasma membrane (i) alters its fluidity and structure (Chen *et al.*, 1991) in addition to the surface potential (Kinraide, 2001), (ii) induces organic

anion release (Osawa and Matsumoto, 2002; Ryan *et al.*, 1995b), (iii) blocks Ca^{2+} transport (Ding *et al.*, 1993b; Pineros and Tester, 1993), and/or (iv) inhibits H^{+}-ATPase activity (Ahn et al., 2002). These changes would alter the plasma membrane potential. However, there are contrasting results reported in the literature about Al^{3+} stress effects on the plasma membrane potential. For example, Al^{3+} stress induced depolarisation in intact roots of Al-sensitive wheat genotype Scout, but not in the Al-resistant genotype Atlas (Miyasaka *et al.*, 1989). In some studies, Al^{3+} induced hyperpolarisation in Al-sensitive but not in Al-tolerant genotypes (Johnson *et al.*, 2005; Kinraide, 1993; Lindberg and Strid, 1997; Wherrett *et al.*, 2005). The reason for contradicting results may be plants either growing (for a few days) or just being conditioned (for a few hours) in the low-pH (≈4.5) medium before root cells being impaled with a measuring electrode (longer time in the low-pH medium may allow plants to recover from low-pH-induced depolarisation) (Kinraide, 1993). Further research, especially on low-pH stress studied separately from Al^{3+} stress, is thus needed to understand Al^{3+}-specific changes in the plasma membrane potential.

2.2.6 Inhibition of nutrient uptake

Long-term exposure to Al^{3+} (from hours to days) results in a deficiency of one or more nutrients, such as Ca, Mg, NH_4-N, P, K and B (cf. Foy, 1988; Grimme, 1983; Keltjens, 1988; Keltjens and Tan, 1993; Lenoble *et al.*, 1996; Mariano and Keltjens, 2005; Mugwira *et al.*, 1980; Rengel, 1990; Rengel and Elliott, 1992; Rengel and Robinson, 1989b). These deficiencies may be due to (i) direct inhibition of uptake system and/or (ii) Al^{3+}-induced impairment of root growth and a consequent decrease in the nutrient-absorbing surface area (Clarkson, 1985). The latter cause of deficiency is common after prolonged exposure to Al^{3+} (hours to days), whereby root growth reduction is associated with decreased nutrient accumulation (see Rengel, 1992 for references). Therefore, long-term Al^{3+} exposure studies may not provide information about specific Al^{3+} effects on nutrient uptake. Further complication with long-term studies is that Al^{3+} may inhibit root growth without reducing nutrient uptake. For example, root growth inhibition under Al^{3+} was observed in Norway spruce, small birch and wheat without reduction in $Ca^{2+}$and/or Mg^{2+} uptake (Godbold and Jentschke, 1998; Göransson and Eldhuset, 1995; Ryan *et al.*, 1997). Hence, short-term Al^{3+} exposure

studies involving direct measurements of ion fluxes are essential for understanding immediate Al^{3+} effects on nutrient uptake.

2.2.6.1 Ca^{2+} uptake

The interaction between Al^{3+} toxicity and Ca^{2+} uptake received considerable attention because symptoms of severe Al^{3+} toxicity resemble Ca^{2+} deficiency in plants (see Foy, 1988; Rengel and Elliott, 1992 for references) and exogenous application of relatively high (millimolar) concentrations of Ca^{2+} alleviated Al^{3+} toxicity in many plant species (Brady *et al.*, 1993; Keltjens and Tan, 1993; Kinraide *et al.*, 2004).

Al^{3+} might inhibit Ca^{2+} influx into intact root cells (Huang *et al.*, 1992; Ryan and Kochian, 1993), protoplasts (Rengel, 1994; Rengel and Elliott, 1992) and the membrane vesicles (Huang *et al.*, 1996; White, 1998) through binding of Al^{3+} on the plasma membrane surface (Al^{3+} exhibits 560-fold higher affinity for plasma membrane surface than does Ca^{2+}) (Akeson *et al.*, 1989). Such binding of Al^{3+} to the plasma membrane surface may block Ca^{2+}-permeable channels in the plasma membrane. Indeed, both the hyperpolarisation-activated Ca^{2+}-permeable channels (Ding *et al.*, 1993a; Kiegle *et al.*, 2000; Very and Davies, 2000) and depolarisation-activated Ca^{2+} channels (Pineros and Tester, 1997; Rengel *et al.*, 1995) are sensitive to Al, but Ca^{2+} influx inhibition was higher in the former (87±7%) (Kiegle *et al.*, 2000) than the latter (only 44%) (Rengel and Zhang, 2003). This Ca^{2+} influx inhibition following Al^{3+} exposure precedes root growth inhibition (Huang *et al.*, 1992; Ryan and Kochian, 1993). Hence, Al^{3+}-induced Ca^{2+} influx inhibition could be one of potential primary causes of Al^{3+} phytotoxicity in plants (Rengel, 1992; Rengel and Zhang, 2003). However, further studies revealed that low concentration of Al^{3+} can inhibit root growth without affecting Ca^{2+} influx, and addition of ameliorating cations (Mg^{2+} and Na^{+}) improved root growth, even though the net Ca^{2+} influx remained inhibited (Ryan and Kochian, 1993; Ryan *et al.*, 1997). Similarly, Al^{3+} caused root hair growth inhibition without affecting Ca^{2+} influx in *Limnobium stoloniferum* (Jones *et al.*, 1995). Poor correlation between Al-induced Ca^{2+} influx inhibition and elongation growth of *Chara* (Reid *et al.*, 1995) indicated that Al-induced inhibition of Ca^{2+} influx alone cannot be a critical factor in triggering the Al toxicity in plants. However, prolonged inhibition of Ca^{2+} influx into Al-treated root cells disrupts Ca nutrition, which in turn exacerbates Al toxicity in plants (Rengel and Zhang, 2003).

2.2.6.2 Mg^{2+} uptake

Mg^{2+} deficiency occurs particularly in highly leached acid soils with low cation exchange capacity (Aitken *et al.*, 1999; Tan *et al.*, 1991; vanPraag *et al.*, 1997). Mg^{2+} is unique among the major biological cations due to the largest hydrated radius (0.428 nm), the smallest ionic radius (0.072 nm), and the highest charge density. Because it binds water molecules three to four orders of magnitude more tightly than do other cations, Mg^{2+} often interacts with other molecules while maintaining its hydration sphere (Maguire and Cowan, 2002). As a result, Mg^{2+} binds quite weakly to the negative charged groups in the root cell wall, so the excess cations like H^+ and Al^{3+} present in acid soils can inhibit Mg^{2+} loading in the apoplasm and uptake across the plasma membrane (Marschner, 1991; Marschner, 1995).

Al^{3+}-induced inhibition of Mg^{2+} uptake has been observed in diverse plant species (Grimme, 1983; Keltjens, 1988; Rengel, 1990; Rengel and Robinson, 1989b). Al^{3+} might cause Mg^{2+} uptake inhibition through competitive interactions between Al^{3+} and plasma membrane transporters for Mg^{2+} (Rengel, 1990; Rengel and Robinson, 1989b). This might be true because *Arabidopsis thaliana* magnesium transporters (*AtMGT1* and *AtMGT10*) are highly sensitive to Al^{3+}, providing potential molecular targets for Al^{3+} toxicity in plants (Li *et al.*, 2001). Overexpression of Mg^{2+} transporter genes in yeast (MacDiarmid and Gardner, 1998) and *Nicotiana benthamiana* (Deng *et al.*, 2006) conferred Al tolerance by potentially alleviating Al-induced magnesium deficiency, but these studies did not provide sufficient evidence of enhanced magnesium uptake in the presence of Al^{3+} ions.

2.2.6.3 K^+ uptake

K^+ is essential for cell division through polymerisation of actin (Alberts *et al.*, 1994) and turgor-dependent cell elongation caused by accumulation of K^+ in the vacuole (Dolan and Davies, 2004; Frensch, 1997; Sano *et al.*, 2007). However, there is no causal relationship between Al^{3+} toxicity and K^+ nutrition in plants because Al^{3+} induced either inhibition (Matsumoto and Yamaya, 1986; Nichol *et al.*, 1993) or an increase in K^+ uptake (Lee and Pritchard, 1984; Lindberg, 1990; Tanoi *et al.*, 2005). The reason for increased K^+ uptake under Al^{3+} stress may be a decrease in net K^+ efflux rather than an increase in uptake (Horst *et al.*, 1992; Olivetti *et al.*, 1995; Sasaki *et al.*,

1995). Indeed, the patch clamp work demonstrated that Al ions decrease the open probability of K^+ inward-rectifying channels through internal blocking (Gassmann and Schroeder, 1994; Liu and Luan, 2001). In contrast, Al induced or maintained K^+ efflux in Al-tolerant wheat genotypes together with enhanced malate release (Osawa and Matsumoto, 2002; Ryan *et al.*, 1995b; Wherrett *et al.*, 2005), probably to balance charges created by exudation of weak organic acid anions (Ma *et al.*, 2001; Matsumoto, 2000; Osawa and Matsumoto, 2002; Ryan *et al.*, 1995b; Wherrett *et al.*, 2005).

2.2.7 Disturbance of ion homeostasis

The maintenance of optimal concentrations of inorganic ions like H^+, K^+, Na^+, Ca^{2+}, and Mg^{2+} (ionic homeostasis) inside plant cells and organelles is pivotal for the functioning of biopolymers (Andreev, 2001). Ion homeostasis in plants is regulated by controlled flux of ions across the plasma membrane and the endomembranes in addition to storage in organelles. Given that Al ions enter the cytoplasm rapidly (Babourina and Rengel, 2009; Silva *et al.*, 2000), they may affect homeostasis of various ions inside the cell.

2.2.7.1 H^+ homeostasis

The change of pH (ΔpH) between the cytoplasm and the apoplasm is the major driving force for the translocation of ions in plant cells. Under no stress, the pH is 7.3-7.6 in the cytoplasm, 4.5-5.9 in vacuoles, ≈7 in mitochondria, 7.2-7.8 in chloroplasts and about 5.5 in the apoplasm (Kurkdjian and Guern, 1989). Thus, cytoplasm is less acidic when compared to vacuoles and the apoplasm (**Figure 2.1**). This pH difference is regulated by proton pumps (H^+-ATPase and H^+-PPase) located in the plasma membrane and the tonoplast, driving H^+ from the cytoplasm to either the apoplasm or the vacuole (Marty, 1999). Hence, disturbance in H^+-ATPase activity by environmental stresses would affect cytoplasmic pH regulation. Indeed, the low-pH treatment caused cytoplasmic acidification (Plieth *et al.*, 1999), whereas the combined low-pH/Al^{3+} treatment alkalinised the cytoplasm of internal root cells of *Arabidopsis thaliana* (Babourina and Rengel, 2009). Though Al^{3+} decreased the H^+-ATPase activity in the plasma membrane vesicles prepared from Al-treated seedlings of barley (Matsumoto, 1988; Matsumoto *et al.*, 1992), wheat (Sasaki *et al.*, 1995) and squash(Ahn *et al.*, 2002; Ahn *et al.*, 2001), inhibition of H^+-ATPase activity appears to

be dependent on Al^{3+} concentration. For example, Al^{3+} concentrations lower than the threshold Al^{3+} phytotoxicity caused up-regulation of H^+-ATPase, whereas phytoxic Al^{3+} concentrations resulted in H^+-ATPase inhibition in maize (Facanha and Okorokova-Facanha, 2002) and soybean roots (Shen *et al.*, 2005). In addition, cytoplasmic pH may also vary depending on the Al^{3+} concentrations used. Thus, more work is needed to understand Al^{3+}concentration influence on cytoplasmic pH homeostasis.

2.2.7.2 Ca^{2+} homeostasis

Being the secondary messenger, free cytosolic Ca^{2+} activities are pivotal for transduction of hormonal and environmental signals to the responsive elements of cellular metabolism (see Rengel and Zhang, 2003 for references). Free cytosolic Ca^{2+} activities in plant cells are usually maintained in the 100–200 nM concentration range (Bush, 1995; Webb *et al.*, 1996) to prevent Ca^{2+} cytotoxicity by the formation of insoluble calcium precipitates with inorganic phosphates in the cytoplasm (Webb *et al.*, 1996). However, Ca^{2+} activities in the cell wall (apoplasm) and other internal organelles (e.g. vacuoles and endoplasmic reticulum) are higher than the cytosolic Ca^{2+} by three to four orders of magnitude (Clarkson, 1984; DuPont *et al.*, 1990; Evans *et al.*, 1991). Low concentrations of cytosolic Ca^{2+} are maintained by ATP-dependent Ca^{2+} pumps and Ca^{2+} exchangers (CaX) in the plasma membrane and the endomembranes via (i) sequestration in different organelles, and (ii) pumping Ca^{2+} into the apoplasm (Evans *et al.*, 1991; Hirschi, 2001; Miedema *et al.*, 2001).

Al^{3+} affects the Ca^{2+} homeostasis maintenance in three ways. Firstly, Ca^{2+} is essential for cross-linking the pectic materials in the cell wall. Aluminium displaces pectin-bound Ca^{2+} because Al has a higher affinity for pectic material than Ca^{2+} (Blamey, 2001). For example, between 90% (Reid *et al.*, 1995) and 99.99% (Taylor *et al.*, 2000) of cell-wall-bound Ca^{2+} is displaced by Al^{3+} in *Chara* internodal cells. Hence, displacement of Ca^{2+} by Al^{3+} would severely alter the physical properties of the cell wall, including extensibility, rigidity and permeability (Horst *et al.*, 2007; Jones *et al.*, 2006; Reid *et al.*, 1995; Tabuchi and Matsumoto, 2001), thereby detrimentally affecting cell division and elongation. However, contradicting results were observed in onion root tips where the particle-induced X-ray emission technique indicated that Ca^{2+} in the root tips was not displaced by Al (Schofield *et al.*, 1998). These discrepancies might be due to different experimental systems and environmental conditions. Secondly, Al^{3+} inhibits

the Ca^{2+} influx (reviewed in 2.2.6.1). Thirdly, Al disturbs cytosolic Ca^{2+} activity, thereby affecting the signal transduction pathways involved in root growth. However, a disagreement exists in the literature about Al effects on cytosolic Ca^{2+} homeostasis and its involvement in Al toxicity.

In many plant species Al^{3+} toxicity caused elevation of cytoplasmic Ca^{2+} activity, with such elevation being higher in Al-sensitive than Al-tolerant genotypes of the same species (Jones *et al.*, 1998a; Ma *et al.*, 2002; Rengel and Zhang, 2003; Zhang and Rengel, 1999). This cytosolic Ca^{2+} rise would play a major role in the expression of Al^{3+} toxicity because the cell responsive elements may stop responding to transient rises in cytosolic Ca^{2+} caused by variety of signals (Rengel and Zhang, 2003). For example, an increase in cytosolic Ca^{2+} caused closure of plasmodesmata (Holdaway-Clarke *et al.*, 2000) and inhibited plasmodesmata-mediated cell-to-cell transport in Al-sensitive wheat root (Sivaguru *et al.*, 2000). In fact, good correlation was observed between Al-induced cytosolic Ca^{2+} rise (within 30 min) and root growth inhibition in wheat genotypes (Zhang and Rengel, 1999), leading to the hypothesis that disruption of Ca^{2+} homeostasis may be the primary cause of Al^{3+} toxicity (Rengel and Zhang, 2003). However, in a recent study on *Arabidopsis*, an Al-induced cytoplasmic Ca^{2+} rise started in the least Al-sensitive mature root zone (in 48 seconds) and proceeded towards the root cap (in 100 seconds). Moreover, the Ca^{2+} rise did not differ among Al-resistant, Al-sensitive and the wild type *Arabidopsis* roots (Rincon-Zachary *et al.*, 2010). Similarly, a lack of correlation between Al-induced growth inhibition and alteration in cytosolic Ca^{2+} in the root hairs of *Arabidopsis thaliana* wild type, sensitive and tolerant genotypes (Jones *et al.*, 1998a) indicated that alteration in cytosolic Ca^{2+} may not be responsible for growth inhibition. In some studies, such as in tobacco cell cultures, Al decreased the cytosolic Ca^{2+} concentration along with growth inhibition (Jones *et al.*, 1998b). More detailed comparison (Plieth *et al.*, 1999) of low-pH and combined low-pH/Al^{3+} effects on cytosolic Ca^{2+} dynamics using *Arabidopsis thaliana* indicated that intact roots responded to low pH by a sustained elevation of cytosolic Ca^{2+}. However, this low-pH-mediated elevation in cytosolic Ca^{2+} activity was abolished in the presence of Al, suggesting that Ca^{2+}-mediated protection mechanism against low pH is irreversibly inhibited by Al (Plieth *et al.*, 1999). More information, especially during the first few seconds of low-pH and Al^{3+} stress, is clearly needed to resolve many discrepancies in the literature.

2.2.7.3 Mg^{2+} homeostasis

Mg^{2+} may play a crucial role in the perception of Al^{3+} toxicity and translocation of this signal into activation of organic acid synthesis and exudation. This is because Mg^{2+} is critical for the activity of many enzymes involved in organic synthesis and metabolism, such as citrate synthase (Boulton and Ratledge, 1980), malate synthase (Howard *et al.*, 2000), malic enzyme (Coleman and Palmer, 1972), malate dehydrogenase (Iglesias and Andreo, 1990), PEPC (phospho*enol*pyruvate carboxylase) (Bandurski, 1955; O'Leary, 1982; Tovar-Mendez *et al.*, 1998), isocitrate dehydrogenase (Doyle *et al.*, 2001; Satoh and Nakamura, 1984) and pyruvate kinase (Podestá and Plaxton, 1991; 1992). Indeed, over-expression of Mg^{2+}-requiring enzymes, for example citrate synthase in canola (Anoop *et al.*, 2003), PEPC in rice (Begum *et al.*, 2009; Osaki *et al.*, 2001), malate dehydrogenase in lucerne (Tesfaye *et al.*, 2001) and isocitrate dehydrogenase in *Pseudomonas fluorescens* (Middaugh *et al.*, 2005) provided Al tolerance by enhancing organic acid synthesis and release. Further, Silva *et al.* (2001a) found that pre-treatment of soybean seedlings with Mg^{2+} and subsequent exposure to Al^{3+} resulted in enhanced citrate secretion within an hour compared with seedlings without Mg^{2+} pre-treatment. This might imply that pre-treatment with Mg^{2+} 'primes' the citrate synthesis mechanism for release of organic acid anions upon exposure to Al^{3+} stress.

Transport of Mg^{2+} into cells may use either negative potential across the plasma membrane or the H^+-ATPase (Shaul, 2002). It is interesting to note that proton pumps (H^+-ATPases) are dependent on Mg^{2+} (that binds to ATP) (Brooker and Slayman, 1983; Costa and de Meis, 1996) for their activity, so that Mg^{2+} is required for its own homeostasis maintenance. For example, Yang *et al.* (2007) found that Al^{3+} stress, in the absence of Mg^{2+} in the growth medium, inhibited H^+-ATPase by 37% in rice bean (*Vigna umbellata*) roots. However, addition of micromolar concentrations of Mg^{2+} in the external medium resulted in up-regulation of plasma membrane H^+-ATPase activity, even though Al^{3+} activity was maintained constant (Yang *et al.*, 2007).

Despite Mg^{2+} involvement in many cellular processes, the literature reports on free Mg^{2+} activity inside the cytoplasm are rare. In particular, there is no information on cytosolic Mg^{2+} activity upon low-pH and Al^{3+} exposure. Available information on cellular Mg^{2+} distribution and homeostasis regulation is reviewed below.

2.2.7.3.1 Distribution of cellular Mg^{2+}

The free levels of Mg^{2+} within the cell compartments (e.g. cytoplasm, vacuole, mitochondria and chloroplasts) are important for ongoing metabolic processes and have to be strictly regulated because there are steep electrochemical gradients for Mg^{2+} across the plasma membrane, tonoplast and other membranes (**Figure 2.1**) (Shaul, 2002). A portion of cellular Mg^{2+} is bound to the cell wall or stored in the vacuoles. The concentration of Mg^{2+} in the cytosol of leaf cells is assumed to be in the range of 2-10 mM (Leigh and Wyn Jones, 1986), andtotal Mg^{2+} concentration of up to 100 mM has been measured in leaf endodermal cells (Stelzer *et al.*, 1990). However, free Mg^{2+} concentration in the cytoplasm should be much lower because Mg^{2+} is chelated by ATP and stored in organelles. Yazaki *et al.* (1988) measured free Mg^{2+} concentration of 0.4 mM in the cytoplasm of Mg-sufficient mung bean root tips compared to 3.9 mM total concentration in the same tissue. Further, they observed that about 90% of the cytoplasmic ATP was complexed with Mg^{2+}. Therefore, low concentration of free Mg^{2+} in the cytoplasm is tightly regulated, with any excess of Mg^{2+} activating its own efflux into the apoplasm or into the vacuole (Marschner, 1995). Stelzer *et al* (1990) observed almost constant concentration of Mg^{2+} (about 13 mM) in the vacuoles of mesophyll and parenchyma cells throughout the experimental period, whereas large variations were observed in the vacuoles of endodermal cells (from 20 to more than 120 mM, average 64 mM) of Norway spruce needles. This high Mg^{2+} vacuolar concentration does not necessarily represent free Mg^{2+}, as large proportion of vacuolar Mg^{2+} is bound to anionic compounds (e.g. SO_4^{2-} and phosphate). In another study, Dietz *et al.* (1992) measured total Mg^{2+} concentration in barley vacuoles as 3-7 mM. Currently, no information was found in the literature about free vacuolar Mg^{2+} concentration in plant cells (Shaul, 2002).

As Mg^{2+} is the coordinating metal ion in the chlorophyll molecule, and under abundant supply about 6% of the total Mg^{2+} is bound to chlorophyll (Marschner, 1995; Scott and Robson, 1990a, b), the chloroplasts require a significant amount of internal Mg^{2+} (**Figure 2.1**) (Demmig and Gimmler, 1979; Huber and Maury, 1980). Schroppelmeier and Kaiser (1988) observed a total Mg^{2+} concentration of about 13-18 mM in spinach chloroplasts. Pottosin and Schonknecht (1996) calculated that Mg^{2+} concentration in the lumen of spinach chloroplasts (by considering the relative volume

of the stroma and lumen) needs to be in the range of 30-50 mM to support the observed 2-mM increase in stromal Mg^{2+} concentration during illumination. Potris and Heldt (1976) reported stroma Mg^{2+} concentration in the order of 5 mM. Other subcellular organelles such as the Golgi apparatus or the endoplasmic reticulum also require Mg^{2+} for normal functioning, but no current reports could be found on Mg^{2+} concentration in these organelles.

2.2.7.3.2 Vacuole: prime organelle in Mg^{2+} homeostasis

The vacuole occupies most of the volume of differentiated cells and is involved in turgor regulation, signal transduction, defence mechanisms, pH maintenance and detoxification of metabolic compounds in the cytosol. In addition, vacuoles play a major role in ion homeostasis (Andreev, 2001; Marschner, 1995). Stelzer *et al.* (1990) demonstrated that Mg^{2+} was the predominant cation in the vacuole of endodermal cells of Norway spruce needles. They observed large variations in Mg^{2+} concentration in vacuoles of endodermal cells. These variations were accompanied by concomitant variations in the major charge-balancing anions (sulphate and phosphate). Hence, it was suggested that the vacuoles of the endodermal cells serve as an Mg^{2+} and anion storage compartment for the maintenance of constant Mg^{2+} concentrations in the adjacent cells.

A potential difference of -20 mV across tonoplast is generally assumed to be a reflection of a steady physiological state (Allen and Sanders, 1996). This indicates that the lumen of the vacuole is positively charged compared to the cytoplasm. Also, the vacuole is more acidic than the cytoplasm (**Figure 2.1**). This clearly shows that transporting Mg^{2+} into the vacuole requires a Mg^{2+}/H^+ antiport transporter like AtMHX (*Arabidobsis thaliana* Magnesium-Proton Exchanger) using the energy of either H^+-ATPase or H^+-PPase (Marty, 1999; Shaul, 2002). The first cloned Mg^{2+} transport gene AtMHX is electrogenic and exchanges proton with divalent cations (Mg^{2+} and Zn^{2+}). It exchanges at least three H^+ ions per Mg^{2+} ion (Shaul, 2002; Shaul *et al.*, 1999). The activity of the Mg^{2+}/H^+ exchanger was also identified from lutoid [a specialized vacuolar-lysosomal compartment involved in rubber biosynthesis (Kang *et al.*, 2000)] membranes of *Heavea brasiliensis* latex – a liquid cytosol (Amalou *et al.*, 1992; Amalou *et al.*, 1994) and in tonoplast from roots of maize (Pfeiffer and Hager 1993). Lutoids accumulated 10-fold higher Mg^{2+} when compared to the latex cytosol (d'Auzac *et al.*, 1989). The K_m value of the Mg^{2+} transporter involved was 2.6 mM, but it was

able to transport Zn^{2+} and Cd^{2+} ions at higher affinity than Mg^{2+}. This transporter appeared to be electro-neutral, exchanging two H^{+} ions per Mg^{2+} ion.

The mechanism and molecular basis for the efflux of Mg^{2+} from the vacuole to the cytosol is unknown. The efflux may occur through either slow activating vacuolar (SV) or fast activating (FV) channels (Shaul, 2002), which are permeable to both mono and divalent cations including Mg^{2+} (Allen and Sanders, 1996; Pottosin *et al.*, 1997; Ward and Schroeder, 1994). The activity of SV channels is regulated by Mg^{2+}, Ca^{2+}, calmodulin, protein kinase, phosphatases, ATP and redox agents (Allen and Sanders, 1996; Bethke and Jones, 1994; Carpaneto *et al.*, 1999; Weiser *et al.*, 1991). In addition, SV channels are activated *in vitro* by membrane potentials that are more positive than physiological potentials of the tonoplast. However, it was demonstrated that *in vivo* activating potential of SV channels could be strongly shifted, suggesting the presence of additional unknown regulatory factors essential for the function of SV channels. Moreover, it was suggested that SV channels may carry both inward and outward currents *in vivo* depending on conditions (Pei *et al.*, 1999).

2.2.7.3.3 Mitochondrial Mg^{2+} regulation

The yeast MRS2 (Mitochondrial RNA Splicing 2) and AtMRS2 (*Arabidopsis thaliana* Mitochondrial RNA Splicing 2) genes may regulate Mg^{2+} transport (**Figure 2.1**) (Bui *et al.*, 1999; Schock *et al.*, 2000). The yeast MRS 2 gene is essential for the splicing of group II intron RNA in mitochondria and for maintenance of the functional respiratory system (Bui *et al.*, 1999). MRS2 and AtMRS2 genes are distantly related to the CorA (Cobalt resistance) group of bacterial Mg^{2+} transporters (Kehres *et al.*, 1998; Smith and Maguire, 1998). The yeast MRS2 protein was localized in the inner membrane of mitochondria and was involved in the maintenance of homeostasis in this organelle (Bui *et al.*, 1999; Gregan *et al.*, 2001; Kolisek *et al.*, 2003). In contrast, green fluorescent protein analysis of AtMRS2-1 suggested that it was not targeted to the mitochondria and was probably localized in the plasma membrane (Li *et al.*, 2001; Schock *et al.*, 2000). Though most of the members of MRS2 family are expressed in the most major organs of the plant (Li *et al.*, 2001; Schock *et al.*, 2000), the precise location of MRS2 needs to be determined (Shaul, 2002). The regulation of Mg^{2+} homeostasis in other subcellular organelles (e.g. the Golgi apparatus, the endoplasmic reticulum, etc) also needs to be characterised.

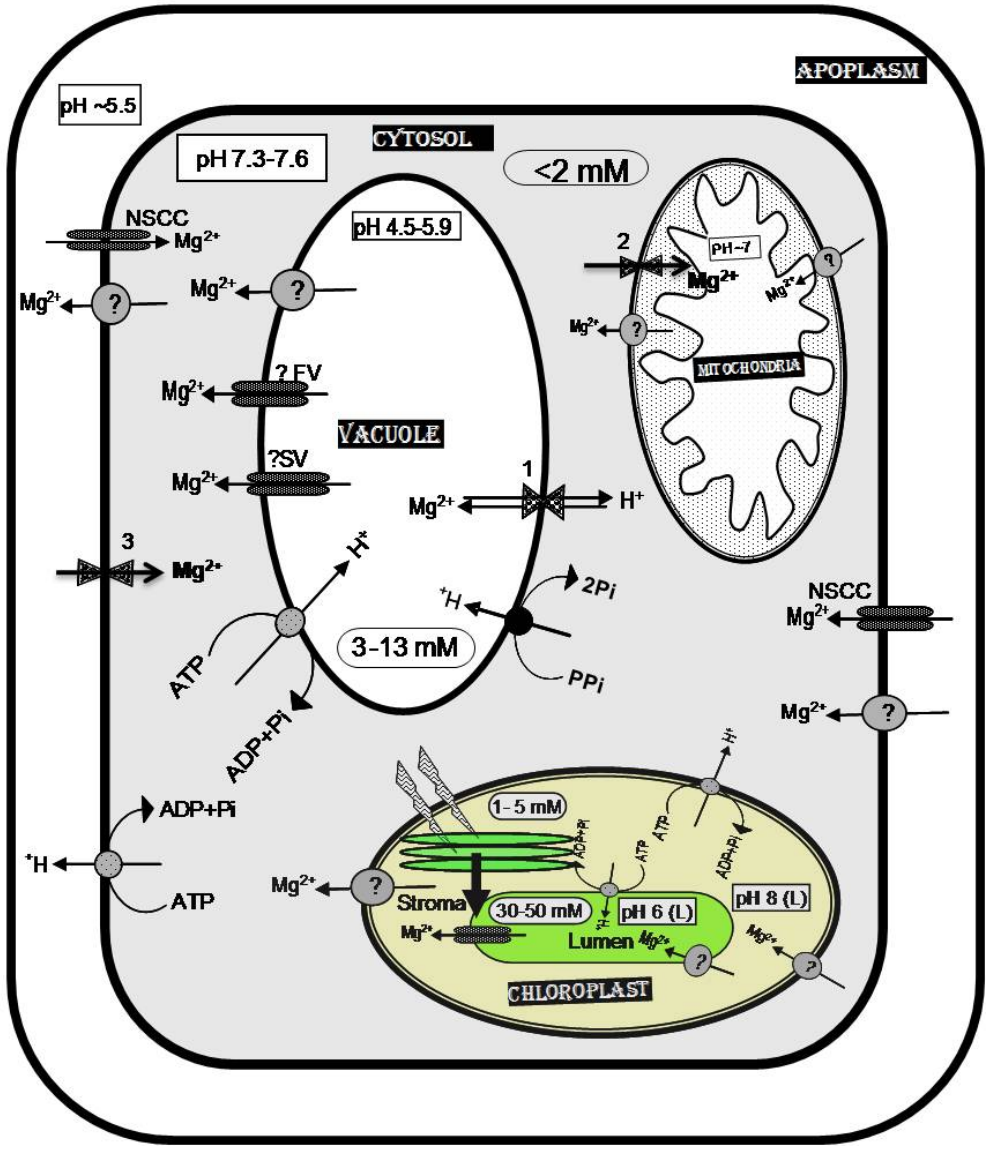

Approximate Mg^{2+} concentration

SV Slow activating voltage channels

FV Fast activating voltage channels

NSCC Non-selective cation channels

(L) Light

? unidentified transport mechanism

ion channel

Carrier protein 1.AtMHX; 2.AtMRS; 3. AtMGT

Figure 2.1 Schematic diagram of Mg^{2+} homeostasis regulation inside the plant cell. All mM concentrations refer to Mg.

2.3 Low-pH toxicity in plants

In mungbean and maize, root growth has been stimulated by low-pH (≤ 4.2) (Blamey *et al.*, 2004; Winch and Pritchard, 1999). But in many plant species, low-pH (≤ 4.2) alone caused root growth inhibition (Arnon and Johnson, 1942; Iuchi *et al.*, 2007; Kidd and Proctor, 2001; Kinraide, 2003; Koyama *et al.*, 2001; Lazof and Holland, 1999; Llugany *et al.*, 1995; Rangel *et al.*, 2005; Sawaki *et al.*, 2009). Thus, our knowledge of H^+ toxicity and the molecular mechanisms of low-pH tolerance is rather limited when compared to Al^{3+} toxicity and tolerance.

Careful examination of low-pH and Al^{3+} rhizotoxicity in *Arabidopsis* indicated that low pH causes irreversible damage to primary and lateral roots, and the pattern of damage is different from Al^{3+} rhizotoxicity (Koyama *et al.*, 2001; Koyama *et al.*, 1995). In addition, an *Arabidopsis* QTL analysis revealed that Al^{3+} tolerance and low-pH tolerance are controlled by different genetic factors (Ikka *et al.*, 2007). In contrast, low-pH hypersensitive *Arabidopsis stop1* (sensitive to proton rhizotoxicity1) mutant is also hypersensitive to Al^{3+} (Iuchi *et al.*, 2007; Sawaki *et al.*, 2009). Therefore, it can be suggested that H^+ and Al^{3+} toxicities are affecting root growth by some separate and some common mechanisms, which would need to be elucidated.

It has been proposed that excess H^+ in low-pH soils competes with other cations for root absorption sites (Marschner, 1991) and/or inhibits H^+-ATPase (Schubert *et al.*, 1990), thereby reducing ion uptake and transport in plants. Indeed, close correlation was observed between H^+ toxicity and a decrease in specific absorption rates of B, P, Ca, Mg, and Fe in maize (Poschenrieder *et al.*, 1995). Thus, alterations in nutrient uptake could play a major role in H^+ toxicity. In particular, displacement of Ca^{2+} by H^+ from pectic polysaccharide network in the cell wall has been suggested as the primary target of proton toxicity in *Arabidopsis* roots (Koyama *et al.*, 2001). Short-term low-pH exposure also induced (i) H^+ influx into the root tissue (Babourina *et al.*, 2001; Babourina *et al.*, 2006; Shabala *et al.*, 1997); (ii) cytoplasmic acidification in *Riccia* rhizoids (Felle, 1988) and protoplasts from wheat roots (Lindberg and Strid, 1997); (iii) K^+ efflux (Babourina *et al.*, 2001; Fawzy *et al.*, 1954) and decreased root K^+ concentration (Kidd and Proctor, 2001); (iv) transient rise in intracellular free Ca^{2+} (Felle, 1988; Plieth *et al.*, 1999); and (v) depolarisation of plasma membrane

(Babourina *et al.*, 2001; Felle, 1988; Shabala *et al.*, 1997). As these effects are inter-related, a classic cause–consequence dilemma needs to be addressed to decipher primary mechanism of low-pH toxicity.

2.4 Common tolerance mechanisms for low-pH and combined low-pH/Al^{3+} stresses

2.4.1 Rhizosphere alkalization

To date, several mechanisms have been proposed for increased plant tolerance to Al^{3+} toxicity (Kochian *et al.*, 2004; Matsumoto, 2000). Some of them (like rhizosphere alkalization) can increase plant tolerance to both low-pH and combined low-pH/Al stresses.

An increase in the rhizosphere pH of 0.1 to 0.2 units may convert a large proportion of rhizotoxic Al^{3+} species into less toxic Al hydroxides and Al phosphates (Kinraide, 1991). Thus, an increase in rhizosphere pH was proposed as the Al^{3+}-exclusion mechanism (Foy *et al.*, 1965; Mugwira and Patel, 1977). Indeed, an Al-induced increase in the rhizosphere pH by 0.15 units enhanced the root growth of Al-tolerant *Arabidopsis thaliana* mutant *alr104* when compared to the wild type (Degenhardt *et al.*, 1998; Larsen *et al.*, 1998).

Previous studies often compared two genotypes differing in Al^{3+} sensitivity at fixed Al^{3+} exposure and reported higher rhizosphere pH in tolerant than sensitive genotypes (Foy *et al.*, 1965; Kollmeier *et al.*, 2000; Miyasaka *et al.*, 1989; Mugwira and Patel, 1977). However, such genotypic differences could be a consequence rather than a cause of differential Al^{3+} tolerance (Kollmeier *et al.*, 2000; Miyasaka *et al.*, 1989) because Al^{3+} application did not enhance surface pH of roots in comparison to the low-pH treatment. Further, comparison of a low-pH and combined low-pH/Al^{3+}-induced root surface pH profile along the longitudinal root axis of maize cultivars revealed that the Al^{3+} treatment resulted in a strong decrease in root surface pH when compared to the low-pH treatment in both Al-sensitive and Al-tolerant cultivars (Kollmeier *et al.*, 2000). Similar results were reported in roots of wheat (Miyasaka *et al.*, 1989), signalgrass, ruzigrass (Wenzl *et al.*, 2001) and squash (Ahn *et al.*, 2002), indicating Al^{3+} affects the rhizosphere alkalinisation process in the low-pH environment.

2.4.2 Reciprocal alleviation of H^+ and Al^{3+} toxicities

Despite root growth inhibition by Al^{3+} toxicity, enhancement of root growth by submicromolar concentrations of Al^{3+} ions under low pH (i.e. H^+ concentration high enough to retard root growth) has been reported in many plant species (Kinraide, 1993; Kinraide and Parker, 1990; Llugany *et al.*, 1995). Principally, three mechanisms have been proposed for alleviation of H^+ toxicity by Al^{3+} ions (Kinraide, 1993) such as (i) Al^{3+} stress can decrease the plasma membrane leakiness induced by H^+ stress (Horst *et al.*, 1992; Staß and Horst, 1995), (ii) Al may stimulate H^+ efflux (Bennet *et al.*, 1987; Calba and Jaillard, 1997; Keltjens, 1988; Kinraide, 1988) that may be essential for root growth at low pH (Yan *et al.*, 1992), and (iii) Al may induce hyperpolarization of the plasma membrane (Johnson *et al.*, 2005; Kinraide, 1993; Lindberg and Strid, 1997; Wherrett *et al.*, 2005) as opposed to low pH inducing depolarisation (Babourina *et al.*, 2001; Felle, 1988; Shabala *et al.*, 1997).

Al^{3+} toxicity is ameliorated by cations in the order of $H^+ \approx Cation^{3+} > Cation^{2+} > Cation^+$ (Kinraide *et al.*, 1992). H^+ ions readily bind to the carboxylate, phosphate and amino groups on the plasma membrane, thereby causing charge reversal of the plasma membrane surface when the pH drops below 4 (Obi *et al.*, 1989). Such charge reversal or reduction of cell surface negativity by H^+ ions decreased Al^{3+} activity at the plasma membrane surface and, in turn, alleviated Al^{3+} toxicity (Kinraide *et al.*, 1992). Thus, reciprocal alleviation of H^+ and Al^{3+} toxicities is dependent on the bioavailability of the intoxicating and ameliorating cations at the plasma membrane surface, which is mainly determined by the plasma membrane surface potential (Kinraide, 2006; Kinraide and Yermiyahu, 2007).

2.5 Specific tolerance of low-pH stress

2.5.1 Enhanced potassium nutrition

Low-pH tolerance and K^+ nutrition appear to be interlinked in plants because addition of K^+ in the external medium alleviated H^+ toxicity in maize (Yan *et al.*, 1992), common bean (Rangel *et al.*, 2005) and sugar beet (Lindberg and Yahya, 1994) through enhanced K^+ uptake. Similarly in *Arabidopsis*, over-expression of *Arabidopsis*

cation:proton antiporter, AtCHX13, enhanced K^+ uptake at low pH (4.3) and consequently improved growth (Zhao *et al.*, 2008b). Further, down-regulation of CIPK23 that encodes the regulatory kinase of major K^+ transporter AKT1 may be responsible for low-pH sensitivity in *stop1* mutant (Iuchi *et al.*, 2007; Sawaki *et al.*, 2009). These results suggest that plant capacity to take up K^+ or retain more K^+ in the tissue may contribute to low-pH tolerance. Nonetheless, Koyama *et al.* (2001) did not observe ameliorative effect of K in H^+-sensitive *Arabidopsis thaliana*, ecotype Landsberg.

2.6 Specific mechanisms of tolerance to Al^{3+} toxicity

Plants evolved two distinct tolerance mechanisms to combat toxic effects of Al^{3+} (i) exclusion of Al from the root apex, thus minimising the amount of Al that would enter the symplasm, and (ii) internal detoxification, whereby plants can accumulate Al in the root and shoot tissues by forming non-toxic Al complexes (Kochian *et al.*, 2004).

2.6.1 Al^{3+} exclusion mechanisms

2.6.1.1 Root cap or root border cells (RBC)

A protective role of root cap, in particular binding of Al^{3+} ions onto the mucilage material, has long been speculated (Horst *et al.*, 1982). However, in maize, removal of the root cap had no effect on the Al-induced inhibition of root growth (Ryan *et al.*, 1993). Therefore, contribution of root cap was discounted from subsequent Al^{3+} toxicity studies. Recently, the importance of root cap cells in Al tolerance have been recognised again through root border cells (RBC) (=living cells that surround root apices of most plant species). Indeed, presence of RBC increased Al tolerance in diverse plant species (Chen *et al.*, 2008; Li *et al.*, 2008; Tamas *et al.*, 2005; Yu *et al.*, 2009; Zhu *et al.*, 2003). Moreover, exposure of root tips that had RBC removed to Al^{3+} in a solid agar medium resulted in stronger fluorescence from Al-selective dye lumogallion compared with intact roots, suggesting that the presence of RBC reduced the amount of Al bound by root tips (Brigham *et al.*, 2001). Hence, maintenance of high RBC density may help plants to protect the root apex from Al toxicity.

2.6.1.2 Cell wall properties

The cation exchange capacity (CEC) of roots may influence the amount of Al binding on the cell wall (Horst, 1995). Thus, plants with relatively low CEC demonstrated enhanced Al tolerance (Blamey *et al.*, 1990; Büscher *et al.*, 1990; Kennedy *et al.*, 1986; Vose and Randall, 1962). This low-CEC-mediated Al tolerance was due to low Al concentration at the plasma membrane surface (Wehr *et al.*, 2003). By contrast, Kinraide (2004) suggested that the cell wall has a negligible effect on Al tolerance. Further, a lack of clear relationship between root CEC and Al tolerance was noticed across many plant species (Horst *et al.*, 2007; Ishikawa *et al.*, 2001), indicating CEC may not have a large and widespread impact on Al tolerance.

2.6.1.3 Phosphorus exudation

Phosphorus (Pi) efflux from roots has the potential to be an Al-resistance mechanism in plants because phosphate ions strongly bind with Al^{3+} ions to form non-toxic Al-phosphate complexes either in the apoplasm, on the root surface, or in the rhizosphere (cf. Taylor, 1991). Al-induced Pi efflux was observed in Al-tolerant sugar beet (Sylvia, 1990), wheat (Pellet *et al.*, 1996) and maize (Pellet *et al.*, 1995). Sylvia (1990) hypothesized that Al-resistant cultivar of sugar beet exuded Pi in a metabolically-dependent manner in the presence of Al^{3+}. In contrast, in wheat, constitutive Pi exudation was observed in Al-tolerant cultivar Atlas 66 (Pellet *et al.*, 1997). However, similar Pi exudation was not observed in another Al-tolerant wheat cultivar (ET3), suggesting Pi exudation may contribute to the multigenic Al tolerance of specific genotypes (Pellet *et al.*, 1996). In rice, low Pi exudation from both the Al-sensitive and Al-tolerant cultivars suggested Pi exudation may not be the main Al tolerance mechanism in rice (Chen and Shen, 2008).

Cell wall phosphate concentration is known to influence Al tolerance in some plants such as buckwheat, in which Al-tolerant cultivar accumulated more Al-bound phosphate in the cell wall compared with Al-sensitive cultivar. However, no difference was observed between these two cultivars in Pi exudation, oxalate exudation or rhizosphere pH (Zheng *et al.*, 2005).

2.6.1.4 Organic acid anion exudation

Among the Al exclusion mechanisms, the best-described one is the root exudation of low-molecular-weight organic acid anions in a range of plant species (Kochian *et al.*, 2004; Kochian *et al.*, 2005; Ryan *et al.*, 2001). In general, organic acid anions with a large number of carboxylate groups chelate Al particularly strongly (Kochian *et al.*, 2004). For example, tricarboxylate citrate^{3-} has a 6- to 8-fold greater capacity to chelate Al than bicarboxylate malate^{2-} (Ryan *et al.*, 2001). Organic acids decrease Al binding to the cell wall surface (Li *et al.*, 2009) and the phophatidylinosytol-4, 5-phosphate in the plasma membrane (Jones and Kochian, 1997), thereby reducing the aluminium toxicity. In addition, complexing of Al by malate increased the hydrolysis of pectates, which in turn enhanced cell wall loosening and cell expansion (Wehr *et al.*, 2003).

Depending on the plant species, Al activates exudation of various organic acid anions, like malate, citrate, oxalate, pyruvate and/or succinate (Kochian *et al.*, 2005; Larsen *et al.*, 1998; Ryan *et al.*, 2001), through organic-anion-permeable plasma membrane channels (Pineros and Kochian, 2001; Sasaki *et al.*, 2004; Zhang *et al.*, 2001). For example, malate is released through aluminium-activated malate transporters in wheat (*TaALMT1*) (Delhaize *et al.*, 2007; Sasaki *et al.*, 2006; Sasaki *et al.*, 2004), *Arabidopsis thaliana* (*AtALMT1*) (Hoekenga *et al.*, 2006) and *Secale cereale* (*ScALMT1*) (Collins *et al.*, 2008; Fontecha *et al.*, 2007). In maize, *ZmALMT1* is not involved in malate transport, but is involved in the specific Al-activated exudation of citrate (Piñeros *et al.*, 2008). Characterisation of *ALMT1* revealed that reversible phosphorylation is important in the transcriptional and post-transcriptional regulation of *ALMT1* (Kobayashi *et al.*, 2007). Citrate efflux occurs through multidrug and toxin efflux (MATE) transporters in *Arabidopsis thaliana* (*AtMATE*) (Liu *et al.*, 2009), wheat (Ryan *et al.*, 2009), barley (*HvMATE1*) (Furukawa *et al.*, 2007) and sorghum (*SbMATE*) (Magalhaes *et al.*, 2007). Some plant species can release more than one organic acid anion in response to Al^{3+} exposure. For example, *Arabidopsis* has been reported to release malate (Hoekenga *et al.*, 2006), citrate (Liu *et al.*, 2009), pyruvate and succinate (Larsen *et al.*, 1998).

Long-term efflux of organic acid anions requires continuous synthesis of organic acids inside the root cells (Basu *et al.*, 1994). Indeed, over-expression of

organic acid synthesising enzymes, viz. phospho*enol*pyruvate carboxylase (PEPC) in rice (Begum *et al.*, 2009; Osaki *et al.*, 2001), malate dehydrogenase in lucerne (Tesfaye *et al.*, 2001) and isocitrate dehydrogenase in *Pseudomonas fluorescens* (Middaugh *et al.*, 2005) conferred Al^{3+} tolerance by enhancing organic acid anion synthesis and release. In this context, shoots also appear to play a key role because removal of shoots reduced the efflux of organic acid anions. Hence, it is hypothesised that *de novo* synthesis of organic acid requires a continued supply of carbohydrates from shoots.

Organic acid anion exudation may occur immediately (classified as pattern I) or after a time delay (classified as pattern II) upon Al^{3+} exposure (Ma *et al.*, 2001; Pineros *et al.*, 2002). For example, wheat and buckwheat follow pattern I because the efflux of malate was detectable in wheat within 5 minutes (Osawa and Matsumoto, 2001) or 15 minutes (Delhaize *et al.*, 1993b; Ryan *et al.*, 1995a), and oxalate efflux was detectable within 30 minutes in buckwheat (Ma *et al.*, 1997c). In contrast, 4-h induction time was required to achieve maximum malate release in *Arabidopsis* (Kobayashi *et al.*, 2007) and citrate release in *Cassia tora* (Ma *et al.*, 1997b), whereas in rye citrate and malate efflux increased steadily during a 10-h period (Li *et al.*, 2000); these species follow pattern II. However in maize, both a rapid efflux as well as a delayed release of citrate (increased during a 48-h period) was observed (Pellet *et al.*, 1995; Pineros and Kochian, 2001).

In a study involving maize genotypes with a diverse genetic background, poor correlation between citrate exudation and Al tolerance was reported. In fact, one of the sensitive genotype exuded highest amount of citrate (Pineros *et al.*, 2005), indicating Al tolerance is quite complex, with more than one type of tolerance mechanisms operating in various plant species.

2.6.1.5 Exudation of other compounds

Phenolics are organic compounds containing one or more hydroxylated aromatic rings; they represent a broad range of compounds including alkaloids, flavonoids, terpenoids and glycosides (Kochian *et al.*, 2004). Exudation of phenolic compounds received attention in relation to Al tolerance due to their capacity to complex Al and also act as strong antioxidants in response to abiotic stresses (Matsumoto *et al.*, 1976a; Ofei-Manu *et al.*, 2001). A better correlation between differential Al tolerance in three

maize genotypes and the rate of Al-stimulated flavonoid (catechin and quercetin) exudation compared with Al-activated organic acid efflux suggested that exudation of phenolics may play a key role in the detoxification of Al in the rhizosphere (Kidd *et al.*, 2001).

Recently, two genes *STAR1* (sensitive to aluminium rhizotoxicity1) formerly known as *Al sensitive1 (als1*) (Ma *et al.*, 2005) and *STAR2* involved in Al tolerance were identified in rice, mostly expressed in the plasma membrane of root cells, except in the epidermal cells of the mature root zone. *STAR1* and *STAR2* form a STAR1-STAR2 complex that functions as an ABC transporter protein to exude UDP-Glc (Huang *et al.*, 2009), an activated form of glucose used as a substrate for glycosyltransferases to synthesize various glycosides (Ross *et al.*, 2001). It has been suggested that exuded UDP-glucose or glycoside derived from UDP-Glc modifies the cell walls by masking the sites for Al binding, resulting in Al tolerance in rice (Huang *et al.*, 2009).

2.6.2 Al tolerance mechanisms

2.6.2.1 Internal detoxification

Internal detoxification of Al can be achieved by formation of non-toxic complexes of Al with organic acids or other chelators; of these complexes can be either sequestered in vacuoles (Larsen *et al.*, 2007; Ma *et al.*, 1997a; Shen *et al.*, 2004b; Shen *et al.*, 2002) or transported away from the Al-sensitive sites (Larsen *et al.*, 2005). Aluminium induced an increase in organic acid concentration in maize roots (Pineros *et al.*, 2002). In addition, inhibition of root growth, deposition of Al-phosphate in the cell wall and accumulation of Al in the vacuole was observed after 4 hours of Al exposure in Al-tolerant maize cultivar (Vázquez, 2002). However, after 24 hours, root elongation was restored, Al was not detected in the cell wall, but increased Al concentration was measured in the vacuole. After 96 hours, Al precipitation was observed only in vacuoles and apoplasm (Vázquez, 2002). Similar observations were made in vacuolated protoplasts of *Chara corallina* after 60 minutes, but vacuolar sequestration was delayed up to 12-24 hours (Taylor *et al.*, 2000). These results suggest that plants may have the capacity to sequester Al as Al-organic acid complex in vacuoles in order to lower cytoplasmic Al concentrations. Indeed, *Arabidopsis ALS1*, a constitutively expressed

gene encoding a half-type ABC transporter protein, was located at the tonoplast. This transporter might be involved in compartmentation of chelated Al into the vacuoles (Larsen *et al.*, 2007). However, it should be borne in mind that no correlation between Al tolerance and internal concentration of organic acid was observed in some plant species (Hayes and Ma, 2003; Mariano and Keltjens, 2004; Pellet *et al.*, 1995; Wenzl *et al.*, 2002).

Even Al-hyperaccumulating plants, such as members of the *Melastomataceae* family and *Camelia* (tea) genus, must remove phytotoxic Al from the sensitive root cells, particularly from the transition root zone at the apex to maintain growth and development (Poschenrieder *et al.*, 2009). It has been hypothesised that a phloem-localised plasma membrane ABC transporter-like protein inducible by Al may remove the potentially toxic Al from sensitive parts of the root (Larsen *et al.*, 2005).

2.7 Characteristics of *Arabidopsis thaliana* mutants that could be important in deciphering Al tolerance mechanisms

2.7.1 Al-resistant *alr104* mutant

Genetic analysis of the Al-resistant mutant, *alr104*, showed that Al resistance was semi-dominant and mapped on chromosome 4 of *Arabidopsis* genome (Larsen *et al.*, 1998). The *alr104* accumulated lower levels of Al in the root tips compared with the wild type. However, it did not exhibit increased release of malate or citrate; instead, there was a 2-fold increase in net H^+ influx localised to the root apex upon Al exposure. This increased H^+ influx alkalinised the rhizosphere to a greater extent than in the wild type roots (Degenhardt *et al.*, 1998; Larsen *et al.*, 1998). Therefore, this mutant can be used to evaluate the potential importance of H^+ fluxes in Al tolerance mechanisms in plants.

2.7.2 Al-sensitive *als5* mutant

Al-sensitive *als5* is a semi-dominant mutant (Larsen *et al.*, 1997b). Staining with morin and hematoxylin dyes indicated that *als5* is defective in the Al-exclusion mechanism. Indeed, *als5* mutant accumulated more Al and callose than the wild type under Al^{3+} stress (Larsen *et al.*, 1996). Thus, *als5* mutant can be used to study Al^{3+} toxicity mechanisms when Al exclusion mechanism is defective.

2.7.3 Al-sensitive *als3* mutant

Al-sensitive loss-of-function mutant *als3* did not differ from the wild type in Al accumulation in the root apex (Larsen *et al.*, 1996). However, in the presence of sub-toxic Al^{3+} concentrations, root growth of *als3* mutant was severely inhibited, whereas the wild type root growth was unaffected. The growth of *als3* primary roots did not recover following rescue to the Al^{3+}-free medium, with severe disturbance of root tissue differentiation also observed. For example, root hair growth occurred at the point just proximal to the root tip. In addition to severe disturbance in root growth, exposure of *als3* mutants to Al^{3+} resulted in complete inhibition of leaf and rosette development and induced callose production in a leaf primordial. These effects were not observed in the wild type (Larsen *et al.*, 1997a; Larsen *et al.*, 1996), indicating *ALS3* is essential for both root and shoot growth under Al^{3+} stress.

Map-based cloning localised *als3-1* mutation to the bottom half of *Arabidopsis* chromosome 2, with substitution of a T for a C in the coding sequence of the gene *at2g37330* (Larsen *et al.*, 2005). Further, *ALS3* encodes an ABC (ATP-binding cassette) transporter-like protein involved in solute transport. Interestingly, closely related homologs of *ALS3* were found in lucerne, rice, maize and even in blue-green algae *Synechocystis sp*, suggesting that *ALS3*-mediated Al tolerance may be universally present in plants. Tissue localisation indicated that *ALS3* was expressed in the root epidermis, cortex and phloem of roots, leaves and flowers (Larsen *et al.*, 2005). Given that *ALS3* shared similarities with a putative bacterial metal-resistance protein (ybbM), it has been speculated that *ALS3* is involved in redistribution of accumulated Al away from Al-sensitive tissues in the form of an Al-organic acid complex, or some other yet-to-be-identified compound required to ameliorate the toxic effects of internalised Al (Larsen, 2009). Further characterisation of *ALS3* is essential for describing *ALS3*-dependent mechanism of Al tolerance.

2.8 Conclusions

Low-pH and Al^{3+} toxicity coexist in acid soils, affecting plant growth. Thus, Al^{3+} toxicity is always studied together with low-pH stress. Much progress has been made on understanding the combined low-pH/Al^{3+} toxicity and tolerance mechanisms

in plants. However, little is known about the low-pH toxicity and tolerance mechanisms in plants.

Al^{3+} toxicity mechanisms are complex and remain unclear. In general, Al^{3+} inhibits root growth by affecting cell division, cell elongation and plasma membrane properties; disturbing cytoskeleton, ion uptake and ion homeostasis; and inducing reactive oxygen species production. Plants also evolved sophisticated Al exclusion and internal Al detoxification mechanisms to cope with the Al-toxic environments. Among the Al tolerance mechanisms, exudation of organic acid anions received considerable attention, leading to the identification of novel genes involved in organic acid anion metabolism and transport. However, many unanswered questions remain, particularly perception of Al^{3+} signal by roots and transduction of this signal to activate specific organic acid anion transport is unknown. In this context, Mg^{2+} is critical for activation of many enzymes involved in the organic acid synthesis and metabolism. However, there is no information available on the dynamics of Mg^{2+} uptake and intracellular homeostasis upon Al^{3+} exposure.

Over many years, experimentation with different species, genotypes and experimental conditions may have led to sometimes confusing information on Al^{3+} toxicity mechanisms. On the other side, large interest in exudation of organic acid anions may have contributed to insufficient knowledge about other potential Al tolerance mechanisms (e.g. reduced cell wall binding, rhizosphere alkalisation, phosphate exudation, internal detoxification) that may be operating. Thus, *Arabidopsis thaliana* mutants differing in Al sensitivity, such as Al-tolerant mutant, *alr104*, which has higher rhizosphere alkalinising capacity, and two Al-sensitive mutants (*als3*, which is defective in redistribution of accumulated Al away from Al-sensitive tissues, and *als5*, which is defective in Al exclusion mechanism) were used in this dissertation together with the wild type (Col-0) to characterise multiple low-pH and Al toxicity and tolerance mechanisms. The low-pH effects were separated from combined low-pH/Al^{3+} effects to establish stress-specific responses of *Arabidopsis thaliana*.

Chapter 3

General Materials and Methods

3.1 Experimental solutions

Aluminium undergoes complex speciation in solution in dependence of pH and various ligands (Kinraide and Parker, 1987). To maintain most of Al in the Al^{3+} form, Al stock solution was prepared in acidified milliQ water (pH ≈4.5). Any further adjustment of pH was done with 0.1 mM HCl.

For long-term experiments, $1/10^{th}$ Hoagland solution, pH 5.5, was used as a basic growth medium (**Table 3.1**). In case of short-term experiments, basic salt medium (BSM) consisting of 0.1 mM $CaCl_2$, 1.0 mM KCl and 0.2 mM $MgCl_2$ (pH 5.5) was used.

Table 3.1 Preparation of $1/10^{th}$ Hoagland solution (values in the paranthesis of final column indicates the concentrations of respective nutrients in $1/10^{th}$ Hoagland solution).

Sl.No	Salt	Molecular Wt. (g)	Stock Solution (g L^{-1})	Stock Solution Conc.	Original Hoagland Conc.	$1/10^{th}$ Hoagland Solution (mL stock soln. L^{-1})
1.	KH_2PO_4	136.09	68.045	0.5 M	0.001 M	0.2 (100 µM)
2.	KNO_3	101.10	50.550	0.5 M	0.005 M	1.0 (500 µM)
3.	$Ca(NO_3)_2.4H_2O$	236.15	118.075	0.5 M	0.005 M	1.0 (500 µM)
4.	$MgSO_4.7H_2O$	246.47	123.235	0.5 M	0.002 M	0.4 (200 µM)
5.	EDTA-Na_2	372.24	7.45	0.5% w/v	0.0005% w/v	0.1
	$FeSO_4.7H_2O$	278.01	5.57			
6.	H_3BO_3	61.83	2.86			0.1
	$MnCl_2.2H_2O$	197.92	1.81			
	$ZnCl_2$	136.28	0.11			
	$CuCl_2.2H_2O$	170.48	0.05			
	$Na_2MoO_4.2H_2O$	241.96	0.025			

3.2 Plant material

Seeds of *Arabidopsis thaliana* L. [Heynh] wild type (ecotype Col-0) and mutants *als3*, *als5* and *r104* in Columbia background were obtained from the Arabidopsis Biological Resource Center (ABRC, The Ohio State University, Columbus, USA).

3.3 Non-invasive microelectrode ion flux estimation (MIFE^{TM})

3.3.1 MIFE theory

MIFE measurements were made as per the principles and methods explained by Newman (2001). Here, only the synopsis is given. The flux measurements of an ion of interest was made at two positions (M_1 = x and M_2 = x + Δx) based on the principle that living cells acquire and release ions from the surrounding solutions and consequently ionic concentration gradients form; if concentration close to the surface is lower than far away position, the net movement of an ion is influx (uptake) and *vice versa* (**Figure 3.1**). Implied assumptions are (i) convection and water uptake are negligibly small, (ii) and unstirred layer conditions are met so that the concentration gradients observed in solution are simply explained by basic diffusion.

The ion diffusion pattern is strongly influenced by geometry of organs/tissues, necessitating different formulae to calculate fluxes. In the case of simplest (plannar) diffusion, the following equation is used:

$$J = c\ u\ z\ F\ g\ (\Delta V/\Delta x)$$

where J= ion flux (mol m^{-2} s^{-1}); c= ion concentration (mol m^{-3}); u = ion mobility (m s^{-1} per Newton mol^{-1}); z = ion valence; F = Faraday number (96500 C mol^{-1}); g = factor found from the measured Nernst slope for the electrode during calibration; ΔV = voltage difference measured by an electrometer between the two positions (V); Δx = distance between the two positions (m).

In my experiments *Arabidopsis* root ion fluxes were measured. Hence, the radius of roots (r) was taken into account (cylindrical geometry). This was done by replacing Δx in the equation above with

$$\Delta x = r^2 [1/ (r + x) - 1/ (r + x+\Delta x)]$$

The 5-s cycle was followed in each position. For calculation, the first two cycles were removed as described by Shabala et al. (1997).

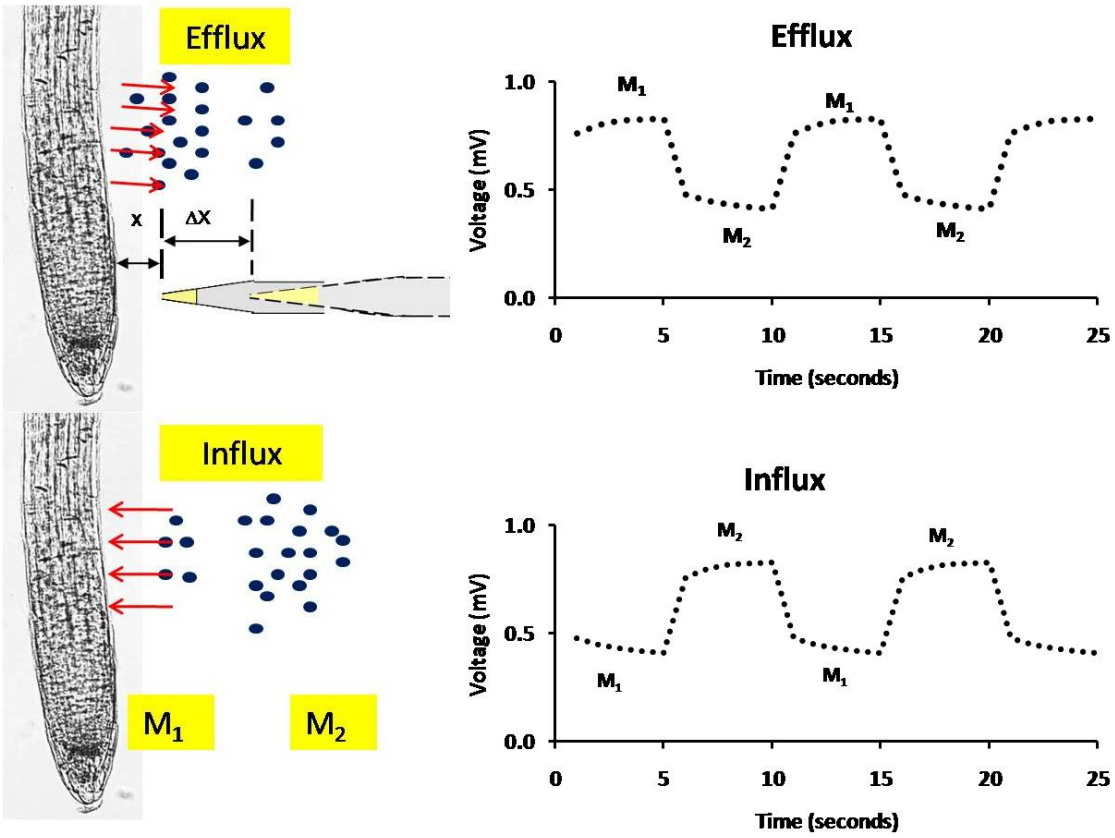

Figure 3.1 Principles of MIFE measurements. The left pane shows the microelectrode positions during measurement; the right pane shows CHART software view of fluxes on the PC-monitor. The top part of the diagram illustrates efflux, and the lower part influx.

In the MIFE system, the DOS-operated software CHART (University of Tasmania, Hobart, Australia) in combination with an analogue-to-digital interface card (DAS08) was used (i) to control data acquisition and write data on the disk, (ii) to automate interactive real-time control of the amplifier configuration and the micromanipulator. The CHART software was also used to calculate an average manipulator (.avm) file. Flux calculation was performed using MFLUX software (University of Tasmania, Hobart, Australia) from the data and log files.

3.3.2 Microelectrode fabrication

Microelectrode blanks were pulled from 1.5-mm outer diameter (OD), 0.86 mm internal diameter (ID) borosilicate glass capillaries (GC 150-10, SDR Clinical Technology, Middle Cove, Australia) by using program 2 [H(eat)=930; P(ull)=100; S =255] of a Sachs-flaming micropipette puller PC-84 (Sutter Instrument Company) to make the final tip diameter < 1 µm. Prepared microelectrode blanks were oven-dried at 225^{o}C over night (or at least for 4 hours); then the container containing electrodes was covered with a steel lid. After 10-15 minutes, 10-50 µL of silanising agent (tributylchlorosilane, Catalogue # 90796, Fluka Chemicals, Busch, Switzerland) was injected under the lid. Ten minutes later the lid was removed, and oven-drying continued for another 30 minutes at 225^{o}C to ensure complete drying. Silanisation is done to make the electrodes hydrophobic so that the liquid ion exchanger (LIX) can be drawn into the tip by capillarity.

The blank electrode base was heated in the flame to make it blunt. A microelectrode was then fixed horizontally under a stereo microscope. The microelectrode tip was broken back to a 2-3 µm diameter (**Figure 3.2**) by adjusting the 3-D micromanipulator.

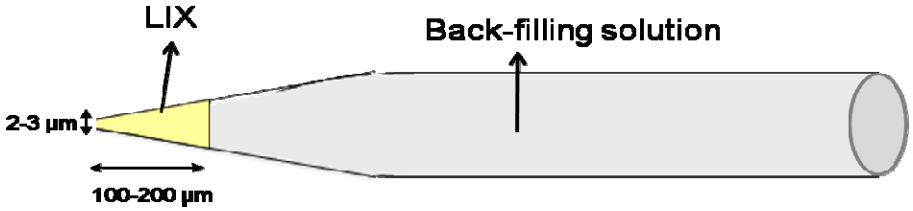

Figure 3.2 Microelectrode filled with liquid ion exchanger (LIX) and back-filling solution

After breaking the microelectrode tip, microelectrode was back-filled with an appropriate back-filling solution (**Table 3.2**) using a syringe with a thin needle. Any air bubble formation inside the capillary was avoided; if it occurred, it was removed by gentle tapping with fingers. Immediately after back-filling, the microelectrode tip was front-filled with the ion-specific LIX by moving the LIX-filling capillary (1.0 mm OD, 0.58 ID pulled as described above and dipped into a stock container of LIX so that it drew a 1-mm column into the electrode tip) mounted on the 3-D micromanipulator to just touch the microelectrode until the column of appropriate LIX (**Table 3.2**) in the

microelectrode was 100-200 μm long (**Figure 3.2**). Microelectrodes were then placed in BSM for at least 30 min (conditioning time) to ensure a stable response during MIFE measurements.

Table 3.2 Ion-specific liquid ion exchanger (LIX) and the back-filling solutions used for preparation of ion-selective microelectrodes

Ion	Liquid ionophore (LIX)	Back-filling solution
Mg^{2+}	Magnesium ionophore I-Cocktail A - Fluka # 63048	500 mM $MgCl_2$
Ca^{2+}	Calcium ionophore I-Cocktail A - Fluka # 21048	500 mM $CaCl_2$
K^+	Potassium ionophore I-Cocktail A - Fluka # 60031	500 mM KCl
H^+	Hydrogen ionophore II-Cocktail A - Fluka # 95297	15 mM NaCl, 40 mM KH_2PO_4 (pH adj. to 6.0 with NaOH)

3.3.3 Reference electrode

Blank electrodes with a relatively wide tip (>100 μm) filled with 100 mM KCl in 2 % w/v agar solution were used as reference electrodes.

3.3.4 Calibration

All the ion-specific microelectrodes were calibrated against a set of three standards covering the expected concentration range of the relevant ion (**Table 3.3**) before and after measurements. Electrodes with calibrated Nernst slopes < 50 mV per decade for monovalent cations and < 25 mV per decade for divalent cations, or with the correlation co-efficient < 0.999 were discarded from measurements.

The ionic strength of solutions affects the calculated intercept of ion-selective microelectrodes in the calibration file. Hence, K^+, Ca^{2+} and Mg^{2+} electrodes were calibrated in the presence of other ions. For example, Ca^{2+} electrodes were calibrated with 0.1, 0.5 and 1.0 mM $CaCl_2$ standards with the background of 0.2 mM $MgCl_2$ + 1.0 mM KCl.

Table 3.3 Ions of interest and calibration standards

Ion	Concentrations of standards for calibration
Mg^{2+}	0.2, 1.0 and 2.0 mM $MgCl_2$ in 0.1 mM $CaCl_2$ + 1.0 mM KCl background
Ca^{2+}	0.1, 0.5 and 1.0 mM $CaCl_2$ in 0.2 mM $MgCl_2$ + 1.0 mM KCl background
K^+	1, 5 and 10 mM KCl in 0.1 mM $CaCl_2$ + 0.2 mM $MgCl_2$ background
H^+	buffers with pH 3.2, 5.0 and 6.0

3.3.5 Setting up vibrating microelectrodes in MIFE system

The ion-selective microelectrodes were fixed on a MMT-5 multi-manipulator (Narishige, Tokyo, Japan) to provide 3-D positioning. Three electrodes were positioned in a line parallel to the root axis 40 µm away from the root surface and with 12-18 µm between electrode tips (**Figure 3.3**). During measurements, the distance between the root surface and microelectrodes was alternating from 40 to 80 µm at the frequency of 0.1 Hz. This was achieved by fixing the microelectrode holders on a three-way hydraulic micromanipulator (WR-88, Narishige, Tokyo, Japan) driven by a computer-controlled stepper motor (MO61-CE08, Superior Electric, Bristol, CT).

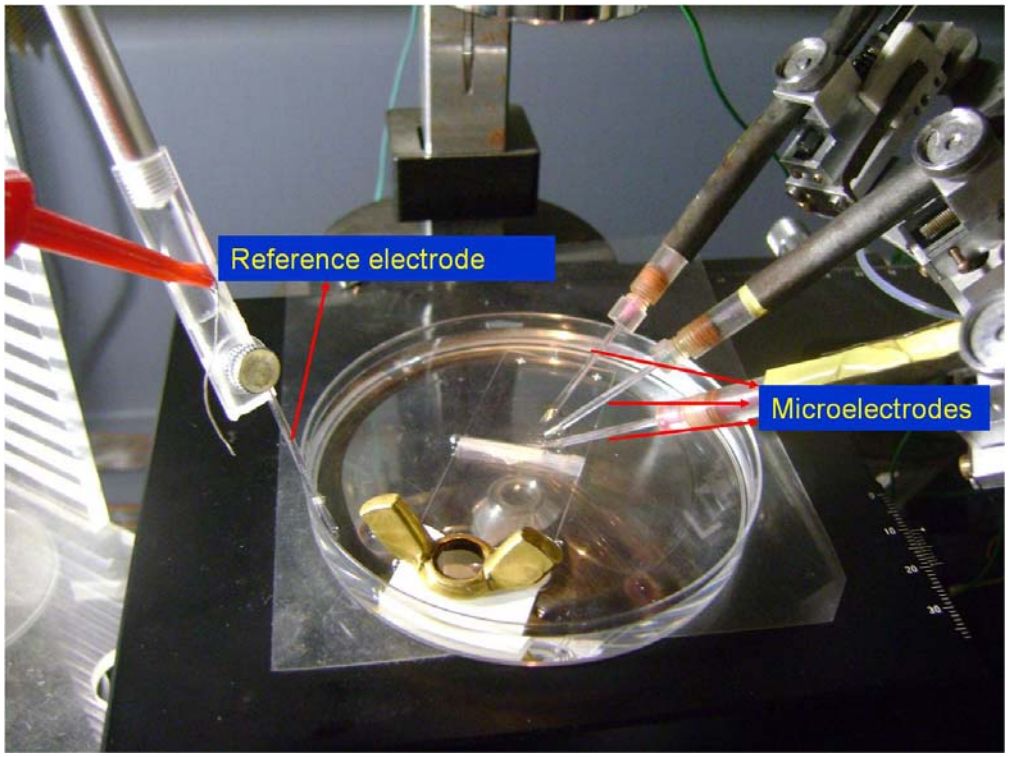

Figure 3.3 Alignment of microelectrodes in the MIFE system

3.4 Fluorescence lifetime imaging (FLIM)

3.4.1 FLIM theory

FLIM works on the principle that the fluorescence light emitted by organic molecules (chromophores) does not only depend on its emission intensity and emission spectrum, but it also has a specific lifetime. The fluorescence lifetime is an inherent characteristic of a chromophore, and thus is independent of chromophore concentration, photobleaching and excitation intensity; however, it depends on the external

environment (e.g., pH and ion concentrations). The fluorescence lifetime was successfully used to measure cell parameters such as pH, ion concentrations or oxygen saturation (Lakowicz and Szmacinski, 1993) and was used for investigating protein or DNA structures by lifetime-sensitive dyes (Knemeyer *et al.*, 2000). This makes FLIM a useful and powerful tool for quantitative imaging at the cellular level (Day, 2005; Day and Schaufele, 2005; Lichtman and Conchello, 2005).

3.5 Statistical analysis

For the different treatments, significant differences between means were assessed by *t*-test and ANOVA using Genstat (10^{th} edition) (VSN International Ltd, Hemel Hempstead, UK).

Chapter 4

Aluminium-dependent dynamics of ion transport in Arabidopsis: Specificity of low pH and aluminium responses

Jayakumar Bose[1], Olga Babourina[1], Sergey Shabala[2] and Zed Rengel[1]

[1]School of Earth and Environment, the University of Western Australia, Crawley WA 6009, Australia

[2]School of Agricultural Science, University of Tasmania, Hobart TAS 7001, Australia

Abstract

Low-pH and Al^{3+} stresses are the major causes of poor plant growth in acidic soils. However, there is still a poor understanding of plant responses to low-pH and Al^{3+} toxicity. Low-pH or combined low-pH and Al^{3+} stress was imposed in order to measure rhizosphere pH, ion fluxes, plasma membrane potential and intracellular H^+ concentration in distal elongation and mature zones along the longitudinal axis of *Arabidopsis thaliana* roots. Low-pH stress facilitated H^+ influx into root tissues and caused cytoplasmic acidification; by contrast, combined low-pH/Al^{3+} treatment either decreased H^+ influx in the distal elongation zone or induced H^+ efflux in the mature zone, leading to cytoplasmic alkalinisation in both zones. Low-pH stress induced an increase in rhizosphere pH in the distal elongation zone, whereas combined low-pH/Al^{3+} stress resulted in lower rhizosphere pH in both root zones compared to the low-pH treatment alone. Low-pH stress facilitated K^+ efflux; the presence of Al^{3+} diminished K^+ efflux or favoured K^+ influx into root tissues. In both zones, low-pH treatment induced plasma membrane depolarisation, which was significantly diminished ($P \leq 0.05$) when combined stresses (low-pH/100 μM Al^{3+}) were imposed. After 60 min of exposure, low pH caused plasma membrane depolarisation, while low pH/100 μM Al^{3+} caused plasma membrane hyperpolarisation. Thus, low pH and Al^{3+} toxicity

differentially affect root tissues and, consequently, the rhizosphere, which might underpin the differential mechanisms of plant adaptation to these abiotic stresses.

Key words: acidity, aluminium toxicity, *Arabidopsis*, distal root elongation zone, H^+ flux, intracellular H^+, K^+ flux, mature root zone, plasma membrane potential

4.1 Introduction

Soil acidity is the major growth-limiting factor for more than 40% of the world's arable land (von Uexkull and Mutert, 1995) In acidic soils, crop plant growth may be limited by various toxicities (H^+, Al^{3+}, Mn^{2+}) and deficiencies (NH_4^+-N, P, Ca^{2+}, Mg^{2+} and MoO_4^{2-}) (for references, see Kidd and Proctor, 2001). Among these complex factors, Al^{3+} and H^+ toxicities are highly correlated with poor plant growth (Rangel *et al.*, 2005). Hence, it is imperative to understand H^+ and Al^{3+} toxicity mechanisms in plants in order to breed genotypes that are more tolerant of these two stresses in acidic soils.

Phytotoxic Al^{3+} is the dominant Al ion when soil pH is below 4.5 (Kochian, 1995). The obvious early symptom of Al^{3+} toxicity is inhibition of root growth, although there is growing evidence suggesting that low pH alone can inhibit root growth in many species, such as lettuce, tomato, Bermuda grass (Arnon and Johnson, 1942), spinach(Yang *et al.*, 2005), grass *Holcus lanathus* L., tree *Betula pendula* Roth (Kidd and Proctor, 2001), common bean (Rangel *et al.*, 2005) and *Arabidopsis* (Koyama *et al.*, 2001). Hence, it is necessary to evaluate the effects of low pH separately from the combination of low pH and Al^{3+} to better understand Al^{3+} toxicity. However, these kinds of experiments are relatively rare (Lazof and Holland, 1999; Samac and Tesfaye, 2003; Vitorello *et al.*, 2005), despite an impressive number of studies investigating Al^{3+} toxicity.

Roots have five distinct zones along the longitudinal axis: root cap, meristem (zone of active cell division), distal elongation zone (DEZ) or transition zone (zone of slow cell growth in length and width), elongation zone (zone of rapid cell growth in length without growth in width) and mature zone (MZ, zone of root hairs). These zones differ distinctly in anatomy, growth pattern and presumably in plant signalling in response to environmental stimuli (Verbelen *et al.*, 2006). It is commonly accepted that

the distal elongation zone is the target site of Al^{3+} toxicity (Illes *et al.*, 2006; Sivaguru and Horst, 1998), even though some results have shown that Al^{3+} affects physiological and biochemical processes in other regions, such as the root cap, meristem, elongation zone and mature zone (Brady *et al.*, 1993; Olivetti *et al.*, 1995; Rengel, 1996).

The mature root zone represents the principal area for nutrient absorption (Bibikova and Gilroy, 2002; Gahoonia and Nielsen, 1998; Parker *et al.*, 2000). For example, Ahn *et al*. (2004b) found that 10 out of 15 K^+ transporters (*KT/KUPs*) were expressed in the mature zone. Hence, it is worthwhile to examine the mature root zone to shed light on nutrient acquisition under low-pH and Al^{3+} stresses.

The initial plant response to low-pH and Al^{3+} stresses is likely to occur at the plasma membrane (PM), because the PM acts as a diffusion barrier for transport processes in order to protect the cell interior (Ahn and Matsumoto, 2006). Low-pH activates rapid H^+ influx into the root tissue (Shabala *et al.*, 1997), thereby depolarising the PM potential (E_m) (Babourina *et al.*, 2001). Al^{3+} may affect the E_m by (i) binding to the PM to alter its fluidity and structure (Chen *et al.*, 1991) and surface potential (Kinraide, 2001), (ii) inducing organic anion release (Osawa and Matsumoto, 2002; Ryan *et al.*, 2001), (iii) blocking Ca^{2+} transport (Ding *et al.*, 1993a; Pineros and Tester, 1993), (iv) inhibiting H^+-ATPase activity (Ahn *et al.*, 2002) and (v) modifying K^+ transport activity (Wherrett *et al.*, 2005). However, there is a great deal of controversy in the literature about whether Al^{3+} stress depolarises (Olivetti *et al.*, 1995; Papernik and Kochian, 1997; Sivaguru *et al.*, 1999; 2003; 2005; Takabatake and Shimmen, 1997) or hyperpolarises E_m (Johnson *et al.*, 2005; Kinraide, 1993; Lindberg and Strid, 1997). To a large extent, this controversy may be explained by the differential effects of low-pH and combined low-pH/Al^{3+} stresses on the activities of H^+ and K^+ transporters as major contributors to E_m.

Changes in E_m directly influence K^+ transport across the PM, as the majority of K^+ channels are voltage-dependent (Krol and Trebacz, 2000). K^+ is essential for (i) cell division through actin polymerisation (Alberts *et al.*, 1994) and (ii) turgor-dependent cell elongation caused by the vacuolar accumulation of K^+ (Frensch, 1997). Both low-pH and Al^{3+} toxicity can affect K^+ flux (Babourina *et al.*, 2001; 2005); however, controversy exists regarding the extent of the effects of Al^{3+} on K^+ flux. Some studies

suggest that Al^{3+} induces K^+ efflux or reduces K^+ uptake (Gassmann and Schroeder, 1994; Liu and Luan, 2001) to balance the charge created by the exudation of organic acid anions (Ma *et al.*, 2001; Matsumoto, 2000; Osawa and Matsumoto, 2002). However, other studies have reported an Al^{3+}-induced decrease in net K^+ efflux, caused by either reducing the conductance of outward-rectifying channels (Horst *et al.*, 1992; Olivetti *et al.*, 1995; Sasaki *et al.*, 1995) or promoting K^+ influx into the root tissue (Tanoi *et al.*, 2005). The reasons for such controversy remain obscure.

The present study used wild type *Arabidopsis thaliana* to test two hypotheses. First, low-pH and combined low-pH/Al^{3+} effects on ion fluxes and plasma membrane potential may be different. Second, the distal elongation zone and the mature zone of *Arabidopsis* roots, being different in anatomy, growth pattern and function, may differ in their responses to low-pH and combined low-pH/Al^{3+} stresses.

4.2 Materials and methods

4.2.1 Short-term experiments

4.2.1.1 Agar culture

Wild type *Arabidopsis thaliana* L. (ecotype Col-0) seeds were surface sterilised with 1% (w/v) calcium hypochlorite, and seedlings were grown in 90-mm Petri dishes under constant fluorescent light (150 µmol $m^{-2}s^{-1}$) and temperature (23-25^oC) in 0.8% (w/w) agar media containing basal salt medium (BSM; 0.1 mM $CaCl_2$ + 1 mM KCl + 0.2 mM $MgCl_2$, pH 5.5). The Petri dishes were oriented upright, allowing the roots to grow down along the agar surface without penetrating it. However, the roots were anchored in the agar by root hairs. Four-to-five-day-old seedlings were used for all short-term experiments.

4.2.1.2 Measurement of rhizosphere pH, H^+ and K^+ fluxes using MIFE®

Net fluxes of H^+, K^+ and rhizosphere pH were measured 40 µm away from the distal elongation zone and mature root zone surfaces using the non-invasive MIFE® system (University of Tasmania, Hobart, Australia) as described by Newman (2001). Microelectrodes were pulled from borosilicate glass capillaries (GC 150-10, SDR Clinical Technology, Middle Cove, Australia), oven dried at 230ºC for approximately 5

h and silanised using tributylchlorosilane (Fluka, catalogue no. 90796). Electrodes were broken back to obtain external tip diameters of 2-3 μm. The electrodes were back-filled with appropriate solutions (0.15 mM NaCl + 0.4 mM KH_2PO_4, adjusted to pH 6.0 using NaOH for the H^+ electrode and 0.5 M KCl for the K^+ electrode). The electrode tips were then front-filled with ionophore cocktails (Fluka, catalogue no. 95297 for H^+ and 60031 for K^+). Prepared electrodes were calibrated in a set of standards (pH from 3.2 to 6.5; K^+ from 0.5 to 10 mM). Electrodes with slope responses of less than 50 mV per decade were discarded.

In the first set of experiments, 4-to-5-day-old seedlings were conditioned in BSM (pH 5.5) for 20 minutes, and ion fluxes were measured along the root axis, concentrating on the following zones: root cap (0-30 μm from the root tip), meristem (30-180 μm), distal elongation zone (180-240 μm), proximal elongation zone (240-480 μm) and mature zone (>680 μm). Given the transparency of *Arabidopsis* roots, root zones were delineated using a 100x magnifying lens attached to the MIFE system (**Figure 4.1**).

In the second set of experiments, 4-to-5-day-old seedlings were conditioned in BSM for 20 minutes followed by either low-pH stress (pH 4.2) or combined low-pH/Al^{3+} stress (50, 100 or 500 μM Al^{3+}, pH 4.2) in the BSM bathing solution; fluxes were measured for 60 minutes. In the third set of experiments, combined low-pH/Al^{3+} stress (0, 10, 25, 50, 75 or 100 μM Al^{3+}, pH 4.2) was sequentially introduced into the bathing solution (starting from the lowest Al^{3+} concentration and proceeding to higher concentrations every 15 minutes) after the first 15 minutes at the control pH (5.5). In the second and third sets of experiments, measurements were made at the distal elongation zone (DEZ; 200 μm from the root tip) and the mature zone (MZ; 700 μm from the root tip) (**Figure 4.1**).

4.2.1.3 Intracellular pH measurements

The pH-sensitive fluorescent dye 2',7'-bis-(2-carboxyethyl)-5-(and-6)-carboxyfluorescein acetoxymethyl ester (BCECF-AM, Molecular Probes, Eugene, OR, USA) was dissolved in dimethyl sulphoxide (DMSO) (Sigma, Castle Hill, Australia) and diluted with a loading solution (0.2 mM $CaCl_2$ and 50 mM mannitol, pH 4.2) to a final concentration of 20 μM. The final concentration of DMSO in the loading solution

was 1% (v/v). The dye was loaded into intact *Arabidopsis* roots for one hour; seedlings were then allowed to recover in BSM for 30 minutes.

In vitro and *in vivo* calibrations for different pH ranges were performed with BCECF potassium salt dissolved in different buffers and an inverted-stage confocal microscope (Leica TCS SP2 AOBS, Leica Microsystems GmbH, Wetzlar, Germany) as described by Nakabayashi *et al.* (2007). Light pulses were generated at a frequency of 80 MHz with a Mai Tai Laser (Spectra Physics, Mountain View, CA, USA). In preliminary experiments, an emission wavelength of 940 nm was found to minimise the contribution from autofluorescence (data not shown). Carbonyl cyanide *m*-chlorophenylhydrazone (CCCP) was used as a protonophore to eliminate the gradient between external and internal H^+ concentrations. Median lifetime, assuming a single exponential decay for BCECF, was used in calibrations (Babourina and Rengel, 2009).

After dye loading and BSM conditioning, seedlings were exposed to low-pH stress (pH 4.2) or 100 µM Al^{3+} (pH 4.2) for 30 minutes. Fluorescence Lifetime IMages (FLIM) of each seedling were collected for 5 min using photomultipliers, and FLIM analysis was performed using electronics (SPC-730; Becker & Hickl, Berlin, Germany) and software (SPC7.22; Becker & Hickl) for time-correlated single-photon counting. The intracellular pH was calculated for all cells (cortex and epidermal) of DEZ and MZ regions according to calibration curves using data analysis software for fluorescence lifetime imaging microscopy systems (SPCImage Version 2.6, MP-FLIM and D-FLIM).

4.2.1.4 Membrane potential (E_m) measurements

The roots of an intact 4-to-5-day-old *Arabidopsis* seedling were gently secured in a measuring chamber in a horizontal position with a Parafilm strip and small plastic blocks. The seedling was then placed in the measuring chamber containing BSM and conditioned for at least 30 minutes.

E_m measurements were conducted according to the procedure outlined by Cuin and Shabala (2005). Borosilicate glass microelectrodes (Shabala and Lew, 2002) (Clarke Electrochemical Instruments, Reading, UK) were filled with 1 M KCl, connected to an IE-251 electrometer (Warner Instruments, Hampden, CT, USA) via an Ag-AgCl half-cell and impaled into the root tissue (DEZ or MZ) with a manually-

operated micromanipulator (MMT-5, Narishige, Tokyo, Japan). E_m was monitored continually using CHART software (for details, see Newman, 2001). Once a stable E_m measurement was obtained for one minute, either low-pH stress (pH 4.2) or combined low-pH/Al^{3+} stress (50 or 100 µM Al^{3+}, pH 4.2) was imposed. E_m measurements were made for approximately 30 minutes. Between eight and twelve plants were measured for every treatment, and the data were averaged.

4.2.2 Long-term experiment

4.2.2.1 Hydroponic culture

Seeds of wild type *Arabidopsis thaliana* L. (ecotype Col-0) were surface sterilised with 1% v/v calcium hypochlorite for 10 minutes and sown on rock-wool strips (1-2 mm thick and 50-60 mm long) in contact with 1/10 Hoagland solution in 250-mL plastic containers kept at 4°C for 2 d to achieve synchronised germination. Seedlings were moved to a growth cabinet with a cycle of 16 h light (150 µmol m^{-2} s^{-1}) and 8 h dark at 20 ±1°C. The nutrient solution was changed daily. After 3 weeks, treatments were imposed in 1/10 Hoagland solution with 0.5 mM homo PIPES buffer (preliminary experiments showed that 0.5 mM buffer was sufficient to maintain desired pH levels for 24 h) for 7 d. Treatments were pH 5.5 with no Al^{3+} or the following range of Al^{3+} concentrations as $AlCl_3$ at pH 4.2: 0, 10, 25, 50, 75, 100 or 250 µM. Solutions were changed daily.

4.2.2.2 Biomass and K^+ concentration measurements

At the end of the experiment, plants were harvested, washed with 100 µM $CaSO_4$, dried in an oven at 70°C for 72 hours and weighed. Shoots and roots were separated, and dried shoots were digested with an HNO_3:$HClO_4$ (10:1) mixture and analysed using inductively-coupled plasma-mass spectrometry (ICP-MS). The experiment was repeated at least two times.

4.2.3 Statistical analysis

For the different treatments, significant differences between means were assessed by *t*-test and ANOVA using Genstat (10th edition) (VSN International Ltd, Hemel Hempstead, UK).

4.3 Results

4.3.1 H^+ and K^+ fluxes along the longitudinal root axis of Arabidopsis at pH 5.5

H^+ and K^+ fluxes were measured along the longitudinal root axis at the root cap, meristem, distal elongation zone, proximal elongation zone and mature zone (**Figure 4.2**). The highest H^+ influx was observed at the distal elongation zone, which is typical for H^+ fluxes along the longitudinal axis at pH less than 5.5 (for references, see Newman, 2001). The highest K^+ efflux was at the meristem zone. The mature zone, with small H^+ efflux and small K^+ influx, was different from the other root zones.

4.3.2 Effect of low pH and combined low pH/Al^{3+} stresses on rhizosphere pH and H^+ and K^+ fluxes

Rhizosphere pH and H^+ and K^+ fluxes were measured at two positions (distal elongation zone and mature zone). Under no stress conditions (pH 5.5), there was net H^+ influx at the distal elongation zone and small net H^+ efflux at the mature zone (**Figure 4.3**, **Figure 4.4**). When low-pH stress was imposed, a net H^+ influx was induced in both distal elongation and mature zones (**Figure 4.3**, **Figure 4.4**). The observed H^+ influx was higher in the distal elongation zone than in the mature zone. Low-pH/Al^{3+} treatments decreased H^+ influx in a dose-dependent manner in the distal elongation zone and induced H^+ efflux during the first 20 min of the 500-µM low-pH/Al^{3+} treatment (**Figure 4.3**A). In the mature zone, all low-pH/Al^{3+} treatments induced H^+ efflux for the first 15 minutes of Al^{3+} exposure in a dose-dependent manner (**Figure 4.4**A). This Al^{3+}-induced net H^+ efflux was decreased after 20 minutes in a low-pH/100-µM Al^{3+} treatment (**Figure 4.4**A).

The difference between H^+ fluxes under low-pH (H^+ influx) and combined low-pH/Al^{3+} stresses (inhibition of H^+ influx in the distal elongation zone and H^+ efflux in the mature zone) was reflected in the rhizosphere pH. In both root zones, low-pH stress induced higher rhizosphere pH than the combined low-pH/Al^{3+} stress (**Figure 4.5**). Low pH induced a net efflux of K^+ ions from the distal elongation zone but not from the mature zone (**Figure 4.6**, **Figure 4.7**). The low-pH-induced K^+ efflux was observed for the duration of the experiment in the distal elongation zone (**Figure 4.6**A). The 50-µM

low-pH/Al^{3+} treatment induced higher K^+ efflux than the low-pH treatment during the first 16 minutes. The low pH/100-µM Al^{3+} treatment induced K^+ efflux during the first 20 minutes, converting to K^+ influx after that time (**Figure 4.6**A) in the distal elongation zone. In the mature zone, low-pH and low-pH/50-µM Al^{3+} treatments induced similar K^+ efflux, but the low-pH/100-µM Al^{3+} treatment induced K^+ influx within a minute of addition (**Figure 4.7**A).

4.3.3 H^+ and K^+ fluxes under sequentially increasing Al^{3+} concentrations

Increasing Al^{3+} treatments (10, 25, 50, 75 and 100 µM, pH 4.2) were gradually introduced after 15 minutes of low pH stress. In the distal elongation zone, low-pH/Al^{3+} treatments decreased H^+ influx (**Figure 4.3**B). In the mature zone, low-pH/Al^{3+} treatments (≥25 µM Al^{3+}) induced H^+ efflux, with 50 µM Al^{3+} treatment inducing the highest H^+ efflux (**Figure 4.4**B). Likewise, a gradual increase in low-pH/Al^{3+} concentration (≥25 µM) decreased K^+ efflux compared to low-pH treatment alone in both zones (**Figure 4.6**B, **Figure 4.7**B).

4.3.4 Effect of low-pH and Al^{3+} stresses on intracellular pH

We measured the intracellular pH of *Arabidopsis thaliana* intact root cells at the distal elongation zone and the mature zone (**Figure 4.8**). After 30 minutes of stress treatment, the low-pH treatment showed an acidification trend, whereas the combined low-pH/Al^{3+} stress significantly alkalinised the intracellular compartments in both root zones compared to control conditions (pH 5.5). The decrease in intracellular pH caused by the low-pH treatment was more pronounced in the distal elongation zone than in the mature zone (**Figure 4.8**).

4.3.5 Effect of low-pH and Al^{3+} stresses on E_m

The resting E_m under no-stress conditions (pH 5.5) was -101 ±2 mV in the distal elongation zone and -110 ±2 mV in the mature zone (**Figure 4.9**). When low-pH stress was introduced, the E_m was depolarised to -51 ±3 mV in the distal elongation zone and -70 ±2 mV in the mature zone within 4 minutes (**Figure 4.9**). Al^{3+} stress depolarised E_m less than the low-pH treatment after 7 minutes at 100 µM Al^{3+} and 25 min at 50 µM Al^{3+} in the distal elongation zone. Membrane potential measurements after 60 minutes

of stress exposure revealed that low-pH/Al^{3+} at either 50 or 100 μM Al^{3+} caused hyperpolarisation beyond the resting potential, while low pH maintained depolarisation in the distal elongation zone (**Figure 4.9**A). In the mature zone, 100 μM Al^{3+} treatment depolarised E_m less than the low-pH treatment after 8 minutes. However, 50 μM Al^{3+} and low-pH treatments caused similar depolarisation up to 60 min (**Figure 4.9**B).

4.3.6 Effect of low-pH and Al^{3+} stresses on plant biomass and shoot nutrient content

Low-pH and low-pH/Al^{3+} treatments reduced plant biomass compared to pH 5.5 conditions (**Figure 4.10**A). All low-pH/Al^{3+} treatments except for 10 μM Al^{3+} caused a greater decrease in biomass than low pH alone (**Figure 4.10**A). Plants grown at ≤25-μM Al^{3+} had negligible amounts of aluminium in their shoots compared to plants treated with higher concentrations (>25 μM) of Al^{3+} (**Figure 4.10**B). Shoot K^+ concentrations did not differ between pH 5.5, low-pH and low-pH/≤25-μM Al^{3+} treatments. However, plants treated with higher concentrations of Al^{3+} (50, 75, 100 and 250 μM, pH 4.2) had higher K^+ concentrations in their shoots compared to low-pH treatment (**Figure 4.10**C).

4.4 Discussion

Al^{3+} stress for plants occurs at low soil pH. However, there are low-pH soils that affect plant growth in which Al^{3+} concentrations are not inhibitory to plant growth (Kinraide, 1990). There is also growing evidence suggesting that these two stresses differ in their inhibition of root growth (Rangel *et al.*, 2005; Yokota and Ojima, 1995). Hence, we separated low-pH effects from combined low-pH/Al^{3+} effects to obtain a deeper understanding of high proton and Al^{3+} toxicities.

An increase in rhizosphere pH of 0.1-0.2 units may convert considerable rhizotoxic Al^{3+} species into less-toxic Al hydroxides and Al phosphates (Kinraide, 1991). Thus, an increase in rhizosphere pH was proposed as the Al^{3+}-detoxification mechanism (Degenhardt *et al.*, 1998; Foy *et al.*, 1965; Kollmeier *et al.*, 2000). Reports often compared two genotypes differing in Al^{3+} sensitivity at fixed Al^{3+} exposures and reported higher rhizosphere pH in tolerant genotypes than in sensitive genotypes (Degenhardt *et al.*, 1998; Foy *et al.*, 1965; Kollmeier *et al.*, 2000; Miyasaka *et al.*, 1989;

Mugwira and Patel, 1977). We also found rhizosphere pH differences between Al^{3+}-sensitive (*als3*, *als5*) and Al^{3+}-tolerant (*alr104*) *Arabidopsis* mutants exposed to 50 μM Al^{3+} (Chapter 6). However, such genotypic differences could be a consequence rather than a cause of differential Al^{3+} tolerance (Kollmeier *et al.*, 2000; Miyasaka *et al.*, 1989). Therefore, it is important to compare H^+ and K^+ fluxes across the root-cell PM as well as E_m and intracellular pH to obtain a better understanding of the plant processes involved in alterations of rhizosphere pH.

We measured immediate-to-short-term root responses to low-pH and combined low-pH/Al^{3+} treatments. In terms of H^+ fluxes, distal elongation and mature zones exhibited a similar response to low-pH stress but markedly different responses to combined low-pH/Al^{3+} stress. In both root zones, low-pH stress induced higher net H^+ influx than low-pH/Al^{3+} (**Figure 4.3**, **Figure 4.4**), which was similar to earlier reports for H^+ flux measurements on wheat roots (Babourina *et al.*, 2006). Thus, low-pH stress alone resulted in higher rhizosphere pH than low-pH/Al^{3+} treatments (**Figure 4.5**). Interestingly, combined low-pH/Al^{3+} treatments inhibited net H^+ influx in the distal elongation zone (**Figure 4.3**) and induced net H^+ efflux in the mature zone (**Figure 4.4**). In both situations, Al^{3+} exposure would result in the relatively higher concentrations of H^+ ions in the rhizosphere. Given that such H^+ concentrations in the rhizosphere would be lower in the distal elongation zone (where H^+ influx was measured) than in the mature zone (H^+ efflux measured) (**Figure 4.3**, **Figure 4.4**), this can explain the higher Al^{3+} sensitivity in the distal elongation zone compared to the mature zone (Kollmeier *et al.*, 2000; Sivaguru and Horst, 1998). By contrast, a higher concentration of H^+ ions in the rhizosphere caused by Al^{3+} stress would further exacerbate Al^{3+} toxicity because of a shift in ionic speciation of Al to increase the proportion of Al^{3+}.

H^+ influx inhibition in the distal elongation zone and H^+ efflux in the mature zone upon Al^{3+} exposure (**Figure 4.3**, **Figure 4.4**) might happen when rapid binding of Al^{3+} ions shifts E_m toward positive values, and a positively-charged PM surface inhibits uptake of H^+ ions from a low-pH environment (Ahn *et al.*, 2004a; Ahn *et al.*, 2001). The threshold phytotoxic Al^{3+} concentration appeared to be 50 μM, because 50 μM Al^{3+} maintained higher E_m depolarisation than 100 μM Al^{3+} in both root zones (**Figure 4.9**).

It is difficult to unambiguously establish a causal relationship between changes in E_m and K^+ and H^+ fluxes measured in this work because of the close relationship among these three parameters. However, several hypotheses can be put forward.

Changes in K^+ fluxes might cause E_m changes. Under low-pH stress, K^+ efflux (**Figure 4.6**, **Figure 4.7**) via potassium outward-rectifying channels (KORC) was activated to limit the extent of low-pH-induced E_m depolarisation (**Figure 4.9**) (Maathuis *et al.*, 1997). Similarly, under the combined low-pH/100-µM Al^{3+} treatment, initial K^+ efflux made a transition to K^+ influx around 20 minutes post-exposure (**Figure 4.6**A) to limit the extent of Al^{3+}-induced hyperpolarisation in the distal elongation zone (**Figure 4.9**A). This K^+ influx could have been activated through potassium inward-rectifying channels (KIRC) because *Arabidopsis thaliana* plants require a minimum of –80 mV or greater negative E_m to activate KIRC (Maathuis and Sanders, 1995).

We suggest that a difference between low-pH and combined low-pH/Al^{3+} stresses might be largely based on the effects of Al^{3+} on K^+ channels. The long-term study (**Figure 4.10**C) showed that Al^{3+} stress resulted in higher shoot K^+ concentrations compared to a low-pH stress alone. Consistent with this observation, in short-term studies, low-pH stress elicited K^+ efflux, whereas 100-µM Al^{3+} stress inhibited K^+ efflux in the distal elongation zone and induced influx in the mature zone (**Figure 4.6**, **Figure 4.7**) (detailed discussion to follow).

Low pH might have induced K^+ efflux because of three reasons. First, low pH depolarised the plasma membrane (**Figure 4.9**), thereby decreasing the electrochemical gradient between the external environment (1 mM K^+) and the root-cell cytosol (90-100 mM; (Maathuis and Sanders, 1993), making K^+ efflux more favourable. Second, during first 30 minutes, low-pH-induced depolarisation was in the range of -53 to -68 mV in the distal elongation zone and -70 to -77 mV in the mature zone (**Figure 4.9**), which could either activate K^+ outward-rectifying channels (KORC activated at E_m potentials less negative than -80 mV) or inactivate K^+ inward-rectifying channels (KIRC requires E_m in the range of -80 to -150 mV for activation) in *Arabidopsis thaliana* (Maathuis and Sanders, 1995), thereby increasing K^+ efflux (**Figure 4.6**, **Figure 4.7**). The third possible reason could have been the activation of K^+/H^+ antiporters, as we found a good

correlation (r = -0.926) between H^+ influx and K^+ efflux in the distal elongation zone. This K^+/H^+ antiporter activity could be similar to Nha1 antiporter activation in yeast under low-pH stress (Banuelos *et al.*, 1998).

The combined low-pH/Al^{3+} stress-induced inhibition of K^+ efflux in the distal elongation zone and K^+ influx in the mature zone (**Figure 4.6**, **Figure 4.7**) can be explained in two ways. First, low-pH/100-µM Al^{3+} treatment induced less depolarisation (and eventually hyperpolarisation at 100 µM Al^{3+} after 60 min) than low pH alone in both root zones studied (**Figure 4.9**). These Al^{3+} effects on E_m could either inactivate membrane K^+ outward-rectifying channels (KORC) (see Krol and Trebacz, 2000) or activate K^+ inward-rectifying channels (KIRC activated at potentials more negative than –80 mV) (Amtmann *et al.*, 1999; Maathuis and Sanders, 1995). However, the activation of K^+ inward-rectifying channels under Al^{3+} stress is controversial because some studies have reported that Al^{3+} blocked K^+ inward-rectifying channels (Gassmann and Schroeder, 1994). Nevertheless, if we compare the onset of K^+ influx (**Figure 4.6**A) with coincident E_m measurements (**Figure 4.9**A), after about 25 minutes of combined low-pH/100-µM Al^{3+} treatment, the E_m became sufficiently negative (more negative than -80 mV) to effect the transition from K^+ efflux to K^+ influx (Maathuis and Sanders, 1995).

Second, low pH/Al^{3+} can directly inhibit Ca^{2+} uptake through depolarisation-activated *Arabidopsis* two-pore channel 1 (AtTPC1) (Furuichi *et al.*, 2001; Lin *et al.*, 2005), thereby disturbing Ca^{2+} homeostasis (Lin *et al.*, 2005; Rengel and Zhang, 2003). In doing so, the Al^{3+} stress might have affected the closure of Ca^{2+}-dependent K^+ efflux channels, namely plasma membrane K^+ outward-rectifying channels (KORC) and non-selective outward-rectifying channels (NORC) (see Krol and Trebacz, 2000). In addition, an increase in cytoplasmic pH in the low-pH/Al^{3+} treatment (**Figure 4.8**) could have also activated K^+ inward-rectifying channels (Hager, 2003).

Another reason for the reported differences in plant responses to low pH and Al^{3+} stresses is based on their capacity to synthesise and exude organic acid anions (OAA) under low-pH/Al^{3+} stress, which has been shown in numerous studies (Kochian *et al.*, 2004; Matsumoto, 2000). Modulation of cytosolic pH by low-pH and Al^{3+} stresses can act as a cellular messenger to activate/inactivate transporters and enzymes

(Roos *et al.*, 2006) and, in turn, to regulate OAA synthesis and subsequent release. An increase in intracellular pH following a combined low-pH/Al^{3+} stress (**Figure 4.8**) would favour deprotonation of OAA in the cytoplasm (Davies, 1986). Furthermore, OAA release from *Arabidopsis* (Hoekenga *et al.*, 2006; Larsen *et al.*, 1998; Liu *et al.*, 2009) would depolarise E_m (for references, see Wherrett *et al.,* 2005).

In summary, the present study clearly separated low-pH stress from combined low-pH/Al^{3+} stresses. Low-pH stress caused pronounced E_m depolarisation, intracellular acidification and K^+ efflux. By contrast, combined low-pH/Al^{3+} treatment caused inhibition of K^+ efflux, more negative E_m and intracellular alkalinisation. Low-pH stress induced H^+ influx at both distal elongation zone and mature zone, whereas combined low-pH/Al^{3+} stress inhibited H^+ influx in distal elongation zone and induced H^+ efflux in mature zone. Thus, low-pH/Al^{3+} stress decreased the capacity of wild type *Arabidopsi*s roots to increase rhizosphere pH in acidic environments.

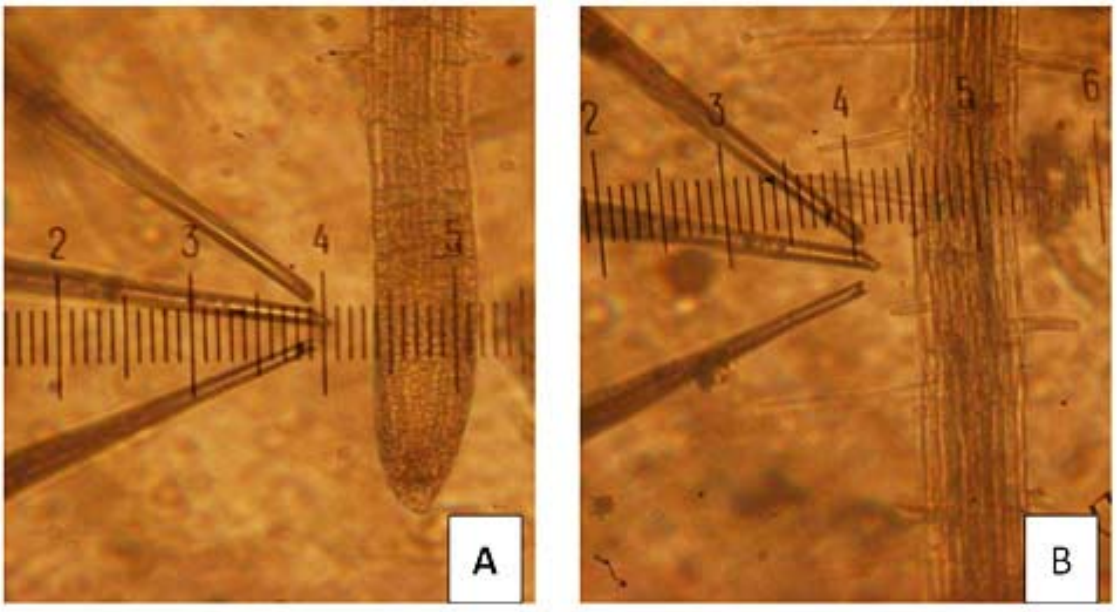

Figure 4.1 Magnified view of ion flux measurements in *Arabidopsis* roots using ion-sensitive microelectrodes at (A) distal elongation zone and (B) mature zone.
One small unit in the scale is equivalent to 12 µm.

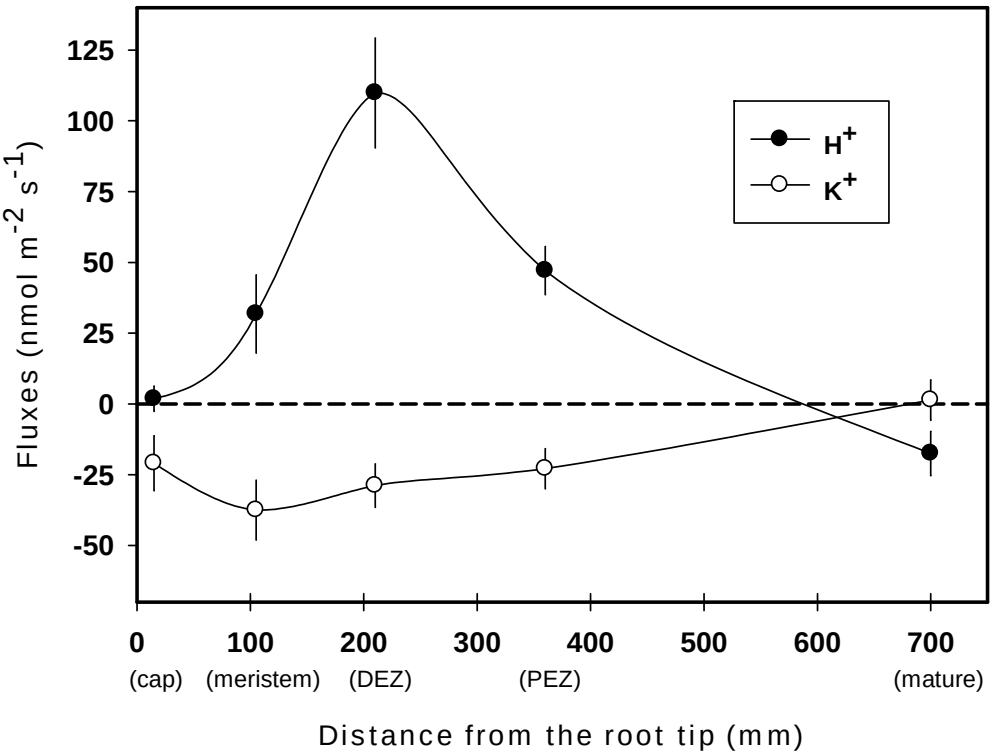

Figure 4.2 H^+ and K^+ fluxes along the longitudinal root axis of four- to five-day-old *Arabidopsis thaliana* seedlings in basal salt medium (0.1 mM $CaCl_2$ + 1 mM KCl + 0.2 mM $MgCl_2$, pH 5.5). Error bars indicate ± SE (n = 6-8 seedlings).

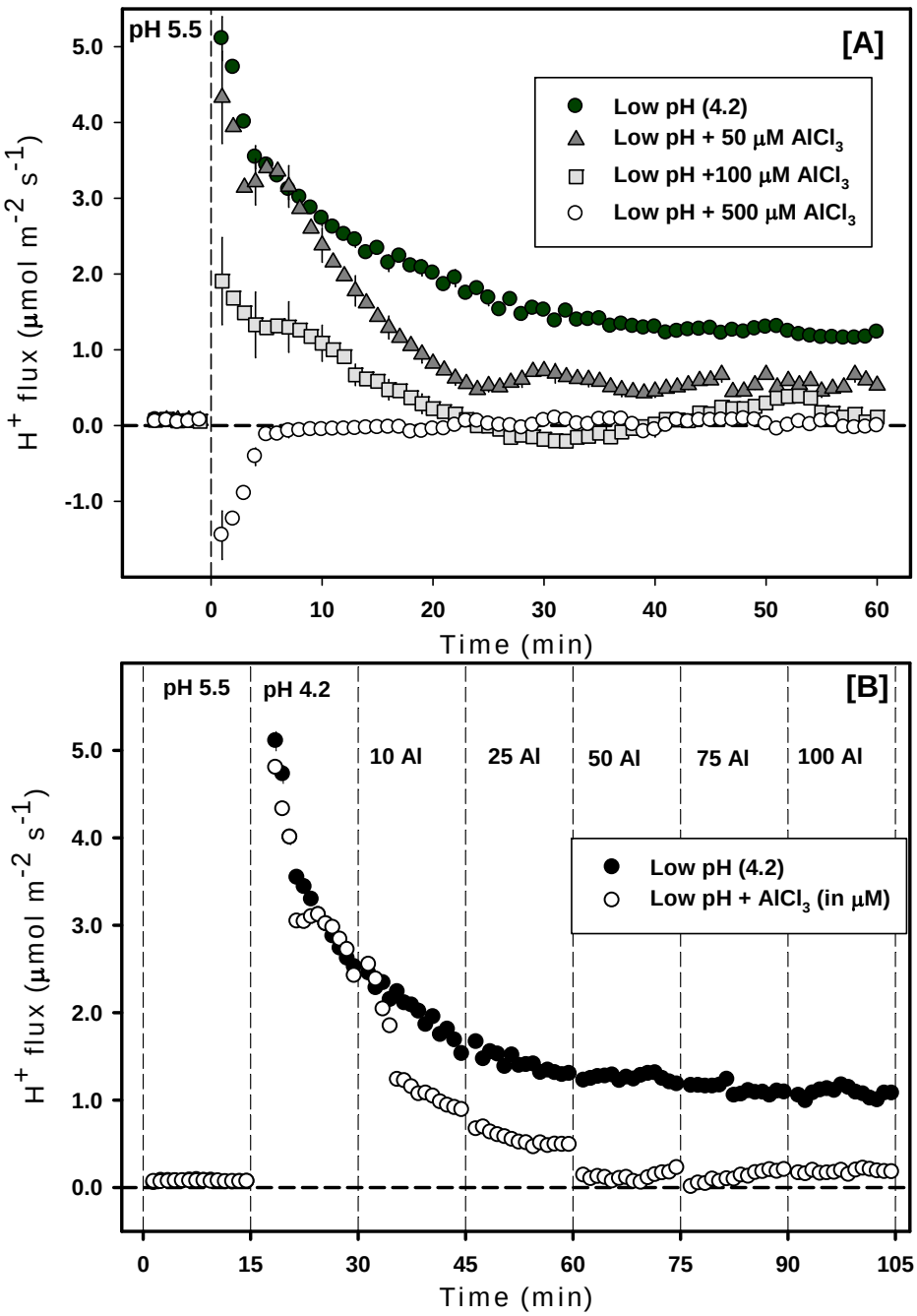

Figure 4.3 H^+ fluxes at the distal elongation zone of four- to five-day-old *Arabidopsis thaliana* seedlings.
[A] Comparison between low-pH and combined low-pH/Al treatments imposed at time = 0; and [B] the effect of sequentially increasing Al concentration at pH 4.2. In [A], the data recorded in the first 5 minutes before time = 0 represent H^+ influx (0.098 ±0.004 μmol $m^{-2}s^{-1}$) at pH 5.5. In [B], the data during the first 15 minutes represent H^+ fluxes at pH 5.5. Error bars indicate ± SE (n = 10-24 seedlings).

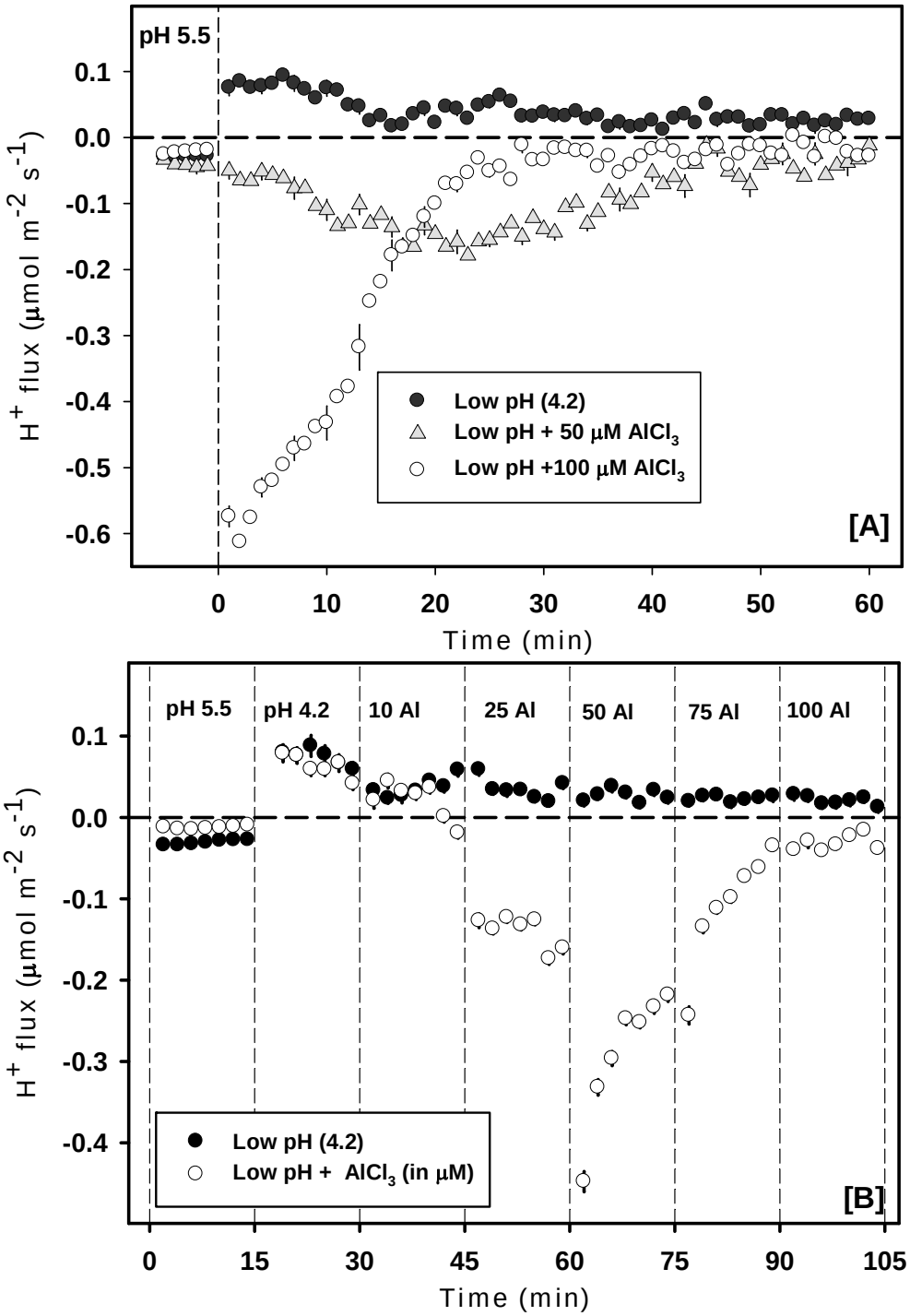

Figure 4.4 H^+ fluxes at the mature zone of four- to five-day-old *Arabidopsis thaliana* seedlings.
[A] Comparison between low-pH and combined low-pH/Al treatments imposed at time = 0; and [B] the effect of sequentially increasing Al concentration at pH 4.2. In [A], the data recorded in the first 5 minutes before time = 0 represent H^+ efflux (-0.046 ±0.008 µmol $m^{-2}s^{-1}$) at pH 5.5. In [B], the data during the first 15 minutes represent H^+ fluxes at pH 5.5. Error bars indicate ± SE (n = 10-24 seedlings).

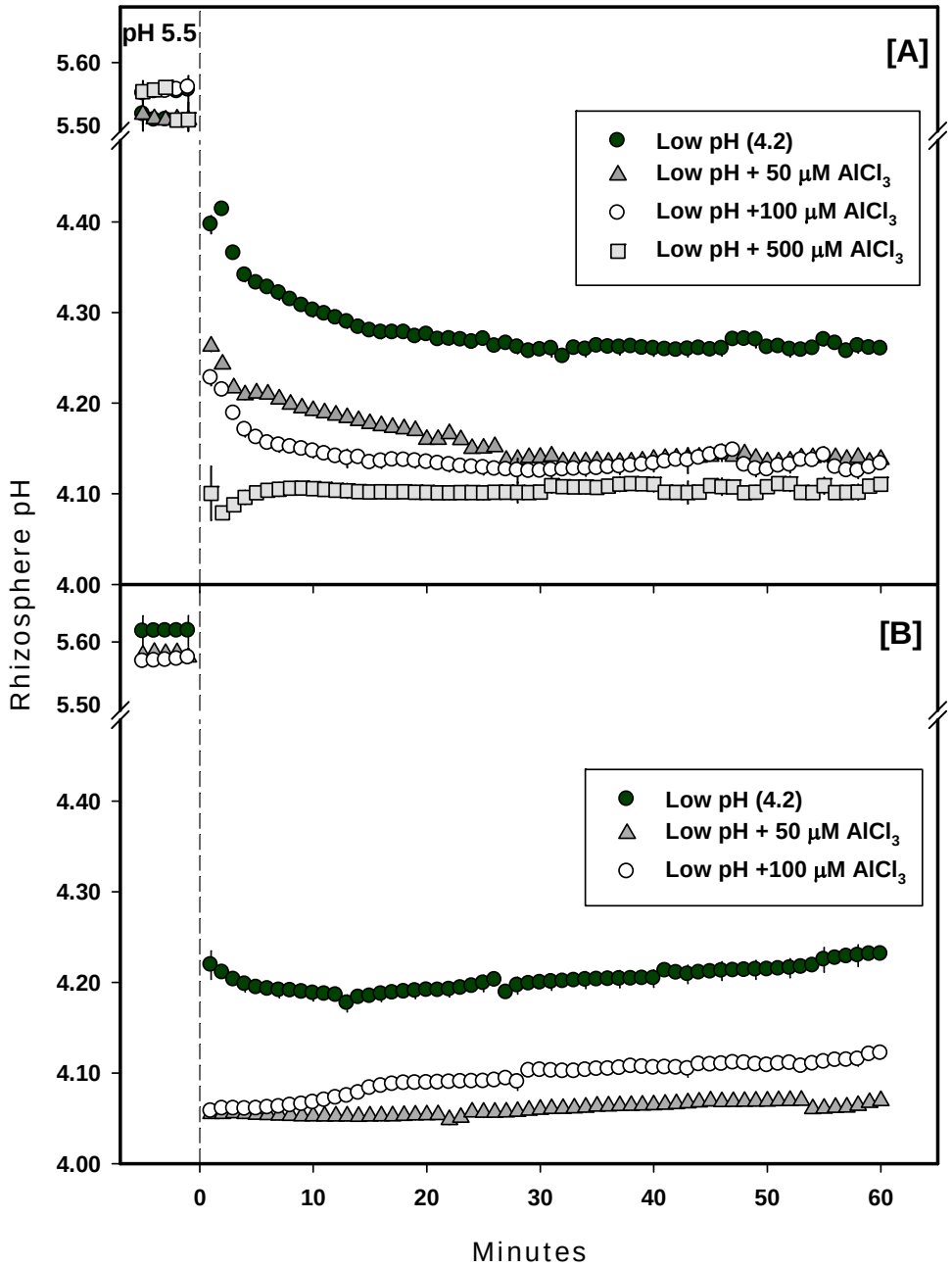

Figure 4.5 Effect of low-pH and combined low-pH/Al treatments on rhizosphere pH measured at [A] distal elongation zone and [B] mature zone of four- to five-day-old *Arabidopsis thaliana* seedlings.
The data recorded in the first 5 minutes before time = 0 represent rhizosphere pH measurements in control solution (pH 5.5). Error bars indicate ± SE (n = 10-24 seedlings).

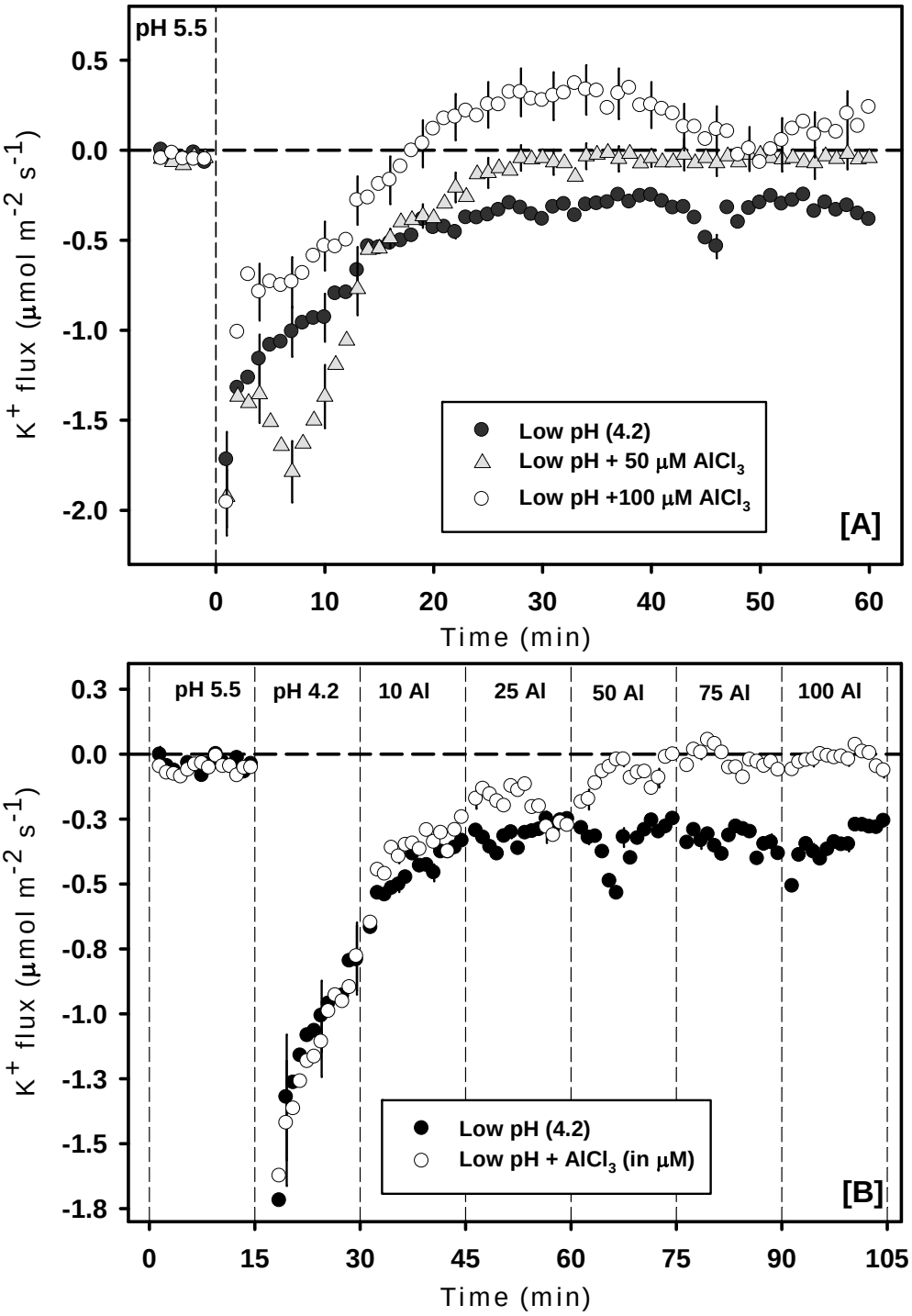

Figure 4.6 K^+ fluxes at the distal elongation zone of four- to five-day-old *Arabidopsis thaliana* seedlings.
[A] Comparison between low-pH and combined low-pH/Al treatments imposed at time = 0; and [B] the effect of sequentially increasing Al concentration at pH 4.2. In [A], the data recorded in the first 5 minutes before time = 0 represent K^+ efflux (-0.037 ±0.018 µmol $m^{-2}s^{-1}$) at pH 5.5. In [B], the data during the first 15 minutes represent K^+ fluxes at pH 5.5. Error bars indicate ± SE (n = 10-24 seedlings).

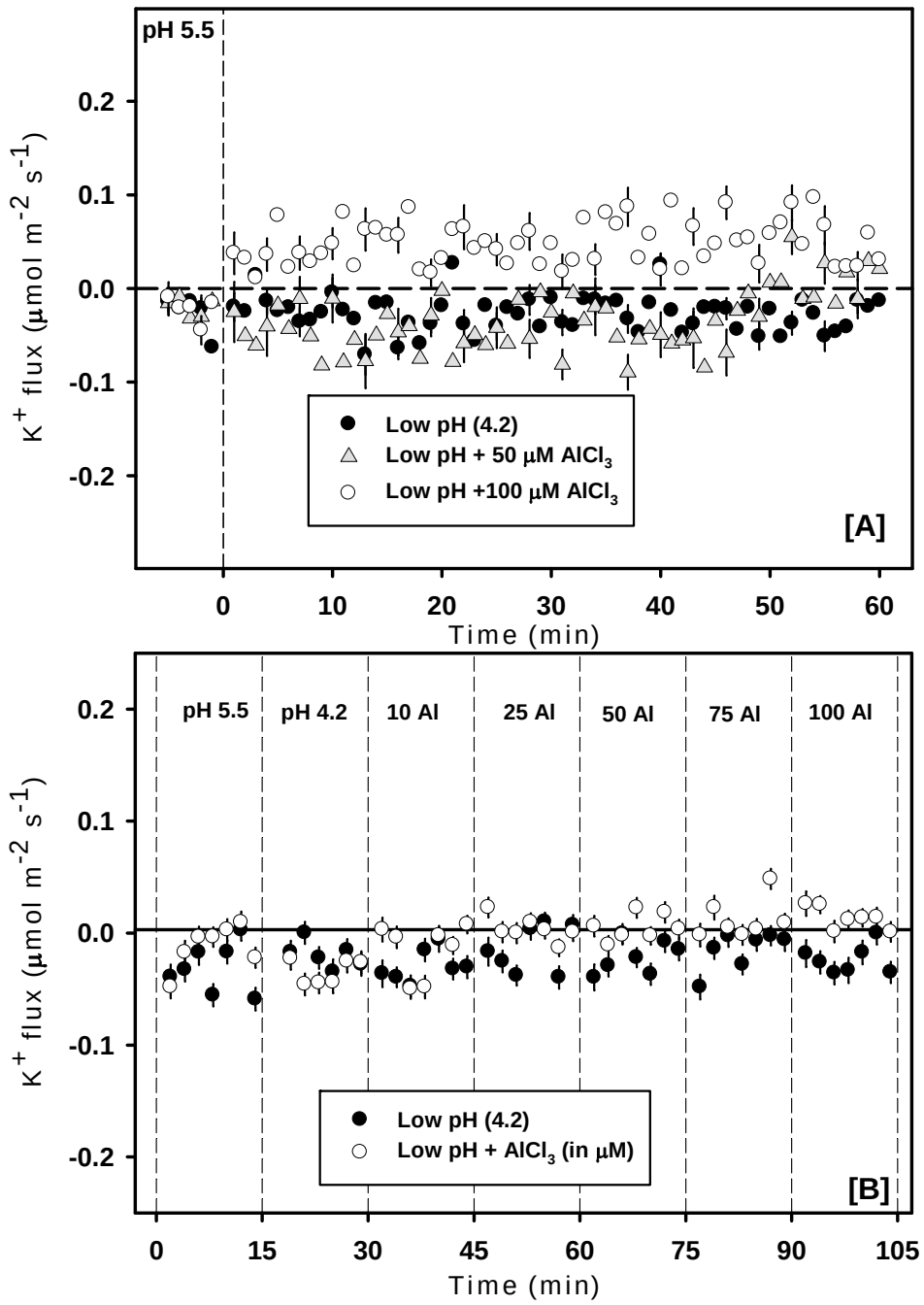

Figure 4.7 K^+ fluxes at the mature zone of four- to five-day-old *Arabidopsis thaliana* seedlings.
[A] Comparison between low-pH and combined low-pH/Al treatments imposed at time = 0; and [B] the effect of sequentially increasing Al concentration at pH 4.2. In [A], the data recorded in the first 5 minutes before time = 0 represent K^+ efflux (-0.012 ±0.008 µmol $m^{-2}s^{-1}$) at pH 5.5. In [B], the data during the first 15 minutes represent K^+ fluxes at pH 5.5. Error bars indicate ± SE (n = 10-24 seedlings).

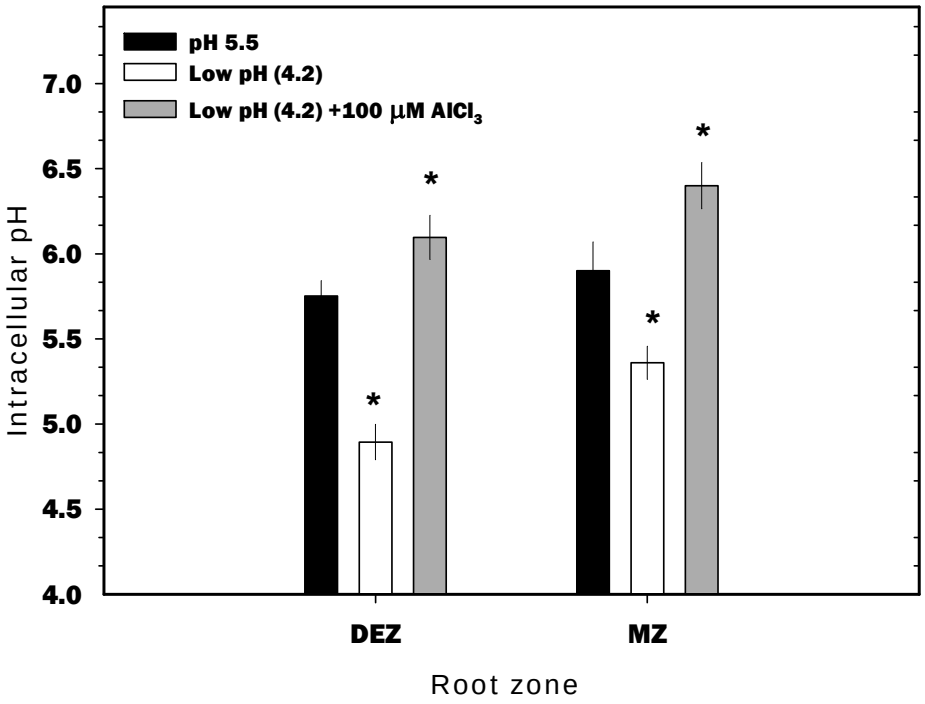

Figure 4.8 Intracellular pH measurements in four- to five-day-old *Arabidopsis thaliana* roots after 30 minutes of low-pH or combined low-pH/Al stress.
Means ± SE (n = 8-12 seedlings). The asterisks indicate values significantly different from the control (pH 5.5) by LSD test at $p \leq 0.05$.

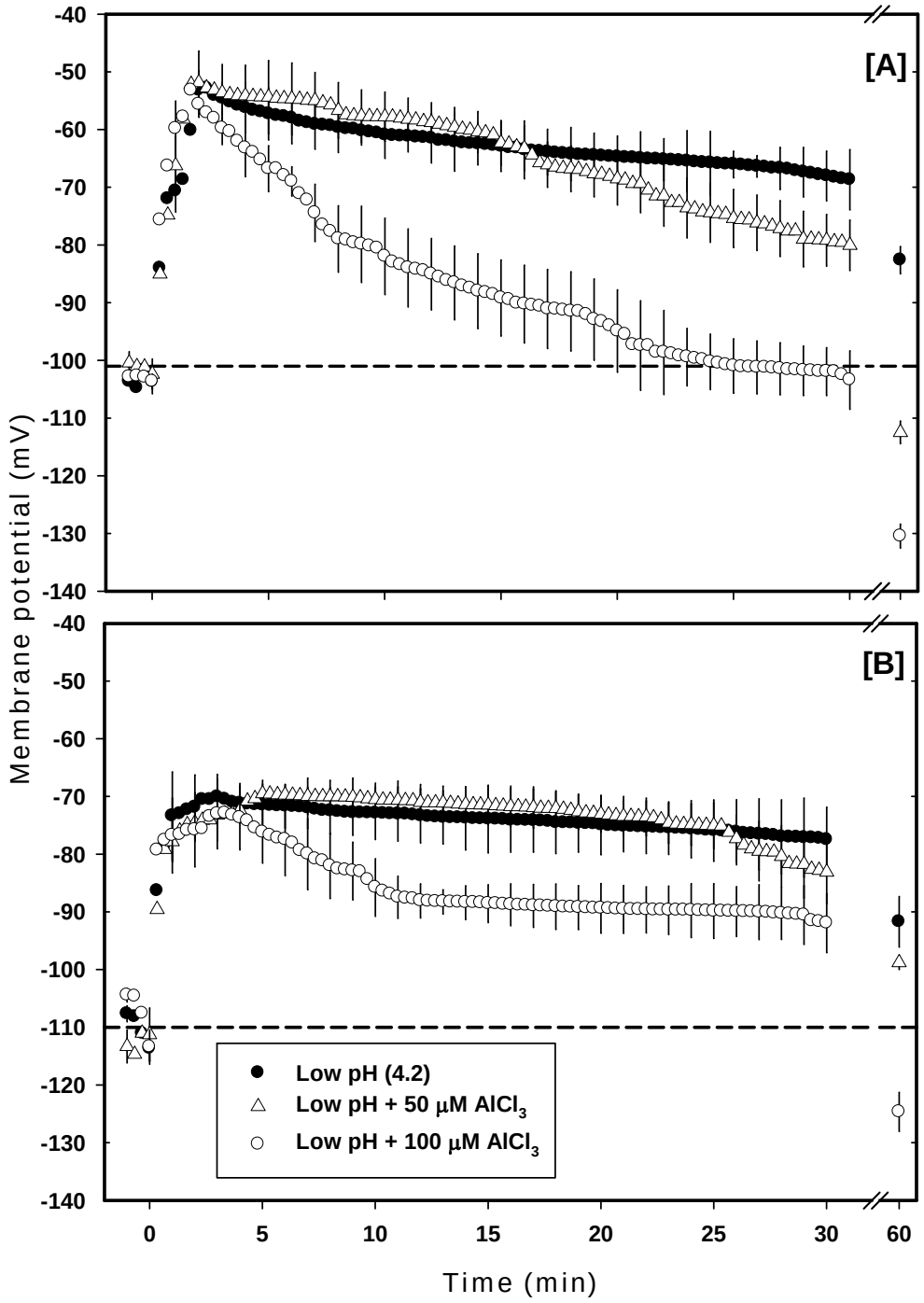

Figure 4.9 Effect of low-pH and combined low-pH/Al treatments imposed at time = 0 on the plasma membrane potential in the [A] distal elongation zone and [B] mature zone of four-to-five-day-old *Arabidopsis thaliana* roots.
Error bars indicate ± SE (n = 8-12 seedlings). The horizontal dotted lines (-101 ±2 mV in [A] and -110 ±2 mV in [B] represent the resting plasma membrane potential at pH 5.5. The symbols for the low-pH treatment during the first minute in [A] were partially covered by the symbols for the other two treatments.

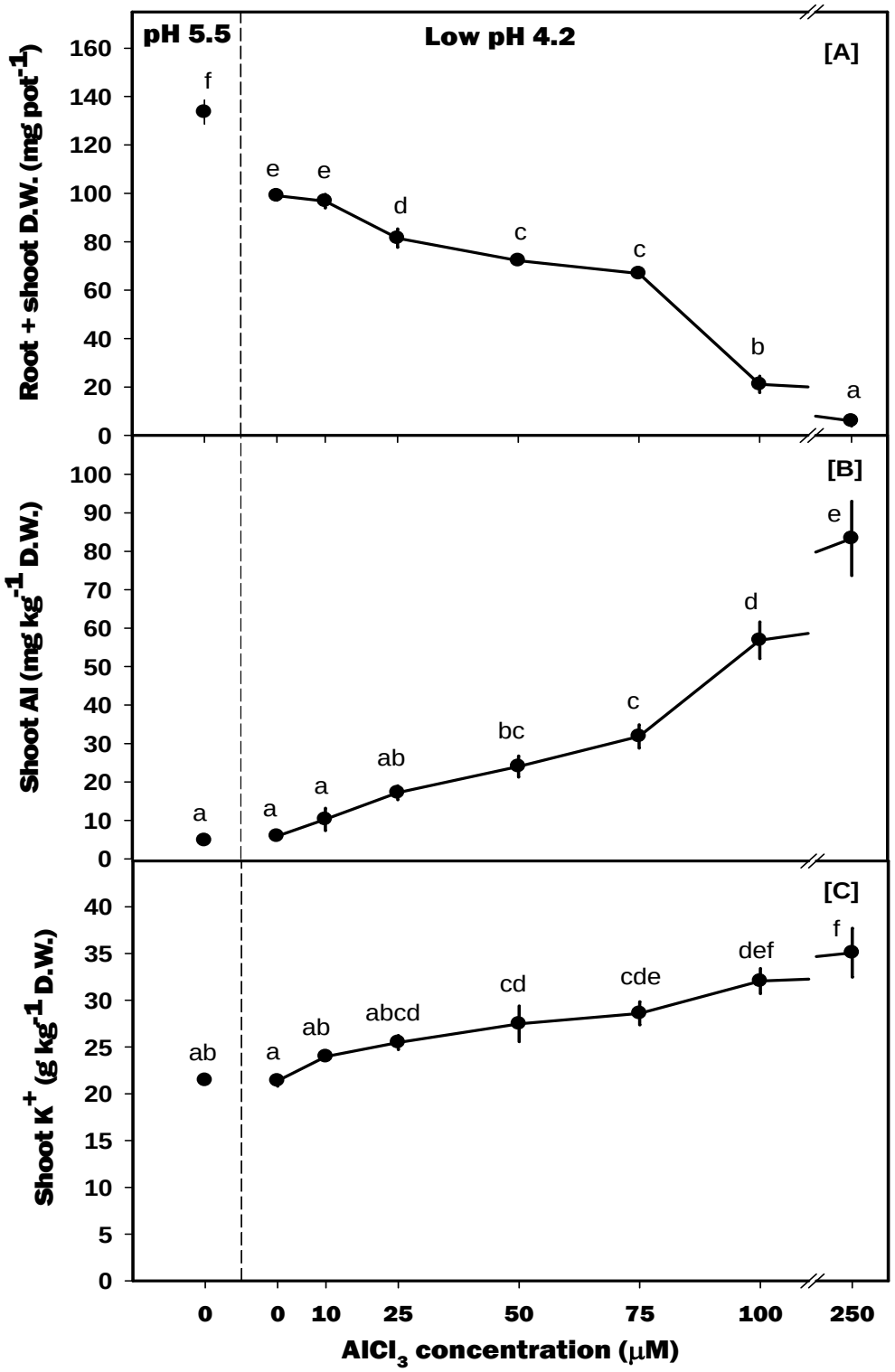

Figure 4.10 Long-term (7-day) effect of low-pH (pH 4.2, 0 μM Al) and aluminium stresses on [A] *Arabidopsis thaliana* shoot + root biomass, [B] shoot Al concentration and [C] shoot K^+ concentration.
Means ± SE (n = 3 replicates). In each graph, points sharing common letters are not significantly different by LSD test at $p \leq 0.05$.

Chapter 5

Aluminium affects Ca^{2+} and Mg^{2+} uptake in the roots of intact *Arabidopsis thaliana* plants

Jayakumar Bose, Olga Babourina and Zed Rengel

School of Earth and Environment, the University of Western Australia, Crawley WA 6009, Australia

Abstract

Al^{3+} toxicity impairs uptake of Ca^{2+} and Mg^{2+}, but the underlying physiology is poorly understood. To elucidate Al^{3+}-induced Ca^{2+} and Mg^{2+} uptake inhibition, *Arabidopsis thaliana* wild type seedlings were used as the model system in the short-term (1 h) and long-term (7 d) exposure to Al^{3+}. In short-term experiments, effects of low-pH and combined low-pH/Al^{3+} stresses on Ca^{2+} and Mg^{2+} fluxes were measured at the distal elongation zone and mature zone of roots using non-invasive microelectrode technique. Intracellular Mg^{2+} concentration was measured in intact root cells for the first time using Mg^{2+}-specific fluorescent dye (Magnesium Green^{TM}).

Moderate Al^{3+} concentrations (50 and 100 μM) induced Mg^{2+} influx in both root zones, resulting in a concomitant rise in intracellular Mg^{2+} concentration. Enhanced Mg^{2+} uptake under moderate concentrations of Al^{3+} might play a crucial role in organic acid synthesis and release. Only high concentrations of Al^{3+} (500 μM) and/or prolonged Al^{3+} exposure reduced Mg^{2+} uptake, suggesting inhibition of activity of plasma membrane cation channels permeable to magnesium. In contrast, all three Al^{3+} concentrations (50, 100 and 500 μM) induced Ca^{2+} efflux in both root zones. Thus, short-term Ca^{2+} fluxes (but not those of Mg^{2+}) are impaired by Al^{3+}, whereas long-term exposure to Al^{3+} has a similar inhibitory effect on accumulation of both Ca^{2+} and Mg^{2+}. Immediate Al^{3+}-induced disturbance in Ca^{2+} uptake may be associated with the primary cause of Al^{3+} toxicity in *Arabidopsis thaliana*.

Key words: acidity, aluminium toxicity, Mg^{2+} flux, Ca^{2+} flux, Fluorescence Life Time Imaging (FLIM), intracellular Mg^{2+}, distal root elongation zone, mature root zone

5.1 Introduction

An early symptom of Al^{3+} toxicity to plants is the inhibition of root growth, becoming measurable within 60 minutes of exposure to very low (μM) concentrations of Al^{3+} (Delhaize and Ryan, 1995; Ownby and Popham, 1989). Thus, roots have been the focus of research to decipher the mechanisms of Al^{3+} toxicity or tolerance in plants. The root apex (Ryan *et al.*, 1993), particularly the distal elongation zone (Illes *et al.*, 2006; Kollmeier *et al.*, 2000; Sivaguru and Horst, 1998), needs to be exposed to Al^{3+} for root growth inhibition to occur. Accordingly, the distal elongation zone needs to be studied in detail for greater understanding of the primary mechanisms of Al^{3+} toxicity and tolerance. Unfortunately, Al^{3+} toxicity studies on the distal elongation zone are relatively rare.

Al^{3+} exposure results in the alteration of many structures and functions in roots, such as (i) disturbance of the cytoskeleton (Amenos *et al.*, 2009; Sivaguru *et al.*, 1999), (ii) changes in the physical properties of the plasma membrane (Ahn and Matsumoto, 2006; Ryan *et al.*, 2007; Tabuchi and Matsumoto, 2001), (iii) inhibition of plasma membrane H^+-ATPase activity in root tip cells (Ahn and Matsumoto, 2006; Ahn *et al.*, 2002; Ahn *et al.*, 2001), (iv) inhibition of cation uptake (Ca^{2+}, Mg^{2+}, K^+, NH_4^+) (Huang *et al.*, 1992; Lazof *et al.*, 1994; Nichol *et al.*, 1993; Rengel and Robinson, 1989b), (v) inhibition of plasmodesmata-mediated transport between cells (Sivaguru *et al.*, 2000), (vi) disturbance in intracellular homeostasis of Ca^{2+} (Plieth *et al.*, 1999; Rengel, 1992; Rengel and Zhang, 2003) and pH (Babourina and Rengel, 2009; Lindberg and Strid, 1997), (vii) induced callose accumulation (Aidemark *et al.*, 2009; Jones *et al.*, 2006; Tahara *et al.*, 2008), and (vii) induction of oxidative stress (Jones *et al.*, 2006; Tahara *et al.*, 2008). These disturbances may directly or indirectly trigger Al^{3+}-induced root growth inhibition.

Among the biochemical and physiological processes affected by Al^{3+}, inhibition of Ca^{2+} and Mg^{2+} uptake received considerable attention because symptoms of severe Al^{3+} toxicity resemble deficiencies of Ca^{2+} (see Foy, 1988; Rengel and Elliott, 1992 for references) and Mg^{2+} (Grimme, 1983; Keltjens, 1988; Rengel, 1990; Rengel and

Robinson, 1989b). Al^{3+}-induced Ca^{2+} and Mg^{2+} deficiency may occur in plants as the result of competitive interactions between Al^{3+} and membrane transporters for Ca^{2+} (Huang *et al.*, 1992; Rengel, 1992; Rengel and Elliott, 1992) and Mg^{2+} (Rengel, 1990; Rengel and Robinson, 1989b) or may simply be due to Al^{3+}-induced impairment of root growth and a consequent decrease in the nutrient-absorbing surface area (Clarkson, 1985). The latter cause of deficiency is common after prolonged exposure to Al^{3+} (hours to days), with root growth reduction being associated with decreased nutrient accumulation (see Rengel, 1992 for references). Therefore, long-term Al^{3+} exposure studies may not provide information about specific Al^{3+} effects on ion transport systems. A further complication with long-term studies is that Al^{3+} may inhibit root growth without reducing $Ca^{2+}$and Mg^{2+} uptake (Godbold and Jentschke, 1998; Göransson and Eldhuset, 1995; Ryan *et al.*, 1997). Hence, short-term Al^{3+} exposure studies involving direct measurements of ion fluxes are essential for understanding immediate Al^{3+} effects on Ca^{2+} and Mg^{2+} uptake.

Average nutrient uptake rates calculated from either gross ion accumulation in plants or ion depletion in nutrient solution represent averaging over time as well as over the whole root system. However, Ca^{2+} and Mg^{2+} fluxes may vary considerably along the root axis and with time (Demidchik *et al.*, 2002; Ferguson and Clarkson, 1975, 1976; Kiegle *et al.*, 2000; Newman, 2001). The mature root zone accounts for more than 90% of root biomass and plays a crucial role in nutrient absorption and transport (Bibikova and Gilroy, 2002; Gahoonia and Nielsen, 1998; Parker *et al.*, 2000). Hence, it is important to characterize the Al^{3+} effects on Ca^{2+} and Mg^{2+} fluxes at the mature root zone in comparison with the elongation root zone that is most sensitive to Al^{3+} toxicity.

The alleviation of Al^{3+} toxicity by relatively high (millimolar) concentrations of Ca^{2+} and Mg^{2+} has been reported for many plant species (Brady *et al.*, 1993; Keltjens and Tan, 1993; Kinraide *et al.*, 2004). Increased ionic strength of the solutions (Noble and Sumner, 1988), reduction in Al^{3+} saturation at the apoplastic exchange sites (Grauer and Horst, 1992) and decreased Al^{3+} activity at the root cell plasma membrane surface (Kinraide, 2003; Kinraide *et al.*, 2004) have been proposed as mechanisms for Al^{3+} toxicity alleviation by Ca^{2+} and Mg^{2+}. Nonetheless, the mechanisms underlying root growth improvement by Ca^{2+} and Mg^{2+} in the presence of constant Al^{3+} activity (Brady *et al.*, 1993; Lazof and Holland, 1999; Silva *et al.*, 2001b; Silva *et al.*, 2001c) are poorly

understood as illustrated by recent reports about micromolar concentrations of Mg^{2+} resulting in non-electrostatic alleviation of Al^{3+} toxicity (Silva *et al.*, 2001a; Yang *et al.*, 2007). Further, over-expression of Mg^{2+} transporter genes in yeast (MacDiarmid and Gardner, 1998) and *Nicotiana benthamiana* (Deng *et al.*, 2006) conferred Al^{3+} tolerance by alleviating Al^{3+}-induced Mg^{2+} deficiency, but these studies did not provide sufficient evidence of enhanced Mg^{2+} uptake in the presence of Al^{3+} ions.

In the present study, Ca^{2+} and Mg^{2+} fluxes were measured at the distal elongation and the mature zones of *Arabidopsis thaliana* roots using ion-sensitive microelectrodes. Short-term (1 h) and long-term (7 d) Al^{3+} exposure studies were compared to characterise primary and secondary effects of Al^{3+} on Ca^{2+} and Mg^{2+} uptake.

5.2 Material and Methods

5.2.1 Long-term experiment

5.2.1.1 Hydroponic culture

Seeds of *Arabidopsis thaliana* L. wild type (ecotype Col-0) were surface sterilised with 1% v/v calcium hypochlorite for 10 minutes and sown on rock-wool strips (1-2 mm thick and 50-60 mm long) in contact with diluted (1/10) Hoagland solution in 250-mL plastic containers kept at 4^{o}C for 2 d to achieve synchronised germination. Seedlings were then moved to a growth cabinet with 16 h light (150 µmol m^{-2} s^{-1}) and 8 h dark at 20±1^{o}C. Nutrient solution was changed daily. After 3 weeks, treatments were imposed in diluted (1/10) Hoagland solution with 0.5 mM homo PIPES buffer for 7 d. Preliminary experiment showed that 0.5 mM homo PIPES concentration was sufficient to keep the pH at a desired level for 24 h, so the solutions were changed daily. Treatments were pH 5.5/no Al, and a range of Al^{3+} concentrations (0, 10, 25, 50, 75, 100 or 250 µM) at pH 4.2 and replicated thrice. The experiment was repeated two times.

5.2.1.2 Biomass and Ca^{2+} and Mg^{2+} concentration measurements

At harvest, shoots and roots were separated, washed in 100 µM $CaSO_4$, rinsed with deionised water and dried in the oven at 70^{o}C for 72 hours and weighed. Oven-

dried shoots were digested with HNO_3:$HClO_4$ (10:1) mixture and analysed using inductively-coupled plasma-mass spectrometry (ICP-MS).

5.2.2 Short-term experiments

5.2.2.1 Agar culture

Arabidopsis thaliana seedlings were grown in 90-mm Petri dishes under constant fluorescent light (150 µmol m^{-2} s^{-1}) and temperature (23-25 ^{o}C) in 0.8% w/w agar media containing basal salt medium (BSM) 0.1 mM $CaCl_2$ + 1 mM KCl + 0.2 mM $MgCl_2$, pH 5.5. The Petri dishes were oriented upright, so roots grew down along the agar surface without penetrating it. However, roots were anchored in the agar by root hairs. Four- to five-day-old seedlings were used for all the short-term experiments.

5.2.2.2 Measurement of Ca^{2+} and Mg^{2+} fluxes using MIFE™

Net fluxes of Ca^{2+} and Mg^{2+} were measured at distal elongation zone (200 µm away from root cap) and mature zone (700 µm away from root cap) using the non-invasive MIFE™ system (University of Tasmania, Hobart, Australia) as described by Newman (2001). Microelectrodes were pulled from borosilicate glass capillaries (GC 150-10, SDR Clinical Technology, Middle Cove, Australia), oven dried at 230 ºC for about 5 h, and silanised using tributylchlorosilane (Fluka catalogue no. 90796). Electrodes were broken back to get the external tip diameter of 2-3 µm. The electrodes were back-filled with appropriate solutions (0.5 M $CaCl_2$ for Ca^{2+} electrode and 0.5 mM $MgCl_2$ for Mg^{2+} electrode). The electrode tips were then front-filled with ionophore cocktails (Fluka catalogue no. 21048 for Ca^{2+} and no. 63048 for Mg^{2+}). Prepared electrodes were calibrated in a set of standards (Ca^{2+} from 0.1 to 1.0 mM with 0.2 mM Mg^{2+} background; Mg^{2+} from 0.2 to 2.0 mM with 0.1 mM Ca^{2+} and 100 µM $AlCl_3$ background). Electrodes with the slope responses of less than 25 mV per decade were discarded.

During the first set of experiments, four- to five-day-old seedlings were conditioned in the BSM (pH 5.5) for 30 minutes followed by imposing either low pH (pH 4.2) or Al treatments (50, 100 or 500 µM $AlCl_3$, pH 4.2) in the BSM bathing solution and measuring fluxes for 60 minutes. In the second set of experiments, combined low-pH/Al treatments (0, 10, 25, 50, 75 and 100 µM $AlCl_3$, pH 4.2) were

sequentially introduced into the bathing solution (starting from the lowest and proceeding to higher Al concentrations every 15 minutes) after the first 15 minutes of pH 5.5.

Because Mg^{2+} ionophore is partially selective for Ca^{2+}, we have simultaneously measured Ca^{2+} and Mg^{2+} fluxes using identically prepared electrodes. The Mg^{2+} fluxes were then recalculated according to the equation described elsewhere (Knowles and Shabala, 2004).

5.2.2.3 Intracellular free Mg^{2+} measurements

The Mg^{2+}-sensitive fluorescent dye Magnesium Green^{TM}-AM, Molecular Probes, Eugene, OR, USA (Glycine, N-[2-(carboxymethoxy)-4-[[(2',7'-dichloro-3',6'-dihydroxy-3-oxospiro[isobenzofuran-1(3H), 9'- [9H] xanthen]-5 yl) carbonyl] amino] phenyl] -N- carboxymethyl-, acetoxymethyl ester) was dissolved in dimethylsulphoxide (DMSO) (Sigma, Castle Hill, Australia) and diluted with a loading solution (0.2 mM $CaCl_2$ and 50 mM mannitol, pH 4.2) to a final concentration of 1.5 μM. Preliminary experiments indicated that 1.5 μM concentration was sufficient for measuring intracellular Mg^{2+} while being sufficiently low to avoid damage to root cells induced by laser scanning (**Figure 5.1**). The final concentration of DMSO in the loading solution was 1% v/v. Preliminary experiments with different recovery times and temperatures revealed that the minimum 10-h recovery period at 25^{o}C was essential for Magnesium Green^{TM}–AM loading into the root tissue (data not shown). Therefore, the dye was loaded into the intact *Arabidopsis* roots for 1 h on ice (Guo *et al.*, 2009), followed by recovery in BSM for 12 h at 25^{0}C.

All the calibration and intracellular Mg^{2+} measurements were done using an inverted-stage confocal microscope (Leica TCS SP2 AOBS, Leica Microsystems GmbH, Wetzlar, Germany). Light pulses were generated at a frequency of 80 MHz with a Mai Tai Laser (Spectra Physics, Mountain View, CA, USA). Emission wavelength of 850 nm was found in preliminary experiments to minimise contribution from autofluorescence (data not shown). Mean lifetime (τ_m), assuming a triple exponential decay for Magnesium-Green^{TM}, was used in calibrations (Szmacinski and Lakowicz, 1996). *In vitro* calibration was performed for the concentration range 0.0 to 1.0 mM Mg^{2+} using Magnesium Green^{TM} pentapotassium salt. A significant shift in τ_m values

was noted between *in vitro* and *in vivo* calibrations (data not shown); thus, *in vivo* calibration was performed for the concentration range 0.0 to 2.0 mM Mg^{2+} using Magnesium Green™–AM (**Figure 5.2**A,B,D,E). For zero free Mg^{2+} concentration, seedlings loaded with Magnesium Green™–AM were incubated for 1 h in BSM containing 200 µM EGTA-AM (Ethylene glycol-bis(beta-aminoethyl ether)-N,N,N',N'-tetraacetic acid-, tetra(acetoxymethyl ester)) and 2.0 mM EGTA (**Figure 5.2**A). For other free Mg^{2+} concentrations, seedlings loaded with Magnesium Green™–AM were perfused with required Mg^{2+} concentration plus 200 µM A23187 ionophore and allowed to equilibrate for 1 h (**Figure 5.2**B). Linear regression analysis confirmed that amplitudes (a1 and a2, **Figure 5.2**D) and τ_m (**Figure 5.2**E) showed a linear response to tested free Mg^{2+} concentrations. Among these parameters, τ_m delineated autofluorescence effectively; thus, τ_m was used for calculating intracellular free Mg^{2+} concentrations (**Figure 5.2**E).

After dye loading and BSM recovery, seedlings were exposed to low pH stress (pH 4.2) or Al^{3+} stress (50, 100 or 500 µM $AlCl_3$, pH 4.2). After 10 minutes of treatment, Fluorescence Lifetime Images (FLIM) were collected for 500 seconds using photomultipliers, and the FLIM analysis was performed using electronics (SPC-730; Becker & Hickl, Berlin, Germany) and software (SPC7.22; Becker & Hickl) for time-correlated single-photon counting (O'Connor and Desmond, 1984). The intracellular free Mg^{2+} was calculated for epidermal cells of the root distal elongation zone according to calibration curves (**Figure 5.2**E) using data analysis software for fluorescence lifetime imaging microscopy systems (SPCImage Version 2.6, MP-FLIM and D-FLIM).

5.2.3 Statistical analysis

Significant differences among means were assessed by *t*-test and ANOVA using Genstat (10th edition) (VSN International Ltd, Hemel Hempstead, UK).

5.3 Results

5.3.1 Long-term experiment

5.3.1.1 Effect of low pH and low pH/Al treatments on plant biomass and shoot nutrient content

Low-pH and low-pH/Al stresses reduced the shoot and root biomass when compared to pH 5.5 (**Figure 5.3**A, B). All Al concentrations, except 10 µM Al, caused a greater biomass decline than the low pH stress alone (**Figure 5.3**A, B). More than 80% decrease in biomass was recorded at 100 and 250 µM Al.

Low pH alone decreased shoot Ca^{2+} concentration by 25% in comparison to pH 5.5 (**Figure 5.4**). The low pH/Al^{3+} treatments (≥ 50 µM) further decreased shoot Ca^{2+} concentration when compared to the low pH treatment (**Figure 5.4**).

Shoot Mg^{2+} concentration did not differ between the low-pH and pH 5.5 treatments (**Figure 5.5**). In contrast, Al stress reduced shoot Mg^{2+} concentration when compared to low pH and pH 5.5. However, such a decline in Mg^{2+} concentration was relatively small (≤10%) up to 75 µM Al, whereas 100 µM Al caused 20% and 250 µM Al around 50% reduction in Mg^{2+} concentration (**Figure 5.5**).

5.3.2 Short-term experiments

5.3.2.1 Effect of low-pH and low-pH/Al^{3+} treatments on Ca^{2+} fluxes

Under control pH 5.5, net Ca^{2+} influx at the distal elongation zone and small transient net efflux at the mature zone were observed (**Figure 5.6**). When low pH stress was imposed, it slightly reduced Ca^{2+} influx at the distal elongation zone (**Figure 5.6**A) and did not alter Ca^{2+} flux at the mature zone (**Figure 5.6**B). Combined low pH/Al^{3+} treatments induced Ca^{2+} efflux in a dose-dependent manner from both root zones within the first minute of treatment commencement (**Figure 5.6**). Initial Al^{3+}-induced Ca^{2+} efflux was higher in the mature zone than the distal elongation zone (**Figure 5.6**). This Al^{3+}-induced Ca^{2+} efflux was measured up to 30 minutes in the distal elongation zone and up to 20 minutes in MZ, followed by Ca^{2+} fluxes oscillating around zero. Interestingly, the 50 µM Al^{3+} treatment shifted Ca^{2+} flux in the distal elongation zone from efflux to influx after 30 minutes and eventually reached the control (0 Al^{3+}, pH

4.2) level after 40 minutes. However, 100 and 500 μM Al^{3+} treatments caused Ca^{2+} fluxes to oscillate around zero in the distal elongation zone after 30 minutes and in the mature zone after 20 minutes (**Figure 5.6**).

5.3.2.2 Effect of low-pH and low-pH/Al treatments on Mg^{2+} fluxes

Under no stress (pH 5.5), net Mg^{2+} influx at the distal elongation zone and net efflux at the mature zone (**Figure 5.7**, **Figure 5.8**) were observed. The low-pH treatment increased net Mg^{2+} influx 10-fold in the distal elongation zone compared with that at pH 5.5, whereas Mg^{2+} fluxes oscillated around zero in the mature zone (**Figure 5.7**, **Figure 5.8**). Interestingly, the combined low-pH/50 μM Al treatment induced higher Mg^{2+} influx in both root zones compared with the low-pH treatment (**Figure 5.7**, **Figure 5.8**). This enhanced Mg^{2+} influx was observed for the entire duration of experiment. The combined low-pH/100 μM Al treatment also induced Mg^{2+} influx in both root zones, but this influx was smaller when compared to the low-pH/50 μM Al treatment, except during the first 10 minutes in the mature zone (**Figure 5.7**). In addition, Mg^{2+} influx induced by the combined low-pH/100 μM Al treatment was variable in the distal elongation zone and even turned into small Mg^{2+} efflux in the period 26-32 minutes after the commencement of the treatment (**Figure 5.7**A). The treatment with high Al concentration (500 μM $AlCl_3$, pH 4.2) caused Mg^{2+} efflux from the distal elongation zone within 5 minutes and from the mature zone in 15 minutes, but then fluxes oscillated around zero until the end of the measuring period (**Figure 5.7**). Sequential introduction of low pH and Al revealed (**Figure 5.8**) that Al concentrations from 25 to 75 μM in the distal elongation zone and 10 to 75 μM in the mature zone increased Mg^{2+} influx when compared to pH 5.5 and pH 4.2. Maximum Mg^{2+} influx was observed under 50 μM Al in both root zones.

5.3.2.3 Effect of low-pH and combined low-pH/Al stresses on intracellular free Mg^{2+}concentration

We measured the intracellular free Mg^{2+} concentration in *Arabidopsis thaliana* intact epidermal root cells at the distal elongation zone (**Figure 5.9**). Under no stress (pH 5.5), 0.92 ± 0.04 mM intracellular Mg^{2+} concentration was recorded. The low-pH treatment caused a non-significant decrease in Mg^{2+} concentration. In contrast, the combined low-pH/50 μM Al stress raised intracellular Mg^{2+} concentration 2-fold,

whereas no difference was observed between the combined low-pH/100 µM Al treatment and control. Among all the treatments, lowest intracellular Mg^{2+} concentration was observed in the combined low-pH/500 µM Al treatment (**Figure 5.9**).

5.4 Discussion

Low-pH and Al^{3+} decreased shoot Ca^{2+} concentration (**Figure 5.4**) after long-term Al^{3+} exposure (7 d). Consistent with this observation, in the short-term study (1 h), Al^{3+} stress inhibited Ca^{2+} uptake in distal elongation and mature root zones of *Arabidopsis thaliana* wild type (**Figure 5.6**). Combined low pH/Al^{3+} treatments induced Ca^{2+} efflux in a dose dependant manner within a minute in both root zones, and the Ca^{2+} efflux persisted in the distal elongation zone for up to 30 min and in the mature zone for 20 min (**Figure 5.6**). This Al^{3+}-induced instantaneous Ca^{2+} efflux might be due to displacement of Ca^{2+} from the apoplasm by Al^{3+} ions (Kinraide and Parker, 1987; Rengel and Zhang, 2003) because Al^{3+} has a stronger affinity for pectin in the cell wall than does Ca^{2+} (Blamey *et al.*, 1990). Ca^{2+} is an integral component of pectin cross-linkages among the cell wall components (Voragen *et al.*, 2009). Hence, displacement of Ca^{2+} by Al^{3+} would severely alter the physical properties of the cell wall, including extensibility, rigidity and permeability (Horst *et al.*, 2007; Jones *et al.*, 2006; Reid *et al.*, 1995; Tabuchi and Matsumoto, 2001), thereby detrimentally affecting cell division and elongation. Ca^{2+} efflux following Al^{3+} exposure occurred in the first minute (**Figure 5.6**), therefore preceding root growth inhibition by a considerable margin. Hence, Al^{3+}-induced Ca^{2+} efflux could be one of the potential primary causes of Al^{3+} phytotoxicity (Rengel, 1992; Rengel and Zhang, 2003), at least in *Arabidopsis thaliana* wild type.

If the initial Al^{3+}-induced Ca^{2+} efflux from the distal elongation zone was the result of Ca^{2+} displacement from the apoplasm, after the equilibrium period (≈30 min) we should have observed Ca^{2+} influx similar to the results obtained in the control treatment (0 Al^{3+}, pH 4.2). However, in the 100 and 500 µM Al^{3+} treatments, Ca^{2+} fluxes at the distal elongation zone did not reach the control (0 Al^{3+}, pH 4.2) level afteraf 60 min (**Figure 5.6**A). Thus, we consider that in the present study Al^{3+} inhibited Ca^{2+} influx (Huang *et al.*, 1992; Rengel and Elliott, 1992) through binding of Al^{3+} on the plasma membrane surface (Al^{3+} exhibits 560-fold higher affinity for plasma membrane surface than does Ca^{2+}) (Akeson *et al.*, 1989). Such binding of Al^{3+} to the

plasma membrane may inhibit hyperpolarisation-activated Ca^{2+}-permeable channels (Ding *et al.*, 1993a; Kiegle *et al.*, 2000; Rengel and Zhang, 2003; Very and Davies, 2000) and also decrease by half the inward current through depolarisation-activated Ca^{2+} channels (Kawano *et al.*, 2004; Pineros and Tester, 1997; Rengel *et al.*, 1995; Rengel and Zhang, 2003).

The combined low-pH/Al^{3+} treatment decreased shoot Mg^{2+} concentration in long-term experiments (7-d exposure) (**Figure 5.5**), whereas short-term experiments (0-60 min) revealed that 50 μM Al induced Mg^{2+} influx (**Figure 5.7**, **Figure 5.8**) and a rise in intracellular Mg^{2+} concentration (**Figure 5.9**). In addition, 500 μM Al^{3+} induced a shift of Mg^{2+} fluxes towards efflux (**Figure 5.7**). Therefore, we observed an aggregate effect of external Al concentration and the time of exposure in long-term experiments. Our study clearly demonstrate competitive interactions between Al^{3+} and membrane transporters for Mg^{2+} (Rengel, 1990; Rengel and Robinson, 1989b) at high Al concentrations (100 and 500 μM Al; **Figure 5.7**). The reason for a decrease in shoot Mg^{2+} concentration at all Al concentrations in long-term experiments can be explained by Al-induced impairment of root growth and a consequent decrease in the nutrient-absorbing surface area (Clarkson, 1985) and/or prolonged Al^{3+} exposure disturbing many biochemical and physiological processes. Thus, secondary effects (not directly caused by Al^{3+}) can affect Mg^{2+} uptake in long-term experiments (Rengel and Robinson, 1989a).

Mg^{2+} is an activator of more enzymes than any other element (eg. RNA polymerases, ATPases, protein kinases, phosphatases, glutathione synthase and carboxylases) and is involved in ion transport and cation balance in plants (see Shaul, 2002 for references). Considering the importance of Mg^{2+} in plants, it is surprising to note that only Yazaki *et al.* (1988) measured free Mg^{2+} concentration (0.4 mM) in the cytoplasm of Mg-sufficient mung bean root tips using *in vivo* ^{31}P NMR spectroscopy. Though intracellular free Mg^{2+} concentration was measured in animal cells using Magnesium-Green™ fluorescent dye (Gotoh *et al.*, 1999; Montezinho *et al.*, 2002; Sharikabad *et al.*, 2001), to our knowledge the present study is the first intracellular Mg^{2+} measurement in plants using Mg-sensitive dyes. Under no stress (pH 5.5) we measured 0.92 ± 0.04 mM Mg^{2+} in the root epidermal cells of distal elongation zone (**Figure 5.9**); this figure is higher than the 0.4 mM reported for mung been root tips

(Yazaki *et al.*, 1988). The reason for this discrepancy is likely due to the fact that the measurements done by Yazaki *et al.* (1988) represented an average for the whole root tip tissues, whereas our measurements were on individual cells in distal elongation zone.

The low-pH treatment did not alter intracellular free Mg^{2+} concentration in *Arabidopsis* root epidermal cells, whereas 50 μM Al^{3+} exposure resulted in a roughly 2-fold increase (to 1.63 ± 0.07 mM) in intracellular free Mg^{2+} concentration (**Figure 5.9**). This rise in intracellular Mg^{2+} concentration might have been due to (i) influx of Mg^{2+} ions into the root tissue from the external medium (**Figure 5.7**, **Figure 5.8**) and/or (ii) intracellular ATP hydrolysis because ATP hydrolysis usually results in increased intracellular Mg^{2+} concentration (Gotoh *et al.*, 1999; Leyssens *et al.*, 1996). Indeed, Al^{3+} concentrations below the phytotoxicity threshold enhanced ATP hydrolysis in maize roots (Facanha and Okorokova-Facanha, 2002) and in fungus *Yarrowia lipolytica* (Lobão *et al.*, 2007).

On the other hand, exposure of *Arabidopsis* roots to Al^{3+} concentrations higher than 50 μM (100 and 500 μM Al^{3+} treatments) decreased intracellular Mg^{2+} concentrations in a dose-dependent manner (**Figure 5.9**). This decline might be explained by the decreased Mg^{2+} influx, or even efflux at 500 μM Al^{3+} (**Figure 5.7**), caused by Al^{3+} inhibition of plasma membrane cation channels because the driving force for Mg^{2+} transport within the first 10 min under these conditions would have been directed inward [driving force for Mg(E^{D}_{Mg}) = -30 to -50 mV]. The driving force calculations were based on external and internal Mg^{2+} concentrations (0.2 mM and 0.9 mM, correspondingly) and E_m during the first 10 min of Al^{3+} application (-50 to -70 mV, **Figure 4.9**).

Based on our results we can propose at least three Mg-related mechanisms that can contribute to amelioration of Al^{3+} toxicity at relatively low Al^{3+} concentrations. Firstly, given that Mg^{2+} is crucial for maintaining H^+-ATPase activity on the plasma membrane (Costa and de Meis, 1996), Al-induced Mg^{2+} influx might have maintained H^+-ATPase activity at the plasma membrane surface, which in turn fuelled other transports, including Al-tolerance-related organic acid anion release (Silva *et al.*, 2001a).

Secondly, elevated Mg^{2+} could stimulate organic acid synthesis and release to detoxify Al^{3+} ions. Intracellular Mg^{2+} regulates many enzymes that are involved in organic acid anion synthesis and metabolism in plants (Coleman and Palmer, 1972; Doyle *et al.*, 2001; Howard *et al.*, 2000; Iglesias and Andreo, 1990). Further, Silva *et al.* (2001a) found that pre-treatment of soybean seedlings with Mg^{2+} and subsequent exposure to Al^{3+} resulted in enhanced citrate secretion within an hour compared with seedlings without Mg^{2+} pre-treatment. This might imply that pre-treatment with Mg^{2+} 'primes' the citrate synthesis mechanism for organic acid release upon exposure to Al^{3+} stress. In our experiments, *Arabidopsis* seedlings were grown or conditioned with 200 µM Mg^{2+}, and Al treatments were imposed in the presence of 200 µM Mg^{2+}; these low Al treatments (50 and 100 µM Al) induced Mg^{2+} influx. Hence, we suggest that the presence of Mg^{2+} in the pre-treatment and subsequent Mg^{2+} influx under mild Al^{3+} stress observed in our experiments might have facilitated synthesis and release of organic acid anions following Al exposure. This hypothesis got support from a recent microarray analysis using *Arabidopsis* wild type (Col-0) in which 50 µM Al^{3+} (pH 4.0) up-regulated activity of Mg^{2+}-requiring malate dehydrogenase (Goodwin and Sutter, 2009).

Thirdly, up-regulation of transporter genes (Zhang *et al.*, 2007), particularly those for high-affinity Mg^{2+} transporters such as *AtMGT1* gene in *Nicotiana benthamiana* (Deng *et al.*, 2006) and *ALR1/ALR2* gene (yeast CorA Mg^{2+} transporters) in *Saccharomyces cerevisiae* (MacDiarmid and Gardner, 1998), can contribute to amelioration of Al^{3+} toxicity. In our studies, 50 µM Al^{3+} exposure caused an instantaneous increase in Mg^{2+} influx into the root cells; hence, we hypothesize that up-regulation of Mg^{2+} transporters by low Al^{3+} concentration might have occurred. High Al^{3+} concentrations (≥100 µM) resulted in lower Mg^{2+} influx or even efflux from the root cells (**Figure 5.7**), suggesting competitive binding of Al^{3+} ions onto the Mg^{2+} transport system (Rengel, 1990; Rengel and Robinson, 1989b). This Al^{3+} binding could have occurred on the *AtMGT1* protein because Li *et al.* (2001) reported inhibition of *AtMGT1* by Al^{3+} ions.

In summary, the lower Mg^{2+} concentration in shoots in long-term experiments is the combined effect of external Al^{3+} concentrations as well as prolonged exposure time (7 d). In short-term experiments, high Al^{3+} treatment (500 µM) most likely affects Mg^{2+}

uptake by inhibiting the activity of plasma membrane Mg^{2+} permeable cation channels. Moderate concentrations of Al^{3+} ($\leq$ 50 µM) enhanced the uptake of Mg^{2+} and raised intracellular Mg^{2+} concentrations, which might play a key role in fueling organic acid synthesis and release to combat moderate Al^{3+} toxicity in acid soils. By contrast, all the low pH/Al^{3+} treatments induced Ca^{2+} efflux from the distal elongation and mature root zones within the first minute. Hence, displacement of Ca^{2+} from sensitive sites together with Ca^{2+} influx inhibition could be among the primary causes of Al^{3+} toxicity in *Arabidopsis thaliana*.

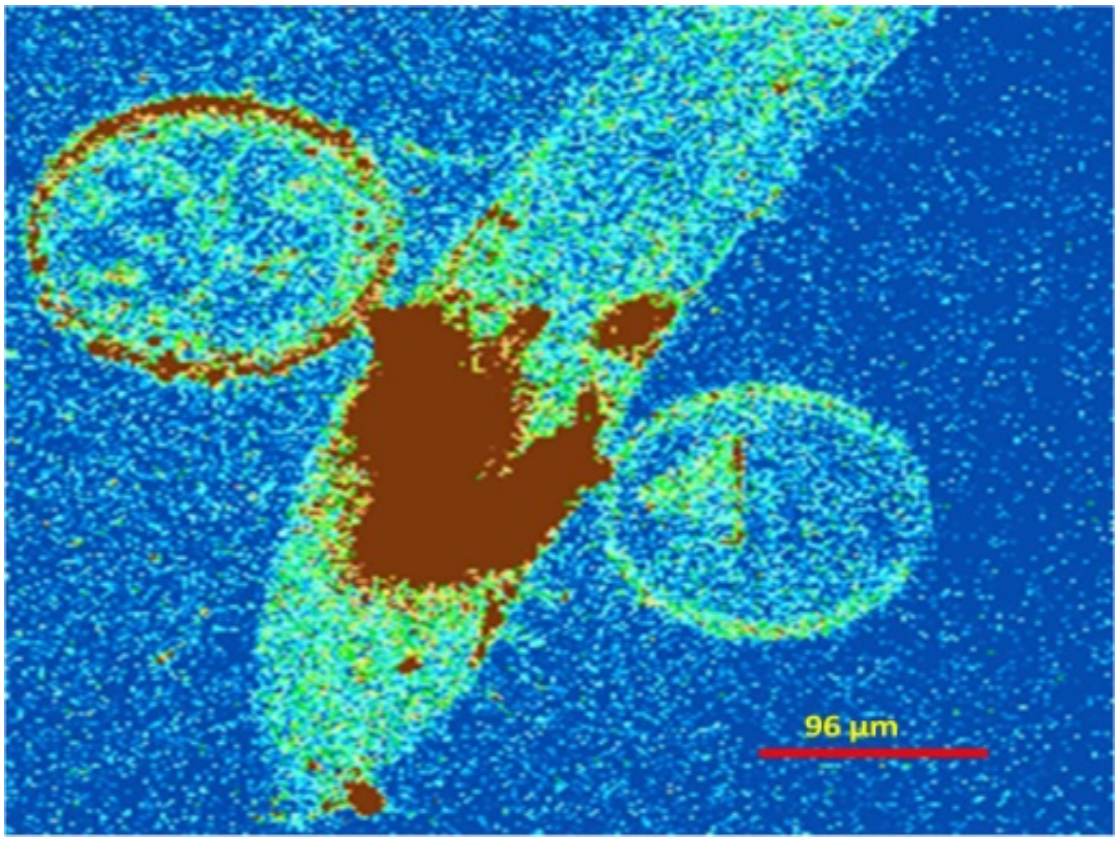

Figure 5.1 Representative conventional confocal image of *Arabidopsis* root bursting, when the roots were treated high ($\geq$ 5 µM) concentrations of Magnesium Green ™ fluorescent dye.

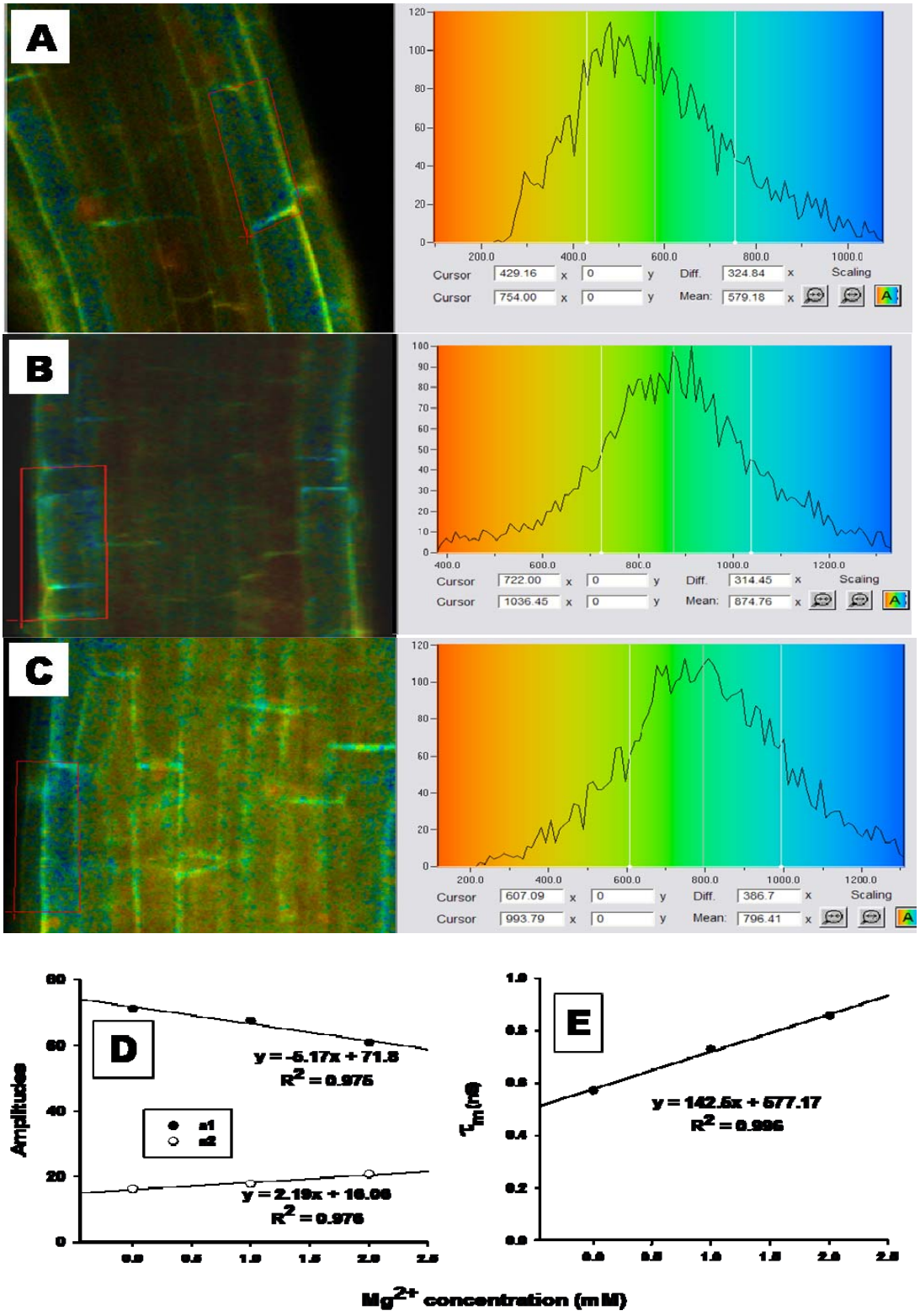

Figure 5.2 Magnesium Green-AM^{TM} fluorescent dye loading in *Arabidopsis thaliana* roots and *in vivo* calibration using fluorescence lifetime imaging (FLIM).
Colour coding of images A and B was based on distribution of fluorescence molecules excited by 850-nm light. Mean lifetime (τ_m) was calculated from triple exponential decay. Red colour lines in images represent regions of interest (epidermal root cells). (A) Effect of 1-h incubation in basal salt medium (BSM; 0.1 mM $CaCl_2$ + 1 mM KCl + 0.2 mM $MgCl_2$, pH 5.5) containing 200 µM EGTA-AM (Ethylene glycol-bis(beta-

aminoethyl ether)-N,N,N',N'-tetraacetic acid-, tetra(acetoxymethyl ester)) and 2.0 mM EGTA on lifetime distribution of fluorescence molecules in *Arabidopsis* root cells (τ_m 579 ps). (B) effect of 1-h perfusion with 2.0 mM Mg^{2+} plus 200 μM A23187 ionophore on lifetime distribution of fluorescence molecules in *Arabidopsis* root cells (τ_m 875 ps). (C) Lifetime distribution of Magnesium Green fluorescence dye in root cells after 1 h of acid loading of 1.5 μM Magnesium Green-AM™ on ice and 12 h of recovery in basal salt medium. The τ_m after Magnesium Green-AM™ loading was 796 ps. The orange/yelow colour indicates lower, and blue colour relatively higher, Mg^{2+} concentration within cells. (D) Amplitudes calculated from triple exponential decay of Magnesium Green-AM™ fluorescence dye for different Mg^{2+} concentrations. (E) *in vivo* calibration curve of mean lifetime (τ_m) used to calculate intracellular Mg^{2+} concentrations.

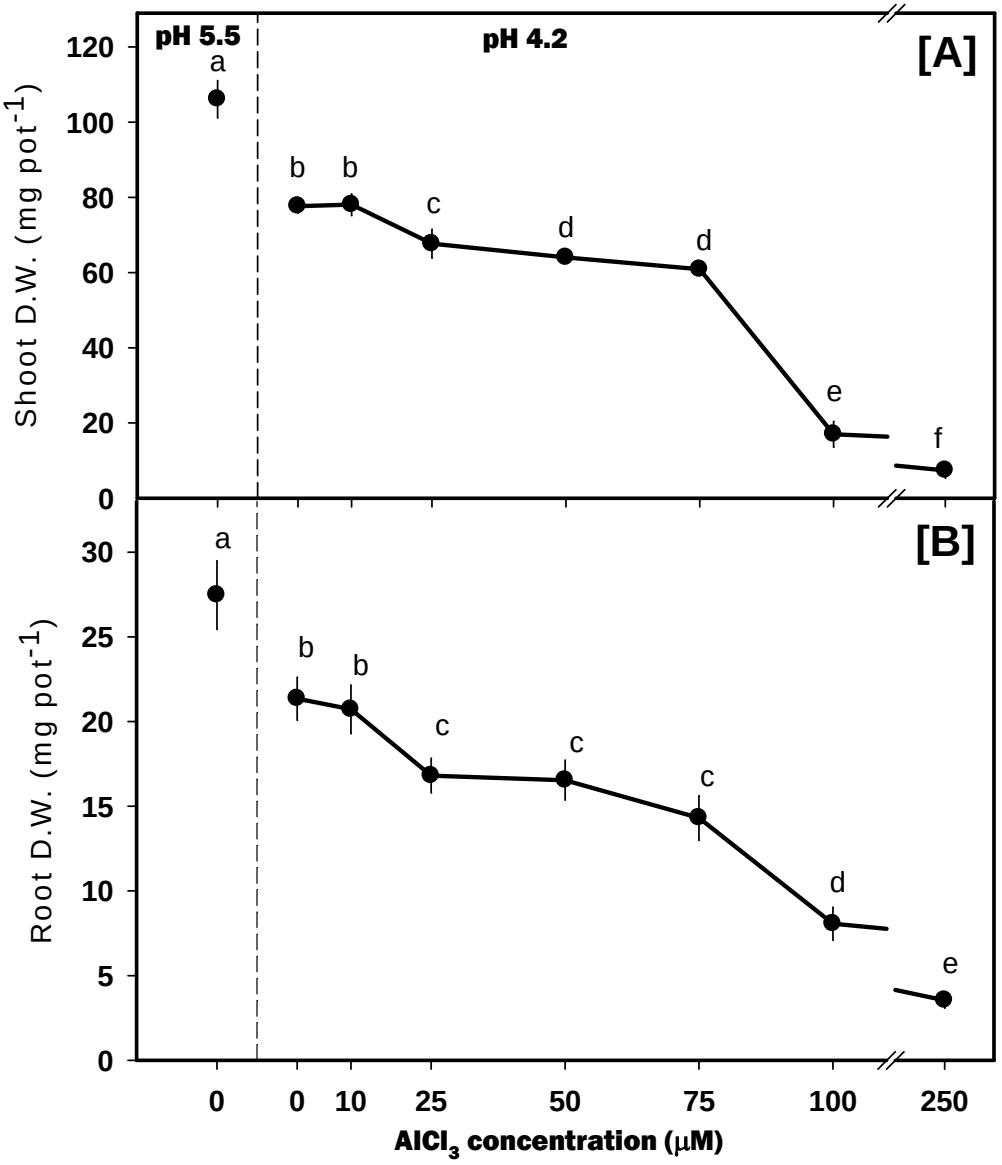

Figure 5.3 Long-term (7 d) effect of low-pH (pH 4.2, 0 μM Al) and combined low-pH/Al stresses on *Arabidopsis thaliana* [A] shoot biomass; and [B] root biomass.

Means ± SE (n = 3 replicates). SE bars are frequently smaller than the data symbol. In each graph, points sharing common letters are not significantly different by LSD test at $p \leq 0.05$.

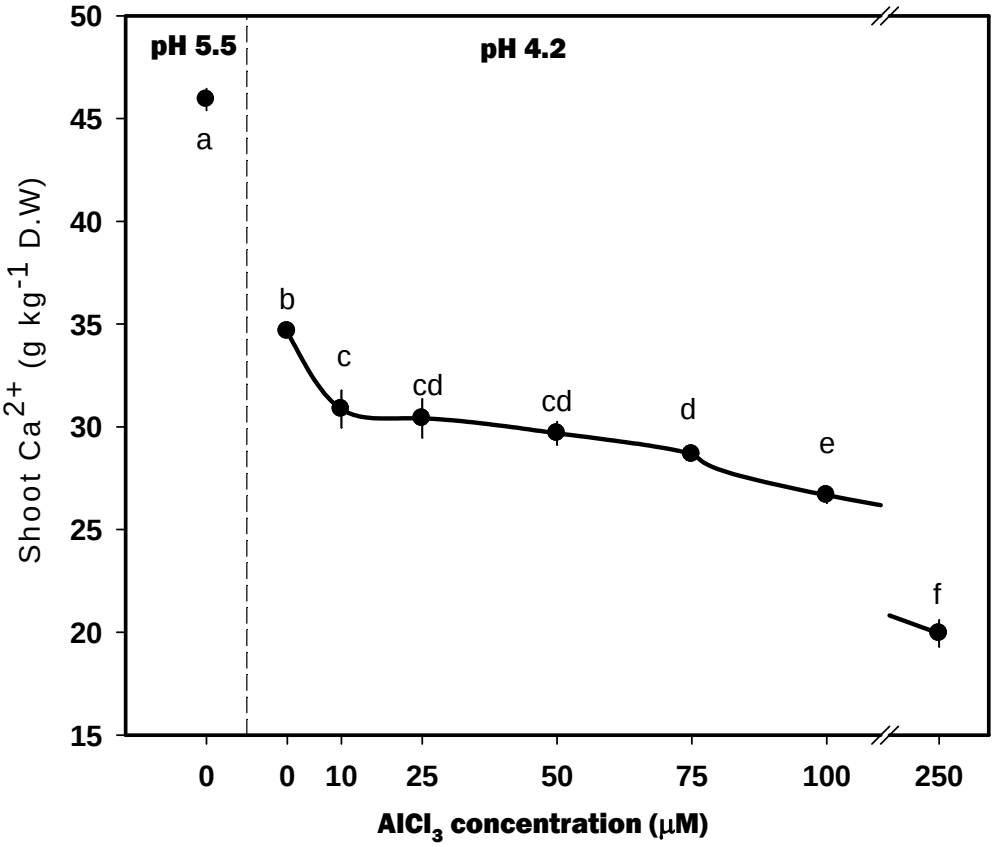

Figure 5.4 Long-term (7 d) effect of low-pH (pH 4.2, 0 μM Al) and combined low-pH/Al stresses on *Arabidopsis thaliana* shoot Ca^{2+}concentration.
Means ± SE (n = 3 replicates). SE bars are frequently smaller than the data symbol. Points sharing common letters are not significantly different by LSD test at $p \leq 0.05$.

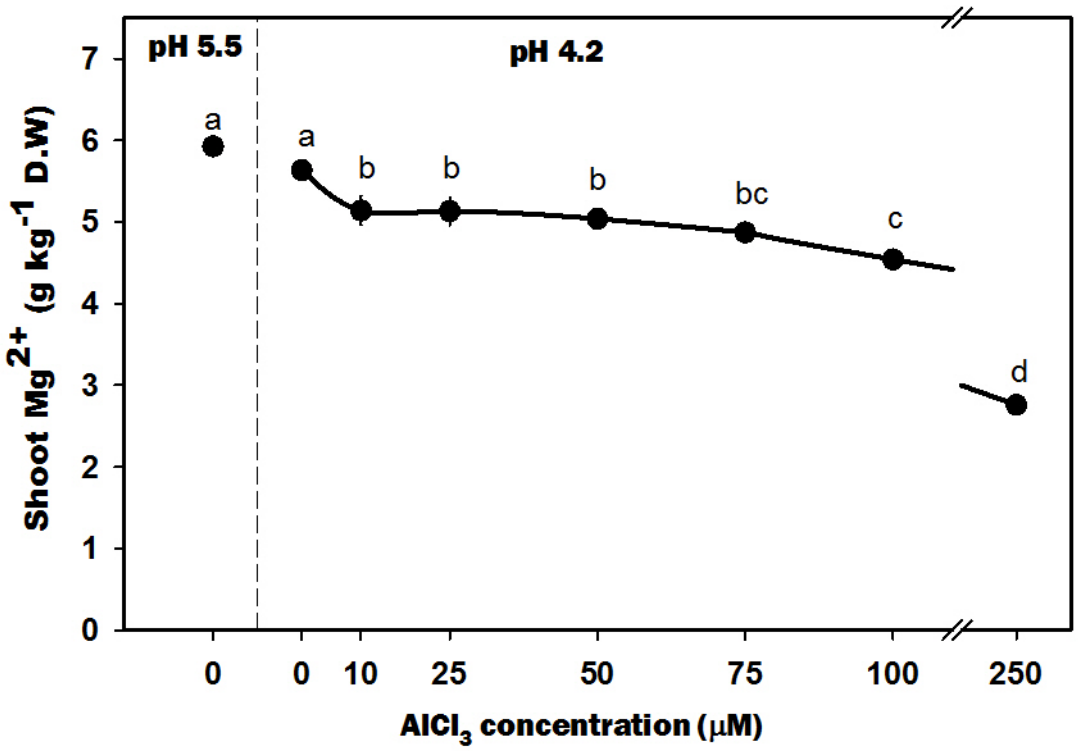

Figure 5.5 Long-term (7 d) effect of low-pH (pH 4.2, 0 μM Al) and combined low-pH/Al stresses on *Arabidopsis thaliana* shoot Mg^{2+}concentration.
Means ± SE (n = 3 replicates). SE bars are frequently smaller than the data symbol. Points sharing common letters are not significantly different by LSD test at $p \leq 0.05$.

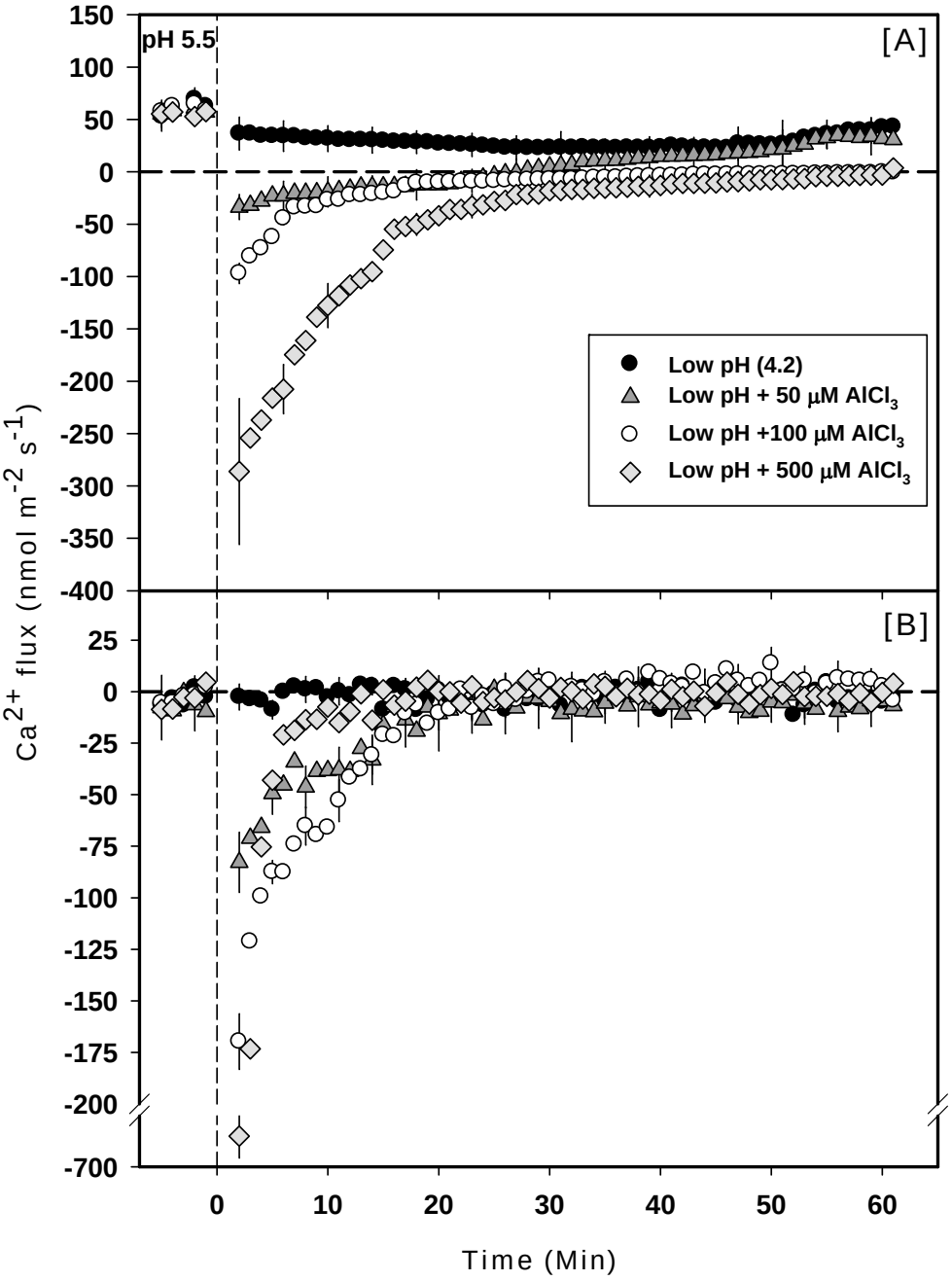

Figure 5.6 Effect of low pH and Al^{3+} stresses on Ca^{2+} fluxes measured at [A] distal elongation zone and [B] mature zone of four- to five-day-old *Arabidopsis thaliana* roots.

Low pH and combined low pH/Al^{3+} treatments imposed at time = 0; the data recorded in the first 5 minutes before time = 0 represent Ca^{2+} fluxes at the respective root zones at pH 5.5. Negative Ca^{2+} flux values indicate Ca^{2+} efflux, and positive values indicate Ca^{2+} influx. Error bars indicate ± SE (n = 6 to 12 plants).

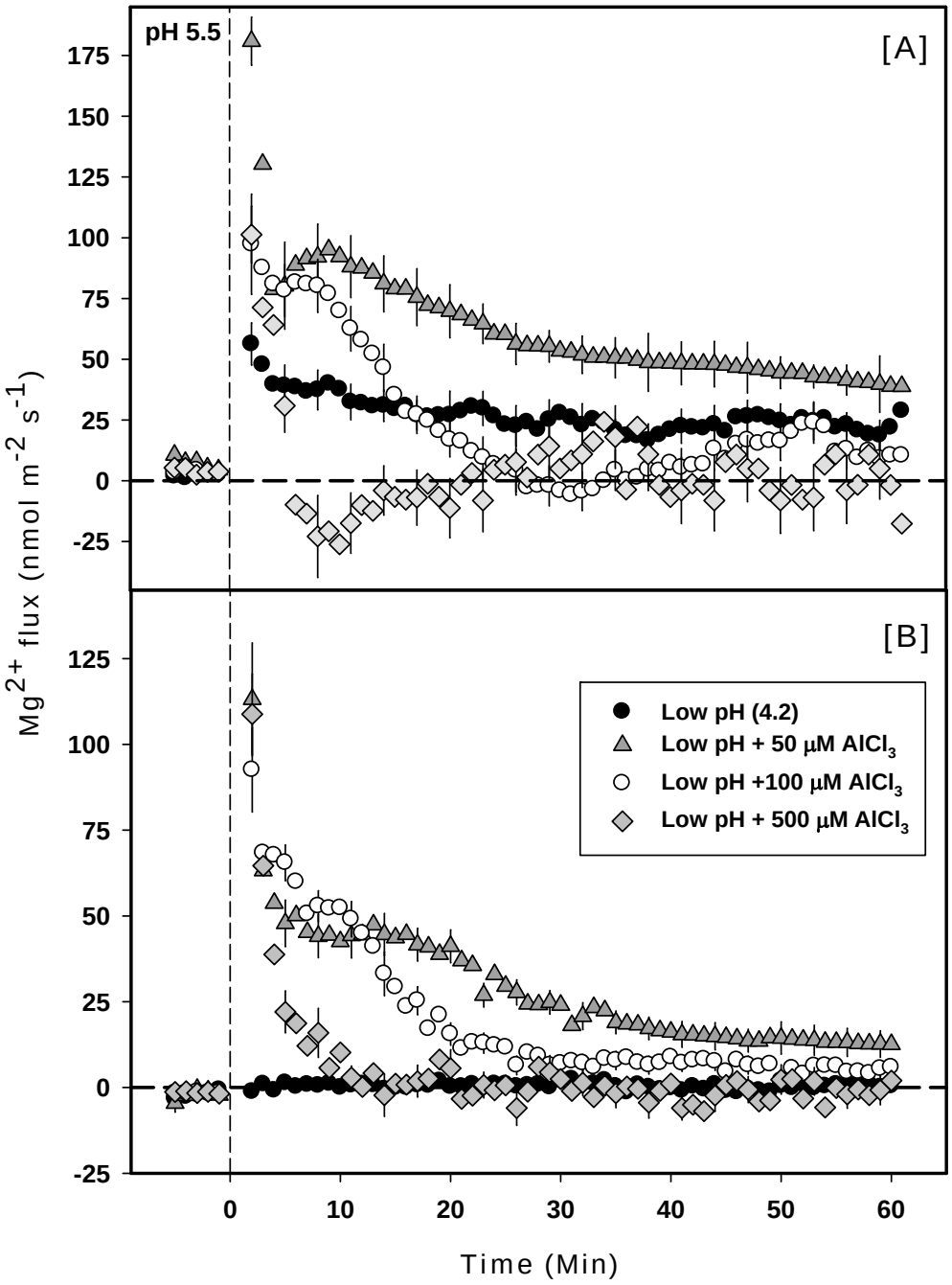

Figure 5.7 Effect of low-pH and combined low-pH/Al stresses on Mg^{2+} fluxes measured at [A] distal elongation zone and [B] mature zone of four- to five-day-old *Arabidopsis thaliana* roots.
Low-pH and combined low-pH/Al treatments imposed at time = 0; the data recorded in the first 5 minutes before time = 0 represent Mg^{2+} fluxes at the respective root zones at pH 5.5. Negative Mg^{2+} flux values indicate Mg^{2+} efflux, and positive values indicate Mg^{2+} influx. Error bars indicate ± SE (n = 6 to 18 plants).

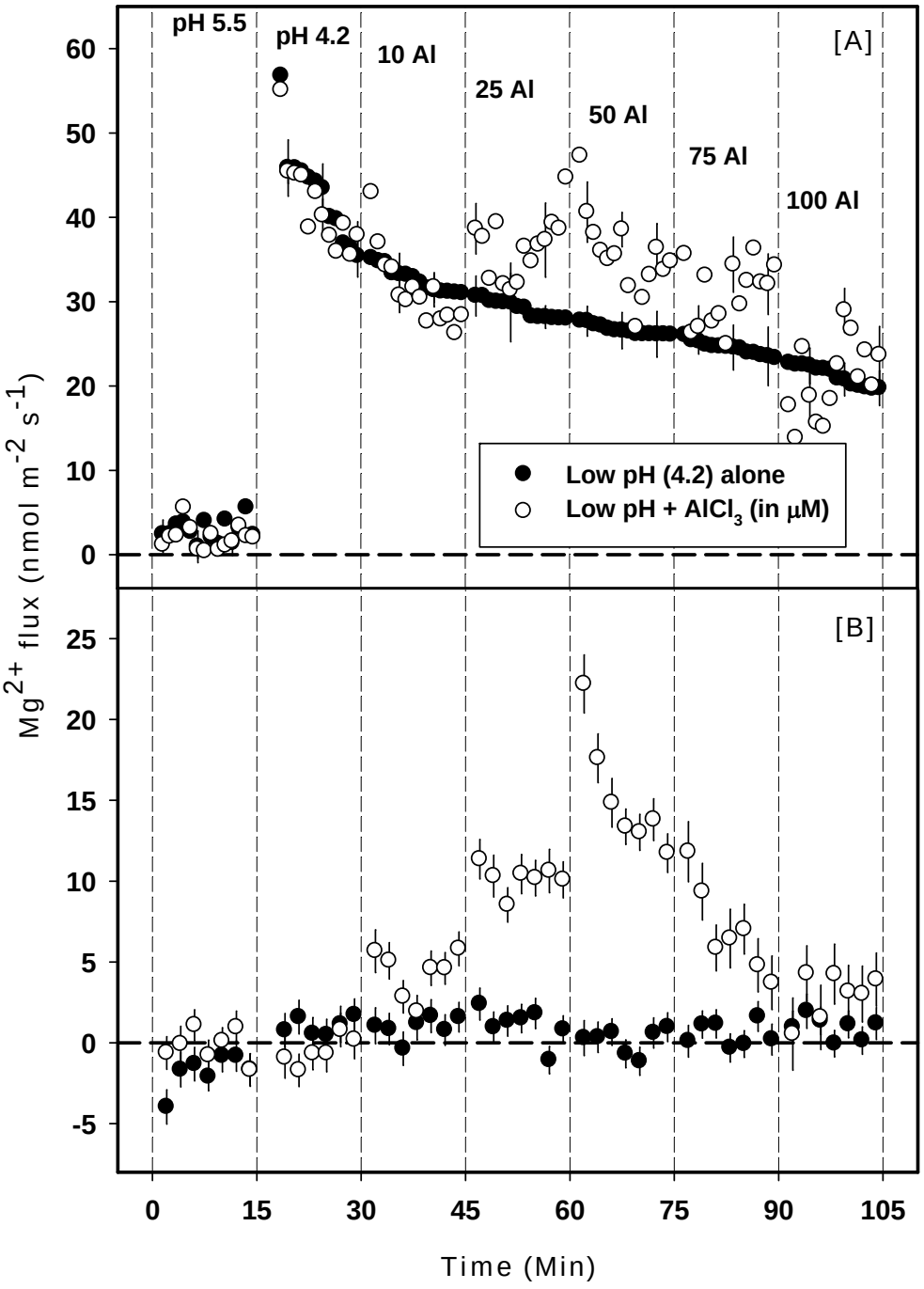

Figure 5.8 Effect of low-pH and gradual addition of Al on Mg^{2+} fluxes measured at [A] distal elongation zone and [B] mature zone of four- to five-day-old *Arabidopsis thaliana* roots.

The data recorded in the first 15 minutes represent Mg^{2+} fluxes at the respective root zones at pH 5.5. The low-pH treatment was imposed at time = 15 minutes, followed by measurements of Mg^{2+} fluxes for up to 105 minutes. Combined low-pH/Al treatments from 0 to 100 μM Al were imposed at 15-minute intervals. Negative Mg^{2+} fluxes indicate Mg^{2+} efflux, and positive values indicate Mg^{2+} influx. Error bars indicate ± SE (n = 10 to 12 plants).

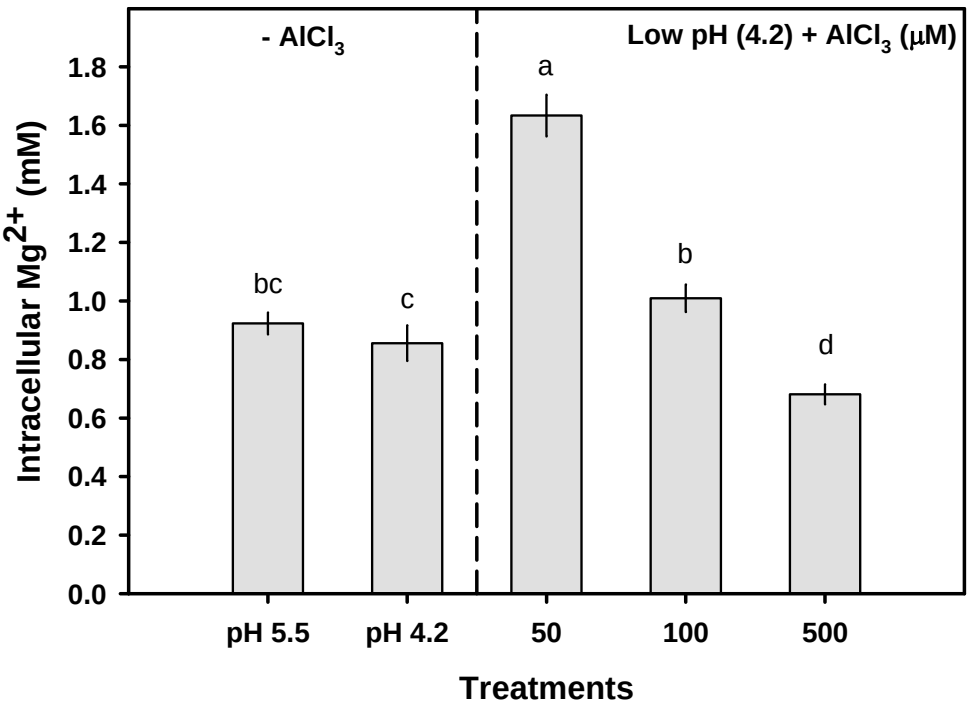

Figure 5.9 Intracellular Mg^{2+} concentration measured in the epidermal cells of elongation root zone of four- to five-day-old *Arabidopsis thaliana* after 10 minutes of the low-pH (4.2) or combined low-pH/Al treatments using Fluorescence Life Time Imaging (FLIM) of Magnesium Green™ dye.
Error bars indicate ± SE (n = 6 to 10 plants). Bars sharing common letters are not significantly different by LSD test at $p \leq 0.001$.

Chapter 6

Aluminium-induced ion transport in Arabidopsis: The relationship between Al tolerance and root ion flux

Jayakumar Bose[1], Olga Babourina[1], Sergey Shabala[2] and Zed Rengel[1]

[1]School of Earth and Environment, the University of Western Australia, Crawley WA 6009, Australia

[2]School of Agricultural Science, University of Tasmania, Hobart TAS 7001, Australia

Abstract

Aluminium rhizotoxicity coincides with low pH; however, it is unclear whether plant tolerance to these two factors is controlled by the same mechanism. To address this question, Al-resistant *alr104* mutant, two Al-sensitive mutants (*als3* and *als5*) and the wild type *Arabidopsis thaliana* were compared in long-term exposure (solution culture) and in short-term experiments (for measuring H^+ and K^+ fluxes, rhizosphere pH and plasma membrane potential, E_m).

Based on biomass accumulation, *als5* and *alr104* showed tolerance to low pH (4.20), whereas *alr104* was tolerant to the combined low-pH/Al treatment (50 μM Al). The sensitivity of *als5* and *als3* mutants to the Al stress was similar. The Al-induced decrease in H^+ influx at the distal elongation zone and Al-induced H^+ efflux at the mature zone were higher in Al-sensitive mutants (*als3* and *als5*) than in the wild type and *alr104* mutant. Under combined low-pH/Al treatment, *alr104* and the wild type had depolarised plasma membranes for the entire 30-min measurement period, whereas in Al-sensitive mutants (*als3* and *als5*), initial depolarisation to around -60 mV became hyperpolarisation at -110 mV after 20 min. At the distal elongation zone, the E_m changes corresponded with the changes in K^+ flux: K^+ efflux was higher in *alr104* and the wild type than in *als3* and *als5* mutants.

In conclusion, Al tolerance in *alr104* mutant correlated with E_m depolarisation, higher K^+ efflux and higher H^+ influx, which led to alkalinisation of the rhizosphere

under the combined low-pH/Al stress. Low-pH tolerance (*als5*) was linked to higher H^+ uptake under low-pH stress, which was abolished by Al exposure.

Keywords: Aluminium toxicity, distal root elongation zone, H^+ flux, K^+ flux, low pH, mature root zone, plasma membrane potential.

6.1 Introduction

Phytotoxic aluminium adversely affects root growth in acidic soils. A number of mechanisms responsible for Al tolerance have been characterised in plants, such as (i) release of organic acid anions(OAA) (e.g. Hoekenga *et al.*, 2006; Kochian *et al.*, 2004; Liu *et al.*, 2009; Ma *et al.*, 1997c; Ryan *et al.*, 2009); (ii) release of phenolic compounds (Kidd *et al.*, 2001); (iii) rhizosphere alkalinisation (Degenhardt *et al.*, 1998); (iv) internal detoxification of Al by complexation with organic acid anions (Ma *et al.*, 2001; Shen *et al.*, 2002) and (v) redistribution of accumulated Al away from sensitive root tissues (Larsen *et al.*, 2005). However, the low pH itself can affect root growth in various plant species (Arnon and Johnson, 1942; Iuchi *et al.*, 2007; Kidd and Proctor, 2001; Kinraide, 2003; Koyama *et al.*, 2001; Lazof and Holland, 1999; Llugany *et al.*, 1995; Rangel *et al.*, 2005; Sawaki *et al.*, 2009). Nevertheless, our knowledge of proton toxicity and the molecular mechanisms underlying low-pH tolerance is rather limited when compared to Al tolerance.

Low-pH tolerance and K^+ nutrition appear to be interlinked in some plants species because the addition of K^+ to the external medium alleviated H^+ toxicity in maize (Yan *et al.*, 1992), common bean (Rangel *et al.*, 2005) and sugar beet (Lindberg and Yahya, 1994). Also, down-regulation of CIPK23, which encodes the regulatory kinase of a major K^+ transporter AKT1, may be responsible for the higher sensitivity of the Arabidopsis *stop1* mutant to low pH (Iuchi *et al.*, 2007; Sawaki *et al.*, 2009). Although the detailed mechanism underlying this phenomenon is unclear, the increased internal K^+ concentration could be due to changes in K^+ transport at the root/soil interface via either increased K^+ uptake or decreased K^+ efflux. Lower K^+ efflux under Al exposure in comparison to low-pH exposure has been reported for soybean cells grown in suspension culture (Stass and Horst 1995), which might indicate Al-induced changes in the plasma membrane potential (E_m) because K^+ transport and accumulation

in roots is highly interlinked to E_m. Hence, E_m and K^+ flux need to be assessed simultaneously to elucidate the role of K^+ nutrition in low-pH tolerance.

In *Arabidopsis*, the patterns of root damage caused by H^+ are distinct from those induced by Al (Koyama *et al.*, 1995). Furthermore, an *Arabidopsis* QTL analysis revealed that Al tolerance and H^+ tolerance are controlled by different genetic factors (Ikka *et al.*, 2007). In contrast, the proton hypersensitive *Arabidopsis stop1* (sensitive to proton rhizotoxicity 1) mutant is also hypersensitive to Al (Iuchi *et al.*, 2007; Sawaki *et al.*, 2009). Therefore, H^+ and Al tolerances could be independent with respect to some genotypes and interlinked in other genotypes of *Arabidopsis thaliana*.

Based on this hypothesis, we studied low-pH tolerance of an Al-resistant mutant, *alr104*, which has a higher rhizosphere alkalinising capacity than the wild type (Degenhardt *et al.*, 1998; Larsen *et al.*, 1998), and two Al-sensitive mutants, *als3* [defective in an ABC transporter-like protein (Larsen *et al.*, 2005)), and *als5* [defective in Al exclusion (Larsen *et al.*, 1996)]. The Al stress is inevitably studied in combination with the low-pH stress; as a result, genotypes more sensitive to one stress were occasionally classified as being tolerant to the other stress (see Lazof and Holland, 1999 for references). Hence, we separated the effects of low pH from combined low-pH/Al effects and re-examined Al susceptibility or tolerance of these *Arabidopsis* mutants by measuring rhizosphere alkalinisation capacity, internal K^+ concentration, changes in the plasma membrane potential (E_m) and the H^+ and K^+ net fluxes. We found that *als5* mutant was tolerant to low pH but sensitive to Al, whereas *alr104* was tolerant and *als3* sensitive to both low pH and Al.

6.2 Material and methods

6.2.1 Long-term exposure experiments: Hydroponic culture

Arabidopsis thaliana L. seeds were surface sterilised with 1% (v/v) calcium hypochlorite for 10 minutes. Seeds were then sown on rock-wool strips (1-2 mm thick and 5-6 cm long) that were placed into 250-mL plastic containers containing $1/10^{th}$ Hoagland solution. The containers were kept at 4^oC for 2 d to achieve synchronised germination. Seedlings were then moved to a growth cabinet with 16 h light (150 µmol m^{-2} s^{-1}) and 8 h dark at 20 ± 1^oC. Three-week-old seedlings (**Figure 6.1**) were used to

conduct two sets of long-term exposure experiments. During the first set of experiments, *Arabidopsis thaliana* L. wild type ecotype Col-0 and Al-sensitive mutant (*als3* and *als5*) seedlings were exposed to either pH 5.5 or 4.2 with or without 0.5 mM homo-PIPES buffer for 10 days in quadruplicate. Nutrient solutions were changed daily. During the treatment period, the bulk solution pH was measured on the second day at 12 and 24 h after the nutrient solution was changed.

During the second set of experiments, 3-week-old seedlings [wild type (ecotype Col-0), *als3*, *als5* and *alr104*] were exposed to pH 5.5 and a range of Al concentrations (0, 10, 25, 50, 75, 100 or 250 μM $AlCl_3$; pH 4.2) in 0.5 mM homo-PIPES buffer for 7 d. The treatments were performed in triplicate, and the treatment solutions were changed daily.

At the end of experiments, shoots and roots were separately harvested, washed with 100 μM $CaSO_4$, rinsed with deionised water, dried in an oven at 70^{o}C for 72 hours and weighed. Dried shoots were digested with a HNO_3:$HClO_4$ (10:1) mixture. The K^+ concentration was analysed using inductively coupled plasma-mass spectrometry (ICP-MS).

6.2.2 Short-term exposure experiments

Arabidopsis thaliana L. wild type (ecotype Col-0), *als3*, *als5* and *alr104* seeds were surface sterilised with 1% (w/v) calcium hypochlorite. Seedlings were grown in 90-mm Petri dishes under constant fluorescent light (150 μmol m^{-2} s^{-1}) and temperature (23-25^{o}C) in 0.8% (w/w) agar media containing basal salt medium (BSM) with 0.1 mM $CaCl_2$, 1 mM KCl and 0.2 mM $MgCl_2$, pH 5.5. The Petri dishes were oriented upright, so the roots grew down along the agar surface without penetrating it. However, roots were anchored in the agar by root hairs.

Four- to five-day-old seedlings of wild type (ecotype Col-0), *als3*, *als5* and *alr104* mutants were conditioned in BSM at pH 5.5 for 20 minutes followed by either low pH (pH 4.2) or combined low-pH/50 μM $AlCl_3$ treatment. All measurements were made at the root distal elongation zone (DEZ; 200 μm away from the root cap) and the mature zone (MZ; 700 μm from the root cap).

Net fluxes of H^+ and K^+ and rhizosphere pH were measured 40 µm away from the root surface using the non-invasive MIFE® system (University of Tasmania, Hobart, Australia) as described by Newman (2001). Microelectrodes were pulled from borosilicate glass capillaries (GC 150-10, SDR Clinical Technology, Middle Cove, Australia), oven dried at 230ºC for about 5 h and silanised using tributylchlorosilane (Fluka catalogue no. 90796). Electrodes with an external tip diameter of 2-3 µm were used. The electrodes were back-filled with the appropriate solution (0.15 mM NaCl and 0.4 mM KH_2PO_4 adjusted to pH 6.0 using NaOH for the H^+ electrode and 0.5 M KCl for the K^+ electrode). The electrode tips were then front-filled with ionophore cocktails (Fluka catalogue no. 95297 for H^+ and no. 60031 for K^+). The prepared electrodes were calibrated with a set of standards (pH from 3.2 to 6.5; K^+ from 0.5 to 10 mM). Electrodes with the slopes of less than 50 mV per 10 units were discarded.

The roots of an intact 4- to 5-day-old *Arabidopsis* seedling were gently secured horizontally in a measuring chamber with a Parafilm strip and small plastic blocks. The seedling was then placed in the measuring chamber containing BSM and conditioned for at least 20 minutes. The E_m measurements were conducted according to the procedure outlined in Cuin and Shabala (2005). The borosilicate glass microelectrodes (Shabala and Lew, 2002) (Clarke Electrochemical Instruments, Reading, UK) were filled with 1 M KCl, connected to an IE-251 electrometer (Warner Instruments, Hampden, CT) via the Ag-AgCl half-cell and inserted into the root tissue (distal elongation zone or mature zone) with a manually operated micromanipulator (MMT-5, Narishige, Tokyo, Japan). The E_m was monitored continually using the CHART software (see Newman 2001 for details). Once a stable measurement of E_m was obtained for 1 minute, treatments with either low pH (pH 4.2) or combined low-pH/50 µM $AlCl_3$ were initiated, and the E_m was measured for about 30 minutes. Eight to twelve plants were measured for every treatment, and the data were averaged.

6.3 Results

6.3.1 Long-term exposure experiments: low pH and low-pH/Al stresses in buffered and non-buffered media

6.3.1.1 Alkalinisation capacity and growth of Arabidopsis mutants under low pH

Measurements of the bulk solution pH were made after 12 h and 24 h (**Figure 6.2**). The results revealed that 0.5 mM homo-PIPES buffer was sufficient to keep the pH around 4.2 or 5.5 (depending on the treatment) for at least 24 hours. In non-buffered medium, within 12 hours the plants increased the media pH from 4.2 to 5.1-5.6 depending on the genotype (**Figure 6.2**). Of the three genotypes tested, mutants *als5* and *als3* were the most and the least effective, respectively, in increasing the media pH.

After 10 days in non-buffered medium, the low-pH treatment decreased the biomass of the wild type and *als3* mutant, whereas low-pH stress enhanced growth of *als5* mutant (**Figure 6.3**); there were no differences in growth of *als5* at the two pHs in the buffered medium. For the wild type and *als3* mutant, biomass was similar in the buffered and non-buffered media.

6.3.1.2 Effect of low pH and Al on root biomass and shoot K^+ concentration

In the homo-PIPES-buffered medium, the low-pH treatment retarded root biomass of the wild type and *als3* mutant, whereas root biomass of *alr104* and *als5* mutants was unaffected. *als3* mutant showed a greater reduction in root biomass in the low pH treatment compared to the wild type (**Figure 6.4**A). The addition of Al severely inhibited root biomass of the Al-sensitive mutants (*als3* and *als5*), even at a low concentration (10 μM), whereas root biomass reduction in the wild type was observed at Al concentrations ≥ 25 μM. Root biomass of Al-resistant mutant *alr104* was inhibited only at ≥ 75 μM Al (**Figure 6.4**A). Al-related root biomass reduction was greater in the sensitive mutants (*als3* and *als5*) compared to the wild type and was the lowest in the resistant mutant (*alr104*).

The shoot K^+ concentration did not differ among the genotypes in the pH 5.5 treatment (**Figure 6.4**B). In low pH treatment, the Al-sensitive mutants (*als5* and especially *als3*) had higher shoot K^+ concentrations compared to the wild type.

Interestingly, the shoot K^+ concentration of Al-resistant mutant *alr104* did not differ from the wild type under any treatment. In all Al treatments, Al-sensitive mutant *als3* had higher shoot K^+ concentrations than any other genotype.

6.3.2 Short-term exposure experiments: microelectrode measurements during low pH and low-pH/Al stresses

6.3.2.1 Rhizosphere pH

In the low-pH treatment, *alr104* and *als5* mutants had higher rhizosphere pH than the wild type and *als3* mutant in both the distal elongation and the mature root zones. No significant rhizosphere pH change was observed between the wild type and *als3* mutant in both root zones, except for the first 12 minutes in distal elongation zone when *als3* mutant demonstrated a slightly lower pH than the wild type (**Figure 6.5**).

The combined low-pH/50 μM Al treatment resulted in lower rhizosphere pH than the low-pH treatment in both root zones of all genotypes tested. However, Al-resistant *alr104* mutant had a rhizosphere pH that was 0.1 ± 0.01 units higher than the wild type in the distal elongation zone. In the mature zone, *alr104* mutant demonstrated a higher pH than the wild type for the first 4 minutes, but there was no significant difference afterwards. Both Al-sensitive mutants had lower rhizosphere pH compared to the wild type and *alr104* in both root zones (**Figure 6.5**).

6.3.2.2 H^+ fluxes

At pH 5.5, a small net H^+ influx in the distal elongation zone and a small net H^+ efflux in the mature zone were observed in all tested genotypes (**Figure 6.6**). The low-pH treatment induced net H^+ influx in both root zones of all genotypes, but the magnitude was greater in the distal elongation than the mature zone. Mutants *alr104* and *als5* exhibited higher H^+ influxes than the wild type and *als3* at both root zones. In the low-pH treatment, *als3* and the wild type had similar H^+ influxes in both root zones, except for the first 12 minutes in the distal elongation zone, where a lower level of H^+ influx was observed in *als3* mutant compared with the wild type.

In the low-pH/Al treatment (50 μM), Al-resistant *alr104* mutant maintained the highest H^+ influx in the distal elongation zone, followed by the wild type; H^+ influx was the lowest in the Al-sensitive mutants (*als3* and *als5*; **Figure 6.6**). In the mature zone,

the 50-μM Al treatment induced H^+ efflux in all genotypes tested for the first 45 minutes. The highest levels of H^+ efflux were observed in *als3* and *als5* mutants. The highest H^+ efflux was observed 17 minutes after 50-μM Al exposure in the Al-sensitive mutants (*als3* and *als5*) and after 22 minutes in the wild type and *alr104* mutant (**Figure 6.6**).

6.3.2.3 K^+ fluxes

The low-pH treatment induced K^+ efflux from the distal elongation zone, which decreased gradually over time in all genotypes (**Figure 6.7**). Among the mutants, *als3* and *als5* had lower K^+ efflux than the wild type and *alr104*. During the first 30 minutes of the low-pH treatment, K^+ efflux was higher in *alr104* mutant than in the wild type, but the opposite occurred between 30 and 60 min after the start of the treatment.

The combined low-pH/50 μM Al treatment generally induced lower K^+ efflux in the distal elongation zone than the low-pH treatment alone after about 10-15 minutes in all genotypes, except for *alr104* mutant which showed little difference between K^+ flux in the low-pH and low-pH/Al treatments (**Figure 6.7**). Interestingly, in the combined low-pH/50 μM Al treatment, the K^+ flux changed from efflux to influx in *als3* and *als5* mutants after 12 and 20 minutes, respectively, whereas the wild type and *alr104* mutant maintained K^+ efflux for the entire 60-min period.

In the mature zone, no distinct differences in K^+ flux were observed between the low-pH and combined low-pH/50 μM Al treatments for all genotypes tested (**Figure 6.8**). There was a tendency toward K^+ efflux for the wild type and *alr104*, whereas the net fluxes oscillated around zero for the two Al-sensitive mutants.

6.3.2.4 Plasma membrane potential (E_m)

The resting E_m (at pH 5.5) of *alr104* mutant was more negative than E_m of the wild type and the Al-sensitive mutants (*als3* and *als5*) in both root zones (**Figure 6.9**, **Figure 6.10**). There was no difference in the resting potential observed between the wild type and the Al-sensitive mutants (*als3* and *als5*) in the distal elongation zone (**Figure 6.9**). However, in the mature zone, the wild type had a more negative resting potential than the sensitive mutants (*als3* and *als5*; **Figure 6.10**).

The low-pH treatment depolarised the plasma membrane in both root zones and in all genotypes, but to different extents. Low pH induced more depolarisation in *als3* and *als5* mutants than the wild type and *alr104* (**Figure 6.9**, **Figure 6.10**).

In the distal elongation zone of the Al-sensitive mutants (**Figure 6.9**), the initial depolarisation of the plasma membrane was less in the combined low-pH/50 μM Al treatment than in the low-pH treatment. E_m depolarisation in the distal elongation zone lasted for 30 min in the wild type and *alr104*. In the Al-sensitive mutants (*als3* and *als5*), E_m depolarisation was maintained for the entire 60-min measuring period in the low-pH treatment, whereas the low-pH/50 μM Al treatment hyperpolarised the plasma membrane after 20 minutes in both Al-sensitive mutants. After 60 min of low-pH/Al treatment, E_m was still depolarised in *alr104*, but became hyperpolarised in the other three genotypes.

In the mature zone of the wild type and *alr104* roots, the low-pH/Al treatment did not induce a significant difference in the depolarisation pattern when compared to the low-pH treatment for up to 60 minutes (**Figure 6.10**). In contrast, in the Al-sensitive mutants, the low-pH/Al treatment depolarised the plasma membrane to a lesser extent than the low-pH treatment. After 60 minutes of low-pH/Al treatment, plasma membrane hyperpolarisation was observed in the Al-sensitive mutants, whereas the wild type and *alr104* maintained depolarised states.

6.4 Discussion

Arabidopsis mutants differed in their responses to low-pH and Al stresses: *als5* grew better in the low-pH treatment (**Figure 6.3**) and poorly in the Al treatment (**Figure 6.4**A), whereas *als3* was sensitive and *alr104* was tolerant to both stresses (**Figure 6.3**, **Figure 6.4**A). These results agree with Ikka *et al*. (2007), who classified 260 *Arabidopsis thaliana* strains into the following four groups based on the results of QTL analysis: (i) Al and low-pH resistant, (ii) Al sensitive but low-pH resistant, (iii) Al sensitive but low-pH resistant and (iv) Al and low-pH sensitive.

Several mechanisms have been proposed for the increased plant tolerance to Al toxicity (Kochian *et al.*, 2004; Matsumoto, 2000), some of which could also increase tolerance to low-pH stress, such as increased rhizosphere alkalinisation. We found that

als5 and *alr104* mutants had higher rhizosphere pH than the wild type and *als3* mutant, reflecting the low-pH tolerances of the former mutants (**Figure 6.2**, **Figure 6.5**). In line with the impaired rhizosphere alkalinisation mechanism in the combined low-pH/Al treatment, the Al-sensitive mutants (*als3* and *als5*) exhibited lower rhizosphere pH in both root zones during short-term exposure experiments when compared with the Al-tolerant genotypes (wild type and *alr104*; **Figure 6.5**). Interestingly, a suppressor mutant of *als3* (*alt1-1*) has enhanced capability for pH adjustment of the rhizosphere (Gabrielson *et al.*, 2006). Our results confirmed that Al-resistant *alr104* mutant has an alkaline rhizosphere under low-pH as well as combined low-pH/Al stresses (Degenhardt *et al.*, 1998). Therefore, rhizosphere alkalinisation as a regulatory mechanism of plant tolerance to low-pH and Al stresses is supported by the data on *alr104*, *als3* and *als5* mutants.

Although rhizosphere pH changes are the net result of the dynamics of cation/anion uptake and release (including H^+, OH^- and organic acids), we cannot separately measure each component using MIFE technique, and it is difficult to establish which ion fluxes are responsible for a specific pattern of pH changes. However, in our study we found a close correlation between rhizosphere pH changes and changes in H^+ flux ($r \geq 0.93$). Thus, H^+ flux across the root tissue is likely to be an important contributor to pH changes in the rhizosphere under low-pH and combined low-pH/Al stresses.

The low-pH treatment induced an increase in H^+ influx in both root zones for all genotypes tested (**Figure 6.6**). This H^+ influx could be the result of (i) passive entry of H^+ from the external media into the root tissue because acidification of the external pH by one unit can increase the H^+ electrochemical gradient across the plasma membrane by 60 mV (Babourina *et al.*, 2001; Yamashita *et al.*, 2003) and/or (ii) decreased activity of H^+-ATPase (Kasamo, 1986; Zhao *et al.*, 2008a). However, a decrease in H^+-ATPase activity under low-pH conditions was not supported by Yan *et al.* (1998; 1992); instead, they reported that re-entry of H^+ ions into the root cells was enhanced at low pH. In any case, this surge of H^+ influx into the root tissue would cause intracellular acidification (Gerendas *et al.*, 1990); **Figure 4.8**), thereby disturbing cytoplasmic pH. Earlier reports showed that the genes regulating cytoplasmic pH were down-regulated in the low-pH-hypersensitive *Arabidopsis stop1* mutant (Iuchi *et al.*, 2007; Sawaki *et al.*, 2009). In our

experiments, higher H^+ influx was observed in the low-pH-tolerant mutants (*als5* and *alr104*) compared to the low-pH-sensitive wild type and *als3* mutant. The low-pH-tolerant mutants maintained relatively higher biomass than the low-pH-sensitive wild type and *als3* (**Figure 6.3**, **Figure 6.4**A). Hence, we propose that the low-pH-tolerant mutants (*als5* and *alr104*) have a better cytoplasmic pH regulatory mechanism than the wild type and *als3* mutant.

The combined low-pH/Al treatment decreased H^+ influx in the distal elongation zone and increased H^+ efflux in the mature root zone for all genotypes tested (**Figure 6.6**). This could result from Al ions either inhibiting H^+ influx or inducing H^+ efflux. These results are consistent with earlier studies on squash roots where Al-treated root apices were not able to alkalinise media to the same extent as in control low-pH media (Ahn *et al.* (2002).

The MIFE technique used in the present study estimates the net H^+ flux across the plasma membrane. Hence, we can only speculate that Al ions, by virtue of their strong affinity for the plasma membrane surface, might have shifted the plasma membrane surface potential towards relatively positive values (Ahn *et al.*, 2004a; Ahn *et al.*, 2001). A positively charged plasma membrane surface would impede the uptake of cations, including H^+ ions. This might explain the observed inhibition of H^+ influx in the distal elongation zone. The H^+ influx inhibition by Al ions would also result in measured enhancement of the H^+ efflux in the mature zone. Furthermore, Ahn *et al.* (2004a) reported that Al ions shifted the plasma membrane surface potential towards positive values in an Al-sensitive (ES8) but not in an Al-tolerant wheat genotype (ET8). Similarly, plasma membrane surface potential differences between *Arabidopsis* genotypes exposed to the low-pH/Al treatment in the present study could have been linked to greater inhibition of H^+ influx and enhanced H^+ efflux in the Al-sensitive mutants (*als3* and *als5*) compared to the wild type and Al-tolerant *alr104* mutant.

As reported in Al-sensitive maize (Calba and Jaillard, 1997) and wheat roots (Kinraide, 1988), enhanced net H^+ release from Al-sensitive mutants (*als3* and *als5*) under Al stress would decrease the net H^+ influx into the distal elongation zone and increase the net H^+ efflux from the mature zone (**Figure 6.6**). Protein kinases can regulate H^+-ATPase activity across the plasma membrane (Trofimova *et al.*, 1997).

Though up-regulation of protein kinases was reported for Al-tolerant genotypes of some plant species (Osawa and Matsumoto, 2001; Shen *et al.*, 2005), protein kinase inhibition by Al ions was observed for Al-sensitive *Arabidopsis stop1* mutant (Sawaki *et al.*, 2009). It is tempting to hypothesise that Al can specifically inhibit the *Arabidopsis* protein kinase PKS5, a negative regulator of the membrane H^+-ATPase, thereby inducing H^+ efflux and acidification of the external medium (cf. Fuglsang *et al.*, 2007).

The low-pH treatment depolarised E_m in all genotypes tested (**Figure 6.9**, **Figure 6.10**). This could be the result of a transient increase in H^+ influx and/or a decrease in H^+-ATPase activity. In the combined low-pH/Al treatment, E_m depolarisation was higher in the Al-tolerant genotypes (wild type and *alr104*) than in the Al-sensitive mutants (*als3* and *als5*) in both root zones (**Figure 6.9**, **Figure 6.10**). Similar results were observed in wheat (Papernik and Kochian, 1997; Wherrett *et al.*, 2005), indicating that *Arabidopsis* and wheat might employ similar mechanisms to combat combined low-pH/Al stress. This Al-induced E_m depolarisation in the Al-tolerant genotypes could be a result of (i) currents carried by the H^+ flux across the plasma membrane (see Raven, 1991 and references there in) because higher H^+ influx in the distal elongation zone or lower H^+ efflux in the mature zone of the Al-tolerant genotypes (*alr104* and wild type) would cause E_m to depolarise more than in the Al-sensitive mutants (*als3* and *als5*), or (ii) release of organic anions from the *Arabidopsis* roots upon Al exposure, which would depolarise E_m (Kollmeier *et al.*, 2001; Olivetti *et al.*, 1995; Papernik and Kochian, 1997). Under Al stress, *Arabidopsis* has been reported to release malate (Hoekenga *et al.*, 2006), citrate (Liu *et al.*, 2009), pyruvate and succinate (Larsen *et al.*, 1998). Characterisation of the AtALMT transporter revealed that *Arabidopsis* falls into the pattern II category (Ma *et al.*, 2001), which requires 4 h of induction time to achieve maximum malate release (Kobayashi *et al.*, 2007). For this reason, malate efflux could not have caused the observed E_m depolarisation in the Al-tolerant genotypes as measured in the present study.

Larsen *et al.*(1998) reported that *alr104* mutant and the wild type release similar amounts of citrate upon Al exposure. Tricarboxylate citrate^{3-} has a six- to eight-fold greater ability to chelate Al than bicarboxylate malate^{2-} (Ryan *et al.*, 2001). Citrate efflux occurs through MATE transporters in *Arabidopsis* (Liu *et al.*, 2009), wheat (Ryan *et al.*, 2009), barley (Furukawa *et al.*, 2007) and sorghum (Magalhaes *et al.*,

2007). The MATE transporters are present in the PM of epidermal cells along the root apex as well as the mature root zone (Furukawa *et al.*, 2007; Magalhaes *et al.*, 2007; Ryan *et al.*, 2009) and rapidly (within 20 min) release citrate following Al exposure (Zhao *et al.*, 2003). The release of citrate^{3-} upon Al exposure from the Al-tolerant genotypes (*alr104* and wild type) would decrease the level of toxic Al ions in the rhizosphere (thereby maintaining E_m depolarisation), whereas smaller citrate release from Al-sensitive genotypes would diminish E_m depolarisation (**Figure 6.9**, **Figure 6.10**).

Given that K^+ transport in plants usually occurs near the electrochemical equilibrium, theoretically any change in E_m would affect K^+ flux. The low-pH treatment caused immediate depolarisation in all tested genotypes (**Figure 6.9**). This E_m depolarisation should lead to increased K^+ efflux from the roots through K^+ channels as shown previously under low-pH conditions (Babourina *et al.*, 2001; Shabala *et al.*, 2006), which was indeed observed in the distal elongation zone of all genotypes in this study (**Figure 6.7**). The combined low-pH/Al treatment caused smaller initial depolarisation in Al-sensitive mutants (both zones) compared with the low-pH treatment (**Figure 6.9**, **Figure 6.10**). This shift in E_m towards less depolarisation or even hyperpolarisation should decrease K^+ efflux or even induce K^+ influx, which was observed in the distal elongation zone of all tested genotypes (**Figure 6.7**). Similar results were reported in soybean suspension cells (Staß and Horst, 1995) and wheat, wherein inhibition of K^+ efflux by Al ions was more pronounced in Al-sensitive Scout than Al-tolerant Atlas wheat (Sasaki *et al.*, 1995). Interestingly, Al treatment hyperpolarised E_m in the distal elongation zone of Al-sensitive Arabidopsis mutants (*als3* and *als5*) after 20 minutes (**Figure 6.9**). K^+ influx occurred together with this E_m hyperpolarisation in the Al-sensitive mutants (**Figure 6.7**), which might have been the result of hyperpolarisation-activated K^+ inward-rectifying channels (KIRC) (Lebaudy *et al.*, 2007; Maathuis and Sanders, 1995).

Regulation of K^+ flux by E_m as observed in the distal elongation zone was not found in mature zone, with no specific pattern of K^+ flux changes recorded under either low-pH or combined low-pH/Al stress (**Figure 6.8**). Indeed, the mature zone has a larger number of K^+ transport systems than the root apex (Ahn *et al.*, 2004b; Hanson

and Kahn, 1957; Vallejo *et al.*, 2005), but not all K^+ transport systems are voltage gated in the mature zone of *Arabidopsis* roots (Lebaudy *et al.*, 2007).

The highest shoot K^+ concentration (**Figure 6.4**B) and lowest K^+ efflux (**Figure 6.7**) observed for *als3* under low-pH stress independently supports the observation of Koyama *et al.* (2001) that K^+ transport in *Arabidopsis* is altered at low pH. The higher shoot K^+ concentration in the Al-sensitive mutants (*als3* and *als5* mutants) could be linked to decreased K^+ efflux or enhanced K^+ influx in the distal elongation zone (**Figure 6.7**), indicating a disturbance in K^+ homeostasis. This shift in K^+ flux towards influx might be due to direct or indirect effect of *ALS3* and *ALS* mutations. ALS3 has been described as a plasma membrane-localised ABC transporter-like protein (Larsen *et al.*, 2005). Although it shares high similarity with other plant ABC transporters, it lacks the ATP-binding cassette. It has been proposed that ALS3 is involved in translocation of Al from Al-sensitive tissues (Larsen *et al.*, 2005). This conclusion is based on its high expression in the phloem. However, 24-h exposure to Al had no effect on *ALS3* expression in the phloem, but changed spatial distribution, shifting *ALS3* expression from external to internal cells (Larsen *et al.*, 2005). In the current study, an immediate difference between the wild type and *als3* mutants in ion fluxes and E_m was observed after exposure to Al. It indicated that ALS3 functioning may be linked to maintenance of E_m depolarisation, K^+ efflux and H^+ influx, and, in a longer term, to K^+ homeostasis . These findings are consistent with physiological studies on plants with *alt1-1* mutation, a suppressor of *als3* mutation, which demonstrated that *alt1-1* mutation positively impacted Al resistance by pH adjustment rather than Al exclusion (Gabrielson *et al.*, 2006).

In summary, the enhanced ability of *als5* and *alr104* mutants to alkalinise the rhizosphere and take up H^+ from a low-pH environment is responsible for the low-pH tolerance in these mutants. Tolerance to combined low-pH/Al stress in the wild type and *alr104* mutant coincided with relatively high resting E_m and continuous E_m depolarisation, high K^+ efflux and high H^+ influx, which are linked to the plant ability to make the rhizosphere less acidic. Low-pH tolerance (*als5* mutant) was associated with higher H^+ uptake under low-pH stress; however, this ability was abolished by exposure to Al. Therefore, the mechanisms that underlie plant tolerance to acidic and Al stresses might be different.

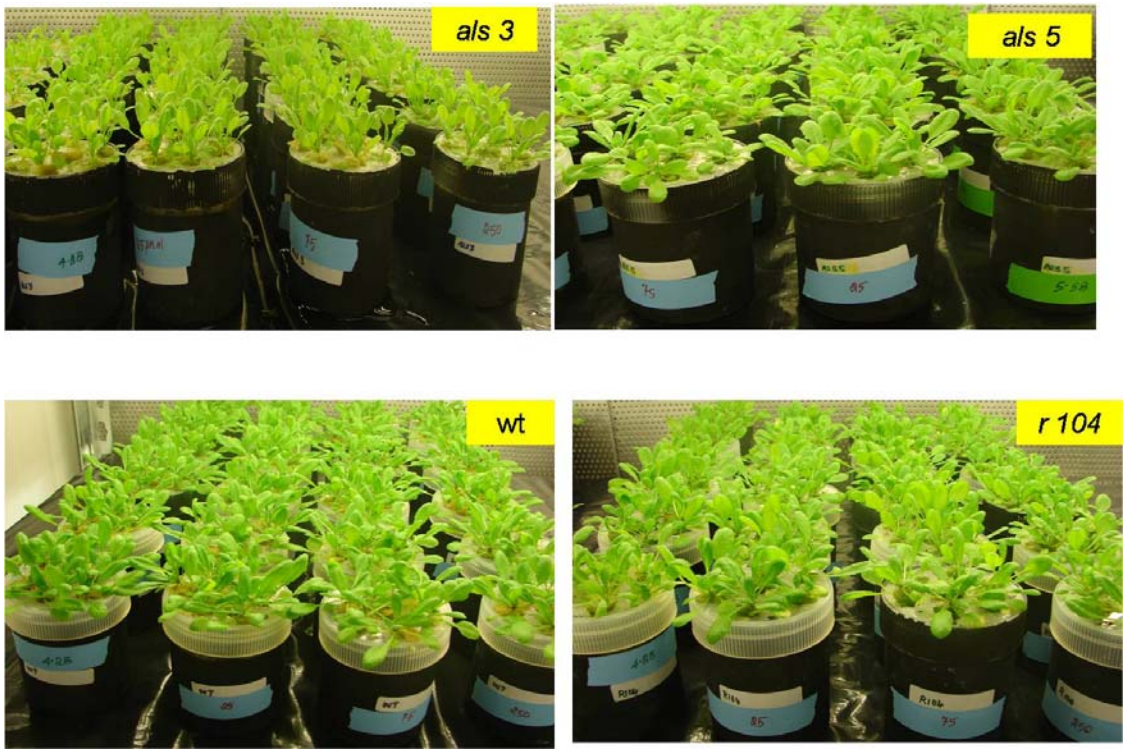

Figure 6.1 Growth of *Arabidopsis* wild type and mutants (*als3*, *als5* and *r104*) in 1/10th Hoagland solution at pH 5.5 in 3 weeks.

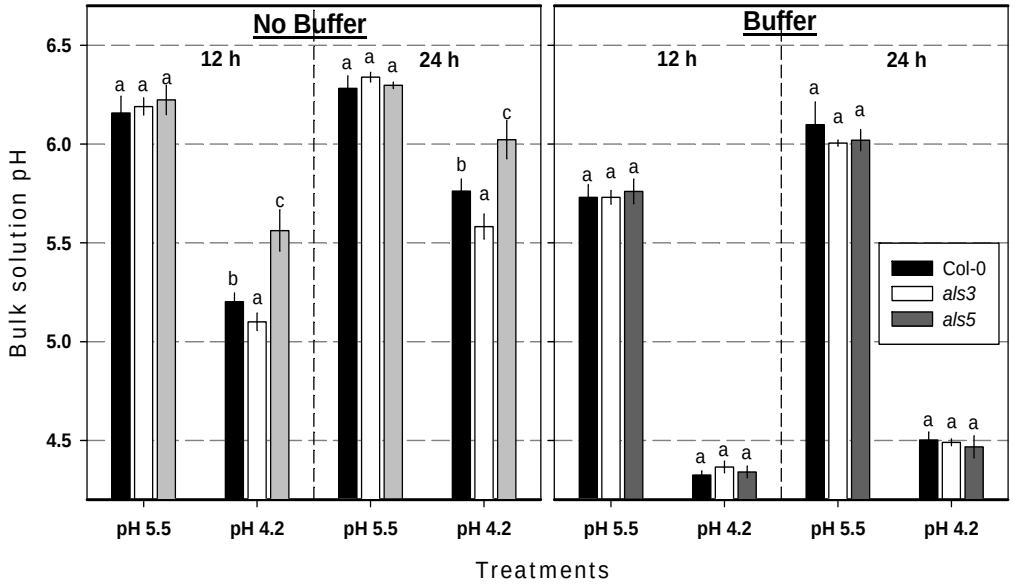

Figure 6.2 Bulk solution pH of *Arabidopsis thaliana* genotypes with and without 0.5 mM HomoPIPES buffer measured on second day at 12 and 24 hours after the nutrient solution change. Mean ± SE (n = 4 replicates).
Within each buffer x pH treatment, different letters represent significant difference by LSD test at p <0.001. *Arabidopsis* seedlings were grown in diluted (1/10) Hoagland solution for 3 weeks; treatments were then imposed for 10 d.

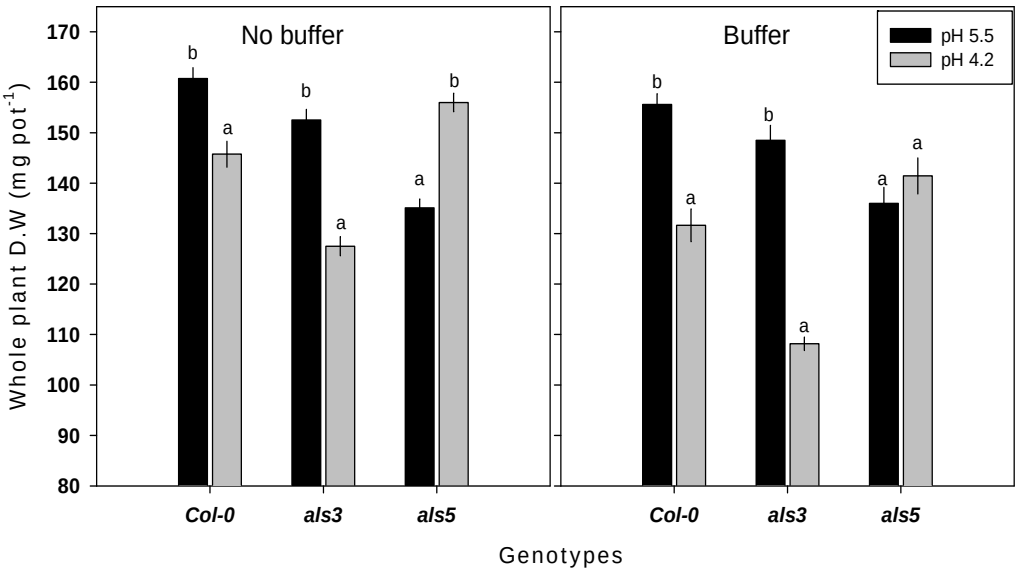

Figure 6.3 Biomass of *Arabidopsis thaliana* genotypes at pH 4.2 with and without 0.5 mM HomoPIPES buffer.
Mean±SE (n = 4 replicates). In each graph, different letters within each genotype represent significant difference between pH 5.5 and pH 4.2 by t-test at $p \leq 0.001$.

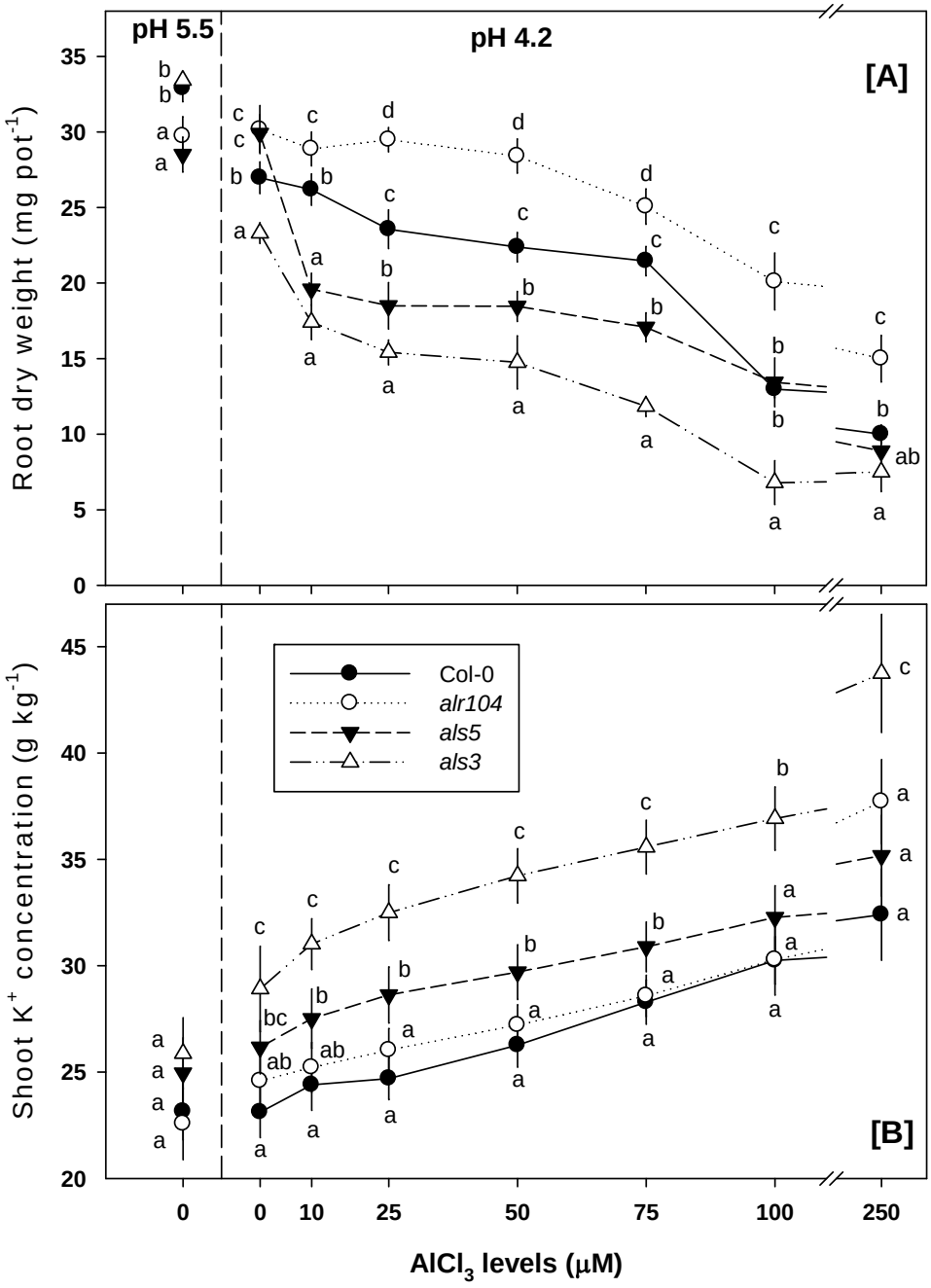

Figure 6.4 Effect of low pH and Al stresses on *Arabidopsis thaliana* root biomass [A] and shoot K^+ concentration [B].
Means ± SE (n = 3 replicates). In each $AlCl_3$ concentration, genotypes sharing a common letter are not significantly different by LSD test at $p \leq 0.05$. *Arabidopsis* seedlings were grown in diluted (1/10) Hoagland solution for 3 weeks, and treatments were then imposed in buffered medium (0.5 mM HomoPIPES) for 7 d.

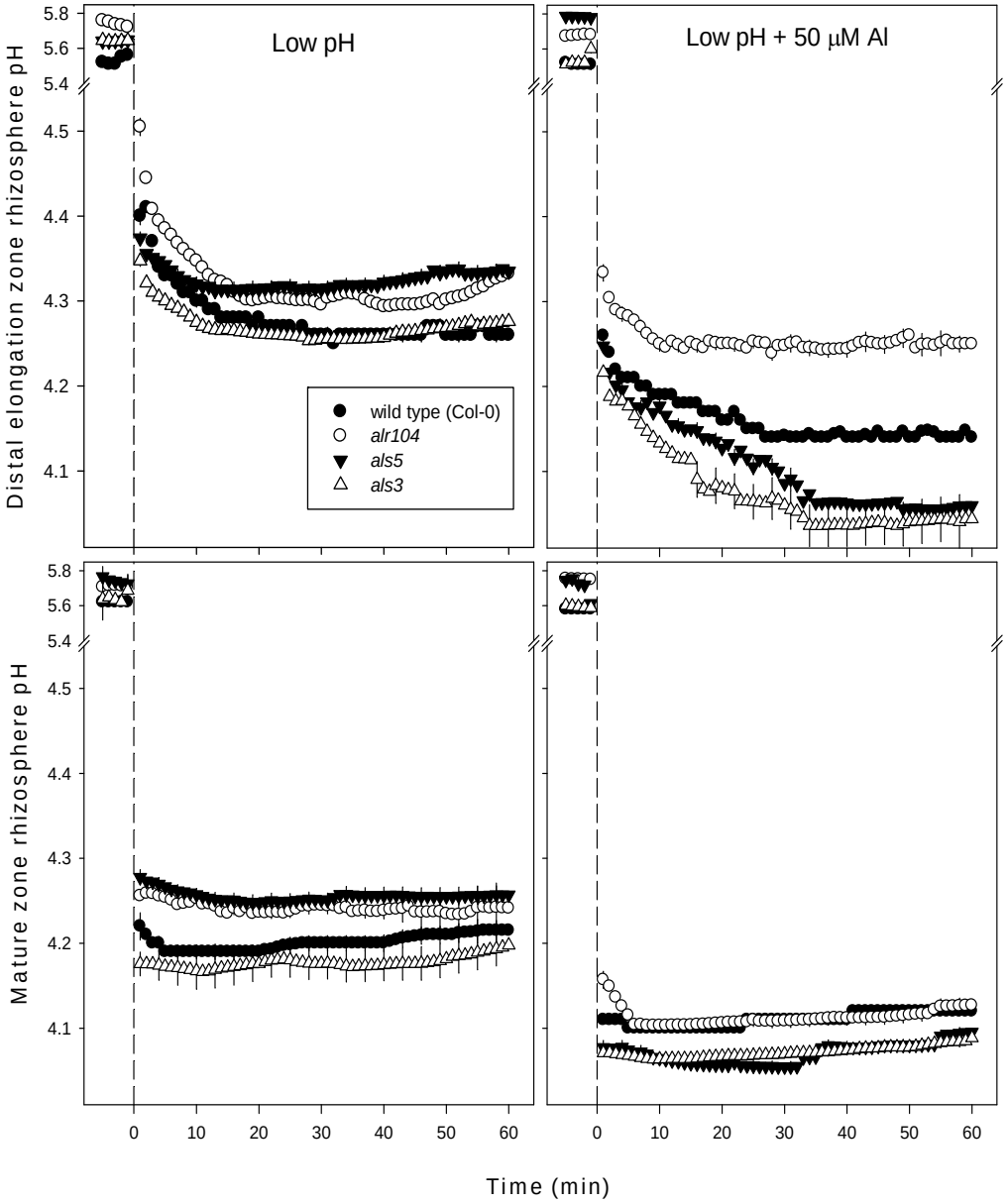

Figure 6.5 Effect of low-pH and combined low-pH/Al treatments on rhizosphere pH at distal elongation zone (top panel) and mature zone (bottom panel) of four- to five-day-old *Arabidopsis thaliana* roots.
The low-pH and combined low-pH/Al treatments were imposed at time = 0; the data recorded in the first 5 minutes before time = 0 represent H^+ fluxes at pH 5.5. Error bars indicate ± SE (n = 10 to 12 seedlings). *Arabidopsis* seedlings were conditioned in basal salt medium (BSM; 0.1 mM $CaCl_2$ + 1 mM KCl + 0.2 mM $MgCl_2$, pH 5.5) for 20 min before treatments were imposed in unbuffered BSM.

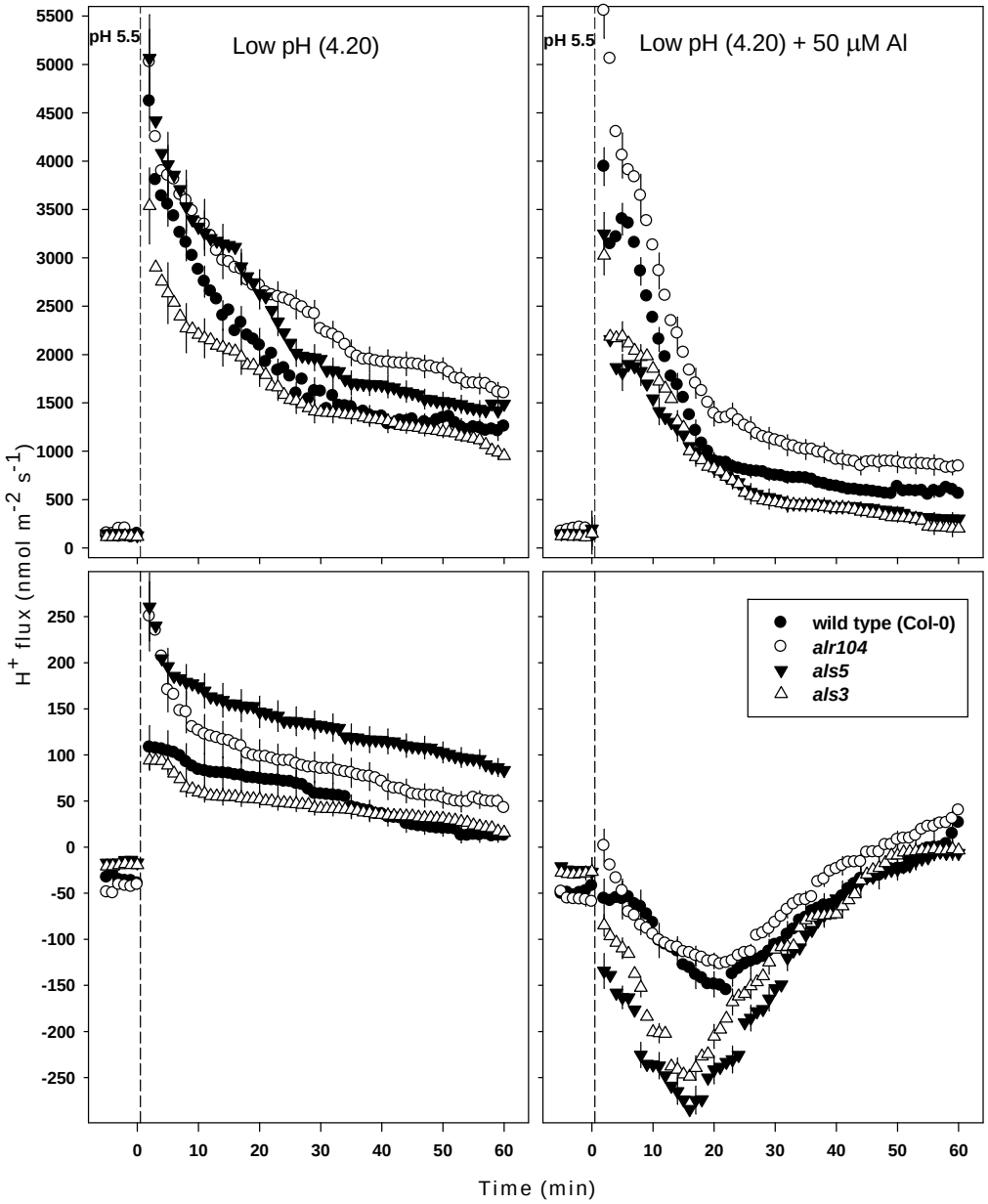

Figure 6.6 Effect of low pH and combined low pH/50 µM Al on H^+ fluxes measured at distal elongation zone (top panel) and mature zone (bottom panel) of four- to five-day-old *Arabidopsis thaliana* roots.
The low-pH and combined low-pH/Al treatments were imposed at time = 0; the data recorded in the first 5 minutes before time = 0 represent H^+ fluxes at pH 5.5. Negative H^+ flux values indicate efflux, and positive values influx. Error bars are ± SE (n = 10 to 12 seedlings). *Arabidopsis* seedlings were conditioned in basal salt medium (BSM; 0.1 mM $CaCl_2$ + 1 mM KCl + 0.2 mM $MgCl_2$, pH 5.5) for 20 min before treatments were imposed in unbuffered BSM.

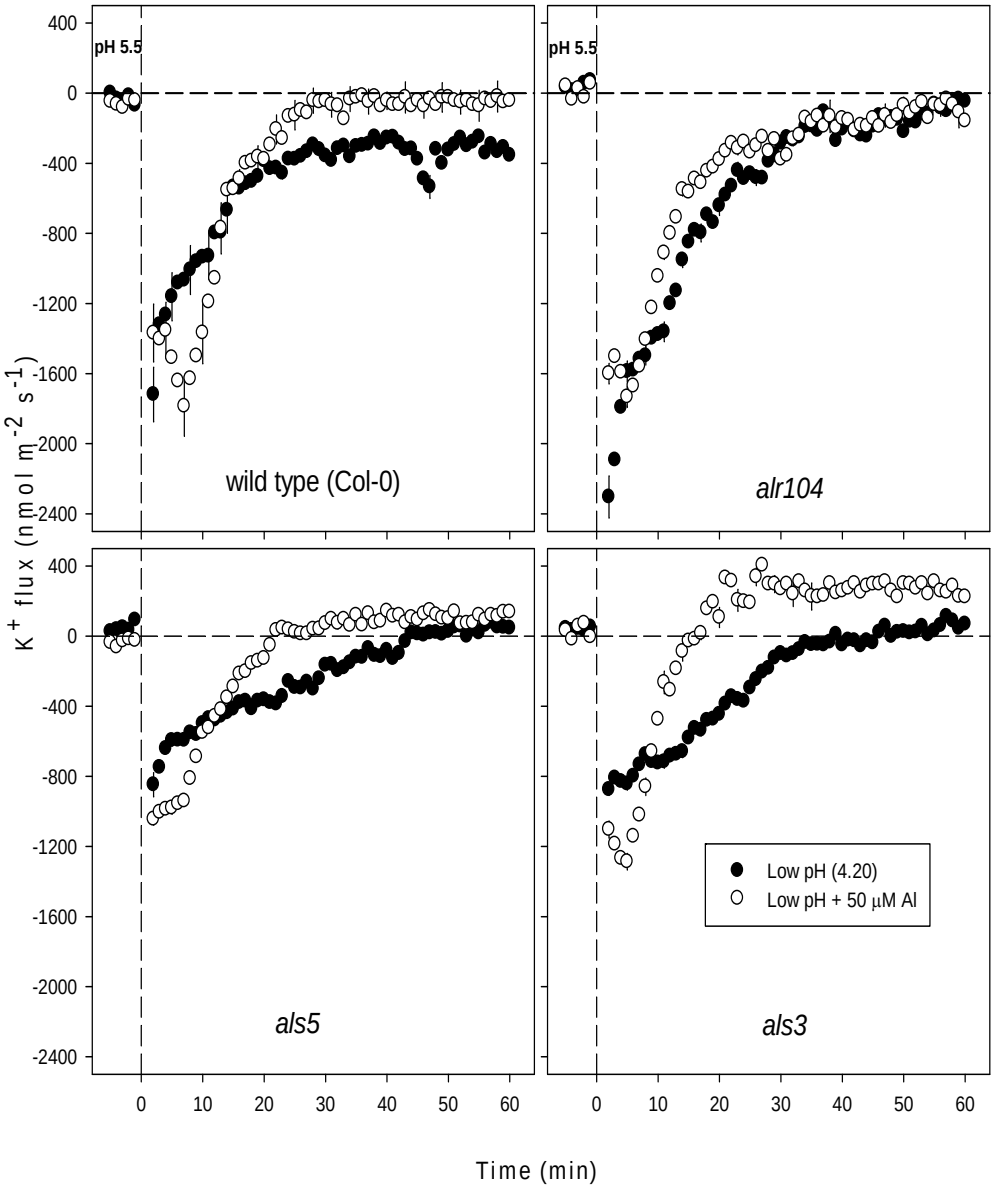

Figure 6.7 Effect of low pH and combined low pH plus 50 μM Al^{3+} on K^+ fluxes measured at distal elongation zone of four- to five-day-old *Arabidopsis thaliana* roots. The low-pH and combined low-pH/Al^{3+} treatments were imposed at time = 0; the data recorded in the first 5 minutes before time = 0 represent K^+ fluxes at pH 5.5. Negative K^+ flux values indicate efflux, and positive values indicate influx. Error bars are ± SE (n = 10 to 12 seedlings). *Arabidopsis* seedlings were conditioned in basal salt medium (BSM; 0.1 mM $CaCl_2$ + 1 mM KCl + 0.2 mM $MgCl_2$, pH 5.5) for 20 min before treatments were imposed in unbuffered BSM.

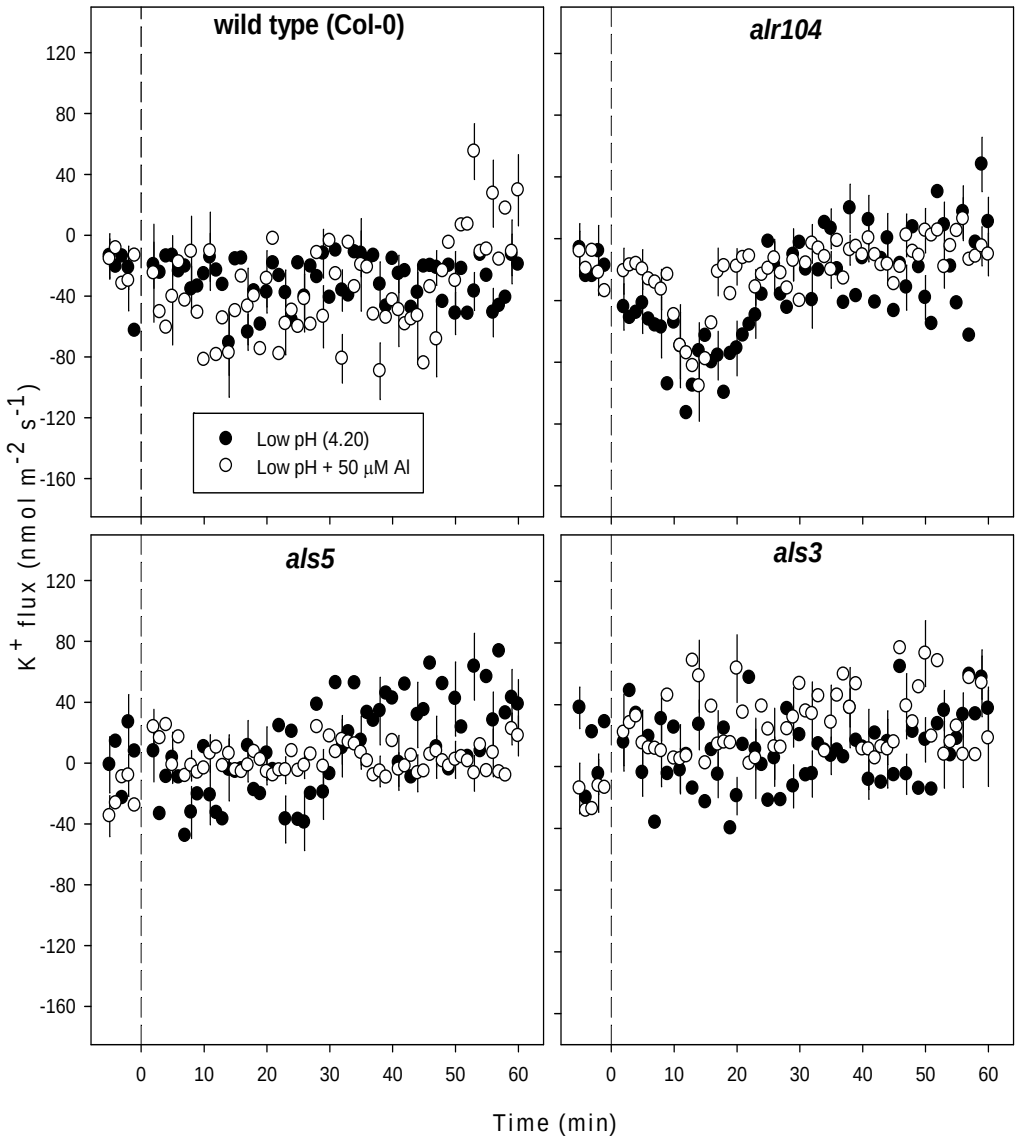

Figure 6.8 Effect of low pH and combined low pH plus 50 μM Al^{3+} on K^+ fluxes measured at mature zone of four- to five-day-old *Arabidopsis thaliana* roots.
The low-pH and combined low-pH/Al^{3+} treatments were imposed at time = 0; the data recorded in the first 5 minutes before time = 0 represent K^+ fluxes at pH 5.5. Negative K^+ flux values indicate efflux and positive values indicate influx. Error bars are ± SE (n = 10 to 12 seedlings). *Arabidopsis* seedlings were conditioned in basal salt medium (BSM; 0.1 mM $CaCl_2$ + 1 mM KCl + 0.2 mM $MgCl_2$, pH 5.5) for 20 min before treatments were imposed in unbuffered BSM.

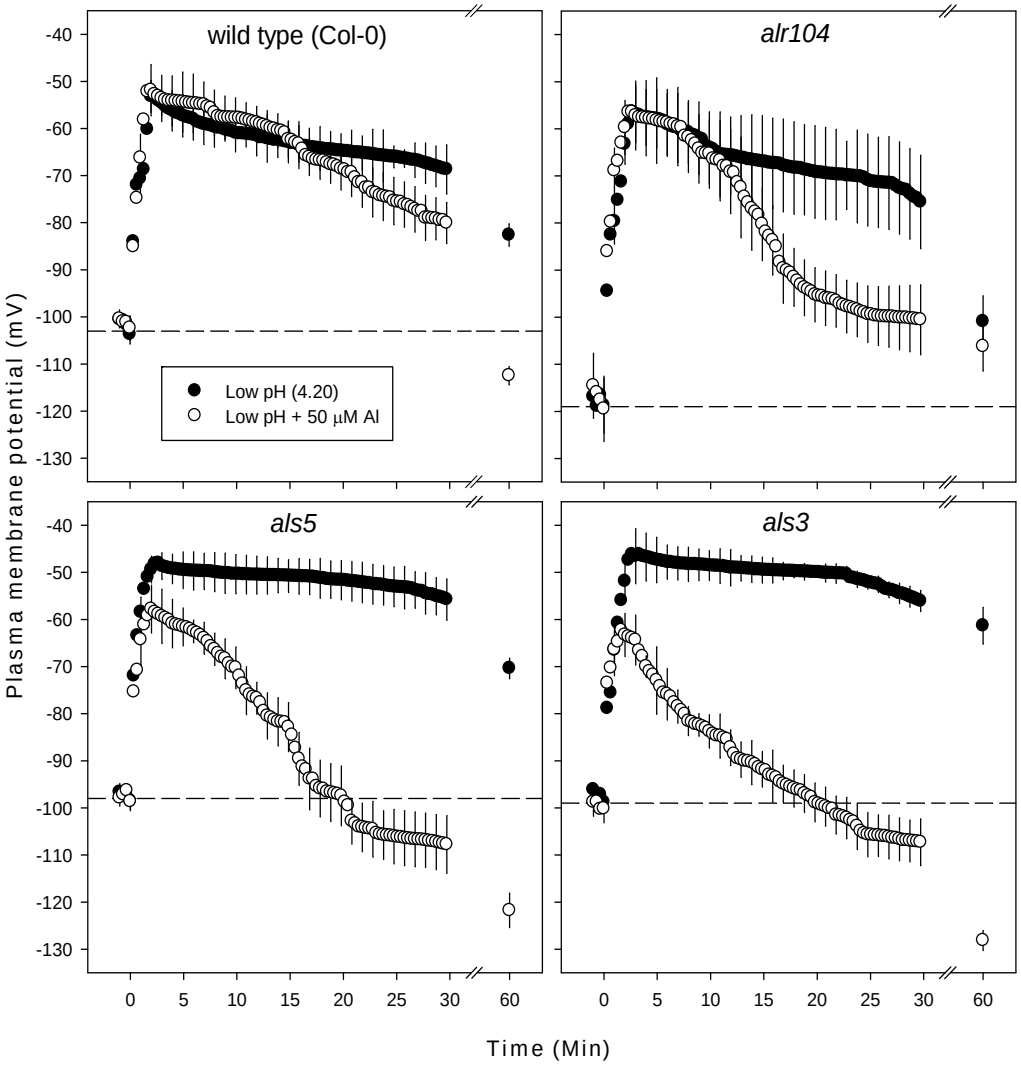

Figure 6.9 Effect of low pH and combined low pH/Al treatments imposed at time = 0 on the plasma membrane potential in the distal elongation zone of four- to five-day-old *Arabidopsis thaliana* roots.
Error bars indicate ± SE (n = 8 to 10 seedlings). The horizontal dotted lines represent the resting plasma membrane potential of respective genotypes at pH 5.5. *Arabidopsis* seedlings were conditioned in basal salt medium (BSM; 0.1 mM $CaCl_2$ + 1 mM KCl + 0.2 mM $MgCl_2$, pH 5.5) for 20 min before treatments were imposed in unbuffered BSM.

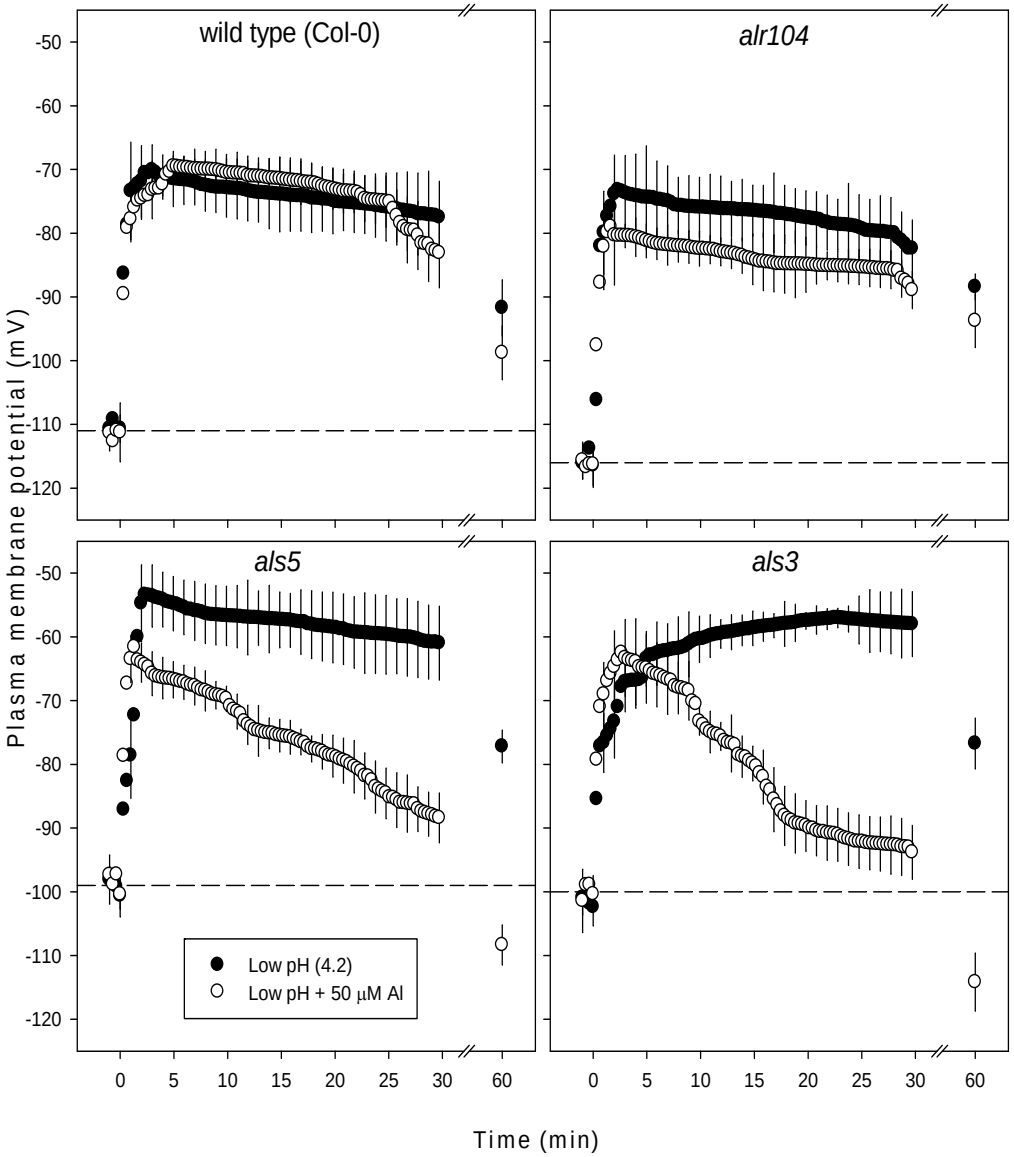

Figure 6.10 Effect of low pH and combined low pH/Al treatments imposed at time = 0 on the plasma membrane potential in the mature zone of four- to five-day-old *Arabidopsis thaliana* roots.
Error bars indicate ± SE (n = 8 to 10 seedlings). The horizontal dotted lines represent the resting plasma membrane potential of respective genotypes at pH 5.5. *Arabidopsis* seedlings were conditioned in basal salt medium (BSM; 0.1 mM $CaCl_2$ + 1 mM KCl + 0.2 mM $MgCl_2$, pH 5.5) for 20 min before treatments were imposed in unbuffered BSM.

Chapter 7

Low-pH and aluminium tolerance in Arabidopsis is linked to increased calcium and magnesium uptake

Jayakumar Bose, Olga Babourina and Zed Rengel

School of Earth and Environment, the University of Western Australia, Crawley WA 6009, Australia

Abstract

Low-pH stress and Al^{3+} toxicity affect root growth in acid soils. The capacity of genotypes to maintain Ca^{2+} and Mg^{2+} uptake from acidic environments may contribute to low-pH and Al tolerance.

To test this hypothesis, Al-tolerant *alr104* mutant, two Al-sensitive mutants (*als5* and *als3*) and the wild type (Col-0) of *Arabidopsis thaliana* were compared for Ca^{2+} and Mg^{2+} uptake under low-pH and combined low-pH/Al^{3+} stresses. Ca^{2+} and Mg^{2+} accumulation in roots was measured in long-term (7 days) exposure experiments. In addition, Ca^{2+} and Mg^{2+} fluxes were determined using ion-sensitive microelectrodes at the distal elongation and mature root zones in short-term (0-60 min) experiments. Intracellular Mg^{2+} concentrations were measured in intact root cells in the distal elongation zone using magnesium-specific fluorescent dye and fluorescent lifetime imaging (FLIM) analysis.

Under low-pH stress, *Arabidopsis* mutants *als5* and *alr104* maintained higher Ca and Mg concentration in roots, and had greater Mg^{2+} influx and less-disturbed Ca^{2+} influx than the wild type and *als3* mutant. In the combined low-pH/Al^{3+} treatment, Al-tolerant genotypes (wild type and *alr104*) maintained higher Ca^{2+} and Mg^{2+} accumulation than Al-sensitive genotypes (*als3* and *als5*). Further, Al-tolerant genotypes (*alr104* and wild types) recovered from Al-induced Ca^{2+} efflux, and had higher Mg^{2+} influx and higher intracellular Mg^{2+} concentration than Al-sensitive mutants (*als3* and *als5*).

In conclusion, increased Ca^{2+} and Mg^{2+} uptake helps *Arabidopsis* genotypes to cope with low-pH and combined low-pH/Al^{3+} stresses. Elevated intracellular Mg^{2+} concentration under Al stress might fuel organic acid synthesis in Al-tolerant genotypes.

Key words: acidity, aluminium toxicity, Mg^{2+} flux, Ca^{2+} flux, Fluorescence Life Time Imaging (FLIM), intracellular Mg^{2+}, distal root elongation zone, mature root zone

7.1 Introduction

The most severe symptom of Al toxicity is the inhibition of root growth, resulting in nutrient imbalance and ultimately reduction of plant growth (Kochian *et al.*, 2005). Indeed, Al interferes with the uptake and/or transport of Ca, Mg, P, Mn, B, Fe, Cu and K (see Silva *et al.*, 2010 for references). Among the nutrients, Al-induced inhibition of Ca and Mg uptake was the most pronounced in diverse plant species (cf. Foy, 1988; Grimme, 1983; Keltjens, 1988; Keltjens and Tan, 1993; Mariano and Keltjens, 2005; Mugwira *et al.*, 1980; Rengel, 1990; Rengel and Elliott, 1992; Rengel and Robinson, 1989b; Silva *et al.*, 2010). However, the magnitude of inhibition was not equal among the genotypes of a given plant species. In this respect, Al-tolerant genotypes recorded higher uptake of Ca and Mg than the sensitive genotypes in maize (Giannakoula *et al.*, 2008; Mariano and Keltjens, 2005), wheat (Silva *et al.*, 2010), sorghum (Baligar *et al.*, 1993) and rice (Sivaguru and Paliwal, 1993), suggesting that the capacity of tolerant genotypes to maintain mineral nutrition in the presence of Al could be an important component of Al tolerance. However, given that most published reports consider relatively long-term Al exposure (hours to days), it remains unclear whether higher Ca and Mg uptake in Al-tolerant genotypes is due to greater root development and/or greater tolerance of uptake mechanisms. Hence, short-term Al exposure studies involving direct measurements of Ca^{2+} and Mg^{2+} fluxes are essential for understanding the immediate effects of Al^{3+} on Ca and Mg uptake mechanisms.

Few short-term Al exposure studies have compared the Ca^{2+} fluxes of Al-tolerant and -sensitive genotypes and the results are contradictory (Rengel and Zhang, 2003). For example, Al rapidly inhibited Ca^{2+} influx into intact root cells of Al-sensitive wheat genotypes (Huang *et al.*, 1992; Ryan and Kochian, 1993). However, further studies revealed that low concentrations of Al can inhibit root growth in an Al-sensitive wheat genotype without affecting Ca^{2+} influx (Ryan and Kochian, 1993; Ryan *et al.*,

1997). Further, addition of ameliorating cations (Mg, Sr or Na) improved root growth of an Al-sensitive wheat genotype, even though the net Ca^{2+} influx remained inhibited (Ryan *et al.*, 1997). These results indicate that Al-induced inhibition of Ca^{2+} influx alone may not be a critical factor causing diminished root growth. On the other hand, under constant Al^{3+} activity, presence of micromolar concentrations of Mg in the rooting media enhanced root growth in soybean (Silva *et al.*, 2001c), rice bean (Yang *et al.*, 2007) and rice (Watanabe and Okada, 2005), suggesting that an ameliorative mechanism of Al^{3+} toxicity by low concentrations of Mg is beyond the pure electrostatic effects. Further, over-expression of Mg transporter genes in yeast (MacDiarmid and Gardner, 1998) and *Nicotiana benthamiana* (Deng *et al.*, 2006) conferred Al tolerance, indicating that enhanced Mg uptake in the presence of Al^{3+} ions may provide Al tolerance. To test this hypothesis, comparison of short-term Mg^{2+} fluxes in genotypes differing in Al tolerance in the presence of constant Al activity is essential.

Nutrient fluxes vary considerably in the different root zones (see Newman, 2001 for references). Indeed, uptake of Ca^{2+} and Mg^{2+} varied between the root apex and the mature zone of barley (Ferguson and Clarkson, 1976), maize (Ryan *et al.*, 1990) and *Arabidopsis* (Guo *et al.*, 2010). The root apex (Ryan *et al.*, 1993), particularly the distal elongation zone (Sivaguru and Horst, 1998), is the primary site of Al stress. The distal elongation root zone also acts as a "plant command centre" to integrate sensory inputs into adaptive mechanisms for diverse environmental stimuli (Baluška *et al.*, 2004). In addition to the root apex, Al-induced gene expression in the mature root zone of *Medicago truncatula* may play a key role in Al tolerance (Chandran *et al.*, 2008). Therefore, Ca^{2+} and Mg^{2+} fluxes need to be studied and compared between these two root zones (namely, distal elongation and mature) to decipher the primary mechanisms of Al^{3+} toxicity and tolerance in plants.

In many plant species Al toxicity caused elevation of intracellular Ca^{2+} activity, with that elevation being more pronounced in Al-sensitive than -tolerant genotypes (see Rengel and Zhang, 2003 for references). Such cytosolic Ca^{2+} spikes may cause closure of plasmodesmata (Holdaway-Clarke *et al.*, 2000) and inhibit plasmodesmata-mediated cell-to-cell transport in Al-sensitive wheat roots (Sivaguru *et al.*, 2000). In contrast, little is known about the dynamics of intracellular Mg^{2+} activity under Al^{3+} stress, even though intracellular Mg^{2+} is pivotal for H^+-ATPase activity (Brooker and Slayman,

1983; Costa and de Meis, 1996) and the activation of many enzymes involved in organic acid synthesis and metabolism (Boulton and Ratledge, 1980; Howard *et al.*, 2000; Shaul, 2002).

Using *Arabidopsis thaliana* as a model system to study complex Al^{3+} toxicity and tolerance mechanisms has many advantages, such as the availability of large collections of mutants differing in growth response to Al-toxic environments, rapid advancement in the knowledge of the *Arabidopsis* genome (including a full sequence), similarities in response between *Arabidopsis* and crop species, short time frames and relatively small space required to screen large numbers of genotypes, *etc*. Thus, *Arabidopsis* Al-tolerant mutant *alr104* (Degenhardt *et al.*, 1998) and two Al-sensitive mutants, *als5* and *als3* (Larsen *et al.*, 1996), along with the wild type (Col-0) were compared in this study. Long-term (7 days) and short-term (0-60 min) effects of Al^{3+} exposure on Ca^{2+} and Mg2+ uptake were compared among the genotypes to examine (i) whether these genotypes indeed differ in Ca^{2+} and Mg2+ uptake and (ii) how the possible changes in Ca^{2+} and Mg2+ uptake relate to the Al^{3+} tolerance of these genotypes.

7.2 Materials and Methods

7.2.1 Long-term exposure experiments: Hydroponic culture

Arabidopsis thaliana L. wild type (ecotype Col-0), *als3*, *als5* and *alr104* seeds were surface sterilised with 1% (v/v) calcium hypochlorite for 10 minutes. Seeds were then sown on rock-wool strips (1-2 mm thick and 5-6 cm long) that were placed into 250-mL plastic containers containing 1/10 Hoagland solution. The containers were kept at 4^{o}C for 2 d to achieve synchronised germination. Seedlings were then moved to a growth cabinet with 16 h light (150 µmol m^{-2} s^{-1}) and 8 h dark at 20 ± 1^{o}C. Three-week-old seedlings were exposed to pH 5.5 and pH 4.2 with a range of Al concentrations (0, 10, 25, 50, 75, 100 or 250 µM $AlCl_3$) in 0.5 mM homo-PIPES buffer for 7 d. The treatments were performed in triplicate. the treatment solutions were changed daily.

At the end of experiments, shoots and roots were separated, washed with 100 µM $CaSO_4$, rinsed with deionised water, dried in an oven at 70^{o}C for 72 hours and weighed. Dried roots were digested with a HNO_3:$HClO_4$ (10:1) mixture. The Ca, Mg

and Al concentrations were analysed using inductively coupled plasma-mass spectrometry (ICP-MS).

7.2.2 Short-term exposure experiments

Arabidopsis thaliana L. wild type (ecotype Col-0), *als3*, *als5* and *alr104* seeds were surface sterilised with 1% (w/v) calcium hypochlorite and seedlings were grown in 90-mm Petri dishes under constant fluorescent light (150 µmol m^{-2} s^{-1}) and temperature (23-25^{o}C) in 0.8% (w/w) agar media containing basal salt medium (BSM) with 0.1 mM $CaCl_2$, 1 mM KCl and 0.2 mM $MgCl_2$, pH 5.5. The Petri dishes were oriented upright, so the roots grew down along the agar surface without penetrating it. However, roots were anchored in the agar by root hairs.

Net fluxes of Ca^{2+} and Mg^{2+} were measured using the non-invasive MIFE^{TM} system (University of Tasmania, Hobart, Australia) as described by Newman (2001). Microelectrodes were pulled from borosilicate glass capillaries (GC 150-10, SDR Clinical Technology, Middle Cove, Australia), oven dried at 230 ºC for about 5 h, and silanised using tributylchlorosilane (Fluka catalogue no. 90796). Electrodes were broken back to get the external tip diameter of 2-3 µm. The electrodes were back-filled with appropriate solutions (0.5 M $CaCl_2$ for Ca^{2+} electrode and 0.5 mM $MgCl_2$ for Mg^{2+} electrode). The electrode tips were then front-filled with ionophore cocktails (Fluka catalogue no. 21048 for Ca^{2+} and no. 63048 for Mg^{2+}). Prepared electrodes were calibrated in a set of standards (Ca^{2+} from 0.1 to 1.0 mM with 0.2 mM Mg^{2+} background; Mg^{2+} from 0.2 to 2.0 mM with 0.1 mM Ca^{2+} and 100 µM $AlCl_3$ background). Electrodes with the slope responses of less than 25 mV per decade were discarded. Since Mg^{2+} ionophore is partially selective for Ca^{2+}, we have simultaneously measured Ca^{2+} and Mg^{2+} fluxes using identically prepared electrodes. The Mg^{2+} fluxes were then recalculated according to the equation described earlier (Knowles and Shabala, 2004).

In the first set of experiments, 4-to-5-day-old seedlings were conditioned in BSM (pH 5.5) for 20 minutes, and Ca^{2+} and Mg^{2+}fluxes were measured along the root axis, concentrating on the following zones: root cap (0-30 µm from the root tip), meristem (30-180 µm), distal elongation zone (180-240 µm), proximal elongation zone (240-480 µm) and mature zone (>680 µm).

In the second set of experiments, 4- to 5-day-old seedlings were conditioned in BSM at pH 5.5 for 20 minutes followed by either low-pH (pH 4.2) or combined low-pH/50 µM $AlCl_3$ treatment; Ca^{2+} and Mg^{2+} fluxes were measured at the distal elongation zone (200 µm away from root cap) and the mature zone (700 µm away from root cap) for 60 minutes.

For intracellular Mg^{2+} measurements, the Mg^{2+}-sensitive fluorescent dye, Magnesium Green™-AM (Molecular Probes, Eugene, OR, USA) was dissolved in dimethyl sulphoxide (DMSO) (Sigma, Castle Hill, Australia) and diluted with a loading solution (0.2 mM $CaCl_2$ and 50 mM mannitol, pH 4.2) to a final concentration of 1.5 µM. The final concentration of DMSO in the loading solution was 1% v/v. The dye was loaded into the intact *Arabidopsis* roots for 1 h on ice (Guo *et al.*, 2009), followed by recovery in BSM for 12 h at 25^0C. Then seedlings were exposed to low pH stress (pH 4.2) or Al^{3+} stress (50 µM $AlCl_3$, pH 4.2). After 10 minutes of treatment, Fluorescence Lifetime Images (FLIM) were collected for 500 seconds using photomultipliers, and the FLIM analysis was performed using electronics (SPC-730; Becker & Hickl, Berlin, Germany) and software (SPC7.22; Becker & Hickl) for time-correlated single-photon counting (O'Connor and Desmond, 1984). The intracellular Mg^{2+} was calculated for epidermal cells of the root distal elongation zone according to calibration curves (**Figure 5.2**E) using data analysis software for fluorescence lifetime imaging microscopy systems (SPCImage Version 2.6, MP-FLIM and D-FLIM).

7.3 Results

7.3.1 Long-term effects of low-pH and combined low-pH/Al^{3+} stresses on root Ca^{2+} and Mg^{2+} accumulation

At pH 5.5, the wild type accumulated slightly more Mg^{2+} in roots when compared to the mutants (**Figure 7.1**A). The low-pH treatment decreased Mg^{2+} accumulation in roots of the wild type and *als3* mutant, but did not affect *alr104* and *als5* mutants. The combined low-pH/Al^{3+} treatments inhibited Mg^{2+} accumulation in all the genotypes, but the inhibition was most pronounced in the Al-sensitive genotypes (*als3* and *als5*) followed by the wild type and was least in the Al-resistant mutant (*alr104*). The lowest Al concentration tested (10 µM) caused more than 55% inhibition of Mg^{2+} accumulation in roots of Al-sensitive mutants (*als3* and *als5*).

The Ca^{2+} accumulation in roots (**Figure 7.1**B) showed a similar pattern to that of Mg^{2+}. The Ca^{2+} accumulation in the wild type roots was higher when compared to the mutants at pH 5.5. The low-pH treatment did not affect Ca^{2+} accumulation in roots of *als5* and *alr104* mutants, but inhibited Ca^{2+} accumulation in roots of wild type and *als3* mutant. Though the combined low-pH/Al^{3+} treatments decreased Ca^{2+} accumulation in all genotypes tested, the magnitude of inhibition varied among the genotypes. Al-induced Ca^{2+} inhibition was least in Al-tolerant *alr104* mutant and most severe in the Al-sensitive mutants (*als3* and *als5*).

7.3.2 Long-term effects of combined low-pH/Al^{3+} exposure on root Al concentration

The combined low-pH/Al^{3+} treatment increased Al concentration in the roots of all four genotypes tested, but to a different extent (**Figure 7.2**). The lowest and highest Al concentrations were observed in Al-tolerant *alr104* and Al-sensitive *als5*, respectively. Interestingly, Al-sensitive mutant *als3* and the wild type had similar Al concentration in roots.

7.3.3 Ca^{2+} and Mg^{2+} fluxes along different root zones of *Arabidopsis* mutants at pH 5.5

Ca^{2+} and Mg^{2+} fluxes were measured along the longitudinal root axis (at the root cap, apical meristem, distal and proximal elongation zone and mature zone) (**Figure 7.3**). Ca^{2+} and Mg^{2+} fluxes followed a similar pattern in all genotypes: influx at the root cap, apical meristem, and the distal and proximal elongation zones, but efflux at the mature zone. Highest influx was observed in the distal elongation zone. Among the genotypes, *alr104* mutant recorded smaller Ca^{2+} (**Figure 7.3**A) and higher Mg^{2+} influx (**Figure 7.3**B) than other genotypes at the apical meristem and the distal elongation zone.

7.3.4 Short-term effects of low-pH and combined low-pH/Al^{3+} stresses on Mg^{2+} fluxes

Under no stress (pH 5.5), small net Mg^{2+} influx at the distal elongation zone and net Mg^{2+} efflux at the mature zone were observed in all genotypes (**Figure 7.4**). The low-pH treatment induced Mg^{2+} influx from the distal elongation zone of all genotypes:

als5 and *alr104* recorded higher Mg^{2+} influx than the wild type and *als3* (**Figure 7.4** top left panel). In the mature zone, the low-pH treatment did not cause any significant change in Mg^{2+} fluxes, with the fluxes oscillating around zero in all genotypes (**Figure 7.4** bottom left panel).

The combined low-pH/Al^{3+} treatment (50 μM) induced higher Mg^{2+} influx than the low-pH treatment. This Al-induced Mg^{2+} influx was observed at both distal elongation and mature zones of all genotypes (**Figure 7.4** right panel). Moreover, Al-induced Mg^{2+} influx at the distal elongation zone was higher than at the mature root zone. Among the genotypes, the wild type and Al-resistant *alr104* mutant recorded higher Al-induced Mg^{2+} influx than the Al-sensitive mutants (*als3* and *als5*).

7.3.5 Short-term effects of low-pH and combined low-pH/Al^{3+} stresses on Ca^{2+} fluxes

At pH 5.5, net Ca^{2+} influx at the distal elongation zone (**Figure 7.5**) and net Ca^{2+} efflux at the mature zone (**Figure 7.6**) were observed in all genotypes tested. Among the genotypes, Al-tolerant mutant *alr104* recorded lower Ca^{2+} influx at the distal elongation zone when compared to other genotypes. However, at the mature zone, no difference was observed among genotypes.

At the distal elongation zone, the low-pH treatment did not inhibit net Ca^{2+} influx into Al-tolerant *alr104* mutant, but inhibited net Ca^{2+} influx into other genotypes (**Figure 7.5**). The magnitude of inhibition was greater in the wild type and *als3* mutant compared with the other two genotypes. Interestingly, recovery of Ca^{2+} influx was observed after 25 minutes in *als5* mutant (**Figure 7.5**). At the mature zone, the low-pH treatment did not induce any observable change in the Ca^{2+} fluxes.

The combined low-pH/Al^{3+} treatment (50 μM) induced Ca^{2+} efflux from both distal elongation and mature zones of all genotypes (**Figure 7.5**, **Figure 7.6**). The initial (1 to 4 min) Al-induced Ca^{2+} efflux was higher at the mature zone in comparison to the distal elongation zone. Among the genotypes, the Al-sensitive mutants (*als3* and *als5*) recorded higher Ca^{2+} efflux than the wild type and Al-resistant *alr104* mutant (**Figure 7.5**, **Figure 7.6**). Further, the Al-sensitive mutants (*als3* and *als5*) did not recover from Al-induced Ca^{2+} efflux, with their Ca^{2+} fluxes oscillating around zero at the distal

elongation zone (**Figure 7.5**). In contrast, the wild type and Al-resistant *alr104* mutant exhibited recovery from Al-induced Ca^{2+} efflux to show Ca^{2+} influx after 20 min of Al treatment (**Figure 7.5**).

7.3.6 Short-term effects of low-pH and combined low-pH/Al^{3+} stresses on intracellular Mg^{2+} concentration

Using Fluorescence Life Time Imaging (FLIM) of Magnesium Green™ dye, dynamics of intracellular Mg^{2+} concentrations were measured in the epidermal cells of distal elongation zone of intact *Arabidopsis thaliana* roots (**Figure 7.7**). Under no stress (pH 5.5), intracellular Mg^{2+} concentration varied among the genotypes. Al-resistant mutant *alr104* recorded highest intracellular Mg^{2+} concentration followed by *als5* ≈ wild type > *als3*. In all genotypes tested, the low-pH treatment did not cause any significant changes in Mg^{2+} concentration compared with the control (pH 5.5). In contrast, the combined low-pH/50 μM Al treatment raised intracellular Mg^{2+} concentration in all genotypes, but to a different extent. The wild type and *alr104* mutant recorded higher intracellular Mg^{2+} concentration than the Al-sensitive mutants (*als3* and *als5*).

7.4 Discussion

Measurements of short-term Ca^{2+} and Mg^{2+} fluxes along the longitudinal root axis of *Arabidopsis thaliana* genotypes demonstrated variability in Ca^{2+} and Mg^{2+} uptake between the root apex (influx) and the mature zone (efflux) at pH 5.5 (**Figure 7.3**). Thes differential transport dynamics between the root apex and the mature zone might be due to the presence of different transport systems. Indeed, in *Arabidopsis,* hyperpolarisation-activated cation currents were observed only in the root elongation zone (Kiegle *et al.*, 2000), whereas non-selective cation channels predominate in the mature root zone (Demidchik *et al.*, 2002). Mutant *alr104* exhibited smaller Ca^{2+} influx (**Figure 7.3**A) than other mutants. However, observed lower Ca^{2+} influx in *alr104* may not affect its root growth, because competitive inhibition of Ca^{2+} influx by a wide range of Mg^{2+} concentrations did not decrease the growth rate of root hair tips in *Limnobium stoloniferum* (Jones *et al.,* 1995). Mutant *alr104* also had higher Mg^{2+} influx (**Figure 7.3**B) and intracellular Mg^{2+} concentration (**Figure 7.7**) compared with other genotypes at pH 5.5, suggesting preferential uptake of Mg^{2+} by this mutant.

Arabidopsis mutants showed a differential response in the treatment with low pH: *alr104* and *als5* mutants recorded higher Mg^{2+} influx and less-disturbed Ca^{2+} influx in the distal elongation zone than the wild type and *als3* mutant (**Figure 7.4**, **Figure 7.5**). Such enhanced Mg^{2+} influx and less-disturbed Ca^{2+} influx in *alr104* and *als5* mutants demonstrate the capacity of these mutants to tolerate low-pH stress (Chapter 6, **Figure 6.3**, **Figure 6.4**A) and confirm that Ca^{2+} and Mg^{2+} may ameliorate H^+ toxicity in *Arabidopsis* (Koyama *et al.*, 2001).

The combined low-pH/Al^{3+} treatment caused Ca^{2+} efflux from both the distal elongation and mature zones in all four genotypes within a minute (**Figure 7.5**, **Figure 7.6**). This initial Ca^{2+} efflux may be due to removal of Ca^{2+} from the apoplasm by Al ions because 85 to 99.9% of Al was found in the apoplasm of root cells (Ma, 2007). Ca^{2+} is essential for cross-linking of pectic material (Voragen *et al.*, 2009). Given that Al has greater affinity for pectic material than Ca^{2+} (Blamey, 2001), displacement of Ca^{2+} from pectic material is inevitable during the first few minutes of Al^{3+} exposure. Indeed, between 90% (Reid *et al.*, 1995) and up to 99.99% (Taylor *et al.*, 2000) of cell-wall-bound Ca^{2+} was displaced by Al in *Chara* internodal cells. Such displacement of Ca^{2+} by Al^{3+} ions would severely alter the physical properties of the cell wall, including extensibility, rigidity and permeability (Horst *et al.*, 2007; Jones *et al.*, 2006; Reid *et al.*, 1995; Tabuchi and Matsumoto, 2001), thereby detrimentally affecting root growth. In this study, initial Al-induced Ca^{2+} efflux was higher in Al-sensitive genotypes (*als3* and *als5*) than the wild type and Al-tolerant *alr104* mutant (**Figure 7.5**, **Figure 7.6**), suggesting extensive displacement of Ca^{2+} by Al^{3+} ions in Al-sensitive mutants. This strong Al-induced Ca^{2+} displacement from Al-sensitive mutants might be due to a relatively high pectin content of Al-sensitive mutants (Blamey *et al.*, 1990; Eticha *et al.*, 2005) and/or a greater activity of pectin methylesterase in these mutants because over-expression of this enzyme in *Solanum tuberosum* resulted in severe Al^{3+} toxicity (Schmohl *et al.*, 2000).

In the distal elongation zone, Ca^{2+} fluxes in Al-tolerant genotypes (wild type and *alr104*) recovered to show influx after the initial Al-induced Ca^{2+} efflux, but Ca^{2+} fluxes of Al-sensitive genotypes oscillated around zero (**Figure 7.5**). Similar results were reported in wheat (Huang *et al.*, 1992; Ryan and Kochian, 1993). Pronounced inhibition of Ca^{2+} influx in Al-sensitive genotypes (*als3* and *als5*) under Al^{3+} stress might be due

to the blockage of Ca^{2+}-permeable channels by Al^{3+} ions in the distal elongation zone. Indeed, hyperpolarisation-activated Ca^{2+}-permeable channels responsible for Ca^{2+} influx in the distal elongation zone were highly sensitive to Al, with about 87±7% inhibition reported in *Arabidopsis* (Kiegle *et al.*, 2000). Moreover, other Ca^{2+}-permeable channels, namely depolarisation-activated channels (Pineros and Tester, 1997; Rengel *et al.*, 1995) and hyperpolarisation-activated mechano-sensitive channels (Ding *et al.*, 1993a), were also sensitive to Al. In Al-sensitive mutants (*als3* and *als5*), Al-induced Ca^{2+} efflux was observed within a minute of Al^{3+} exposure followed by Ca^{2+} influx inhibition; hence, disturbance in Ca^{2+} uptake could be one of potential primary causes of Al^{3+} phytotoxicity in *Arabidopsis* (cf. Rengel and Zhang, 2003).

The combined low-pH/Al^{3+} exposure resulted in enhanced Mg^{2+} influx from both distal elongation and mature zones of the wild type and Al-tolerant mutant (*alr104*) (**Figure 7.4**). Given that intracellular Mg^{2+} concentration was higher (1.1 to 1.6 mM) than the external Mg^{2+} concentration (0.2 mM), observed Mg^{2+} influx under Al stress was against the electrochemical gradient. Thus, involvement of high-affinity Mg^{2+} transporters in the wild type and *alr104* mutant cannot be ignored. Indeed, over-expression of *Arabidopsis* plasma membrane high-affinity Mg^{2+} transporter (*AtMGT1* gene) in *Nicotiana benthamiana* increased Al tolerance (Deng *et al.*, 2006) by enhancing Mg^{2+} uptake from a Mg^{2+}-deficient medium. Apart from *AtMGT1*, over-expression of the *ALR1/ALR2* gene (yeast CorA Mg^{2+} transporters) in *Saccharomyces cerevisiae* also improved Al^{3+} tolerance (MacDiarmid and Gardner, 1998).

Efflux of H^+ by electrogenic proton-extruding ATPase is the main driving force for nutrient absorption by plants, especially under stress conditions (Newman, 2001). The Mg^{2+} activity inside the cytoplasm is pivotal for the regulation of H^+-ATPase activity (Brooker and Slayman, 1983; Costa and de Meis, 1996). In fact, ATP hydrolysis usually results in increased intracellular Mg^{2+} concentration in animal cells (Gotoh *et al.*, 1999; Leyssens *et al.*, 1996). Moreover, increased free Mg^{2+} (K_s= 2.9 mM) activated H^+-ATPase activity in maize roots at pH 6.0 (Costa and de Meis, 1996). In contrast, Al stress inhibited H^+-ATPase by 37% in rice bean (*Vigna umbellata*) roots in the absence of Mg^{2+} in a growth medium (Yang *et al.*, 2007). However, addition of micromolar concentration (10 μM) of Mg^{2+} in the external medium restored plasma membrane H^+-ATPase activity, even though Al^{3+} activity was maintained constant

(Yang *et al.*, 2007). Taken together, our data suggest a relatively higher H^+-ATPase activity in Al-tolerant (*alr104* and wild type) vs. Al-sensitive genotypes (*als3* and *als5*), given that the tolerant genotypes recorded larger Mg^{2+} influx from the distal elongation and mature zones (**Figure 7.4**) and higher intracellular Mg^{2+} concentration (**Figure 7.7**) than the Al-sensitive genotypes.

In *Arabidopsis*, exudation of organic acid anions, such as malate through AtALMT transporter (Hoekenga *et al.*, 2006), citrate through MATE transporter (Liu *et al.*, 2009), and pyruvate and succinate (Larsen *et al.*, 1998) have been reported under Al stress. the addition of a micromolar concentration of Mg^{2+} in the external medium alleviated Al^{3+} toxicity by enhancing exudation of citrate in soybean (Silva *et al.*, 2001a) and rice bean (Yang *et al.*, 2007). In this respect, Mg^{2+} acts as a co-factor for many enzymes involved in organic acid synthesis, such as citrate synthase (Boulton and Ratledge, 1980), malate synthase (Howard *et al.*, 2000), malic enzyme (Coleman and Palmer, 1972), malate dehydrogenase (Iglesias and Andreo, 1990), phospho*enol*pyruvate carboxylase (PEPC) (Tovar-Mendez *et al.*, 1998), isocitrate dehydrogenase (Doyle *et al.*, 2001), and pyruvate kinase (Podestá and Plaxton, 1992). Moreover, over-expression of Mg^{2+}-requiring enzymes, *viz*. citrate synthase in canola (Anoop *et al.*, 2003), PEPC in rice (Begum *et al.*, 2009), malate dehydrogenase in lucerne (Tesfaye *et al.*, 2001) and isocitrate dehydrogenase in *Pseudomonas fluorescens* (Middaugh *et al.*, 2005) provided Al tolerance by enhancing organic acid synthesis and release.

Al-tolerant *Arabidopsis* mutant *alr104* and the wild type exude similar levels of citrate upon Al^{3+} exposure (Larsen *et al.*, 1998). Hence, larger Mg^{2+} influx (**Figure 7.4**) coupled with higher intracellular Mg^{2+} (**Figure 7.7**) in the Al-tolerant (wild type and *alr104*) compared with the Al-sensitive genotypes would trigger organic acid synthesis to form an organic acid-Al complex inside the cytoplasm and/or to exude organic acid anions into the rhizosphere. In contrast, low Mg^{2+} influx (**Figure 7.4**) and intracellular Mg^{2+} (**Figure 7.7**) upon Al^{3+} exposure in the Al-sensitive mutants (*als3* and *als5*) would hamper organic acid production in the cytoplasm. This could be the reason why *als3* mutant was unable to detoxify Al as Al-organic acid complex inside the cytoplasm and to remobilize Al away from the sensitive sites in the root tissue using ALS3 (a phloem-localized ABC-transporter like protein) (Larsen *et al.*, 2005).

Differential uptake of Al could account for differences in Al tolerance among the genotypes (Delhaize *et al.*, 1993a). Indeed, Al-tolerant *Arabidopsis* mutant *alr104* had the lowest and Al-sensitive mutant *als5* the highest Al concentration in roots (**Figure 7.2**). The lowest Al concentration in *alr104* mutant was due to superior Al-exclusion mechanism through Al-induced increase in rhizophere pH (Degenhardt *et al.*, 1998). The highest Al concentration in *als5* mutant (**Figure 7.2**), confirmed that this mutant is defective in the Al-exclusion mechanism (Larsen *et al.*, 1996). Interestingly, root Al concentration in the wild type and Al-sensitive mutant *als3* was similar (**Figure 7.2**), even though root growth inhibition by Al was more severe in *als3* mutant than the wild type. The reason for greater root growth inhibition in *als3* mutant than the wild type is due to inability of this mutant to acquire Ca^{2+} and Mg^{2+} from an Al^{3+}-toxic environment.

Exposure of *Arabidopsis* mutants to the combined low-pH/Al^{3+} treatment for 7 days resulted in inhibition of Ca and Mg accumulation in all four genotypes (**Figure 7.1**). This was clearly an aggregate effect of the presence of Al ions as well as a decrease in nutrient-absorbing root surface area (Clarkson, 1985) as the result of prolonged Al^{3+} exposure (7 days). However, the inhibition was lower in Al-tolerant *alr104* mutant and the wild type than in the Al-sensitive mutants (*als3* and als5), suggesting the Al-tolerant genotypes maintained relatively less-disturbed Ca and Mg uptake compared with the Al-sensitive genotypes.

In summary, the enhanced capacity of *als5* and *alr104* mutants to take up Ca^{2+} and Mg^{2+} from a low-pH environment may help these mutants to cope with low-pH stress. Compared with *als3* and *als5*, relatively higher tolerance to the combined low-pH/Al^{3+} stress in the wild type and *alr104* mutant coincided with greater Mg^{2+} influx, higher intracellular Mg^{2+} and lower inhibition of Ca^{2+} uptake. Elevated intracellular Mg^{2+} might play a key role in organic acid synthesis and release in Al-tolerant genotypes. In contrast, large Al-induced Ca^{2+} efflux followed by inhibition of Ca^{2+} influx and inability to take up Mg^{2+} from Al-containing environments may be responsible for poor growth of Al-sensitive genotypes.

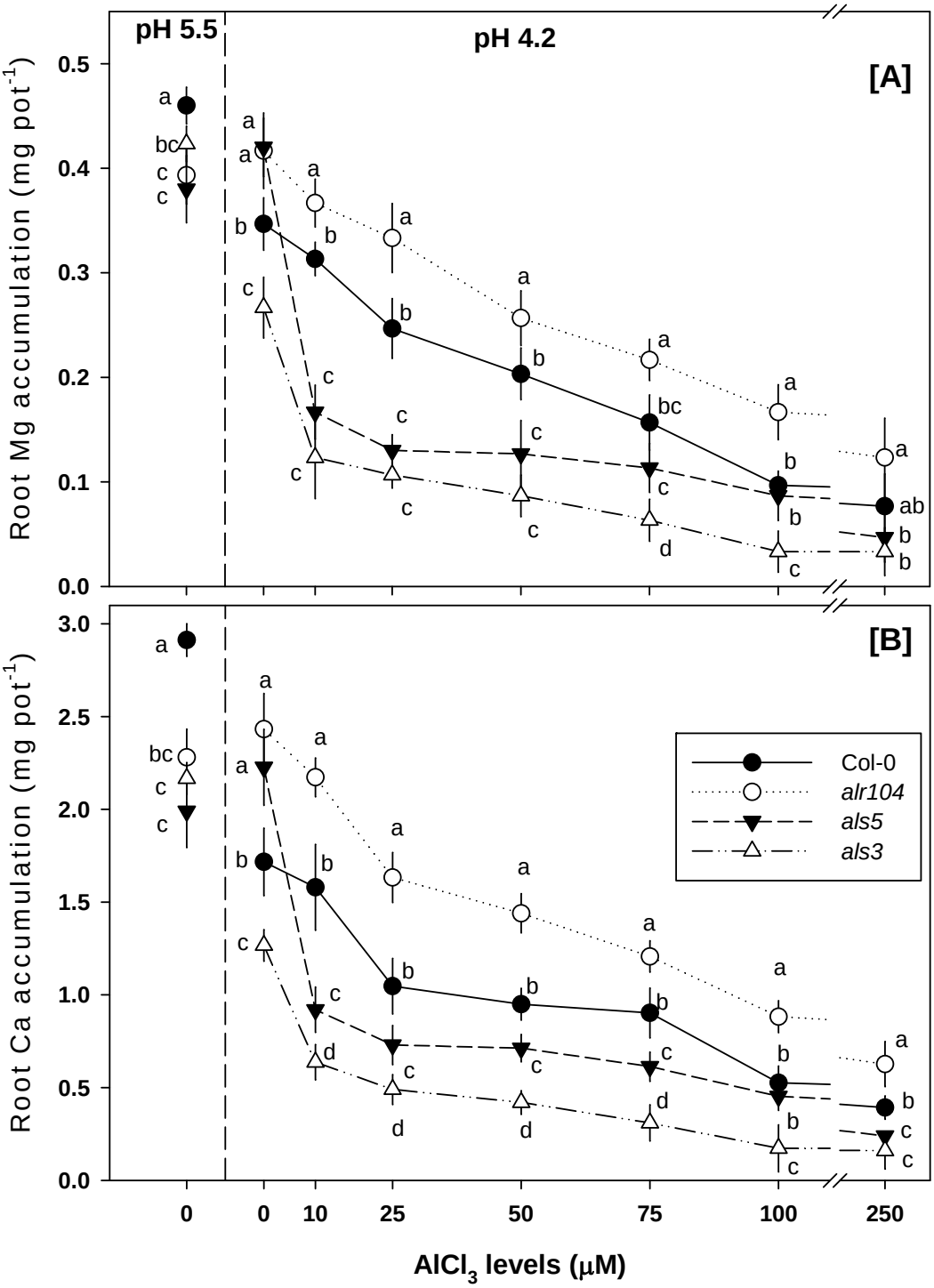

Figure 7.1 Long-term (7 d) effects of low-pH (pH 4.2, 0 μM Al) and combined low-pH/Al^{3+} stresses on [A] Mg; and [B] Ca accumulation in *Arabidopsis thaliana* roots. Means ± SE (n = 3 replicates). In each graph, points sharing common letters are not significantly different by LSD test at $p \leq 0.05$. *Arabidopsis* seedlings were grown in diluted (1/10) Hoagland solution for 3 weeks followed by treatments being imposed in buffered medium (0.5 mM HomoPIPES) for 7 d.

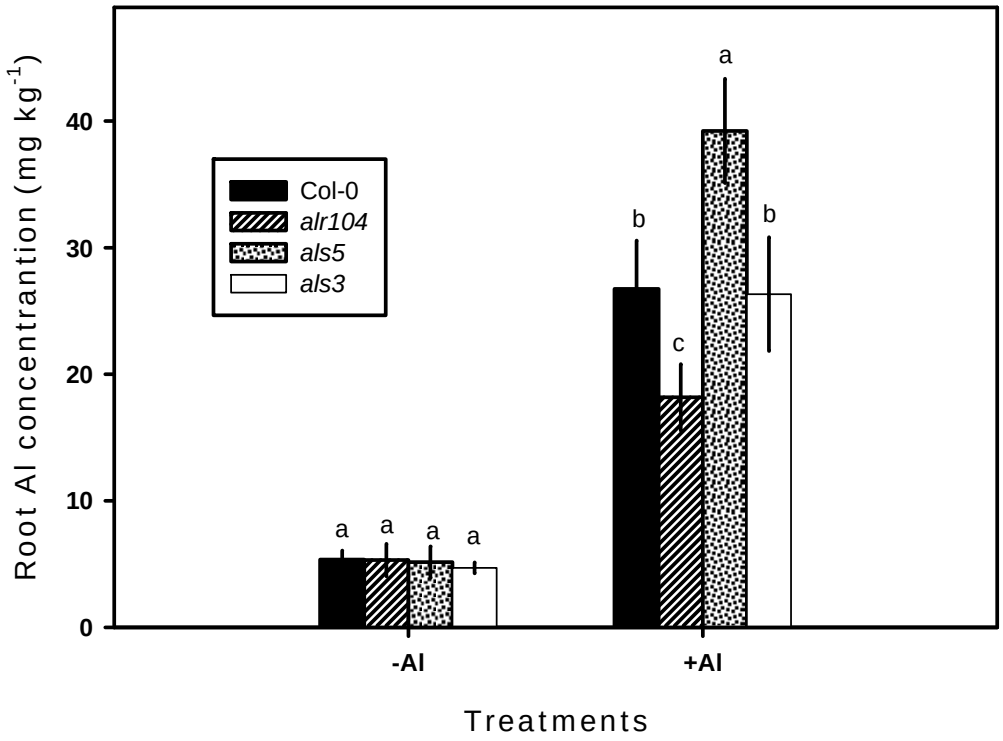

Figure 7.2 Al concentrations in the roots of *Arabidopsis thaliana* after 7 days with (+Al) or without (-Al) aluminium stress.
The data for no Al treatments (-Al, pH 5.50 and 4.20) and Al treatments (+ Al, 10, 25, 50, and 75 µM $AlCl_3$, pH 4.20) were pooled and averaged. Means ± SE (n = 4 to 15 replicates). In each group, bars sharing common letters are not significantly different by LSD test at $p \leq 0.05$. *Arabidopsis* seedlings were grown in diluted (1/10) Hoagland solution for 3 weeks followed by treatments being imposed in buffered medium (0.5 mM HomoPIPES) for 7 d.

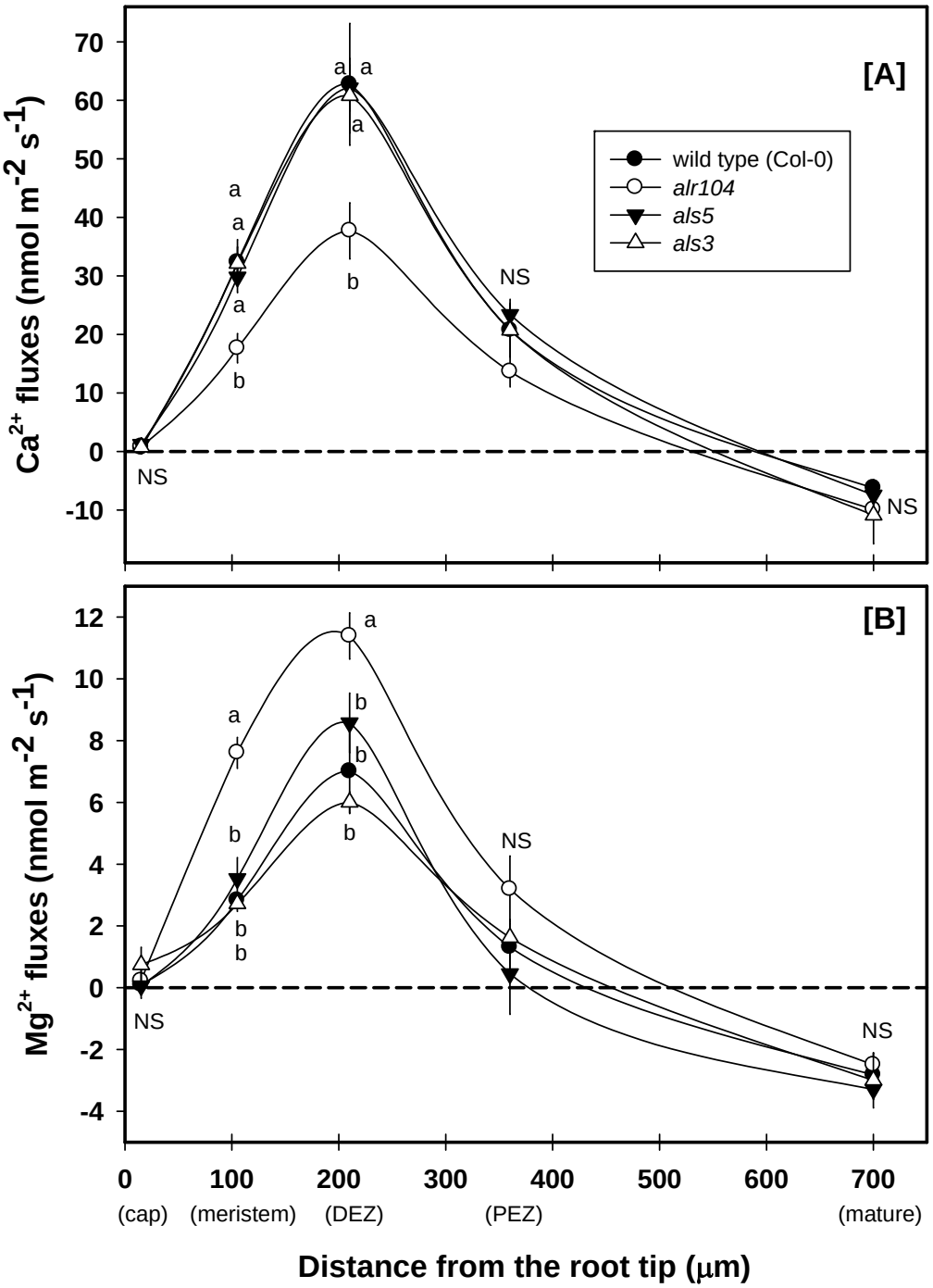

Figure 7.3 Ca^{2+} and Mg^{2+} fluxes along the longitudinal root axis of four- to five-day-old *Arabidopsis thaliana* seedlings in basal salt medium (0.1 mM $CaCl_2$ + 1 mM KCl + 0.2 mM $MgCl_2$, pH 5.5).
Error bars indicate ± SE (n = 6-8 seedlings). In each graph, points sharing common letters are not significantly different by LSD test at $p \leq 0.05$. NS indicates non-significant difference.

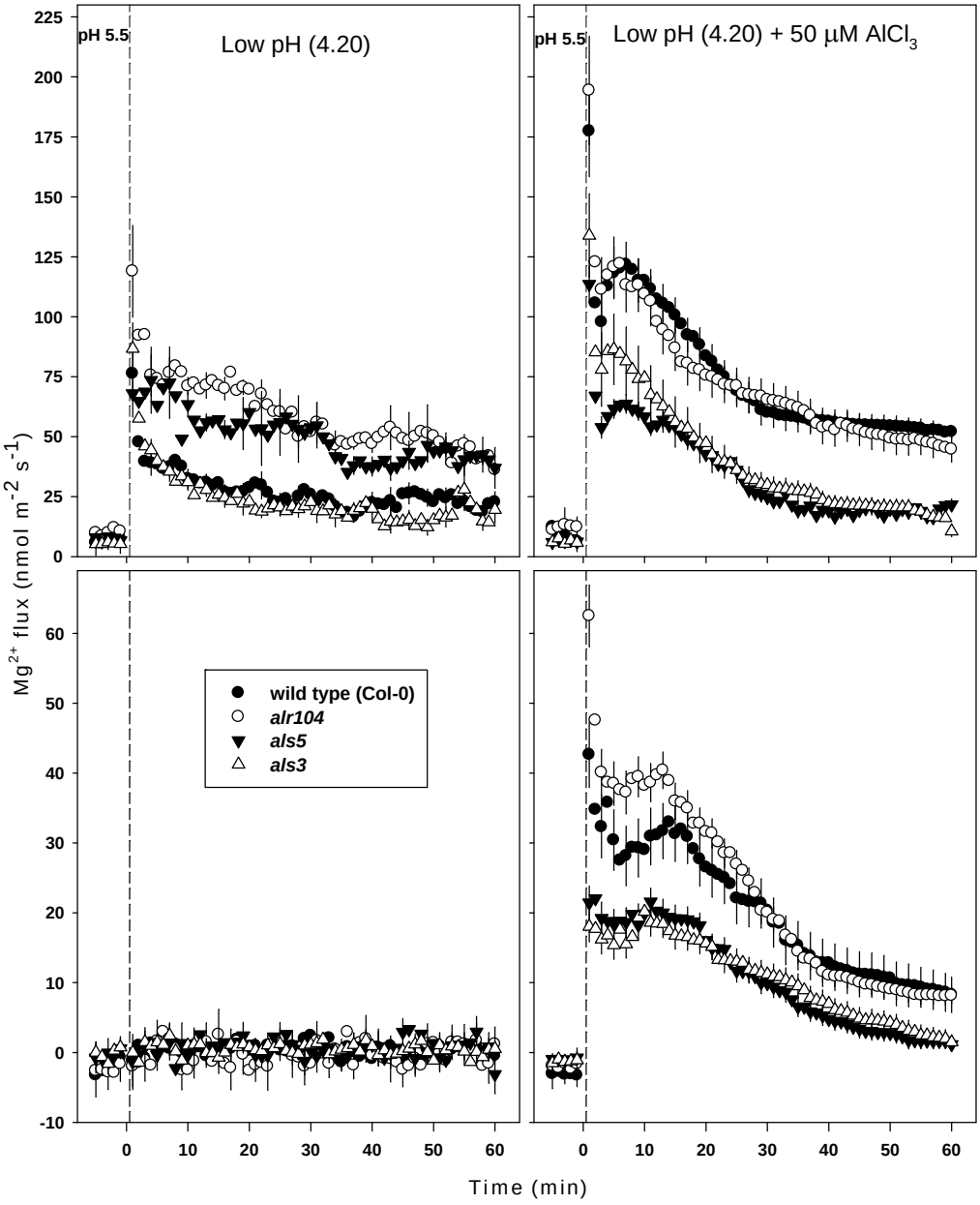

Figure 7.4 Effect of low-pH and combined low-pH/50 µM $AlCl_3$ stresses on Mg^{2+} fluxes measured at the distal elongation zone (top panel) and the mature zone (bottom panel) of four- to five-day-old *Arabidopsis thaliana* roots.
The low-pH and combined low-pH/Al^{3+} treatments were imposed at time = 0; the data recorded in the 5 minutes before time = 0 represent Mg^{2+} fluxes at the respective root zones at pH 5.5. Negative Mg^{2+} flux values indicate Mg^{2+} efflux, and positive values indicate Mg^{2+} influx. Error bars indicate mean ± SE (n = 6 to 15 seedlings). *Arabidopsis* seedlings were conditioned in basal salt medium (BSM; 0.1 mM $CaCl_2$ + 1 mM KCl + 0.2 mM $MgCl_2$, pH 5.5) for 20 min before treatments were imposed in unbuffered BSM.

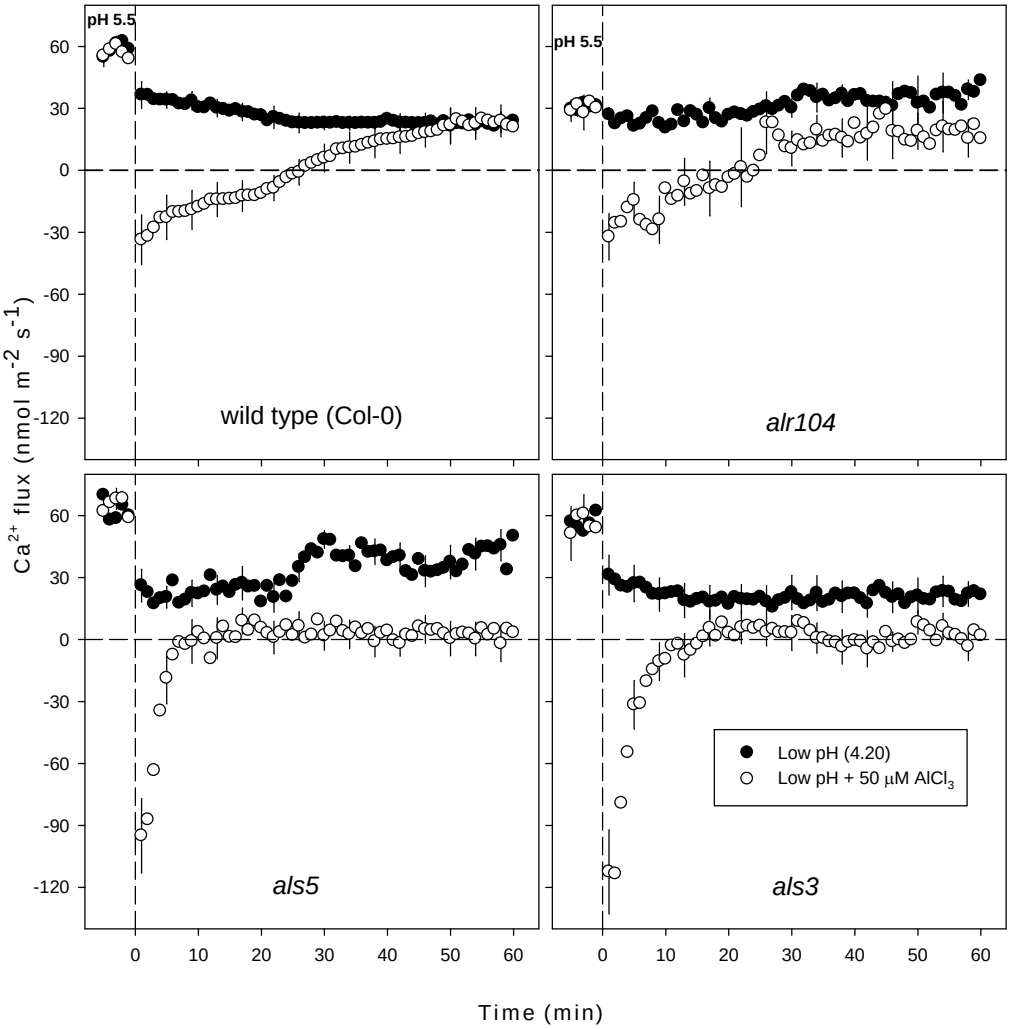

Figure 7.5 Effect of low-pH and combined low-pH/50 μM $AlCl_3$ on Ca^{2+} fluxes measured at the distal elongation zone of four- to five-day-old *Arabidopsis thaliana* roots.
The low-pH and combined low-pH/Al^{3+} treatments were imposed at time = 0; the data recorded in the 5 minutes before time = 0 represent Ca^{2+} fluxes at pH 5.5. Negative Ca^{2+} flux values indicate efflux, and positive values indicate influx. Error bars are ± SE (n = 10 to 14 seedlings). *Arabidopsis* seedlings were conditioned in basal salt medium (BSM; 0.1 mM $CaCl_2$ + 1 mM KCl + 0.2 mM $MgCl_2$, pH 5.5) for 20 min before treatments were imposed in unbuffered BSM.

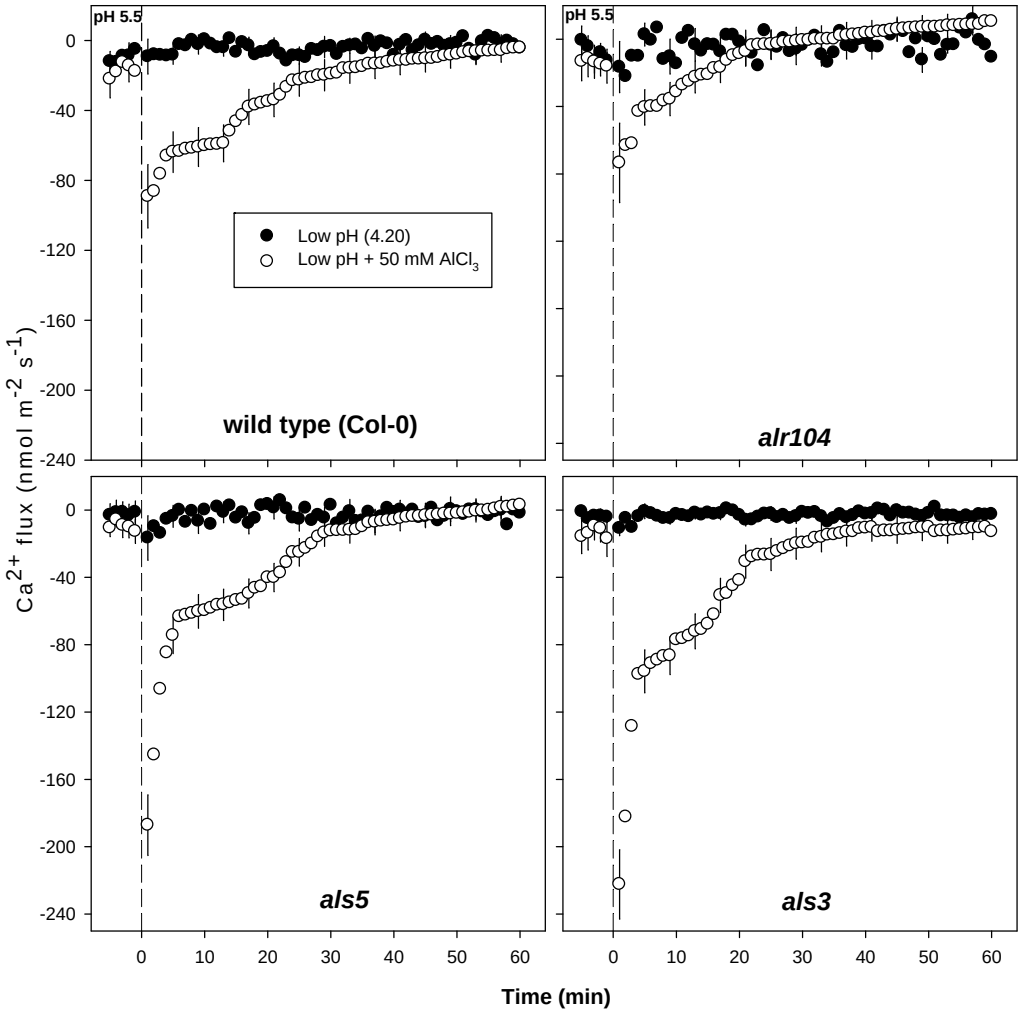

Figure 7.6 Effect of low-pH and combined low-pH/50 µM $AlCl_3$ on Ca^{2+} fluxes measured at the mature zone of four- to five-day-old *Arabidopsis thaliana* roots.
Low-pH and combined low-pH/Al^{3+} treatments were imposed at time = 0; the data recorded in the 5 minutes before time = 0 represent Ca^{2+} fluxes at pH 5.5. Negative Ca^{2+} flux values indicate efflux, and positive values indicate influx. Error bars are ± SE (n = 10 to 14 seedlings). *Arabidopsis* seedlings were conditioned in basal salt medium (BSM; 0.1 mM $CaCl_2$ + 1 mM KCl + 0.2 mM $MgCl_2$, pH 5.5) for 20 min before treatments were imposed in unbuffered BSM.

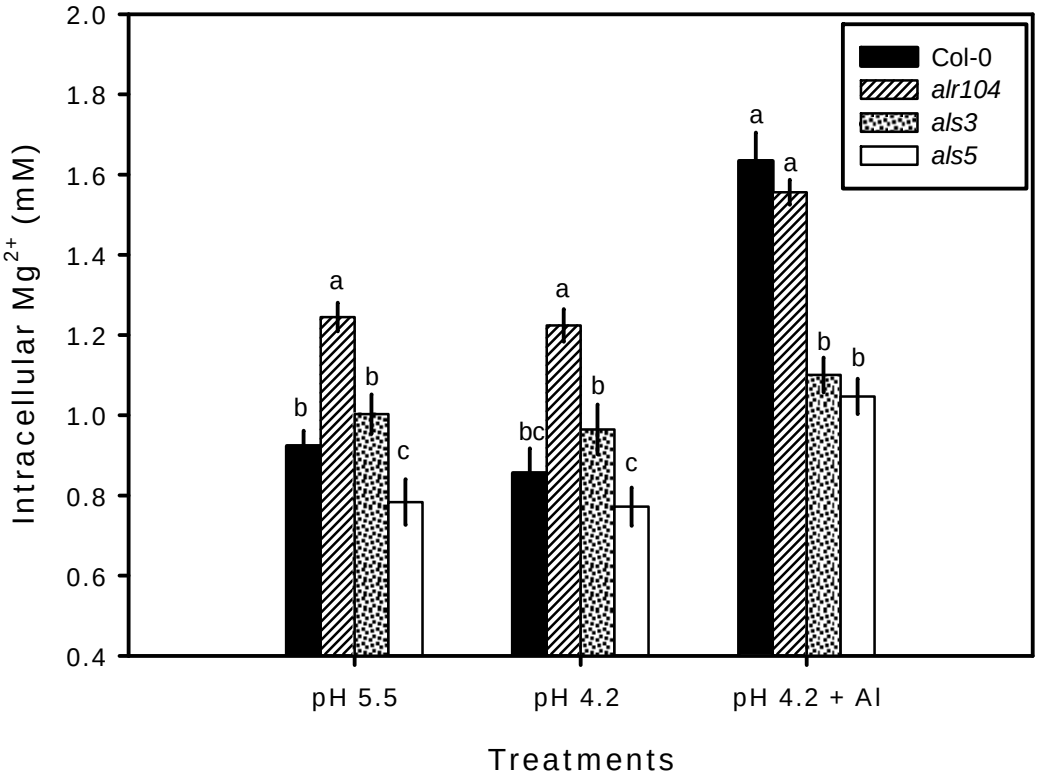

Figure 7.7 Intracellular Mg^{2+} concentration measured in the epidermal cells of distal elongation root zone of four- to five-day-old *Arabidopsis thaliana* after 10 minutes of the low-pH (4.2) or combined low-pH/50 µM $AlCl_3$ treatments using Fluorescence Life Time Imaging (FLIM) of Magnesium Green™ dye.
Error bars indicate ± SE (n = 6 to 10 plants). Bars sharing common letters are not significantly different by LSD test at $p \leq 0.05$.

Chapter 8

General discussion

Characterisation of the *Arabidopsis* wild type demonstrated that the effects of low-pH stress on ion fluxes, membrane potential and intracellular pH are distinctly different from those caused by the combined low-pH/Al^{3+} stress (**Figure 8.1**). Further, *Arabidopsis* mutants differed in their responses to low-pH and combined low-pH/Al^{3+} stresses: *als5* was tolerant to low pH but sensitive to Al^{3+} stress, whereas *als3* was sensitive and *alr104* tolerant to both stresses.

8.1 Differential effects of low-pH and combined low-pH/Al^{3+} stresses

8.1.1 H^+ fluxes and intracellular pH

The low-pH treatment induced H^+ influx in both the distal elongation and the mature root zones of the wild type (**Figure 4.3**, **Figure 4.4**). This influx might be due to either passive entry of H^+ from the external media into the root tissue down the electrochemical gradient (**Figure 8.1**) (Babourina *et al.*, 2001; Yamashita *et al.*, 2003) or decreased activity of the H^+-ATPase (Kasamo, 1986; Zhao *et al.*, 2008a). In any case, net H^+ influx into the root tissue may cause intracellular acidification (Gerendas *et al.*, 1990); **Figure 4.8**), thereby disturbing the cytoplasmic pH homeostasis. Earlier reports showed that genes controlling cytoplasmic pH were down-regulated in the low-pH-hypersensitive *Arabidopsis stop1* mutant (Iuchi *et al.*, 2007; Sawaki *et al.*, 2009). Thus, cytoplasmic acidification may be responsible for poor root growth in the treatments with low pH only. Interestingly, low-pH tolerance of *als5* and *alr104* mutants coincided with high H^+ influx (**Figure 6.6**), suggesting that aforementioned mutants may possess effective mechanisms to prevent cytoplasmic acidification despite high H^+ influx from the external environment; in contrast, such mechanisms would be absent/ineffective in the low-pH-sensitive mutant (*als3*).

Transient changes in cytoplasmic pH are pivotal for the signal cascades to elicit defence mechanisms or developmental processes in response to a variety of environmental stimuli (Roos *et al.*, 2006). Similarly, modulation of cytosolic pH by

low-pH and Al^{3+} stresses (**Figure 8.1**) can act as a secondary messenger to activate/inactivate transporters and enzymes and, in turn, regulate synthesis of organic acid anions and their subsequent release. An increase in intracellular pH towards pH ≈ 6.5 following a combined low-pH/Al^{3+} stress was observed in *Arabidopsis* wild type (**Figure 4.8**). This rise in intracellular pH would favour deprotonation of organic acids inside the cytoplasm (Davies, 1986) and potentially their exudation into the rhizosphere.

The distal elongation zone and the mature zone showed markedly different responses under combined low-pH/Al^{3+} treatments. Al^{3+} stress inhibited net H^+ influx in the distal elongation zone (**Figure 4.3**) and induced net H^+ efflux in the mature zone (**Figure 4.4**). Hence, in both zones, Al^{3+} exposure would result in increased concentrations of H^+ ions in the rhizosphere. Based on this observation, one can speculate that higher H^+ concentrations in the rhizosphere (i) may be a defence mechanism employed by the plants to decrease binding of Al^{3+} in the apoplasm (Kinraide, 1993), and (ii) may exacerbate Al^{3+} toxicity because of a shift in ionic speciation of Al to increase the proportion of Al^{3+}. In this study, Al-sensitive mutants (*als3* and *als5*) showed greater inhibition of H^+ influx in the distal elongation zone as well as greater H^+ efflux in the mature zone compared with Al-tolerant mutant (*alr104*) (**Figure 6.6**). Thus, relatively high H^+ concentration in the rhizosphere of the Al-sensitive genotypes increased the proportion of Al^{3+}, thereby affecting root growth.

8.1.2 Rhizosphere pH

Characterisation of *Arabidopsis* wild type showed that the low-pH treatment increased rhizosphere pH in the distal elongation and mature zones, whereas the combined low-pH/Al^{3+} treatment resulted in lowering of rhizosphere pH in both root zones. Similar observations were noted in other plant species (Kollmeier *et al.*, 2000; Miyasaka *et al.*, 1989; Wenzl *et al.*, 2001), suggesting Al^{3+} stress affects normal rhizosphere alkalisation process required to cope with low-pH environments.

The capacity of genotypes to increase rhizosphere pH has been proposed as one of the mechanisms underlying Al tolerance (Degenhardt *et al.*, 1998; Foy *et al.*, 1965); such alkalinisation of the rhizosphere could also increase tolerance to low-pH stress. Indeed, *als5* and *alr104* mutants had higher rhizosphere pH than the wild type and *als3* mutant, reflecting the tolerance of the former mutants to low pH (**Figure 6.5**). In line

with the impaired rhizosphere alkalinisation mechanism in the combined low-pH/Al^{3+} treatment, the Al-sensitive mutants (*als3* and *als5*) exhibited lower rhizosphere pH in both root zones when compared with the Al-tolerant genotypes (wild type and *alr104*). These findings provide independent support to previous reports that a suppressor mutant of *als3* (*alt1-1*) has enhanced capacity to increase rhizosphere pH (Gabrielson *et al.*, 2006) and that Al-resistant *alr104* mutant has an alkaline rhizosphere under low-pH as well as combined low-pH/Al^{3+} stresses (Degenhardt *et al.*, 1998). Therefore, differential rhizosphere alkalinisation as a mechanism of differential tolerance to low-pH and Al stresses is supported by findings on *alr104*, *als3* and *als5* mutants in this study.

Given that rhizosphere pH changes are the net result of the dynamics of cation/anion uptake and release (including H^+, OH^- and organic acid anions), it is difficult to establish which ion fluxes (and in which direction) are responsible for a specific pattern of pH changes in the rhizosphere. However, a close correlation between rhizosphere pH changes and changes in H^+ flux ($r \geq 0.93$) were observed in this study (**Figures 4.3, 4.4, 4.5**). Thus, H^+ flux in the root tissue is likely to be an important contributor to pH changes in the rhizosphere under low-pH and combined low-pH/Al^{3+} stresses.

8.1.3 K^+ fluxes

In the wild type, low-pH stress elicited K^+ efflux, whereas combined low-pH/100-µM Al stress inhibited K^+ efflux in the distal elongation and induced influx in the mature root zone (**Figure 8.1**). A close link was noted between the plasma membrane potential (E_m) and K^+ fluxes in plants under low-pH and combined low-pH/Al^{3+} stresses. For example, low-pH stress depolarised the E_m, which may either activate K^+ outward-rectifying channels (KORC are activated at E_m potentials less negative than -80 mV) or inactivate K^+ inward-rectifying channels (KIRC requires E_m in the range of -80 to -150 mV for activation), thereby resulting in net K^+ efflux (Maathuis *et al.*, 1997). Similarly, combined low-pH/Al^{3+} stress at first slightly depolarised and subsequently hyperpolarised the E_m, which could either inactivate KORC or activate KIRC, thereby resulting in inhibition of K^+ efflux in the distal elongation zone and induced influx in the mature zone (Maathuis and Sanders, 1995).

K^+ is essential for cell division through polymerisation of actin (Alberts *et al.*, 1994) and turgor-dependent cell elongation caused by accumulation of K^+ in the vacuole (Dolan and Davies, 2004; Frensch, 1997; Sano *et al.*, 2007). Thus, the plant capacity to take up K^+ or retain more K^+ in the tissue has been previously suggested as the low-pH tolerance mechanism, but this hypothesis was not supported in the present thesis because low-pH-sensitive *als3* mutant retained more K^+ in shoots (**Figure 6.4**B) and showed lower K^+ efflux (**Figure 6.7**) than low-pH-tolerant *alr104* mutant.

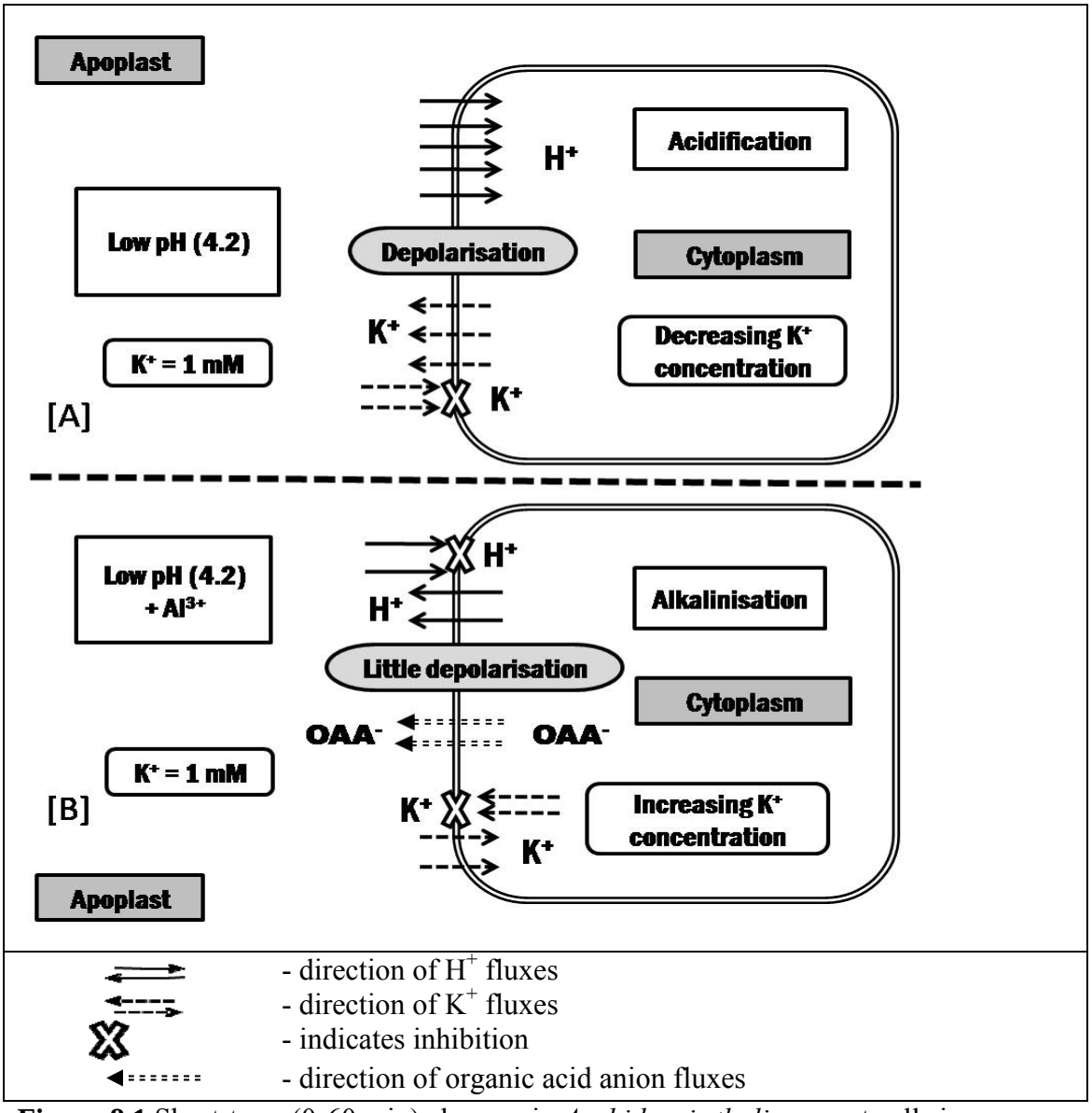

Figure 8.1 Short-term (0-60 min) changes in *Arabidopsis thaliana* root cells in response to [A] low pH stress (H^+ influx and K^+ efflux were activated, and the plasma membrane was depolarized) and [B] Al^{3+} stress (H^+ influx and K^+ efflux were inhibited, H^+ efflux and K^+ influx promoted, and the plasma membrane was less depolarized when compared to low-pH stress). The cytoplamic pH is around 7.0 and K^+ concentration is about 84 mM in unstressed roots.

The Al-sensitive mutants (*als3* and *als5*) had the higher shoot K^+ concentration in comparison with the wild type and *alr104* mutant under combined low-pH/Al^{3+} stress. Consistent with this observation, the combined low-pH/Al stress either decreased K^+ efflux or enhanced K^+ influx in the distal elongation zone in the Al-sensitive mutants (*als3* and *als5*) (**Figure 6.7**), indicating a disturbance in K^+ homeostasis. This shift in K^+ flux towards net influx might be due to a direct or indirect effect of *ALS* mutations. *ALS3* encodes a plasma membrane-localised ABC transporter-like protein that lacks an ATP-binding cassette (Larsen *et al.*, 2005). Given that *ALS3* is highly expressed in the phloem, it is hypothesised that ALS3 is involved in translocation of Al away from Al-sensitive tissues (Larsen *et al.*, 2005). However, 24-h exposure to Al^{3+} showed no effect on *ALS3* expression in the phloem, but changed spatial distribution in other cells, shifting *ALS3* expression from external to internal cells (Larsen *et al.*, 2005). In the current study, an immediate difference between the wild type and *als3* mutants in K^+ fluxes and E_m was observed after exposure to combined low-pH/Al^{3+} stress. Thus, ALS3 functioning may be linked to E_m depolarisation, K^+ efflux and, in a longer term, regulation of K^+ homeostasis. Indeed, higher tolerance to combined low-pH/Al^{3+} stress in the wild type and *alr104* mutant compared with the Al-sensitive mutants (*als3* and *als5*) coincided with higher K^+ efflux and better K^+ homeostasis maintenance as well as a higher resting E_m and more intense E_m depolarisation throughout the combined low-pH/Al^{3+} stress period.

8.1.4 Ca^{2+} fluxes

Low-pH and combined low-pH/Al^{3+} stresses decreased shoot Ca^{2+} concentration (**Figure 5.4**) after long-term Al^{3+} exposure (7 d) of *Arabidopsis thaliana* wild type. Consistent with this observation, in the short-term study (1 h), low-pH and combined low-pH/Al^{3+} stress inhibited Ca^{2+} uptake in the distal elongation and mature root zones (**Figure 5.6**). Combined low-pH/Al^{3+} treatments induced Ca^{2+} efflux within a minute in both root zones. This Al^{3+}-induced instantaneous Ca^{2+} efflux might be due to displacement of Ca^{2+} from the apoplasm by Al^{3+} ions (Kinraide and Parker, 1987; Rengel and Zhang, 2003) because Al^{3+} has stronger affinity for pectin in the cell wall than does Ca^{2+} (Blamey *et al.*, 1990). Displacement of Ca^{2+} by Al^{3+} would severely alter

physical properties of the cell wall, including extensibility, rigidity and permeability (Horst *et al.*, 2007; Jones *et al.*, 2006; Reid *et al.*, 1995; Tabuchi and Matsumoto, 2001), thereby detrimentally affecting cell division and elongation. This Ca^{2+} efflux occurred in the first minute of Al^{3+} exposure, therefore likely preceding root growth inhibition. Hence, Al^{3+}-induced Ca^{2+} efflux could be one of potential primary causes of Al^{3+} phytotoxicity (Rengel, 1992; Rengel and Zhang, 2003).

If the initial Al^{3+}-induced Ca^{2+} efflux from the distal elongation zone was the result of Ca^{2+} displacement from the apoplasm, after the equilibrium period (≈30 min) the Ca^{2+} fluxes should have shown Ca^{2+} influx similar to that in the low-pH treatment (0 Al^{3+}, pH 4.2). Indeed, such recovery was observed under low concentration of Al^{3+} (50 µM Al), but under high concentrations of Al^{3+} (100 and 500 µM Al) Ca^{2+} fluxes oscillated around zero at the distal elongation zone and did not reach Ca^{2+} influx similar to the low-pH treatment (0 Al^{3+}, pH 4.2) for up to 60 min (**Figure 5.6**A). Thus, Al^{3+} concentrations higher than 50 µM inhibited Ca^{2+} influx in the wild type (Huang *et al.*, 1992; Rengel and Elliott, 1992).

Maintenance of Ca^{2+} influx is essential for root growth (Schiefelbein *et al.*, 1992); thus, capacity of genotypes to maintain Ca^{2+} influx from low-pH environments may contribute to low-pH tolerance. This hypothesis was supported in this study because mutants tolerant to low pH (*alr104* and *als5*) recorded higher Ca^{2+} influx in the distal elongation zone than the wild type and *als3* mutant in the low-pH treatment (**Figure 7.5**).

The combined low-pH/50 µM Al^{3+} stress caused Ca^{2+} efflux from both distal elongation and mature root zones within a minute in all four genotypes (**Figure 7.5**, **Figure 7.6**). Interestingly, initial Al-induced Ca^{2+} efflux was higher in the Al-sensitive genotypes (*als3* and *als5*) than the wild type and Al-tolerant *alr104* mutant, suggesting extensive displacement of apoplastic Ca^{2+} by Al ions in the Al-sensitive mutants. This strong Al-induced Ca^{2+} displacement from Al-sensitive mutants suggests that these Al-sensitive mutants (i) may have high pectin content (Blamey *et al.*, 1990; Eticha *et al.*, 2005) and/or (ii) exert high activity of pectin methylesterase because over-expression of this enzyme in *Solanum tuberosum* resulted in severe Al toxicity (Schmohl *et al.*, 2000).

In the distal elongation zone, Ca^{2+} fluxes in Al-tolerant genotypes (wild type and *alr104*) recovered to show net influx after the initial Al-induced Ca^{2+} efflux, but Ca^{2+} influx in Al-sensitive genotypes remained inhibited (**Figure 7.5**). Similar results were reported in wheat (Huang *et al.*, 1992; Ryan and Kochian, 1993). Pronounced inhibition of Ca^{2+} influx in the Al-sensitive *Arabidopsis* genotypes (*als3* and *als5*) under Al stress might have been due to the blockage of Ca^{2+}-permeable channels by Al ions in the distal elongation zone. Given that combined low-pH/50 µM Al stress caused less depolarisation and eventual hyperpolarisation of E_m in the Al-sensitive mutants (*als3* and *als5*; **Figure 6.9**), it may be suggested that Al^{3+} stress inhibited hyperpolarisation-activated Ca^{2+}-permeable channels in Al-sensitive mutants (Kiegle *et al.*, 2000). Moreover, other Ca^{2+}-permeable channels, namely depolarisation-activated channels (Pineros and Tester, 1997; Rengel *et al.*, 1995) and hyperpolarisation-activated mechano-sensitive channels (Ding *et al.*, 1993a), were also sensitive to Al^{3+}.

8.1.5 Mg^{2+} fluxes and intracellular Mg^{2+} concentration

Al^{3+} toxicity impairs uptake of Mg^{2+}, but the underlying physiology, particularly the primary and secondary effects of Al^{3+} toxicity on Mg^{2+} uptake, is poorly understood. Thus, short-term (1 h) and long-term (7 d) Al^{3+} exposure studies were compared in this thesis. Despite intracellular Mg^{2+} being involvement in many cellular processes, there is no information on cytosolic Mg^{2+} activity upon low-pH and Al^{3+} exposure. To my knowledge, the present study reports the first intracellular Mg^{2+} measurement in plants using Mg-sensitive dye and fluorescent lifetime imaging (FLIM) analysis.

Combined low-pH/Al^{3+} stress decreased shoot Mg^{2+} concentration in long-term experiments (**Figure 5.5**), whereas short-term experiments revealed that Al^{3+} stress (50 µM) induced Mg^{2+} influx (**Figure 5.7**) into the root tissue and increased intracellular Mg^{2+} concentration (**Figure 5.9**) of *Arabidopsis thaliana* wild type. This apparent disagreement between short- and long-term Al^{3+} effects can be explained by Al-induced impairment of root growth and a consequent decrease in the nutrient-absorbing surface area (Clarkson, 1985) and/or prolonged Al^{3+} exposure disturbing many biochemical and physiological processes; thus, secondary effects (not directly caused by Al^{3+}) can affect Mg^{2+} uptake in long-term experiments (Rengel and Robinson, 1989a).

On the other hand, exposure of *Arabidopsis* roots to Al^{3+} concentrations higher than 50 μM (treatments with 100 and 500 μM Al) decreased intracellular Mg^{2+} concentrations in a dose-dependent manner (**Figure 5.9**). This decline might have been due to decreased Mg^{2+} influx, or even Mg^{2+} efflux at 500 μM Al (Figs. 3), caused by Al inhibition of plasma membrane cation channels because the driving force for Mg^{2+} transport (E^{D}_{Mg}) within the first 10 min under these conditions would have been directed inward [-30 to -50 mV]. The driving force calculations were based on external and internal Mg^{2+} concentrations (0.2 mM and 0.9 mM, respectively) and E_m during the first 10 min of Al^{3+} application (-50 to -70 mV; **Figure 4.9**A).

In the low-pH treatment, *alr104* and *als5* mutants had higher Mg^{2+} influx in the distal elongation zone than the wild type and *als3* mutant (**Figure 7.4**). Such enhanced Mg^{2+} influx in *alr104* and *als5* mutants might contribute to low-pH stress tolerance because an addition of Mg^{2+} ameliorated H^{+} toxicity in *Arabidopsis* (Koyama *et al.*, 2001).

The combined low-pH/50 μM Al^{3+} exposure resulted in enhanced Mg^{2+} influx into both distal elongation and mature root zones of the wild type and Al-tolerant mutant (*alr104*) (**Figure 7.4**). Considering intracellular Mg^{2+} concentration was higher (0.9 to 1.3 mM) than Mg^{2+} concentration in the rooting medium (0.2 mM), observed Mg^{2+} influx under combined low-pH/Al^{3+} stress was against the electrochemical gradient. Further, over-expression of *Arabidopsis* plasma membrane high-affinity Mg^{2+} transporter (*AtMGT1* gene) in *Nicotiana benthamiana* increased Al tolerance by enhancing Mg^{2+} uptake from Mg^{2+}-deficient medium (Deng *et al.*, 2006). Thus, it is possible that some high-affinity Mg^{2+} transporters might have been activated in the wild type and *alr104* mutant following Al^{3+} exposure.

It should be borne in mind that Mg^{2+} is a co-factor for many enzymes involved in organic acid synthesis (**Chapter 7.4**). Indeed, over-expression of Mg^{2+}-requiring enzymes provided Al tolerance by enhancing organic acid synthesis and release (**Chapter 7.4**). Al-tolerant *Arabidopsis* mutant *alr104* and the wild type exude similar amounts of citrate upon Al exposure (Larsen *et al.*, 1998). Hence, larger Mg^{2+} influx (**Figure 7.4**) coupled with higher intracellular Mg^{2+} (**Figure 7.7**) in the Al-tolerant (wild type and *alr104*) compared with the Al-sensitive genotypes would enhance

organic acid synthesis to potentially form organic acid-Al complex in the cytoplasm and/or to exude organic acid anions into the rhizosphere. In contrast, low Mg^{2+} influx and low intracellular Mg^{2+} in Al-sensitive mutants (*als3* and *als5*) upon Al exposure would hamper organic acid production in the cytoplasm.

Al^{3+} stress inhibited H^+-ATPase in rice bean (*Vigna umbellata*) roots in the absence of Mg^{2+} in a growth medium. However, addition of 10 μM concentration of Mg^{2+} in the external medium restored plasma membrane H^+-ATPase activity, even though Al^{3+} activity was maintained constant (Yang *et al.*, 2007). Intracellular Mg^{2+} is involved in the regulation of H^+-ATPase (Brooker and Slayman, 1983; Costa and de Meis, 1996). In fact, ATP hydrolysis usually results in increased intracellular Mg^{2+} concentration in animal cells (Gotoh *et al.*, 1999; Leyssens *et al.*, 1996). Moreover, elevated free Mg^{2+} (K_s= 2.9 mM) activated H^+-ATPase in maize roots vesicles (Costa and de Meis, 1996). In light of these literature reports and considering findings reported here [higher Mg^{2+} influx into the distal elongation and mature zones (**Figure 7.4**) and higher intracellular Mg^{2+} concentration (**Figure 7.7**) in the Al-tolerant (wild type and *alr104*) than Al-sensitive genotypes (*als3* and *als5*)], it could be suggested that a relatively higher H^+-ATPase activity existed in Al-tolerant vs. Al-sensitive genotypes.

Chapter 9

Conclusions and Future Work

This project clearly demonstrated that low-pH and combined low-pH/Al^{3+} stresses differentially affect root tissues and, consequently, the chemistry of the rhizosphere. Low-pH stress induced H^+ influx, intracellular acidification, rhizosphere alkalization, K^+ efflux and depolarisation of plasma membrane. By contrast, Al^{3+} stress inhibited H^+ influx, rhizosphere alkalinisation and K^+ efflux, promoted H^+ efflux, intracellular alkalinisation and K^+ influx, and depolarised the plasma membrane only slightly when compared to low-pH stress.

Among the *Arabidopsis* mutants tested, *als5* grew well under low-pH stress and poorly under Al^{3+} stress, whereas *als3* was sensitive and *alr104* tolerant to both stresses, suggesting that low-pH and combined low-pH/Al^{3+} tolerances are controlled by some common and some distinct mechanisms. The capacity of some *Arabidopsis* genotypes to alkalinise the rhizosphere and take up H^+ from a low-pH environment is linked to the tolerance to low-pH and combined low-pH/Al^{3+} stresses. The capacity of *Arabidopsis* genotypes to maintain Ca^{2+} influx from low-pH environments contributed to low-pH tolerance, whereas the capacity of genotypes to recover from initial Al-induced Ca^{2+} efflux to achieve Ca^{2+} influx coincided with combined low-pH/Al^{3+} tolerance. In the case of Mg^{2+}, enhanced Mg^{2+} influx helped the genotypes to cope with low-pH and combined low-pH/Al^{3+} stresses. Maintenance of K^+ efflux together with E_m depolarisation coincided with Al tolerance. However, retention of high K^+ in shoots and/or low K^+ efflux from root tissue under low-pH stress did not contribute to low-pH tolerance.

The initial Al-induced Ca^{2+} efflux was relatively high in the Al-sensitive mutants, suggesting higher pectin or activity of pectin methyl esterase in the Al-sensitive mutants than the Al-tolerant mutant. Future work should measure pectin or pectin methyl esterase activity in mutants differing in Al sensitivity to address this hypothesis.

This project developed a new method to measure intracellular Mg^{2+} concentration dynamics using Mg^{2+}-specific fluorescent dye and fluorescent lifetime imaging (FLIM) analysis. Measured intracellular Mg^{2+} concentrations ranged from 0.77±0.05 to 1.63±0.07 mM depending on the treatment. Al^{3+} stress enhanced Mg^{2+} influx and elevated cytosolic Mg^{2+} concentration in Al-tolerant genotypes. Considering a pivotal role of intracellular Mg^{2+} in regulation of H^{+}-ATPase activity and organic acid synthesising enzymes, this elevated Mg^{2+} may fuel organic acid synthesis in the cytoplasm of Al-tolerant genotypes for subsequent release into the rhizosphere. Further work, particularly to characterize activities of H^{+}-ATPase and organic acid synthesising enzymes in Al-tolerant genotypes together with monitoring cytosolic Mg^{2+} concentration, is eagerly awaited to address this hypothesis.

The low-pH and moderate level of Al^{3+} stress enhanced Mg^{2+} influx in tolerant genotypes, but the Mg^{2+} transport mechanism behind this observation is unclear. Characterisation of *Arabidopsis* mutants which are defective in Mg^{2+} transporters or cation channels may help to decipher Mg^{2+} uptake mechanisms from low-pH and Al-toxic environments. The preliminary experiment on *Arabidopsis* cyclic nucleotide-gated channel (AtCNGC10) showed its capacity to transport Mg^{2+}(Guo *et al.*, 2010), with antisense lines (A2 and A3) of this channel having greater sensitivity to low-pH and Al^{3+} stress than the wild type. Thus, further work on the AtCNGC10 channel may characterise potential involvement of cyclic nucleotide-gated channels in low-pH and Al^{3+} tolerance.

Molecular characterisation of *als3* resulted in identification of ALS3 as a plasma membrane-localised ABC transporter-like protein; however, such information is not available for *alr104* and *als5* mutants. Future characterization of *alr104* and *als5* mutants at the molecular level would pave way for identification of genes that are essential for low-pH and combined low-pH/Al^{3+} tolerance.

References

Ahn SJ, Matsumoto H. 2006. The role of the plasma membrane in the response of plant roots to aluminum toxicity. *Plant Signaling & Behavior* **1**, 37-45.

Ahn SJ, Rengel Z, Matsumoto H. 2004a. Aluminum-induced plasma membrane surface potential and H^+-ATPase activity in near-isogenic wheat lines differing in tolerance to aluminum. *New Phytologist* **162**, 71-79.

Ahn SJ, Shin R, Schachtman DP. 2004b. Expression of KT/KUP genes in *Arabidopsis* and the role of root hairs in K^+ uptake. *Plant Physiology* **134**, 1135-1145.

Ahn SJ, Sivaguru M, Chung GC, Rengel Z, Matsumoto H. 2002. Aluminium-induced growth inhibition is associated with impaired efflux and influx of H^+ across the plasma membrane in root apices of squash (*Cucurbita pepo*). *Journal of Experimental Botany* **53**, 1959-1966.

Ahn SJ, Sivaguru M, Osawa H, Chung GC, Matsumoto H. 2001. Aluminum inhibits the H^+-ATPase activity by permanently altering the plasma membrane surface potentials in squash roots. *Plant Physiology* **126**, 1381-1390.

Aidemark M, Andersson C-J, Rasmusson A, Widell S. 2009. Regulation of callose synthase activity *in situ* in alamethicin-permeabilized *Arabidopsis* and tobacco suspension cells. *BMC Plant Biology* **9**, 27.

Aitken RL, Dickson T, Hailes KJ, Moody PW. 1999. Response of field-grown maize to applied magnesium in acidic soils in north-eastern Australia. *Australian Journal of Agricultural Research* **50**, 191-198.

Akeson MA, Munns DN, Burau RG. 1989. Adsorption of Al^{3+} to phosphatidylcholine vesicles. *Biochimica et Biophysica Acta (BBA) - Biomembranes* **986**, 33-40.

Alberts B, Bray D, Lewis J, Raff M, Roberts K, Watson JD. 1994. *Molecular Biology of the Cell*. New York & London: Garland Publishing, Inc

Allen GJ, Sanders D. 1996. Control of ionic currents in guard cell vacuoles by cytosolic and luminal calcium. *Plant Journal* **10**, 1055-1069.

Amalou Z, Gibrat R, Brugidou C, Trouslot P, Dauzac J. 1992. Evidence for an amiloride-inhibited $Mg^{2+}/2H^{+}$ antiporter in lutoid (vacuolar) vesicles from latex of *Hevea brasiliensis*. *Plant Physiology* **100**, 255-260.

Amalou Z, Gibrat R, Trouslot P, Dauzac J. 1994. Solubilization and reconstitution of the $Mg^{2+}/2H(+)$ antiporter of the lutoid tonoplast from *Hevea brasiliensis* latex. *Plant Physiology* **106**, 79-85.

Amenos M, Corrales I, Poschenrieder C, Illes P, Baluska F, Barcelo J. 2009. Different effects of aluminum on the actin cytoskeleton and brefeldin a-sensitive vesicle recycling in root apex cells of two maize varieties differing in root elongation rate and aluminum tolerance. *Plant and Cell Physiology* **50**, 528-540.

Amtmann A, Jelitto TC, Sanders D. 1999. K^{+}-selective inward-rectifying channels and apoplastic pH in Barley roots. *Plant Physiology* **120**, 331-338.

Andreev IM. 2001. Functions of the vacuole in higher plant cells. *Russian Journal of Plant Physiology* **48**, 672-680.

Anoop VM, Basu U, McCammon MT, McAlister-Henn L, Taylor GJ. 2003. Modulation of citrate metabolism alters aluminum tolerance in yeast and transgenic canola overexpressing a mitochondrial citrate synthase. *Plant Physiology* **132**, 2205-2217.

Arnon DI, Johnson CM. 1942. Influence of hydrogen ion concentration on the growth of higher plants under controlled conditions. *Plant Physiology* **17**, 525-539.

Babourina O, Hawkins B, Lew RR, Newman I, Shabala S. 2001. K^{+} transport by *Arabidopsis* root hairs at low pH. *Australian Journal of Plant Physiology* **28**, 635-641.

Babourina O, Ozturk L, Cakmak I, Rengel Z. 2006. Reactive oxygen species production in wheat roots is not linked with changes in H^{+} fluxes during acidic and aluminium stresses. *Plant Signaling & Behavior* **1**, 71-76.

Babourina O, Rengel Z. 2009. Uptake of aluminium into *Arabidopsis* root cells measured by fluorescent lifetime imaging. *Annals of Botany* **104**, 189-195.

Babourina O, Voltchanskii K, Newman I, Rengel Z. 2005. Ca^{2+} effects on K^{+} fluxes in *Arabidopsis* seedlings exposed to Al^{3+}. *Soil Science and Plant Nutrition* **51**, 733-736.

Baligar VC, Schaffert RE, Dos Santos HL, Pitta GVE, De C Filho B. 1993. Growth and nutrient uptake parameters in sorghum as influenced by aluminum. *Agronomy Journal* **85**, 1068-1074.

Baluška F, Mancuso S, Volkmann D, Barlow P. 2004. Root apices as plant command centres: the unique 'brain-like'status of the root apex transition zone. *Biologia (Bratislava)* **59**, 7–19.

Bandurski RS. 1955. Further studies on the enzymatic synthesis of oxalacetate from phosphorylenolpyruvate and carbon dioxide. *Journal of Biological Chemistry* **217**, 137-150.

Banuelos MA, Sychrova H, Bleykasten-Grosshans C, Souciet JL, Potier S. 1998. The Nha1 antiporter of *Saccharomyces cerevisiae* mediates sodium and potassium efflux. *Microbiology* **144**, 2749-2758.

Basu U, Godbold D, Taylor GJ. 1994. Aluminum resistance in *Triticum aestivum* associated with enhanced exudation of malate. *Journal of Plant Physiology* **144**, 747-753.

Begum HH, Osaki M, Watanabe T, Shinano T. 2009. Mechanisms of aluminum tolerance in phosphoenolpyruvate carboxylase transgenic rice. *Journal of Plant Nutrition* **32**, 84-96.

Bennet RJ, Breen CM, Fey MV. 1987. The effects of aluminium on root cap function and root development in *Zea mays* L. *Environmental and Experimental Botany* **27**, 91–104.

Bethke PC, Jones RL. 1994. Ca2(+)-calmodulin modulates ion channel activity in storage protein vacuoles of barley aleurone cells. *Plant Cell* **6**, 277-285.

Bibikova T, Gilroy S. 2002. Root hair development. *Journal of Plant Growth Regulation* **21**, 383-415.

Blamey FPC. 2001. The role of the root cell wall in aluminum toxicity. In: Ae N, Arihara J, Okada K, Srinivasan A, eds. *Plant nutrient acquisition: New perspectives*. Tokyo, Japan: Springer Verlag, 201-226.

Blamey FPC, Edmeades DC, Wheeler DM. 1990. Role of root cation-exchange capacity in differential aluminum tolerance of *Lotus* species. *Journal of Plant Nutrition* **13**, 729 - 744.

Blamey FPC, Nishizawa NK, Yoshimura E. 2004. Timing, magnitude, and location of initial soluble aluminum injuries to mungbean roots. *Soil Science and Plant Nutrition* **50**, 67-76.

Bolan NS, Hedley MJ, White RE. 1991. Processes of soil acidification during nitrogen cycling with emphasis on legume based pastures. *Plant and Soil* **134**, 53-63.

Boscolo PRS, Menossi M, Jorge RA. 2003. Aluminum-induced oxidative stress in maize. *Phytochemistry* **62**, 181-189.

Boulton CA, Ratledge C. 1980. Regulatory studies on citrate synthase in Candida 107, an oleaginous yeast. *Microbiology* **121**, 441-447.

Brady DJ, Edwards DG, Asher CJ, Blamey FPC. 1993. Calcium amelioration of aluminum toxicity effects on root hair development in soybean [*Glycine max* (L) Merr]. *New Phytologist* **123**, 531-538.

Brady NC, Weil RR. 1990. *Nature and properties of soils*. New york: Macmillan Publishing Company.

Brigham LA, Hawes MC, Miyasaka SC. 2001. Avoidance of aluminium toxicity: Role of root border cells. In: Horst WJ, Schenk MK, Bürkert A, Claassen N, Flessa H, Frommer WB, Goldbach H, Olfs HW, Römheld V, Sattelmacher B, Schmidhalter U, Schubert S, Wirén Nv, Wittenmayer L, eds. *Plant Nutrition - Food security and sustainability of agro-ecosystems through basic and applied research*, Vol. 92. Dordrecht: Kluwer Academic Publishers, 452-453.

Brooker RJ, Slayman CW. 1983. Effects of Mg^{2+} ions on the plasma membrane [H^+]-ATPase of *Neurospora crassa*. II. Kinetic studies. *Journal of Biological Chemistry* **258**, 8833-8838.

Büscher P, Koedam N, Van Speybroeck D. 1990. Cation-exchange properties and adaptation to soil acidity in bryophytes. *New Phytologist* **115**, 177-186.

Bui DM, Gregan J, Jarosch E, Ragnini A, Schweyen RJ. 1999. The bacterial magnesium transporter CorA can functionally substitute for its putative homologue Mrs2p in the yeast inner mitochondrial membrane. *Journal of Biological Chemistry* **274**, 20438-20443.

Bush DS. 1995. Calcium regulation in plant cells and its role in signaling. *Annual Review of Plant Biology* **46**, 95-122.

Cakmak I, Horst WJ. 1991. Effect of aluminium on lipid peroxidation, superoxide dismutase, catalase, and peroxidase activities in root tips of soybean (*Glycine max*). *Physiologia Plantarum* **83**, 463-468.

Calba H, Jaillard B. 1997. Effect of aluminium on ion uptake and H^+ release by maize. *New Phytologist* **137**, 607-616.

Carpaneto A, Cantu AM, Gambale F. 1999. Redox agents regulate ion channel activity in vacuoles from higher plant cells. *FEBS Letters* **442**, 129-132.

Chandran D, Sharopova N, Ivashuta S, Gantt JS, VandenBosch KA, Samac DA. 2008. Transcriptome profiling identified novel genes associated with aluminum toxicity, resistance and tolerance in *Medicago truncatula*. *Planta* **228**, 151-166.

Chen JP, Sucoff EI, Stadelmann EJ. 1991. Aluminum and temperature alteration of cell membrane permeability of *Quercus rubra*. *Plant Physiology* **96**, 644-649.

Chen RF, Shen RF. 2008. Root phosphate exudation and pH shift in the rhizosphere are not responsible for aluminum resistance in rice. *Acta Physiologiae Plantarum* **30**, 817-824.

Chen W, Liu P, Xu G, Cai M, Yu H, Chen M. 2008. Effects of A1~(3+) on the biological characteristics of cowpea root border cells. *Acta Physiologiae Plantarum* **30**, 303-308.

Clarkson DT. 1965. The effect of aluminium and some other trivalent metal cations on cell division in the root apices of *Allium cepa*. *Annals of Botany* **29**, 309-315.

Clarkson DT. 1984. Calcium transport between tissues and its distribution in the plant. *Plant Cell and Environment* **7**, 449-456.

Clarkson DT. 1985. Factors affecting mineral nutrient acquisition by plants. *Annual Review of Plant Biology* **36**, 77-115.

Coleman JOD, Palmer JM. 1972. The Oxidation of Malate by Isolated Plant Mitochondria. *European Journal of Biochemistry* **26**, 499-509.

Collins NC, Shirley NJ, Saeed M, Pallotta M, Gustafson JP. 2008. An *ALMT1* gene cluster controlling aluminum tolerance at the *Alt4* locus of rye (*Secale cereale* L.). *Genetics* **179**, 669-682.

Costa MS, de Meis L. 1996. Regulation of plasma membrane H^+-ATPase from corn root by Mg^{2+} and pH. *Biochimica et Biophysica Acta* **1279**, 214-218.

Cuin TA, Shabala S. 2005. Exogenously supplied compatible solutes rapidly ameliorate NaCl-induced potassium efflux from Barley roots. *Plant and Cell Physiology* **46**, 1924-1933.

d'Auzac J, Jacob J, Chrestin H. 1989. The composition of latex from *Hevea brasiliensis* as a laticiferous cytoplasm In: d'Auzac J, Jacob J, Chrestin H, eds. *Physiology of rubber tree latex*. Boca Raton: FL: CRC Press, 59–96.

Darko E, Ambrus H, Stefanovits-Banyai E, Fodor J, Bakos F, Barnaba B. 2004. Aluminium toxicity, Al tolerance and oxidative stress in an Al-sensitive wheat genotype and in Al-tolerant lines developed by in vitro microspore selection. *Plant Science* **166**, 583-591.

Davies DD. 1986. The fine control of cytosolic pH. *Physiologia Plantarum* **67**, 702-706.

Day RN. 2005. Imaging protein behavior inside the living cell. *Molecular and Cellular Endocrinology* **230**, 1-6.

Day RN, Schaufele F. 2005. Imaging molecular interactions in living cells. *Molecular Endocrinology* **19**, 1675-1686.

De Campos JMS, Viccini LF. 2003. Cytotoxicity of aluminum on meristematic cells of *Zea mays* and *Allium cepa*. *Caryologia* **56**, 65-73.

De Cnodder T, Vissenberg K, Van Der Straeten D, Verbelen JP. 2005. Regulation of cell length in the *Arabidopsis thaliana* root by the ethylene precursor 1-aminocyclopropane-1-carboxylic acid: a matter of apoplastic reactions. *New Phytologist* **168**, 541-550.

Degenhardt J, Larsen PB, Howell SH, Kochian LV. 1998. Aluminum resistance in the *Arabidopsis* mutant *alr*-104 is caused by an aluminum-induced increase in rhizosphere pH. *Plant Physiology* **117**, 19-27.

Delhaize E, Craig S, Beaton CD, Bennet RJ, Jagadish VC, Randall PJ. 1993a. Aluminum tolerance in wheat (*Triticum aestivum* L.) I. Uptake and distribution of aluminum in root apices. *Plant Physiology* **103**, 685-693.

Delhaize E, Gruber BD, Ryan PR. 2007. The roles of organic anion permeases in aluminium resistance and mineral nutrition. *FEBS Letters* **581**, 2255-2262.

Delhaize E, Ryan PR. 1995. Aluminum toxicity and tolerance in plants. *Plant Physiology* **107**, 315-321.

Delhaize E, Ryan PR, Randall PJ. 1993b. Aluminum tolerance in wheat (*Triticum aestivum* L.): II. Aluminum-stimulated excretion of malic acid from root apices. *Plant Physiology* **103**, 695-702.

Demidchik V, Bowen HC, Maathuis FJM, Shabala SN, Tester MA, White PJ, Davies JM. 2002. *Arabidopsis thaliana* root non-selective cation channels mediate calcium uptake and are involved in growth. *Plant Journal* **32**, 799-808.

Demidchik V, Shabala SN, Coutts KB, Tester MA, Davies JM. 2003. Free oxygen radicals regulate plasma membrane Ca^{2+}-and K^{+}-permeable channels in plant root cells. *Journal of Cell Science* **116**, 81-88.

Demmig B, Gimmler H. 1979. Effect of divalent cation fluxes across the chloroplast envelope and on photosynthesis of intact chloroplasts. *Zeitschrift fuer Naturforschung* **24C**, 233–241.

Deng W, Luo K, Li D, Zheng X, Wei X, Smith W, Thammina C, Lu L, Li Y, Pei Y. 2006. Overexpression of an *Arabidopsis* magnesium transport gene, AtMGT1, in *Nicotiana benthamiana* confers Al tolerance. *Journal of Experimental Botany* **57**, 4235-4243.

Dietz KJ, Schramm M, Lang B, Lanzlschramm A, Durr C, Martinoia E. 1992. Characterization of the epidermis from barley primary leaves. 2. the role of the epidermis in ion compartmentation. *Planta* **187**, 431-437.

Ding JP, Badot PM, Pickard BG. 1993a. Aluminium and hydrogen ions inhibit a mechanosensory calcium-selective cation channel. *Australian Journal of Plant Physiology* **20**, 771-778.

Ding JP, Badot PM, Pickard BG. 1993b. Aluminum and hydrogen ions inhibit a mechanosensory calcium-selective cation channel. *Australian Journal of Plant Physiology* **20**, 771-778.

Dolan L, Davies J. 2004. Cell expansion in roots. *Current Opinion in Plant Biology* **7**, 33-39.

Doncheva S, Amenos M, Poschenrieder C, Barcelo J. 2005. Root cell patterning: a primary target for aluminium toxicity in maize. *Journal of Experimental Botany* **56**, 1213-1220.

Doyle SA, Beernink PT, Koshland DE. 2001. Structural basis for a change in substrate specificity: Crystal structure of S113E isocitrate dehydrogenase in a complex with isopropylmalate, Mg^{2+}, and NADP. *Biochemistry* **40**, 4234-4241.

DuPont FM, Bush DS, Windle JJ, Jones RL. 1990. Calcium and proton transport in membrane vesicles from barley roots. *Plant Physiology* **94**, 179-188.

Eticha D, Stass A, Horst WJ. 2005. Cell-wall pectin and its degree of methylation in the maize root-apex: significance for genotypic differences in aluminium resistance. *Plant Cell and Environment* **28**, 1410-1420.

Evans DE, Briars SA, Williams LE. 1991. Active calcium transport by plant cell membranes. *Journal of Experimental Botany* **42**, 285-303.

Exley C. 2004. The pro-oxidant activity of aluminum. *Free Radical Biology and Medicine* **36**, 380-387.

Ezaki B, Gardner RC, Ezaki Y, Matsumoto H. 2000. Expression of aluminum-induced genes in transgenic Arabidopsis plants can ameliorate aluminum stress and/or oxidative stress. *Plant Physiology* **122**, 657-666.

Facanha AR, Okorokova-Facanha AL. 2002. Inhibition of phosphate uptake in corn roots by aluminum-fluoride complexes. *Plant Physiology* **129**, 1763-1772.

Fawzy H, Overstreet R, Jacobson L. 1954. The influence of hydrogen ion concentration on cation absorption by barley roots. *Plant Physiology* **29**, 234-237.

Felle H. 1988. Cytoplasmic free calcium in *Riccia fluitans* L. and *Zea mays* L.: Interaction of Ca^{2+} and pH? *Planta* **176**, 248-255.

Ferguson IB, Clarkson DT. 1975. Ion transport and endodermal suberization in the roots of *Zea mays*. *New Phytologist* **75**, 69-79.

Ferguson IB, Clarkson DT. 1976. Simultaneous uptake and translocation of magnesium and calcium in barley (*Hordeum vulgare* L.) roots. *Planta* **128**, 267-269.

Fontecha G, Silva-Navas J, Benito C, Mestres MA, Espino FJ, Hernández-Riquer MV, Gallego FJ. 2007. Candidate gene identification of an aluminum-activated organic acid transporter gene at the *Alt4* locus for aluminum tolerance in rye (*Secale cereale* L.). *TAG Theoretical and Applied Genetics* **114**, 249-260.

Foreman J, Demidchik V, Bothwell JHF, Mylona P, Miedema H, Torres MA, Linstead P, Costa S, Brownlee C, Jones JDG. 2003. Reactive oxygen species produced by NADPH oxidase regulate plant cell growth. *Nature* **422**, 442-446.

Foy CD. 1988. Plant adaptation to acid, aluminum-toxic soils. *Communications in Soil Science and Plant Analysis* **19**, 959-987.

Foy CD, Burns GR, Brown JC, Fleming AL. 1965. Differential aluminum tolerance of two wheat varieties associated with plant-induced pH changes around their roots. *Soil Science Society of America Journal* **29**, 64-67.

Frensch J. 1997. Primary responses of root and leaf elongation to water deficits in the atmosphere and soil solution. *Journal of Experimental Botany* **48**, 985-999.

Fuglsang AT, Guo Y, Cuin TA, Qiu Q, Song C, Kristiansen KA, Bych K, Schulz A, Shabala S, Schumaker KS, Palmgren MG, Zhu J-K. 2007. *Arabidopsis* protein kinase PKS5 inhibits the plasma membrane H^+-ATPase by preventing interaction with 14-3-3 protein. *Plant Cell* **19**, 1617-1634.

Furuichi T, Cunningham KW, Muto S. 2001. A putative two pore channel AtTPC1 mediates Ca^{2+} flux in Arabidopsis leaf cells. *Plant and Cell Physiology* **42**, 900-905.

Furukawa J, Yamaji N, Wang H, Mitani N, Murata Y, Sato K, Katsuhara M, Takeda K, Ma JF. 2007. An aluminum-activated citrate transporter in barley. *Plant and Cell Physiology* **48**, 1081-1091.

Gabrielson KM, Cancel JD, Morua LF, Larsen PB. 2006. Identification of dominant mutations that confer increased aluminium tolerance through mutagenesis of the Al-sensitive *Arabidopsis* mutant, *als3-1*. *Journal of Experimental Botany* **57**, 943-951.

Gahoonia TS, Nielsen NE. 1998. Direct evidence on participation of root hairs in phosphorus (P-32) uptake from soil. *Plant and Soil* **198**, 147-152.

Galloway JN. 1989. Atmospheric acidification: projections for the future. *Ambio*, 161-166.

Gassmann W, Schroeder JI. 1994. Inward-rectifying K^+ channels in root hairs of wheat - a mechanism for aluminum-sensitive low-affinity K^+ uptake and membrane-potential control. *Plant Physiology* **105**, 1399-1408.

Gerendas J, Ratcliffe RG, Sattelmacher B. 1990. ^{31}P nuclear magnetic resonance evidence for differences in intracellular pH in the roots of maize seedlings grown with nitrate or ammonium. *Journal of plant physiology (Germany, FR)* **137**, 125-128.

Giannakoula A, Moustakas M, Mylona P, Papadakis I, Yupsanis T. 2008. Aluminum tolerance in maize is correlated with increased levels of mineral nutrients, carbohydrates and proline, and decreased levels of lipid peroxidation and Al accumulation. *Journal of Plant Physiology* **165**, 385-396.

Godbold DL, Jentschke G. 1998. Aluminium accumulation in root cell walls coincides with inhibition of root growth but not with inhibition of magnesium uptake in Norway spruce. *Physiologia Plantarum* **102**, 553-560.

Goodwin SB, Sutter TR. 2009. Microarray analysis of *Arabidopsis* genome response to aluminum stress. *Biologia Plantarum* **53**, 85-99.

Göransson A, Eldhuset TD. 1995. Effects of aluminium ions on uptake of calcium, magnesium and nitrogen in *Betula pendula* seedlings growing at high and low nutrient supply rates. *Water Air and Soil Pollution* **83**, 351-361.

Gotoh H, Kajikawa M, Kato H, Suto K. 1999. Intracellular Mg^{2+} surge follows Ca^{2+} increase during depolarization in cultured neurons. *Brain Research* **828**, 163-168.

Goulding KWT, Bailey NJ, Bradbury NJ, Hargreaves P, Howe M, Murphy DV, Poulton PR, Willison TW. 1998. Nitrogen deposition and its contribution to nitrogen cycling and associated soil processes. *New Phytologist* **139**, 49-58.

Grauer UE, Horst WJ. 1992. Modeling cation amelioration of aluminum phytotoxicity. *Soil Science Society of America Journal* **56**, 166-172.

Gregan J, Kolisek M, Schweyen RJ. 2001. Mitochondrial Mg^{2+} homeostasis is critical for group II intron splicing in vivo. *Genes & Development* **15**, 2229-2237.

Grimme H. 1983. Aluminium induced magnesium deficiency in oats. *Zeitschrift für Pflanzenernährung und Bodenkunde* **146**, 666-676.

Guo K-M, Babourina O, Rengel Z. 2009. Na^+/H^+ antiporter activity of the *SOS1* gene: lifetime imaging analysis and electrophysiological studies on Arabidopsis seedlings. *Physiologia Plantarum* **137**, 155-165.

Guo KM, Babourina O, Christopher DA, Borsic T, Rengel Z. 2010. The cyclic nucleotide-gated channel AtCNGC10 transports Ca^{2+} and Mg^{2+} in Arabidopsis. *Physiologia Plantarum*, DOI:10.1111/j.1399-3054.2010.01366.x.

Hager A. 2003. Role of the plasma membrane H^+-ATPase in auxin-induced elongation growth: historical and new aspects. *Journal of Plant Research* **116**, 483-505.

Hanson JB, Kahn JS. 1957. The kinetics of potassium accumulation by corn roots as a function of cell maturity. *Plant Physiology* **32**, 497-498.

Hayes JE, Ma JF. 2003. Al-induced efflux of organic acid anions is poorly associated with internal organic acid metabolism in triticale roots. *Journal of Experimental Botany* **54**, 1753-1759.

Hirschi K. 2001. Vacuolar H^+/Ca^{2+} transport: who's directing the traffic? *Trends in Plant Science* **6**, 100-104.

Hoekenga OA, Maron LG, Pineros MA, Cancado GMA, Shaff J, Kobayashi Y, Ryan PR, Dong B, Delhaize E, Sasaki T, Matsumoto H, Yamamoto Y, Koyama H, Kochian LV. 2006. *AtALMT1*, which encodes a malate transporter, is identified as one of several genes critical for aluminum tolerance in *Arabidopsis*. *Proceedings of the National Academy of Sciences* **103**, 9738-9743.

Holdaway-Clarke TL, Walker NA, Hepler PK, Overall RL. 2000. Physiological elevations in cytoplasmic free calcium by cold or ion injection result in transient closure of higher plant plasmodesmata. *Planta* **210**, 329-335.

Horst WJ. 1995. The role of the apoplast in aluminium toxicity and resistance of higher plants: a review. *Zeitschrift für Pflanzenernährung und Bodenkunde* **158**, 419-428.

Horst WJ, Asher CJ, Cakmak I, Szulkiewicz P, Wissemeier AH. 1992. Short-term responses of soybean roots to aluminum. *Journal of Plant Physiology* **140**, 174-178.

Horst WJ, Kollmeier M, Schmohl N, Sivaguru M, Wang Y, Felle HH, Hedrich R, Schröder W, Staß A. 2007. Significance of the root apoplast for aluminium toxicity and resistance of maize. In: Sattelmacher B, Horst WJ, eds. *The apoplast of higher plants: Compartment of storage, transport and reactions*. Netherlands: Springer, 49-66.

Horst WJ, Wagner A, Marschner H. 1982. Mucilage protects root meristems from aluminium injury. *Zeitschriftfur Pflanzenphysiolgie* **105**, 435-444.

Howard BR, Endrizzi JA, Remington SJ. 2000. Crystal structure of escherichia coli malate synthase G complexed with magnesium and glyoxylate at 2.0 A resolution: mechanistic implications. *Biochemistry* **39**, 3156-3168.

Huang CF, Yamaji N, Mitani N, Yano M, Nagamura Y, Ma JF. 2009. A bacterial-type ABC transporter is involved in aluminum tolerance in rice. *The Plant Cell Online* **21**, 655-667.

Huang JW, Pellet DM, Papernik LA, Kochian LV. 1996. Aluminum interactions with voltage-dependent calcium transport in plasma membrane vesicles isolated from roots of aluminum-sensitive and-resistant wheat cultivars. *Plant Physiology* **110**, 561-569.

Huang JW, Shaff JE, Grunes DL, Kochian LV. 1992. Aluminum effects on calcium fluxes at the root apex of aluminum-tolerant and aluminum-sensitive wheat cultivars. *Plant Physiology* **98**, 230-237.

Huber S, Maury W. 1980. Effects of magnesium on intact chloroplasts I Evidence for activation of (sodium) potassium/proton exchange across the chloroplast envelope. *Plant Physiology* **65**, 350–354.

Iglesias AA, Andreo CS. 1990. NADP-dependent malate dehydrogenase (decarboxylating) from sugar cane leaves. *European Journal of Biochemistry* **192**, 729-733.

Ikka T, Kobayashi Y, Iuchi S, Sakurai N, Shibata D, Kobayashi M, Koyama H. 2007. Natural variation of *Arabidopsis thaliana* reveals that aluminum resistance and proton resistance are controlled by different genetic factors. *Theoretical and Applied Genetics* **115**, 709-719.

Illes P, Schlicht M, Pavlovkin J, Lichtscheidl I, Baluska F, Ovecka M. 2006. Aluminium toxicity in plants: internalization of aluminium into cells of the transition zone in *Arabidopsis* root apices related to changes in plasma membrane potential, endosomal behaviour, and nitric oxide production. *Journal of Experimental Botany* **57**, 4201-4213.

Ishikawa S, Wagatsuma T, Takano T, Tawaraya K, Oomata K. 2001. The plasma membrane intactness of root-tip cells is a primary factor for Al-tolerance in cultivars of five species. *Soil Science and Plant Nutrition* **47**, 489-502.

Iuchi S, Koyama H, Iuchi A, Kobayashi Y, Kitabayashi S, Kobayashi Y, Ikka T, Hirayama T, Shinozaki K, Kobayashi M. 2007. Zinc finger protein STOP1 is critical for proton tolerance in *Arabidopsis* and coregulates a key gene in aluminum tolerance. *Proceedings of the National Academy of Sciences* **104**, 9900-9905.

Johnson VJ, Tsunoda M, Murray TF, Sharma RP. 2005. Decreased membrane fluidity and hyperpolarization in aluminum-treated PC-12 cells correlates with increased production of cellular oxidants. *Environmental Toxicology and Pharmacology* **19**, 221-230.

Jones DL, Blancaflor EB, Kochian LV, Gilroy S. 2006. Spatial coordination of aluminium uptake, production of reactive oxygen species, callose production and wall rigidification in maize roots. *Plant Cell and Environment* **29**, 1309-1318.

Jones DL, Gilroy S, Larsen PB, Howell SH, Kochian LV. 1998a. Effect of aluminum on cytoplasmic Ca^{2+} homeostasis in root hairs of *Arabidopsis thaliana* (L.). *Planta* **206**, 378-387.

Jones DL, Kochian LV. 1997. Aluminum interaction with plasma membrane lipids and enzyme metal binding sites and its potential role in Al cytotoxicity. *FEBS Letters* **400**, 51-57.

Jones DL, Kochian LV, Gilroy S. 1998b. Aluminum induces a decrease in cytosolic calcium concentration in BY-2 tobacco cell cultures. *Plant Physiology* **116**, 81-89.

Jones DL, Shaff JE, Kochian LV. 1995. Role of calcium and other ions in directing root hair tip growth in *Limnobium stoloniferum*. *Planta* **197**, 672-680.

Kang H, Kang MY, Han KH. 2000. Identification of natural rubber and characterization of rubber biosynthetic activity in fig tree. *Plant Physiology* **123**, 1133-1142.

Kasamo K. 1986. Purification and properties of the plasma membrane H^+ translocating adenosine triphosphatase of *Phaseolus mungo* L roots. *Plant Physiology* **80**, 818-824.

Kawano T, Kadono T, Fumoto K, Lapeyrie F, Kuse M, Isobe M, Furuichi T, Muto S. 2004. Aluminum as a specific inhibitor of plant *TPC1* Ca^{2+} channels. *Biochemical and Biophysical Research Communications* **324**, 40-45.

Kehres D, Lawyer C, Maguire M. 1998. The CorA magnesium transporter gene family *Microbial & Comparitive Genomics* **3**, 151–169.

Keltjens WG. 1988. Short-term effects of Al on nutrient uptake, H^+ efflux, root respiration and nitrate reductase activity of two sorghum genotypes differing in Al-susceptibility. *Communications in Soil Science and Plant Analysis* **19**, 1155 - 1163.

Keltjens WG, Tan K. 1993. Interactions between aluminium, magnesium and calcium with different monocotyledonous and dicotyledonous plant species. *Plant and Soil* **155-156**, 485-488.

Kennedy CW, Smith W, Ba MT. 1986. Root cation exchange capacity of cotton cultivars in relation to aluminium toxicity. *Journal of Plant Nutrition* **9**, 1123-1133.

Kidd PS, Llugany M, Poschenrieder C, Gunse B, Barcelo J. 2001. The role of root exudates in aluminium resistance and silicon-induced amelioration of aluminium toxicity in three varieties of maize (*Zea mays* L.). *Journal of Experimental Botany* **52**, 1339-1352.

Kidd PS, Proctor J. 2001. Why plants grow poorly on very acid soils: are ecologists missing the obvious? *Journal of Experimental Botany* **52**, 791-799.

Kiegle E, Gilliham M, Haseloff J, Tester M. 2000. Hyperpolarisation-activated calcium currents found only in cells from the elongation zone of *Arabidopsis thaliana* roots. *Plant Journal* **21**, 225-229.

Kinraide TB. 1988. Proton extrusion by wheat roots exhibiting severe aluminum toxicity symptoms. *Plant Physiology* **88**, 418-423.

Kinraide TB. 1990. Assessing the rhizotoxicity of the aluminate ion, $Al(OH)_4^-$. *Plant Physiology* **93**, 1620-1625.

Kinraide TB. 1991. Identity of the rhizotoxic aluminium species. *Plant and Soil* **134**, 167-178.

Kinraide TB. 1993. Aluminum enhancement of plant growth in acid rooting media - a case of reciprocal alleviation of toxicity by 2 toxic cations. *Physiologia Plantarum* **88**, 619-625.

Kinraide TB. 1994. Use of a Gouy-Chapman-Stern model for membrane-surface electrical potential to interpret some features of mineral rhizotoxicity. *Plant Physiology* **106**, 1583-1592.

Kinraide TB. 2001. Ion fluxes considered in terms of membrane-surface electrical potentials. *Australian Journal of Plant Physiology* **28**, 605-616.

Kinraide TB. 2003. Toxicity factors in acidic forest soils: attempts to evaluate separately the toxic effects of excessive Al^{3+} and H^+ and insufficient Ca^{2+} and Mg^{2+} upon root elongation. *European Journal of Soil Science* **54**, 323-333.

Kinraide TB. 2004. Possible influence of cell walls upon ion concentrations at plasma membrane surfaces. Toward a comprehensive view of cell-surface electrical effects upon ion uptake, intoxication, and amelioration. *Plant Physiology* **136**, 3804-3813.

Kinraide TB. 2006. Plasma membrane surface potential (ψ_{PM}) as a determinant of ion bioavailability: A critical analysis of new and published toxicological studies and a simplified method for the computation of plant ψ_{PM}. *Environmental Toxicology and Chemistry* **25**, 3188-3198.

Kinraide TB, Parker DR. 1987. Cation amelioration of aluminum toxicity in wheat. *Plant Physiology* **83**, 546-551.

Kinraide TB, Parker DR. 1990. Apparent phytotoxicity of mononuclear hydroxy-aluminum to four dicotyledonous species. *Physiologia Plantarum* **79**, 283-288.

Kinraide TB, Pedler JF, Parker DR. 2004. Relative effectiveness of calcium and magnesium in the alleviation of rhizotoxicity in wheat induced by copper, zinc, aluminum, sodium, and low pH. *Plant and Soil* **259**, 201-208.

Kinraide TB, Ryan PR, Kochian LV. 1992. Interactive effects of Al^{3+}, H^{+}, and other cations on root elongation considered in terms of cell-surface electrical potential. *Plant Physiology* **99**, 1461-1468.

Kinraide TB, Yermiyahu U. 2007. A scale of metal ion binding strengths correlating with ionic charge, Pauling electronegativity, toxicity, and other physiological effects. *Journal of Inorganic Biochemistry* **101**, 1201-1213.

Knemeyer JP, Marme N, Sauer M. 2000. Probes for detection of specific DNA sequences at the single-molecule level. *Analytical Chemistry* **72**, 3717-3724.

Knowles A, Shabala S. 2004. Overcoming the problem of non-ideal liquid ion exchanger selectivity in microelectrode ion flux measurements. *Journal of Membrane Biology* **202**, 51-59.

Kobayashi Y, Hoekenga OA, Itoh H, Nakashima M, Saito S, Shaff JE, Maron LG, Pineros MA, Kochian LV, Koyama H. 2007. Characterization of *AtALMT1* expression in aluminum-inducible malate release and its role for rhizotoxic stress tolerance in Arabidopsis. *Plant Physiology* **145**, 843-852.

Kochian LV. 1995. Cellular mechanisms of aluminum toxicity and resistance in plants. *Annual Review of Plant Physiology and Plant Molecular Biology* **46**, 237-260.

Kochian LV, Hoekenga OA, Piñeros MA. 2004. How do crop plants tolerate acid soils? Mechanisms of aluminum tolerance and phosphorous efficiency. *Annual Review of Plant Biology* **55**, 459-493.

Kochian LV, Pineros MA, Hoekenga OA. 2005. The physiology, genetics and molecular biology of plant aluminum resistance and toxicity. *Plant and Soil* **274**, 175-195.

Kolisek M, Zsurka G, Samaj J, Weghuber J, Schweyen RJ, Schweigel M. 2003. Mrs2p is an essential component of the major electrophoretic Mg^{2+} influx system in mitochondria. *The EMBO Journal* **22**, 1235-1244.

Kollmeier M, Dietrich P, Bauer CS, Horst WJ, Hedrich R. 2001. Aluminum activates a citrate-permeable anion channel in the aluminum-sensitive zone of the maize root apex. A comparison between an aluminum-sensitive and an aluminum-resistant cultivar. *Plant Physiology* **126**, 397-410.

Kollmeier M, Felle HH, Horst WJ. 2000. Genotypical differences in aluminum resistance of maize are expressed in the distal part of the transition zone. Is reduced basipetal auxin flow involved in inhibition of root elongation by aluminum? *Plant Physiology* **122**, 945-956.

Koyama H, Toda T, Hara T. 2001. Brief exposure to low-pH stress causes irreversible damage to the growing root in *Arabidopsis thaliana*: pectin-Ca interaction may play an important role in proton rhizotoxicity. *Journal of Experimental Botany* **52**, 361-368.

Koyama H, Toda T, Yokota S, Dawair Z, Hara T. 1995. Effects of aluminum and pH on root growth and cell viability in *Arabidopsis thaliana* strain Landsberg in hydroponic culture. *Plant and Cell Physiology* **36**, 201-205.

Krol E, Trebacz K. 2000. Ways of ion channel gating in plant cells. *Annals of Botany* **86**, 449-469.

Kurkdjian A, Guern J. 1989. Intracellular pH: measurement and importance in cell activity. *Annual Review of Plant Biology* **40**, 271-303.

Lakowicz JR, Szmacinski H. 1993. Fluorescence lifetime-based sensing of pH, Ca^{2+}, K^{+} and glucose. *Sensors and Actuators B: Chemical* **11**, 133-143.

Larsen PB. 2009. Unraveling the mechanisms underlying aluminum-dependent root growth inhibition. In: Jenks MA, Wood AJ, eds. *Genes for Plant Abiotic Stress*: Wiley-Blackwell, 113-142.

Larsen PB, Cancel J, Rounds M, Ochoa V. 2007. *Arabidopsis ALS1* encodes a root tip and stele localized half type ABC transporter required for root growth in an aluminum toxic environment. *Planta* **225**, 1447-1458.

Larsen PB, Degenhardt J, Tai C-Y, Stenzler LM, Howell SH, Kochian LV. 1998. Aluminum-resistant Arabidopsis mutants that exhibit altered patterns of aluminum accumulation and organic acid release from roots. *Plant Physiology* **117**, 9-17.

Larsen PB, Geisler MJB, Jones CA, Williams KM, Cancel JD. 2005. *ALS3* encodes a phloem-localized ABC transporter-like protein that is required for aluminum tolerance in Arabidopsis. *Plant Journal* **41**, 353-363.

Larsen PB, Kochian LV, Howell SH. 1997a. Al inhibits both shoot development and root growth in *als3*, an Al-sensitive Arabidopsis mutant. *Plant Physiology* **114**, 1207-1214.

Larsen PB, Stenzler LM, Tai CY, Degenhardt J, Howell SH, Kochian LV. 1997b. Molecular and physiological analysis of *Arabidopsis* mutants exhibiting altered sensitivities to aluminium. *Plant and Soil* **192**, 3-7.

Larsen PB, Tai CY, Kochian LV, Howell SH. 1996. Arabidopsis mutants with increased sensitivity to aluminum. *Plant Physiology* **110**, 743-751.

Lazof D, Rincón M, Rufty T, Mackown C, Carter T. 1994. Aluminum accumulation and associated effects on $^{15}NO_3^-$ influx in roots of two soybean genotypes differing in Al tolerance. *Plant and Soil* **164**, 291-297.

Lazof DB, Holland MJ. 1999. Evaluation of the aluminium-induced root growth inhibition in isolation from low pH effects in *Glycine max*, *Pisum sativum* and *Phaseolus vulgaris*. *Australian Journal of Plant Physiology* **26**, 147-157.

Lebaudy A, Véry A-A, Sentenac H. 2007. K^+ channel activity in plants: Genes, regulations and functions. *FEBS Letters* **581**, 2357-2366.

Lee J, Pritchard M. 1984. Aluminium toxicity expression nutrient uptake, growth and root morphology of *Trifolium repens* L. cv. 'Grasslands Huia'. *Plant and Soil* **82**, 101-116.

Leigh R, Wyn Jones R. 1986. Cellular compartmentation in plant nutrition: the selective cytoplasm and the promiscuous vacuole. In: Tinker B, Lauchli A, eds. *Advances in Plant Nutrition 2*. New Yark: Praeger Scientific, 249–279.

Lenoble ME, Blevins DG, Sharp RE, Cumbie BG. 1996. Prevention of aluminium toxicity with supplemental boron. I. Maintenance of root elongation and cellular structure. *Plant, Cell & Environment* **19**, 1132-1142.

Leyssens A, Nowicky AV, Patterson L, Crompton M, Duchen MR. 1996. The relationship between mitochondrial state, ATP hydrolysis, $[Mg^{2+}]i$ and $[Ca^{2+}]i$ studied in isolated rat cardiomyocytes. *Journal of Physiology* **496**, 111-128.

Li L, Tutone AF, Drummond RSM, Gardner RC, Luan S. 2001. A novel family of magnesium transport genes in *Arabidopsis*. *Plant Cell* **13**, 2761-2775.

Li R, Cai M, Liu P, Xu G, Liang H, Zhou Z. 2008. Border cells alleviating aluminum toxicity in soybean root tips. *ACTA AGRONOMICA SINICA* **34**, 318-325.

Li XF, Ma JF, Matsumoto H. 2000. Pattern of aluminum-induced secretion of organic acids differs between rye and wheat. *Plant Physiology* **123**, 1537-1544.

Li Y-Y, Yue-Jiao Z, Yuan Z, Jian-Li Y, Shao-Jian Z. 2009. Protecting cell walls from binding aluminum by organic acids contributes to aluminum resistance. *Journal of Integrative Plant Biology* **51**, 574-580.

Lichtman JW, Conchello JA. 2005. Fluorescence microscopy. *Nature Methods* **2**, 910-919.

Lin C, Yu Y, Kadono T, Iwata M, Umemura K, Furuichi T, Kuse M, Isobe M, Yamamoto Y, Matsumoto H, Yoshizuka K, Kawano T. 2005. Action of aluminum, novel TPC1-type channel inhibitor, against salicylate-induced and cold-shock-induced calcium influx in tobacco BY-2 cells. *Biochemical and Biophysical Research Communications* **332**, 823-830.

Lindberg S. 1990. Aluminium interactions with K^+ ($^{86}Rb^+$) and $^{45}Ca^{2+}$ fluxes in three cultivars of sugar beet (*Beta vulgaris*). *Physiologia Plantarum* **79**, 275-282.

Lindberg S, Strid H. 1997. Aluminium induces rapid changes in cytosolic pH and free calcium and potassium concentrations in root protoplasts of wheat (*Triticum aestivum*). *Physiologia Plantarum* **99**, 405-414.

Lindberg S, Yahya A. 1994. Effects of pH and mineral nutrition supply on K (+) ((86) Rb (+)) influx and plasma membrane ATPase activity in roots of sugar beets. *Journal of plant physiology (Germany)* **144**, 150-155.

Liu J, Magalhaes JV, Shaff J, Kochian LV. 2009. Aluminum-activated citrate and malate transporters from the MATE and ALMT families function independently to confer Arabidopsis aluminum tolerance. *The Plant Journal* **57**, 389-399.

Liu K, Luan S. 2001. Internal aluminum block of plant inward K^+ channels. *Plant Cell* **13**, 1453-1465.

Llugany M, Poschenrieder C, Barceló J. 1995. Monitoring of aluminium-induced inhibition of root elongation in four maize cultivars differing in tolerance to aluminium and proton toxicity. *Physiologia Plantarum* **93**, 265-271.

Lobão F, A., Arnoldo RF, Lev AO, Keilla RD, Anna LO-F. 2007. Aluminum impairs morphogenic transition and stimulates H^+ transport mediated by the plasma membrane ATPase of *Yarrowia lipolytica*. *FEMS Microbiology Letters* **274**, 17-23.

Ma JF. 2007. Syndrome of aluminum toxicity and diversity of aluminum resistance in higher plants. *International Review of Cytology* **264**, 225-253.

Ma JF, Hiradate S, Nomoto K, Iwashita T, Matsumoto H. 1997a. Internal detoxification mechanism of Al in hydrangea (Identification of Al form in the leaves). *Plant Physiology* **113**, 1033-1039.

Ma JF, Nagao S, Huang CF, Nishimura M. 2005. Isolation and characterization of a rice mutant hypersensitive to Al. *Plant and Cell Physiology* **46**, 1054-1061.

Ma JF, Ryan PR, Delhaize E. 2001. Aluminium tolerance in plants and the complexing role of organic acids. *Trends in Plant Science* **6**, 273-278.

Ma JF, Shen R, Nagao S, Tanimoto E. 2004. Aluminum targets elongating cells by reducing cell wall extensibility in wheat roots. *Plant and Cell Physiology* **45**, 583-589.

Ma JF, Zheng SJ, Matsumoto H. 1997b. Specific secretion of citric acid induced by Al stress in *Cassia tora* L. *Plant and Cell Physiology* **38**, 1019-1025.

Ma JF, Zheng SJ, Matsumoto H, Hiradate S. 1997c. Detoxifying aluminium with buckwheat. *Nature* **390**, 569-570.

Ma Q, Rengel Z, Kuo J. 2002. Aluminium toxicity in rye (*Secale cereale*): Root growth and dynamics of cytoplasmic Ca^{2+} in intact root tips. *Annals of Botany* **89**, 241-244.

Maathuis FJM, Ichida AM, Sanders D, Schroeder JI. 1997. Roles of higher plant K^+ Channels. *Plant Physiology* **114**, 1141-1149.

Maathuis FJM, Sanders D. 1993. Energization of potassium uptake in *Arabidopsis thaliana*. *Planta* **191**, 302-307.

Maathuis FJM, Sanders D. 1995. Contrasting roles in ion transport of two K^+-channel types in root cells of *Arabidopsis thaliana*. *Planta* **197**, 456-464.

MacDiarmid CW, Gardner RC. 1998. Overexpression of the *Saccharomyces cerevisiae* aagnesium transport system confers resistance to aluminum ion. *Journal of Biological Chemistry* **273**, 1727-1732.

Magalhaes JV, Liu J, Guimaraes CT, Lana UGP, Alves VMC, Wang Y-H, Schaffert RE, Hoekenga OA, Pineros MA, Shaff JE, Klein PE, Carneiro NP, Coelho CM, Trick HN, Kochian LV. 2007. A gene in the multidrug and toxic compound extrusion (MATE) family confers aluminum tolerance in sorghum. *Nature Genetics* **39**, 1156-1161.

Maguire ME, Cowan JA. 2002. Magnesium chemistry and biochemistry. *Biometals* **15**, 203-210.

Mannion AM. 1998. Global environmental change: The causes and consequences of disruption to biogeochemical cycles. *The Geographical Journal* **164**, 168-182.

Mariano ED, Keltjens WG. 2004. Variation for aluminum resistance among maize genotypes evaluated with three screening methods. *Communications in Soil Science and Plant Analysis* **35**, 2617-2637.

Mariano ED, Keltjens WG. 2005. Long-term effects of aluminum exposure on nutrient uptake by maize genotypes differing in aluminum resistance. *Journal of Plant Nutrition* **28**, 323-333.

Marschner H. 1991. Mechanisms of adaptation of plants to acid soils. *Plant and Soil* **134**, 1-20.

Marschner H. 1995. *Mineral Nutrition of Higher Plants*. London,San Diego: Academic Press.

Marty F. 1999. Plant vacuoles. *Plant Cell* **11**, 587-600.

Matsumoto H. 1988. Inhibition of proton transport activity of microsomal membrane vesicles of barley roots by aluminum. *Soil Science and Plant Nutrition* **34**, 499-506.

Matsumoto H. 2000. Cell biology of aluminum toxicity and tolerance in higher plants. *International Review of Cytology* **200**, 1-46.

Matsumoto H, Hirasawa E, Morimura S, Takahashi E. 1976a. Localization of aluminum in tea leaves. *Plant Cell Physiology* **17**, 627-631.

Matsumoto H, Hirasawa E, Torikai H, Takahashi E. 1976b. Localization of absorbed aluminium in pea root and its binding to nucleic acids. *Plant and Cell Physiology* **17**, 127-137.

Matsumoto H, Yamamoto Y, Kasai M. 1992. Changes of some properties of the plasma membrane-enriched fraction of barley roots related to aluminum stress: membrane-associated ATPase, aluminum and calcium. *Soil Science and Plant Nutrition* **38**, 411-411.

Matsumoto H, Yamaya T. 1986. Inhibition of potassium uptake and regulation of membrane-associated Mg^{2+} -ATPase activity of pea roots by aluminum. *Soil Science and Plant Nutrition* **32**, 179-188.

Meriga B, Krishna Reddy B, Rajender Rao K, Ananda Reddy L, Kavi Kishor PB. 2004. Aluminium-induced production of oxygen radicals, lipid peroxidation and DNA damage in seedlings of rice (*Oryza sativa*). *Journal of Plant Physiology* **161**, 63-68.

Middaugh J, Hamel R, Jean-Baptiste G, Beriault R, Chenier D, Appanna VD. 2005. Aluminum triggers decreased aconitase activity via Fe-S cluster disruption and the overexpression of isocitrate dehydrogenase and isocitrate lyase: A metabolic network mediating cellular survival. *Journal of Biological Chemistry* **280**, 3159-3165.

Miedema H, Bothwell JHF, Brownlee C, Davies JM. 2001. Calcium uptake by plant cells–channels and pumps acting in concert. *Trends in Plant Science* **6**, 514-519.

Miyasaka SC, Kochian LV, Shaff JE, Foy CD. 1989. Mechanisms of aluminum tolerance in wheat - an investigation of genotypic differences in rhizosphere pH, K^+, and H^+ transport, and root cell membrane potentials. *Plant Physiology* **91**, 1188-1196.

Montezinho L, Fonseca C, Geraldes C, Castro M. 2002. Quantification and localization of intracellular free Mg in bovine chromaffin cells. *Metal-Based Drugs* **9**, 69-80.

Morimura E, Takahashi E, Matsumoto H. 1978. Association of aluminium with nuclei and inhibition of cell division in onion (*Allium cepa*) roots. *Zeitschrift fuer Pflanzenphysiologie (Germany, FR)* **88**, 395-408.

Mugwira LM, Patel SU. 1977. Root zone pH changes and ion uptake imbalances by triticale, wheat, and rye. *Agronomy Journal* **69**, 719-722.

Mugwira LM, Patel SU, Fleming AL. 1980. Aluminium effects on growth and Al, Ca, Mg, K and P levels in triticale, wheat and rye. *Plant and Soil* **57**, 467-470.

Nakabayashi T, Wang HP, Tsujimoto K, Miyauchi S, Kamo N, Ohta N. 2007. A correlation between pH and fluorescence lifetime of 2',7'-bis(2-carboxyethyl)-5(6)-carboxyfluorescein (BCECF) *in vivo* and *in vitro*. *Chemistry Letters* **36**, 206-207.

Newman IA. 2001. Ion transport in roots: measurement of fluxes using ion-selective microelectrodes to characterize transporter function. *Plant Cell and Environment* **24**, 1-14.

Nichol BE, Oliveira LA, Glass ADM, Siddiqi MY. 1993. The effects of aluminum on the influx of calcium, potassium, ammonium, nitrate, and phosphate in an aluminum-sensitive cultivar of barley (*Hordeum vulgare* L.). *Plant Physiology* **101**, 1263-1266.

Noble AD, Sumner ME. 1988. Calcium and Al interactions and soybean growth in nutrient solutions. *Communications in Soil Science and Plant Analysis* **19**, 1119 - 1131.

O'Leary MH. 1982. Phosphoenolpyruvate carboxylase: An enzymologist's view. *Annual Review of Plant Physiology* **33**, 297-315.

O'Connor DV, Desmond P. 1984. *Time-correlated single photon counting*. London: Academic Press.

Obi I, Ichikawa Y, Kakutani T, Senda M. 1989. Electrophoretic studies on plant protoplasts I. pH dependence of zeta potentials of protoplasts from various sources. *Plant and Cell Physiology* **30**, 439-444.

Ofei-Manu P, Wagatsuma T, Ishikawa S, Tawaraya K. 2001. The plasma membrane strength of the root-tip cells and root phenolic compounds are correlated with Al tolerance in several common woody plants. *Soil Science and Plant Nutrition* **47**, 359-376.

Olivetti GP, Cumming JR, Etherton B. 1995. Membrane-potential depolarization of root cap cells precedes aluminum tolerance in snapbean. *Plant Physiology* **109**, 123-129.

Ono K, Yamamoto Y, Hachiya A, Matsumoto H. 1995. Synergistic inhibition of growth by aluminum and iron of tobacco (*Nicotiana tabacum* L.) cells in suspension culture. *Plant and Cell Physiology* **36**, 115-125.

Osaki M, Nursyamsi D, Begum HH, Watanabe T. 2001. Study on aluminium resistance in relation to organic-acid anion exudation from roots of PEPC transgenic rice plants. In: Horst WJ, Schenk MK, Bürkert A, Claassen N, Flessa H, Frommer WB, Goldbach H, Olfs HW, Römheld V, Sattelmacher B, Schmidhalter U, Schubert S, Wirén Nv, Wittenmayer L, eds. *Plant Nutrition - Food security and sustainability of agro-ecosystems through basic and applied research*, Vol. 92. Netherlands: Kluwer Academic Publishers, 514-515.

Osawa H, Matsumoto H. 2001. Possible involvement of protein phosphorylation in aluminum-responsive malate efflux from wheat root apex. *Plant Physiology* **126**, 411-420.

Osawa H, Matsumoto H. 2002. Aluminium triggers malate-independent potassium release via ion channels from the root apex in wheat. *Planta* **215**, 405-412.

Ownby J, Popham H. 1989. Citrate reverses the inhibition of wheat root growth caused by aluminum. *Journal of Plant Physiology* **135**, 588-591.

Papernik LA, Kochian LV. 1997. Possible involvement of Al-induced electrical signals in Al tolerance in wheat. *Plant Physiology* **115**, 657-667.

Parker JS, Cavell AC, Dolan L, Roberts K, Grierson CS. 2000. Genetic interactions during root hair morphogenesis in *Arabidopsis*. *Plant Cell* **12**, 1961-1974.

Pei ZM, Ward JM, Schroeder JI. 1999. Magnesium sensitizes slow vacuolar channels to physiological cytosolic calcium and inhibits fast vacuolar channels in fava bean guard cell vacuoles. *Plant Physiology* **121**, 977-986.

Pellet DM, Grunes DL, Kochian LV. 1995. Organic acid exudation as an aluminum-tolerance mechanism in maize (*Zea mays* L.). *Planta* **196**, 788-795.

Pellet DM, Papernik LA, Jones DL, Darrah PR, Grunes DL, Kochian LV. 1997. Involvement of multiple aluminium exclusion mechanisms in aluminium tolerance in wheat. *Plant and Soil* **192**, 63-68.

Pellet DM, Papernik LA, Kochian LV. 1996. Multiple aluminum-resistance mechanisms in wheat (roles of root apical phosphate and malate exudation). *Plant Physiology* **112**, 591-597.

Piñeros M, A., Cançado G, M. A. , Maron L, G. , Lyi S, M., Menossi M, Kochian L, V. 2008. Not all ALMT1-type transporters mediate aluminum-activated organic acid responses: the case of *ZmALMT1*- an anion-selective transporter. *The Plant Journal* **53**, 352-367.

Pineros M, Tester M. 1993. Plasma-membrane Ca^{2+} channels in roots of higher plants and their role in aluminum toxicity. *Plant and Soil* **156**, 119-122.

Pineros M, Tester M. 1997. Calcium channels in higher plant cells: Selectivity, regulation and pharmacology. *Journal of Experimental Botany* **48**, 551-577.

Pineros MA, Kochian LV. 2001. A patch-clamp study on the physiology of aluminum toxicity and aluminum tolerance in maize. Identification and characterization of Al^{3+}-induced anion channels. *Plant Physiology* **125**, 292-305.

Pineros MA, Magalhaes JV, Carvalho Alves VM, Kochian LV. 2002. The physiology and biophysics of an aluminum tolerance mechanism based on root citrate exudation in maize. *Plant Physiology* **129**, 1194-1206.

Pineros MA, Shaff JE, Manslank HS, Carvalho Alves VM, Kochian LV. 2005. Aluminum resistance in maize cannot be solely explained by root organic acid exudation. A comparative physiological study. *Plant Physiology* **137**, 231-241.

Plieth C, Sattelmacher B, Hansen UP, Knight MR. 1999. Low-pH-mediated elevations in cytosolic calcium are inhibited by aluminium: a potential mechanism for aluminium toxicity. *Plant Journal* **18**, 643-650.

Podestá FE, Plaxton WC. 1991. Kinetic and regulatory properties of cytosolic pyruvate kinase from germinating castor oil seeds. *Biochemical Journal* **279**, 495-501.

Podestá FE, Plaxton WC. 1992. Plant cytosolic pyruvate kinase: a kinetic study. *Biochimica et Biophysica Acta* **1160**, 213-220.

Portis A, Heldt H. 1976. Light-dependent changes of the Mg^{2+} concentration in the stroma in relation to the Mg^{2+} dependency of CO_2 fixation in intact chloroplasts. *Biochimica et Biophysica Acta* **449**, 434–436.

Poschenrieder C, Amenos M, Corrales I, Doncheva S, Barcelo J. 2009. Root behavior in response to aluminum toxicity. In: Baluska F, ed. *Plant-Environment Interactions*. Berlin Heidelberg: Springer-Verlag 21-43.

Poschenrieder C, Gunsé B, Corrales I, Barceló J. 2008. A glance into aluminum toxicity and resistance in plants. *Science of the Total Environment* **400**, 356-368.

Poschenrieder C, Llugany M, Barceló J. 1995. Short-term effects of pH and aluminium on mineral nutrition in maize varieties differing in proton and aluminium tolerance. *Journal of Plant Nutrition* **18**, 1495-1507.

Pottosin, II, Schonknecht G. 1996. Ion channel permeable for divalent and monovalent cations in native spinach thylakoid membranes. *Journal of Membrane Biology* **152**, 223-233.

Pottosin II, Tikhonova LI, Hedrich R, Schonknecht G. 1997. Slowly activating vacuolar channels can not mediate Ca^{2+}-induced Ca^{2+} release. *Plant Journal* **12**, 1387-1398.

Rangel AF, Mobin M, Rao IM, Horst WJ. 2005. Proton toxicity interferes with the screening of common bean (*Phaseolus vulgaris* L.) genotypes for aluminium resistance in nutrient solution. *Journal of Plant Nutrition and Soil Science* **168**, 607-616.

Raven JA. 1991. Terrestrial rhizophytes and H^+ currents circulating over at least a millimetre: An obligate relationship? *New Phytologist* **117**, 177-185.

Reid RJ, Tester MA, Smith FA. 1995. Calcium/aluminium interactions in the cell wall and plasma membrane of *Chara*. *Planta* **195**, 362-368.

Rengel Z. 1990. Competitive Al^{3+} inhibition of net Mg^{2+} uptake by intact *Lolium multiflorum* roots : II. Plant age effects. *Plant Physiology* **93**, 1261-1267.

Rengel Z. 1992. Role of calcium in aluminium toxicity. *New Phytologist* **121**, 499-513.

Rengel Z. 1994. Effects of Al, rare earth elements, and other metals on net $^{45}Ca^{2+}$ uptake by *Amaranthus* protoplasts. *Journal of Plant Physiology* **143**, 47-51.

Rengel Z. 1996. Uptake of aluminium by plant cells. *New Phytologist* **134**, 389-406.

Rengel Z. 2004. Aluminium cycling in the soil-plant-animal-human continuum. *Biometals* **17**, 669-689.

Rengel Z, Elliott DC. 1992. Mechanism of aluminum inhibition of net $^{45}Ca^{2+}$ uptake by amaranthus protoplasts. *Plant Physiology* **98**, 632-638.

Rengel Z, Pineros M, Tester M. 1995. Transmembrane calcium fluxes during Al stress. *Plant and Soil* **171**, 125-130.

Rengel Z, Robinson DL. 1989a. Aluminum effects on growth and macronutrient uptake by annual ryegrass. *Agronomy Journal* **81**, 208-215.

Rengel Z, Robinson DL. 1989b. Competitive Al^{3+} inhibition of net Mg^{2+} uptake by intact *Lolium multiflorum* roots : I. Kinetics. *Plant Physiology* **91**, 1407-1413.

Rengel Z, Zhang WH. 2003. Role of dynamics of intracellular calcium in aluminium toxicity syndrome. *New Phytologist* **159**, 295-314.

Richards KD, Schott EJ, Sharma YK, Davis KR, Gardner RC. 1998. Aluminum induces oxidative stress genes in *Arabidopsis thaliana*. *Plant Physiology* **116**, 409-418.

Rincon-Zachary M, Teaster ND, Sparks JA, Valster AH, Motes CM, Blancaflor EB. 2010. Fluorescence resonance energy transfer-sensitized emission of Yellow Cameleon 3.60 reveals root zone-specific calcium signatures in Arabidopsis in response to aluminum and other trivalent cations. *Plant Physiology* **152**, 1442-1458.

Roos W, Viehweger K, Dordschbal B, Schumann B, Evers S, Steighardt J, Schwartze W. 2006. Intracellular pH signals in the induction of secondary pathways - The case of *Eschscholzia californica*. *Journal of Plant Physiology* **163**, 369-381.

Ross J, Li Y, Lim EK, Bowles DJ. 2001. Higher plant glycosyltransferases. *Genome Biology* **2**, 3004.3001-3004.3006.

Rowell DL, Wild A. 1985. Causes of soil acidification: a summary. *Soil Use and Management* **1**, 32-33.

Ryan PR, Delhaize E, Jones DL. 2001. Function and mechanism of organic anion exudation from plant roots. *Annual Review of Plant Physiology and Plant Molecular Biology* **52**, 527-560.

Ryan PR, Delhaize E, Randall PJ. 1995a. Characterisation of Al-stimulated efflux of malate from the apices of Al-tolerant wheat roots. *Planta* **196**, 103-110.

Ryan PR, Delhaize E, Randall PJ. 1995b. Characterization of Al-stimulated efflux of malate from the apices of Al-tolerant wheat roots. *Planta* **196**, 103-110.

Ryan PR, Ditomaso JM, Kochian LV. 1993. Aluminium toxicity in roots: An investigation of spatial sensitivity and the role of the root cap. *Journal of Experimental Botany* **44**, 437-446.

Ryan PR, Kochian LV. 1993. Interaction between aluminum toxicity and calcium uptake at the root apex in near-isogenic lines of wheat (*Triticum aestivum* L.) differing in aluminum tolerance. *Plant Physiology* **102**, 975-982.

Ryan PR, Liu Q, Sperling P, Dong B, Franke S, Delhaize E. 2007. A higher plant Δ8 sphingolipid desaturase with a preference for (Z)-isomer formation confers aluminum tolerance to yeast and plants. *Plant Physiology* **144**, 1968-1977.

Ryan PR, Newman IA, Shields B. 1990. Ion fluxes in corn roots measured by microelectrodes with ion-specific liquid membranes. *Journal of Membrane Science* **53**, 59-69.

Ryan PR, Raman H, Gupta S, Horst WJ, Delhaize E. 2009. A second mechanism for aluminum resistance in wheat relies on the constitutive efflux of citrate from roots. *Plant Physiology* **149**, 340-351.

Ryan PR, Reid RJ, Smith FA. 1997. Direct evaluation of the Ca^{2+}-displacement hypothesis for Al toxicity. *Plant Physiology* **113**, 1351-1357.

Samac DA, Tesfaye M. 2003. Plant improvement for tolerance to aluminum in acid soils - a review. *Plant Cell Tissue and Organ Culture* **75**, 189-207.

Sano T, Becker D, Ivashikina N, Wegner LH, Zimmermann U, Roelfsema MRG, Nagata T, Hedrich R. 2007. Plant cells must pass a K^+ threshold to re-enter the cell cycle. *Plant Journal* **50**, 401-413.

Sasaki M, Kasai M, Yamamoto Y, Matsumoto H. 1995. Involvement of plasma membrane potential in the tolerance mechanism of plant roots to aluminum toxicity. *Plant and Soil* **171**, 119-124.

Sasaki T, Ryan PR, Delhaize E, Hebb DM, Ogihara Y, Kawaura K, Noda K, Kojima T, Toyoda A, Matsumoto H. 2006. Sequence upstream of the wheat (*Triticum aestivum* L.) *ALMT1* gene and its relationship to aluminum resistance. *Plant and Cell Physiology* **47**, 1343-1354.

Sasaki T, Yamamoto Y, Ezaki B, Katsuhara M, Ahn SJ, Ryan PR, Delhaize E, Matsumoto H. 2004. A wheat gene encoding an aluminum-activated malate transporter. *The Plant Journal* **37**, 645-653.

Satoh Y, Nakamura Y. 1984. Characteristics of the reverse reaction of $NADP^+$-isocitrate dehydrogenase from castor bean seeds. *Physiologia Plantarum* **62**, 561-565.

Sawaki Y, Iuchi S, Kobayashi Y, Kobayashi Y, Ikka T, Sakurai N, Fujita M, Shinozaki K, Shibata D, Kobayashi M, Koyama H. 2009. STOP1 regulates multiple genes that protect Arabidopsis from proton and aluminum toxicities. *Plant Physiology* **150**, 281-294.

Schiefelbein JW, Shipley A, Rowse P. 1992. Calcium influx at the tip of growing root-hair cells of *Arabidopsis thaliana*. *Planta* **187**, 455-459.

Schmohl N, Pilling J, Fisahn J, Horst WJ. 2000. Pectin methylesterase modulates aluminium sensitivity in *Zea mays* and *Solanum tuberosum*. *Physiologia Plantarum* **109**, 419-427.

Schock I, Gregan J, Steinhauser S, Schweyen R, Brennicke A, Knoop V. 2000. A member of a novel *Arabidopsis thaliana* gene family of candidate Mg^{2+} ion transporters complements a yeast mitochondrial group II intron-splicing mutant. *Plant Journal* **24**, 489–501.

Schofield RMS, Pallon J, Fiskesjö G, Karlsson G, Malmqvist KG. 1998. Aluminum and calcium distribution patterns in aluminum-intoxicated roots of *Allium cepa* do not support the calcium-displacement hypothesis and indicate signal-mediated inhibition of root growth. *Planta* **205**, 175-180.

Scholz-Starke J, Gambale F, Carpaneto A. 2005. Modulation of plant ion channels by oxidizing and reducing agents. *Archives of Biochemistry and Biophysics* **434**, 43-50.

Schroppelmeier G, Kaiser WM. 1988. Ion homeostasis in chloroplasts under salinity and mineral Deficiency.1. Solute concentrations in leaves and chloroplasts from spinach plants under NaCl or $NaNO_3$ salinity. *Plant Physiology* **87**, 822-827.

Schubert S, Schubert E, Mengel K. 1990. Effect of low pH of the root medium on proton release, growth, and nutrient uptake of field beans (*Vicia faba*). *Plant and Soil* **124**, 239-244.

Scott BJ, Robson AD. 1990a. Changes in the content and form of magnesium in the 1st trifoliate leaf of subterranean clover under altered or constant root supply. *Australian Journal of Agricultural Research* **41**, 511-519.

Scott BJ, Robson AD. 1990b. Distribution of magnesium in subterranean clover (*Trifolium subterraneum* L) in relation to supply. *Australian Journal of Agricultural Research* **41**, 499-510.

Shabala S, Demidchik V, Shabala L, Cuin TA, Smith SJ, Miller AJ, Davies JM, Newman IA. 2006. Extracellular Ca^{2+} ameliorates NaCl-induced K^+ loss from Arabidopsis root and leaf cells by controlling plasma membrane K^+-permeable channels. *Plant Physiology* **141**, 1653-1665.

Shabala SN, Lew RR. 2002. Turgor regulation in osmotically stressed Arabidopsis epidermal root cells. Direct support for the role of inorganic ion uptake as revealed by concurrent flux and cell turgor measurements. *Plant Physiology* **129**, 290-299.

Shabala SN, Newman IA, Morris J. 1997. Oscillations in H^+ and Ca^{2+} ion fluxes around the elongation region of corn roots and effects of external pH. *Plant Physiology* **113**, 111-118.

Sharikabad MN, Ostbye KM, Brors O. 2001. Increased $[Mg^{2+}]_o$ reduces Ca^{2+} influx and disruption of mitochondrial membrane potential during reoxygenation. *American Journal of Physiology - Heart and Circulatory Physiology* **281**, H2113-H2123.

Shaul O. 2002. Magnesium transport and function in plants: the tip of the iceberg. *Biometals* **15**, 309-323.

Shaul O, Hilgemann DW, de-Almeida-Engler J, Van Montagu M, Inze D, Galili G. 1999. Cloning and characterization of a novel Mg^{2+}/H^{+} exchanger. *Embo Journal* **18**, 3973-3980.

Shen H, He LF, Sasaki T, Yamamoto Y, Zheng SJ, Ligaba A, Yan XL, Ahn SJ, Yamaguchi M, Sasakawa H, Matsumoto H. 2005. Citrate secretion coupled with the modulation of soybean root tip under aluminum stress. Up-regulation of transcription, translation, and threonine-oriented phosphorylation of plasma membrane H^{+}-ATPase. *Plant Physiology* **138**, 287-296.

Shen J, Tang C, Rengel Z, Zhang F. 2004a. Root-induced acidification and excess cation uptake by N_2-fixing *Lupinus albus* grown in phosphorus-deficient soil. *Plant and Soil* **260**, 69-77.

Shen R, Iwashita T, Ma JF. 2004b. Form of Al changes with Al concentration in leaves of buckwheat. *Journal of Experimental Botany* **55**, 131-136.

Shen R, Ma J, Kyo M, Iwashita T. 2002. Compartmentation of aluminium in leaves of an Al-accumulator, *Fagopyrum esculentum* Moench. *Planta* **215**, 394-398.

Silva IR, Smyth TJ, Israel DW, Raper CD, Rufty TW. 2001a. Magnesium ameliorates aluminum rhizotoxicity in soybean by increasing citric acid production and exudation by roots. *Plant and Cell Physiology* **42**, 546-554.

Silva IR, Smyth TJ, Israel DW, Raper CD, Rufty TW. 2001b. Magnesium is more efficient than calcium in alleviating aluminum rhizotoxicity in soybean and its ameliorative effect is not explained by the Gouy-Chapman-Stern model. *Plant and Cell Physiology* **42**, 538-545.

Silva IR, Smyth TJ, Israel DW, Rufty TW. 2001c. Altered aluminum inhibition of soybean root elongation in the presence of magnesium. *Plant and Soil* **230**, 223-230.

Silva IR, Smyth TJ, Moxley DF, Carter TE, Allen NS, Rufty TW. 2000. Aluminum accumulation at nuclei of cells in the root tip. Fluorescence detection using lumogallion and confocal laser scanning microscopy. *Plant Physiology* **123**, 543-552.

Silva S, Pinto-Carnide O, Martins-Lopes P, Matos M, Guedes-Pinto H, Santos C. 2010. Differential aluminium changes on nutrient accumulation and root differentiation in an Al sensitive vs. tolerant wheat. *Environmental and Experimental Botany* **68**, 91-98.

Šimonovicová M, Huttova J, Mistrik I, Široká B, Tamas L. 2004a. Peroxidase mediated hydrogen peroxide production in barley roots grown under stress conditions. *Plant Growth Regulation* **44**, 267-275.

Šimonovicová M, Huttová J, Mistrik I, Široká B, Tamas L. 2004b. Root growth inhibition by aluminum is probably caused by cell death due to peroxidase-mediated hydrogen peroxide production. *Protoplasma* **224**, 91-98.

Sivaguru M, Baluska F, Volkmann D, Felle HH, Horst WJ. 1999. Impacts of aluminum on the cytoskeleton of the maize root apex. Short-term effects on the distal part of the transition zone. *Plant Physiology* **119**, 1073-1082.

Sivaguru M, Fujiwara T, Samaj J, Baluska F, Yang Z, Osawa H, Maeda T, Mori T, Volkmann D, Matsumoto H. 2000. Aluminum-induced 1––3-$^{\beta}$ -$_{D}$-Glucan inhibits cell-to-cell trafficking of molecules through plasmodesmata. A new mechanism of aluminum toxicity in plants. *Plant Physiology* **124**, 991-1006.

Sivaguru M, Horst WJ. 1998. The distal part of the transition zone is the most aluminum-sensitive apical root zone of maize. *Plant Physiology* **116**, 155-163.

Sivaguru M, Paliwal K. 1993. Differential aluminum tolerance in some tropical rice cultivars. II. mechanism of aluminum tolerance. *Journal of Plant Nutrition* **16**, 1717-1732.

Sivaguru M, Pike S, Gassmann W, Baskin TI. 2003. Aluminum rapidly depolymerizes cortical microtubules and depolarizes the plasma membrane: Evidence that these responses are mediated by a glutamate receptor. *Plant and Cell Physiology* **44**, 667-675.

Sivaguru M, Yamamoto Y, Rengel Z, Ahn S, Matsumoto H. 2005. Early events responsible for aluminum toxicity symptoms in suspension cultured tobacco cells. *New Phytologist* **165**, 99-109.

Smith RL, Maguire ME. 1998. Microbial magnesium transport: Unusual transporters searching for identity. *Molecular Microbiology* **28**, 217-226.

Staß A, Horst WJ. 1995. Effect of aluminium on membrane properties of soybean (*Glycine max*) cells in suspension culture. *Plant and Soil* **171**, 113-118.

Stelzer R, Lehmann H, Kramer D, Luttge U. 1990. X-ray microprobe analyses of vacuoles of spruce needle mesophyll, endodermis and transfusion parenchyma cells at different seasons of the year. *Botanica Acta* **103**, 415-423.

Street HE. 1966. The physiology of root growth. *Annual Review of Plant Physiology* **17**, 315-344.

Sylvia L. 1990. Aluminium interactions with K^+($^{86}Rb^+$) and $^{45}Ca^{2+}$ fluxes in three cultivars of sugar beet (*Beta vulgaris*). *Physiologia Plantarum* **79**, 275-282.

Szmacinski H, Lakowicz JR. 1996. Fluorescence lifetime characterization of magnesium probes: Improvement of Mg^{2+} dynamic range and sensitivity using phase-modulation fluorometry. *Journal of Fluorescence* **6**, 83-95.

Tabuchi A, Matsumoto H. 2001. Changes in cell-wall properties of wheat (*Triticum aestivum*) roots during aluminum-induced growth inhibition. *Physiologia Plantarum* **112**, 353-358.

Tahara K, Yamanoshita T, Norisada M, Hasegawa I, Kashima H, Sasaki S, Kojima K. 2008. Aluminum distribution and reactive oxygen species accumulation in root tips of two Melaleuca trees differing in aluminum resistance. *Plant and Soil* **307**, 167-178.

Takabatake R, Shimmen T. 1997. Inhibition of electrogenesis by aluminum in characean cells. *Plant and Cell Physiology* **38**, 1264-1271.

Tamas L, Budikova S, Huttova J, Mistrik I, Šimonovi ová M, Široká B. 2005. Aluminum-induced cell death of barley-root border cells is correlated with peroxidase- and oxalate oxidase-mediated hydrogen peroxide production. *Plant Cell Reports* **24**, 189-194.

Tamás L, Šimonovi ová M, Huttová J, Mistr k I. 2004. Aluminium stimulated hydrogen peroxide production of germinating barley seeds. *Environmental and Experimental Botany* **51**, 281-288.

Tan KZ, Keltjens WG, Findenegg GR. 1991. Role of magnesium in combination with liming in alleviating acid-soil stress with the aluminum-sensitive sorghum genotype-Cv323. *Plant and Soil* **136**, 65-71.

Tang C, Raphael C, Rengel Z, Bowden JW. 2000. Understanding subsoil acidification: effect of nitrogen transformation and nitrate leaching. *Australian Journal of Soil Research* **38**, 837-850.

Tanoi K, Junko H, Kazutoshi S, Yoshitake H, Hiroki N, Tomoko MN. 2005. Analysis of potassium uptake by rice roots treated with aluminum using a positron emitting nuclide, ^{38}K. *Soil Science and Plant Nutrition* **51**, 715-717.

Taylor GJ. 1991. Current views of the aluminum stress response: the physiological basis of tolerance. *Current topics in plant biochemistry and physiology* **10**, 57-93.

Taylor GJ, McDonald-Stephens JL, Hunter DB, Bertsch PM, Elmore D, Rengel Z, Reid RJ. 2000. Direct measurement of aluminum uptake and distribution in single cells of *Chara corallina*. *Plant Physiology* **123**, 987-996.

Tesfaye M, Temple SJ, Allan DL, Vance CP, Samac DA. 2001. Overexpression of malate dehydrogenase in transgenic alfalfa enhances organic acid synthesis and confers tolerance to aluminum. *Plant Physiology* **127**, 1836-1844.

Tovar-Mendez A, Rodriguez-Sotres R, Lopez-Valentin DM, Munoz-Clares RA. 1998. Re-examination of the roles of PEP and Mg^{2+} in the reaction catalysed by the phosphorylated and non-phosphorylated forms of phosphoenolpyruvate carboxylase from leaves of *Zea mays* - Effects of the activators glucose 6-phosphate and glycine. *Biochemical Journal* **332**, 633-642.

Trofimova MS, Smolenskaya IN, Drabkin AV, Galkin AV, Babakov AV. 1997. Does plasma membrane H^+-ATPase activation by fusicoccin involve protein kinase? *Physiologia Plantarum* **99**, 221-226.

Valadez-Gonzalez N, Colli-Mull JG, Brito-Argaez L, Muñoz-Sánchez JA, Aguilar JJZ, Castano E, Hernández-Sotomayor SMT. 2007. Differential effect of aluminum on DNA synthesis and CDKA activity in two *Coffea arabica* cell lines. *Journal of Plant Growth Regulation* **26**, 69-77.

Vallejo AJ, Peralta ML, Santa-Maria GE. 2005. Expression of potassium-transporter coding genes, and kinetics of rubidium uptake, along a longitudinal root axis. *Plant, Cell & Environment* **28**, 850-862.

vanPraag HJ, Weissen F, Dreze P, Cogneau M. 1997. Effects of aluminium on calcium and magnesium uptake and translocation by root segments of whole seedlings of Norway spruce (*Picea abies* Karst). *Plant and Soil* **189**, 267-273.

Vázquez MD. 2002. Aluminum exclusion mechanism in root tips of maize (*Zea mays* L.): lysigeny of aluminum hyperaccumulator cells. *Plant Biology (Stuttgart)* **4**, 234-249.

Verbelen JP, De Cnodder T, Le J, Vissenberg K, Baluška F. 2006. The root apex of *Arabidopsis thaliana* consists of four distinct zones of cellular activities: meristematic zone, transition zone, fast elongation zone, and growth terminating zone. *Plant Signaling & Behavior* **1**, 296-304.

Very A-A, Davies JM. 2000. Hyperpolarization-activated calcium channels at the tip of *Arabidopsis* root hairs. *Proceedings of the National Academy of Sciences of the United States of America* **97**, 9801-9806.

Vitorello VA, Capaldi FR, Stefanuto VA. 2005. Recent advances in aluminum toxicity and resistance in higher plants. *Brazilian Journal of Plant Physiology* **17**, 129-143.

von Uexkull HR, Mutert E. 1995. Global extent, development and economic impact of acid soils. *Plant and Soil* **171**, 1-15.

Voragen A, Coenen G-J, Verhoef R, Schols H. 2009. Pectin, a versatile polysaccharide present in plant cell walls. *Structural Chemistry* **20**, 263-275.

Vose PB, Randall PJ. 1962. Resistance to aluminium and manganese toxicities in plants related to variety and cation-exchange capacity. *Nature* **196**, 85-86.

Vries W, Breeuwsma A. 1987. The relation between soil acidification and element cycling. *Water, Air, & Soil Pollution* **35**, 293-310.

Wang H, Inukai Y, Yamauchi A. 2006. Root development and nutrient uptake. *Critical Reviews in Plant Sciences* **25**, 279 - 301.

Ward JM, Schroeder JI. 1994. Calcium activated K^+ channels and calcium-induced calcium release by slow vacuolar ion channels in guard cell vacuoles implicated in the control of stomatal closure. *Plant Cell* **6**, 669-683.

Watanabe T, Okada K. 2005. Interactive effects of Al, Ca and other cations on root elongation of rice cultivars under low pH. *Annals of Botany* **95**, 379-385.

Webb AAR, McAinsh MR, Taylor JE, Hetherington AM. 1996. Calcium ions as intracellular second messengers in higher plants. *Advances in Botanical Research* **22**, 45-96.

Wehr JB, Menzies NW, Blamey FPC. 2003. Model studies on the role of citrate, malate and pectin esterification on the enzymatic degradation of Al-and Ca-pectate gels: possible implications for Al-tolerance. *Plant Physiology et Biochemistry* **41**, 1007-1010.

Weiser T, Blum W, Bentrup FW. 1991. Calmodulin regulates the Ca^{2+}-dependent slow vacuolar ion channel in the tonoplast of *Chenopodium rubrum* suspension cells. *Planta* **185**, 440-442.

Wenzl P, Chaves AL, Patiño GM, Mayer JE, Rao IM. 2002. Aluminum stress stimulates the accumulation of organic acids in root apices of *Brachiaria* species. *Journal of Plant Nutrition and Soil Science* **165**, 582-588.

Wenzl P, Patino GM, Chaves AL, Mayer JE, Rao IM. 2001. The high level of aluminum resistance in signalgrass is not associated with known mechanisms of external aluminum detoxification in root apices. *Plant Physiology* **125**, 1473-1484.

Wherrett T, Ryan PR, Delhaize E, Shabala S. 2005. Effect of aluminium on membrane potential and ion fluxes at the apices of wheat roots. *Functional Plant Biology* **32**, 199-208.

White PJ. 1998. Calcium channels in the plasma membrane of root cells. *Annals of Botany* **81**, 173-183.

Winch S, Pritchard J. 1999. Acid-induced wall loosening is confined to the accelerating region of the root growing zone. *Journal of Experimental Botany* **50**, 1481-1487.

Yamamoto Y, Hachiya A, Matsumoto H. 1997. Oxidative damage to membranes by a combination of aluminum and iron in suspension-cultured tobacco cells. *Plant and Cell Physiology* **38**, 1333-1339.

Yamamoto Y, Kobayashi Y, Devi SR, Rikiishi S, Matsumoto H. 2002. Aluminum toxicity is associated with mitochondrial dysfunction and the production of reactive oxygen species in plant cells. *Plant Physiology* **128**, 63-72.

Yamashita K, Mimura T, Shimazaki K-i. 2003. Evidence for nucleotide-dependent passive H^+ transport protein in the plasma membrane of barley roots. *Plant and Cell Physiology* **44**, 55-61.

Yan F, Feuerle R, Schaffer S, Fortmeier H, Schubert S. 1998. Adaptation of active proton pumping and plasmalemma ATPase activity of corn roots to low root medium pH. *Plant Physiology* **117**, 311-319.

Yan F, Schubert S, Mengel K. 1992. Effect of low root medium pH on net proton release, root respiration, and root growth of corn (*Zea mays* L.) and broad bean (*Vicia faba* L.). *Plant Physiology* **99**, 415-421.

Yang JL, You JF, Li YY, Wu P, Zheng SJ. 2007. Magnesium enhances aluminum-induced citrate secretion in rice bean roots (*Vigna umbellata*) by restoring plasma membrane H^+-ATPase activity. *Plant and Cell Physiology* **48**, 66-73.

Yang JL, Zheng SJ, He YF, Matsumoto H. 2005. Aluminium resistance requires resistance to acid stress: a case study with spinach that exudes oxalate rapidly when exposed to Al stress. *Journal of Experimental Botany* **56**, 1197-1203.

Yazaki Y, Asukagawa N, Ishikawa Y, Ohta E, Sakata M. 1988. Estimation of cytoplasmic free Mg^{2+} levels and phosphorylation potentials in Mung bean root tips by *in vivo* ^{31}P NMR spectroscopy. *Plant and Cell Physiology* **29**, 919-924.

Yermiyahu U, Brauer DK, Kinraide TB. 1997. Sorption of aluminum to plasma membrane vesicles isolated from roots of Scout 66 and Atlas 66 cultivars of wheat. *Plant Physiology* **115**, 1119-1125.

Yokota S, Ojima K. 1995. Physiological response of root tip of alfalfa to low pH and aluminium stress in water culture. *Plant and Soil* **171**, 163-165.

Yu M, Shen R, Liu J, Chen R, Xu M, Yang Y, Xiao H, Wang H, Wang C. 2009. The role of root border cells in aluminum resistance of pea (*Pisum sativum*) grown in mist culture. *Journal of Plant Nutrition and Soil Science* **172**, 528-534.

Zhang J, He Z, Tian H, Zhu G, Peng X. 2007. Identification of aluminium-responsive genes in rice cultivars with different aluminium sensitivities. *Journal of Experimental Botany* **58**, 2269-2278.

Zhang WH, Rengel Z. 1999. Aluminium induces an increase in cytoplasmic calcium in intact wheat root apical cells. *Australian Journal of Plant Physiology* **26**, 401-410.

Zhang WH, Ryan PR, Tyerman SD. 2001. Malate-permeable channels and cation channels activated by aluminum in the apical cells of wheat roots. *Plant Physiology* **125**, 1459-1472.

Zhao J, Barkla B, Marshall J, Pittman J, Hirschi K. 2008a. The *Arabidopsis cax3* mutants display altered salt tolerance, pH sensitivity and reduced plasma membrane H^+-ATPase activity. *Planta* **227**, 659-669.

Zhao J, Cheng N-H, Motes CM, Blancaflor EB, Moore M, Gonzales N, Padmanaban S, Sze H, Ward JM, Hirschi KD. 2008b. AtCHX13 is a plasma membrane K^+ transporter. *Plant Physiology* **148**, 796-807.

Zhao Z, Ma JF, Sato K, Takeda K. 2003. Differential Al resistance and citrate secretion in barley (*Hordeum vulgare* L.). *Planta* **217**, 794-800.

Zheng SJ, Yang JL, He YF, Yu XH, Zhang L, You JF, Shen RF, Matsumoto H. 2005. Immobilization of aluminum with phosphorus in roots is associated with high aluminum resistance in buckwheat. *Plant Physiology* **138**, 297-303.

Zhu M, Ahn S, Matsumoto H. 2003. Inhibition of growth and development of root border cells in wheat by Al. *Physiologia Plantarum* **117**, 359-367.